Thèse de Doctorat

pour obtenir le grade de

Docteur de Sorbonne Université

ED386 - École Doctorale Sciences Mathématiques de Paris Centre
Spécialité : « Mathématiques Appliquées »

présentée par

Victor FOURNET

Sous la direction de **Bruno DESPRÉS**
co-dirigé par **Christophe BUET**

Mathematical and Numerical Study of Thick Spray Models

Présentée et soutenue publiquement le 22 Janvier 2025 à Sorbonne Université
devant un jury composé de :

Emmanuel Grenier	Professeur	Beijing Institute of Technology	Rapporteur
Julien Mathiaud	Professeur	Université de Rennes (IRMAR)	Rapporteur
Laurent Boudin	Maitre de conférence	Sorbonne Université (LJLL)	Examinateur
Frédérique Charles	Professeure	Université Grenoble Alpes (LJK)	Présidente du jury
Bruno Després	Professeur	Sorbonne Université (LJLL)	Directeur de thèse
Christophe Buet	Directeur de recherche	CEA-DAM-DIF	Co-directeur de thèse

Remerciements

J'arrive finalement à la fin de mon doctorat. Cela fait longtemps que je pense à ce moment et je dois dire que ça fait très bizarre d'écrire ces lignes. Entre le début et la fin de ma thèse, j'ai beaucoup appris et cela n'aurait pas pu se faire tout seul. Je profite donc de ce moment pour remercier celles et ceux qui m'ont accompagné pendant cette aventure.

Je tiens tout d'abord à remercier mes directeurs de thèse Christophe Buet et Bruno Després. Merci à Christophe qui, dès mon arrivée au CEA, m'a fait confiance, tu m'as toujours soutenu et tu as fait en sorte que tout se passe bien, surtout sur le plan administratif (tu sais comme cette partie me passionne !). Merci Bruno pour tout ce que tu m'as appris. J'ai toujours été impressionné par ta faculté à être sur de nombreux projets en même temps et, malgré ça, je me suis senti toujours accompagné pendant ma thèse. Vous avez tous les deux su me laisser apprendre par moi-même tout en m'évitant de partir dans la mauvaise direction, ce qui, avec votre enthousiasme et votre bonne humeur, a fait que cette thèse a été une période très agréable. Nos longues heures de réunions vont me manquer. J'ai énormément appris à vos côtés et je suis très fier d'être votre élève.

Je remercie Emmanuel Grenier et Julien Mathiaud pour avoir accepté de rapporter cette thèse et avoir lu en profondeur mon manuscrit. Je remercie également Frédérique Charles et Laurent Boudin pour avoir accepté de faire partie de mon jury de thèse.

Merci à Laurent Desvillettes et Ayman Moussa d'avoir fait partie de mon comité de suivi. Vos conseils et votre regard extérieur sur le déroulement de ma thèse m'ont été très précieux.

Merci à Stéphane D-P. Même si tu n'as pas à proprement parler participé au déroulement de ma thèse, tu as encadré mon stage avec Christophe à mon arrivée au CEA et tout ce que tu m'as appris pendant ce stage, notamment sur l'écriture et le débuggage de code numérique, m'a grandement aidé tout au long de ma thèse.

En presque quatre ans au CEA, j'ai rencontré de nombreux doctorants et stagiaires qui ont rendu le quotidien très agréable. Merci à Paul, Axelle, Manu, Valentin, Julie, Claire, Alexianne, Alexandre, Gabriel, Isaïe, Mickaël, Luc, Clément, Mina, Arzhela et Yohan pour ces années passées ensemble. Je n'oublierai jamais nos débats, qui ont, à leur manière, fait avancer la civilisation humaine, que ce soit dans notre bureau, autour d'un café ou dans le froid de la cantine de Teratec. Merci de m'avoir supporté au quotidien et pour tous les bons moments.

Je remercie toutes les personnes que j'ai rencontrées au CEA qui m'ont aidé, que ce soit sur le plan scientifique ou administratif. Merci Stéphane J., Emmanuel, Philippe, Patricia, Céline, Alain et Agnès.

Merci à Lucas pour ton soutien et nos discussions qui m'ont beaucoup aidé à mieux comprendre les sprays !

Merci à Alessandro, Charlène, Marthe, Robin, Baptiste, Helen, Sara, Erwan, Mélanie, Antoine, Serena et Mathilde. Votre compagnie, que ce soit autour d'une bière, d'une pizza ou simplement lors des nombreuses soirées passées ensemble pendant (et avant) ma thèse, m'a beaucoup aidé.

Merci Romain d'être mon ami depuis toutes ces années.

Merci à mes parents, qui m'ont soutenu tout au long de ma vie, m'ont toujours poussé à faire ce que j'aime et se sont toujours sacrifiés pour moi. Merci de m'aimer comme vous le faites. Merci à mon frère Martin de me rendre aussi fier, et merci à Sarah de prendre soin de lui.

Gracias, Esther, por tu amor, por todos los buenos momentos que hemos pasado juntos, por tu apoyo y por tomarte el tiempo de corregir mi manuscrito. Esta tesis no habría sido lo mismo sin ti.

Résumé

Cette thèse est consacrée à la modélisation, à l'analyse mathématique et à l'analyse numérique d'un système d'équations aux dérivées partielles décrivant l'évolution d'une suspension de particules neutres dans un fluide ambiant, souvent désignée sous le nom de spray. La phase dispersée est modélisée par les équations de la théorie cinétique, tandis que la phase continue est décrite par les équations de la mécanique des fluides. Nous nous concentrons en particulier sur le cas des sprays dits épais.

Le Chapitre 2 est consacré au problème de la construction de solutions pour le système des sprays épais. Nous introduisons un nouveau système dans lequel les termes singuliers sont régularisés et nous démontrons l'existence et l'unicité de solutions avec une régularité de type Sobolev, localement en temps.

Le Chapitre 3 explore l'analogie entre le système des sprays épais et le système de Vlasov-Poisson décrivant un plasma électrostatique. Nous montrons qu'en l'absence de friction, le système des sprays épais présente une propriété d'amortissement linéaire de l'énergie acoustique, analogue à l'amortissement de Landau bien connu en physique des plasmas. Cet effet est illustré par des résultats numériques.

Le Chapitre 4 est consacré à la simulation numérique du système des sprays épais. Nous proposons une approche combinant des méthodes existantes : une méthode semi-Lagrangienne pour la phase dispersée, couplée à une méthode de type Volume Fini pour la phase continue. Nous abordons également le problème de la limite de packing et introduisons deux méthodes permettant de conserver cette limite au niveau discret. Enfin, nous présentons des résultats numériques.

Summary

This thesis is dedicated to the modeling, mathematical analysis, and numerical analysis of a partial differential equation system describing the evolution of a suspension of neutral particles in a surrounding fluid, often referred to as a spray. The dispersed phase is modeled by the equations of kinetic theory, while the continuous phase is described by the equations of fluid mechanics. We focus particularly on the case of so-called thick sprays.

Chapter 2 is devoted to the problem of constructing solutions for the thick spray system. We introduce a new system in which singular terms are regularized, and we prove the existence and uniqueness of solutions with Sobolev regularity, locally in time.

Chapter 3 explores the analogy between the thick spray system and the Vlasov-Poisson system describing an electrostatic plasma. We demonstrate that, in the absence of friction, the thick spray system exhibits a property of linear damping of acoustic energy, analogous to Landau damping, which is well known in plasma physics. This effect is illustrated by numerical results.

Chapter 4 is dedicated to the numerical simulation of the thick spray system. We present an approach that combines existing methods: a semi-Lagrangian method for the dispersed phase, coupled with a finite volume method for the continuous phase. We also address the packing limit issue and introduce two methods to preserve this packing limit at the discrete level. Finally, we present numerical results.

List of publications

The research in this thesis has been published in the following works:

- [63] V. Fournet, C. Buet, and B. Després. Local-in-time existence of strong solutions to an averaged thick sprays model. *Kinetic and Related Models*, 2024, 17(4): 606-633. doi: 10.3934/krm.2023034
- [28] C. Buet, B. Després, and V. Fournet. Analog of Linear Landau Damping in a coupled Vlasov-Euler system for thick sprays. Accepted in *Communications in Mathematical Sciences*, 2024.
- [62] V. Fournet. Investigation on the stability in a thick spray model. Accepted in *ESAIM: Proceedings and Surveys*, 2024.

Contents

Chapter 1

Introduction

This introductory chapter introduces the main system of partial differential equations studied in this thesis. We start by defining the concept of a spray, after which we present an overview of the content covered in each chapter.

1.1 Introduction to spray models

This thesis is dedicated to the modelisation and to the mathematical and numerical study of thick sprays. The term *spray* (or aerosol) refers to the suspension of small particles (like dust specks or small droplets) inside a carrying fluid. This description while quite general, encompasses an important number of physical phenomena at different scales. This includes but is not limited to: aerosols for medical use [24, 25], combustion mechanism in engines [5], aerosols in the atmosphere [90], or the modelling of gas giants and exoplanets in astrophysics [66].

Being fundamentally a multiphase flow, there exists a quite large variety of possible mathematical description of a spray [45]:

- **Microscopic level.** A first possibility is to consider each of the particles as dispersed fluid bubbles, where the dynamics in the interior and in the exterior (that is, the dynamics of the carrying fluid) of each bubble is described by a system of Navier Stokes equations. The problem is then not only to describe the position and the velocity of the droplets, but also to describe the free boundary of the droplets. As such, this kind of modelisation is very costly to simulate and only a small number of particles can be considered [109].
- **Macroscopic level.** Another possibility is to instead consider the spray as a two-phase fluids problem (sometimes called "Eulerian-Eulerian"), and to describe the particles and the fluid with two coupled Euler or Navier-Stokes equations. In this approach the interface between the two fluids has disappeared because at the scale of the fluid it is microscopic, and the two fluids are described by their respective volume fractions. This approach is less costly from the numerical point of view, but its numerical discretization remains a difficult problem because such models usually contain nonconservative products. Moreover this kind of model usually leads to ill-posedness due to of a lack of hyperbolicity [64, 67, 120].

In this thesis, we consider a description that lies on the interface between these two, that is, at the **mesoscopic level**. While the fluid is described by macroscopic quantities governed by fluid mechanic equations, the particles are described from a statistical point of view, where we use the **kinetic theory**. Such a way of modelling a spray has been introduced by Williams in [118], and are sometimes called "Eulerian-Lagrangian" or "gas-particles" models.

1.1.1 Kinetic theory

The purpose of the kinetic theory is the modelling of a large number of particles. It was originally introduced by Maxwell [95] to describe the behavior of an ideal gas [31, 32, 65, 115]. Instead of describing each particle with a system of ordinary differential equations, the kinetic theory aims to give a description of the collective motion of a cloud of particles. From a mathematical perspective, the main object of the kinetic theory is a nonnegative distribution function $f := f(t,\boldsymbol{x},\boldsymbol{v})$ on a phase space. Here, $\boldsymbol{x}$ is the position of the particles (living in a space domain $\Omega \subset \mathbf{R}^d$) and $\boldsymbol{v} \in \mathbf{R}^d$ represents their velocity. For any t (on a time interval

$[0,T]$, $T > 0$ or $[0, +\infty))$ the quantity $f(t,\boldsymbol{x},\boldsymbol{v})\mathrm{d}x\mathrm{d}v$ is the number of particles in an element volume $\mathrm{d}x\mathrm{d}v$. It should be noted that pointwise values of f are actually meaningless from a physical point of view (it is not a measurable quantity). A physicist would be interested in integrals of the form $\int f(t,\cdot,\boldsymbol{v})\varphi(\boldsymbol{v})\,\mathrm{d}v$. For instance, the spatial density, average velocity and the average kinetic energy of the particles are expressed as

$$\varrho_f(t,\boldsymbol{x}) = \int_{\mathbf{R}^3} f(t,\boldsymbol{x},\boldsymbol{v})\,\mathrm{d}v$$

$$\varrho_f \boldsymbol{u}_f(t,\boldsymbol{x}) = \int_{\mathbf{R}^3} \boldsymbol{v} f(t,\boldsymbol{x},\boldsymbol{v})\,\mathrm{d}v$$

$$E_f(t,\boldsymbol{x}) = \int_{\mathbf{R}^3} \frac{|\boldsymbol{v}|^2}{2} f(t,\boldsymbol{x},\boldsymbol{v})\,\mathrm{d}v$$

Hereafter, we present a hierarchy of kinetic models, increasing in complexity.

Free transport equation. The first and simplest example of kinetic equation is the free transport equation

$$\partial_t f + \boldsymbol{v} \cdot \nabla_x f = 0. \tag{1.1}$$

This equation describes the free streaming of particles moving in a straigh line. It is a linear transport equation and as such it can be explicitly solved by the method of characteristics. By denoting f_0 the initial condition, it writes

$$f(t,\boldsymbol{x},\boldsymbol{v}) = f_0(\boldsymbol{x} - \boldsymbol{v}t,\boldsymbol{v}).$$

Linear Vlasov equation. If we consider particles which are subject to an external force (e.g. an electromagnetic field, or the forces induced by the flow of an ambient fluid), the distribution function obeys the following equation

$$\partial_t f + \boldsymbol{v} \cdot \nabla_x f + \nabla_v \cdot (\boldsymbol{\Gamma} f) = 0. \tag{1.2}$$

where $\boldsymbol{\Gamma}$ is an external force field which does not depend on f. Again, this equation is solved by the characteristics method

$$f(t,\boldsymbol{x},\boldsymbol{v}) = f_0\left(\mathbf{X}(0;t,\boldsymbol{x},\boldsymbol{v}), \mathbf{V}(0;t,\boldsymbol{x},\boldsymbol{v})\right),$$

where $(\mathbf{X}, \mathbf{V})$ are solutions of the following system of ordinary differential equation

$$\begin{cases} \dfrac{\mathrm{d}}{\mathrm{d}s}\mathbf{X}(s;t,\boldsymbol{x},\boldsymbol{v}) = \mathbf{V}(s;\boldsymbol{x},\boldsymbol{v}) \\ \dfrac{\mathrm{d}}{\mathrm{d}s}\mathbf{V}(s;t,\boldsymbol{x},\boldsymbol{v}) = \boldsymbol{\Gamma}(t,\mathbf{X}(s;t,\boldsymbol{x},\boldsymbol{v}),\mathbf{V}(s;t,\boldsymbol{x},\boldsymbol{v})), \end{cases} \tag{1.3}$$

and

$$(\mathbf{X}(t;t,\boldsymbol{x},\boldsymbol{v}), \mathbf{V}(t;t,\boldsymbol{x},\boldsymbol{v})) = (\boldsymbol{x},\boldsymbol{v}).$$

Boltzmann equation. In some applications, one needs to take into account the interactions between particles.

$$\partial_t f + \boldsymbol{v} \cdot \nabla_x f = \mathcal{Q}(f,f). \tag{1.4}$$

Typically, the operator $\mathcal{Q}(f,f)$ represents the (binary) collision between particles. We refer for the reader interested in such equations to Villani's review [115].

Vlasov-Poisson equations One of the simplest nonlinear kinetic equations, and one of the simplest models for plasmas and the dynamics of galaxies, is the Vlasov-Poisson equations [9, 77, 80, 116]:

$$\begin{cases} \partial_t f + \boldsymbol{v} \cdot \nabla_x f + \mathbf{E} \cdot \nabla_v f = 0 \\ \mathbf{E} = -\nabla_x \phi \\ -\Delta\phi = \displaystyle\int_{\mathbf{R}^3} f(t,\boldsymbol{x},\boldsymbol{v})\,\mathrm{d}v. \end{cases} \tag{1.5}$$

Here, there is no external force, the force acting on the particles is the self-induced electric field $\boldsymbol{\Gamma}(t,\boldsymbol{x},\boldsymbol{v}) = \mathbf{E}(t,\boldsymbol{x})$. This system couples a Vlasov equation with a Poisson equation. Notice that $\mathbf{E}$ does not depend on $\boldsymbol{v}$ and therefore is placed outside the ∇_v operator.

In contrast with the Boltzmann equation (1.4), this equation is time-reversible. However, it surprisingly displays an irreversible behavior, the so-called *Landau damping* [81]. In his pioneering article [81], Landau studied the equation (1.5) linearized around a Gaussian equilibrium for the particles, and concluded that small perturbations of the electric field must decay at an exponential rate. We shall return to this in Chapter 3.

Vlasov-Maxwell equations The previously introduced Vlasov-Poisson equations are an approximation of the more complete and complex Vlasov-Maxwell equations

$$\begin{cases} \partial_t f + \boldsymbol{v} \cdot \nabla_x f + \left(\mathbf{E} + \dfrac{1}{c}\widehat{\boldsymbol{v}} \times \mathbf{B}\right) \cdot \nabla_v f = 0 \\ \dfrac{1}{c}\partial_t \mathbf{B} + \operatorname{curl} \mathbf{E} = 0 \\ -\dfrac{1}{c}\partial_t \mathbf{E} + \operatorname{curl} \mathbf{B} = \dfrac{1}{c}\displaystyle\int_{\mathbf{R}^3} f(t,\boldsymbol{x},\boldsymbol{v})\widehat{\boldsymbol{v}}\,\mathrm{d}v \\ \operatorname{div} \mathbf{E} = \displaystyle\int_{\mathbf{R}^3} f(t,\boldsymbol{x},\boldsymbol{v})\,\mathrm{d}v \\ \operatorname{div} \mathbf{B} = 0 \end{cases} \tag{1.6}$$

with $\widehat{\boldsymbol{v}} = \frac{\boldsymbol{v}}{\sqrt{1+|\boldsymbol{v}|^2/c^2}}$. Despite the fact that $\boldsymbol{\Gamma}$ depends explicitly on $\boldsymbol{v}$, it is divergence-free in the velocity variable $\nabla_v \cdot \boldsymbol{\Gamma} = 0$ and the force can be put inside or outside the ∇_v operator. We recover the Vlasov-Poisson equations (1.5) when $c \to +\infty$ (which translates that the velocities of the particles are negligible compared to the speed of light, $\boldsymbol{v} \ll c$).

1.1.2 Fluid mechanics

Throughout this work, we will only consider compressible, inviscid fluids. The fluid will be described by macroscopic quantities such as its density $\varrho(t,\boldsymbol{x}) \in \mathbf{R}^+$, its velocity $\boldsymbol{u}(t,\boldsymbol{x}) \in \mathbf{R}^d$

and its internal energy $e(t,\boldsymbol{x}) \in \mathbf{R}^+$. The governing equations of the fluid are obtained from the conservation principles of the mass, momentum and total energy. Without external forces, the conservation laws lead to the so-called Euler system [68, 82, 85, 86]

$$\begin{cases} \partial_t \varrho + \nabla_x \cdot (\varrho \boldsymbol{u}) = 0 \\ \partial_t(\varrho \boldsymbol{u}) + \nabla_x(\varrho \boldsymbol{u} \otimes \boldsymbol{u}) + \nabla_x p = 0 \\ \partial_t(\varrho e) + \nabla_x \cdot (\varrho e \boldsymbol{u}) + p \nabla_x \cdot \boldsymbol{u} = 0. \end{cases} \tag{1.7}$$

This set of equations describes a compressible, inviscid fluid, in contrast with the Navier-Stokes equations which take into account viscosity. The pressure $p : \mathbf{R}^+ \to \mathbf{R}$ here is not an unknown quantity, it is a given function obtained from thermodynamical considerations. For instance, for a perfect gas, one has $p(\rho,e) = (\gamma - 1)\rho e$ where $\gamma > 1$ is the adiabatic index. Another important example is the case of a barotropic pressure law $p(\rho) = a\rho^\gamma$ with $a > 0$ and $\gamma > 1$. In this case, the energy equation becomes redundant and one only needs the first two equations to obtain a complete system.

1.1.3 Model for spray

We now turn to the main system under consideration in this thesis. We will present a thin spray model, before turning to the main topic of this thesis, the thick spray model.

We consider only spherical, *monodisperse* particles, which means that they all have the same radius $r_p > 0$ and density $\rho_p > 0$. We denote $m_\star = \frac{4}{3}\pi r_p \rho_p$ the mass of a given particle. We refer to [2, 55, 64, 117] for recent works on polydisperse sprays. We also do not consider thermal effects for the particles and the distribution function f is only dependent on time, position and velocity, $f := f(t,\boldsymbol{x},\boldsymbol{v})$.

In this manuscript, we adopt the classification system proposed by O'Rourke [97], which is based on the volume fraction of the dispersed phase

$$1 - \alpha(t,\boldsymbol{x}) = \frac{m_\star}{\rho_p} \int_{\mathbf{R}^3} f(t,\boldsymbol{x},\boldsymbol{v})\, \mathrm{d}v,$$

where $\alpha(t,\boldsymbol{x})$ represents the fluid volume fraction. The classification is as follows:

- $1-\alpha(t,x) \ll 10^{-3}$: **Very Thin Spray.** In this case, the volume occupied by the particles is so minimal that they do not influence the fluid dynamics. The particles' behavior is entirely dictated by the fluid, with no feedback on the fluid dynamics.
- $1 - \alpha(t,x) \ll 1$: **Thin Spray.** Here, the retroaction of the forces exerted by the fluid on the particles must be considered.
- $1 - \alpha(t,x) \sim 0.1$: **Thick Spray.** In this regime, the volume occupied by the particles is significant compared to that of the fluid, necessitating an explicit inclusion of the volume fraction in the fluid equations.

1.1.3.1 Thin spray model

In the thin spray regime, the fluid volume fraction α is nearly equal to 1, indicating that the total volume occupied by the particles is negligible compared to that of the fluid. Consequently, the volume fraction α does not explicitly appear in the governing equations. A typical model that describes the evolution of a thin spray is often referred to as a Vlasov-Euler system (or Vlasov-Navier-Stokes for viscous fluids) and is expressed as follows [11, 12, 91, 92]:

$$\begin{cases} \partial_t \rho + \nabla_x \cdot (\rho \boldsymbol{u}) = 0 \\ \partial_t (\rho \boldsymbol{u}) + \nabla_x \cdot (\rho \boldsymbol{u} \otimes \boldsymbol{u}) + \nabla_x p = - \iint m_\star f \boldsymbol{\Gamma} \, \mathrm{d}v \mathrm{d}e_p \\ \partial_t (\rho E) + \nabla_x \cdot \left(\rho \left(E + \dfrac{p}{\rho} \right) \right) = - \int m_\star f \left(\boldsymbol{\Gamma} \cdot \boldsymbol{v} + \phi \right) \mathrm{d}v \\ \partial_t f + \boldsymbol{v} \cdot \nabla_x f + \nabla_v \cdot (\boldsymbol{\Gamma} f) + \partial_{e_p} (f \phi) = 0 \\ p = P_1 \left(\rho, E - \dfrac{|\boldsymbol{u}|^2}{2} \right) \\ m_\star \boldsymbol{\Gamma} = D_\star (\boldsymbol{u} - \boldsymbol{v}) \\ m_\star \phi = C(T_g - T_p) \\ T_g = T_1 \left(\rho, E - \dfrac{|\boldsymbol{u}|^2}{2} \right) \\ T_p = T_2 \left(\rho, E - \dfrac{|\boldsymbol{u}|^2}{2} \right). \end{cases} \tag{1.8}$$

In this model, $m_\star$ represents the mass of the particles, while T_g and T_p denote the temperatures of the gas and particles, respectively. The first three equations of this system represent conservation equations for the gas. The fourth equation is the Vlasov equation describing the dynamics of the particles. The interaction between the particles and the fluid is characterized by a drag force, along with heat exchange between the two phases. Here, $\boldsymbol{\Gamma}$ represents the drag force, with the drag coefficient $D_\star$ determined semi-empirically. The functions P_1, T_1, and T_2 are derived from physical laws and vary according to different applications.

This system and its variants have been extensively studied from both mathematical and numerical perspectives; see [11, 12, 24, 25, 54, 91].

1.1.3.2 Thick spray model

In this section, we are interested in the thick spray regime. In this case, the volume fraction of the particles is no longer negligible, and the quantity α appears explicitly in the system. It typically concerns flows where the volume fraction is $\alpha \approx 0.8$ or $\alpha \approx 0.9$. In this thesis, such models will be refered to as thick sprays or thick spray models.

A typical thick spray model reads [23, 49, 52, 53, 97]

$$\begin{cases} \partial_t(\alpha\varrho) + \nabla_x \cdot (\alpha\varrho\boldsymbol{u}) = 0 \\ \partial_t(\alpha\varrho\boldsymbol{u}) + \nabla_x \cdot (\alpha\varrho\boldsymbol{u}\otimes\boldsymbol{u}) + \nabla_x p - \nu\boldsymbol{\mathcal{A}}\boldsymbol{u} = -\displaystyle\int_{\mathbf{R}^3} m_\star \mathbf{\Gamma} f \,\mathrm{d}v \\ \partial_t(\alpha\varrho e) + \nabla_x \cdot (\alpha\varrho e\boldsymbol{u}) + p(\partial_t\alpha + \nabla_x\cdot(\alpha\boldsymbol{u})) = \displaystyle\int_{\mathbf{R}^3} \left(m_\star\mathbf{\Gamma} + \frac{m_\star}{\rho_p}\nabla_x p \right) \cdot (\boldsymbol{v}-\boldsymbol{u}) \,\mathrm{d}v \\ \partial_t f + \boldsymbol{v}\cdot\nabla_x f + \nabla_v\cdot(\mathbf{\Gamma} f) = \kappa\mathcal{Q}(f,f) \\ \alpha = 1 - \dfrac{m_\star}{\rho_p}\displaystyle\int_{\mathbf{R}^3} f\,\mathrm{d}v. \end{cases} \tag{1.9}$$

This system consist of a coupling between a modified compressible Euler system and a Vlasov-Boltzmann equation. The first equation is the conservation of the mass of the fluid. The second equation is the balance law for the momentum of the fluid. The operator $\boldsymbol{\mathcal{A}}\boldsymbol{u}$ is a generic elliptic operator(for instance $\boldsymbol{\mathcal{A}}\boldsymbol{u} = \Delta\boldsymbol{u}$) which models diffusion processes in the gas. Notice the retroaction of the force applied on the particles by the gas on the right-hand-side, inducing a transfert of momentum form the particle phase to the fluid phase. The third equation is the balance law for the internal energy of the fluid. The integral on the right-hand-side corresponds to the transfer of energy from the particles to the fluid. Finally, the fourth equation is a Vlasov-Boltzmann equation that governs the evolution of the particle phase space distribution f. The force field $\mathbf{\Gamma}$ models the forces applied on the particles by the fluid and external forces like gravity. The right-hand-side $\mathcal{Q}(f,f)$ models the interactions between the particles, such as collisions, coalescence (two particles merging together), fragmentation (a particle dividing itself into two or more particles). The constant κ is positive real number that is sometimes refered to as the Knudsen number. Finally, the volume fraction of the fluid $\alpha(t,\boldsymbol{x})$ appears in the fluid part of the system.

Let us detail the force field $\mathbf{\Gamma}$ that couples the particle phase and the fluid phase. In the absence of external forces, the force is usually [5, 45, 53, 97] composed of two terms

$$m_\star\mathbf{\Gamma} = \mathbf{F}_{\text{drag}} + \mathbf{F}_{\text{press}}.$$

- The drag force $\mathbf{F}_{\text{drag}}$ is due the resistance of the fluid to the motion of the particles. One of the more common expressions for this quantity that can be found in the litterature [12, 97, 104] is a nonlinear function of $\boldsymbol{u}(t,\boldsymbol{x}) - \boldsymbol{v}$ that reads

$$\mathbf{F}_{\text{drag}}(t,\boldsymbol{x}) = \frac{1}{2}\pi r_p^2 \varrho(t,\boldsymbol{x}) C_d |\boldsymbol{u}(t,\boldsymbol{x}) - \boldsymbol{v}|(\boldsymbol{u}(t,\boldsymbol{x}) - \boldsymbol{v}),$$

  where C_d is an adimensionnal drag coefficient whose value is given in a semi-empirical way. Some formulae can be found in the litterature. For instance, in the KIVA-II code of Los Alamos [5], the formula used writes

$$C_d = \frac{24}{\mathrm{Re}}\left(1 + \frac{1}{6}\mathrm{Re}^{2/3}\right)$$

  where $\mathrm{Re} = \frac{2\varrho|\boldsymbol{u}-\boldsymbol{v}|r_p}{\mu}$ is the particule Reynolds number and μ is the dynamic viscosity of the fluid. When the Reynolds number is not too large (see [36, 48]), a reasonable approximation is

$$C_d = \frac{24}{\mathrm{Re}},$$

so the drag force writes

$$\mathbf{F}_{\text{drag}} = \frac{C\mu}{r_p^2 \rho_p}(\boldsymbol{u} - \boldsymbol{v}).$$

A common simplification (see again [36, 48]) is to consider a constant viscosity, so the drag force writes

$$\mathbf{F}_{\text{drag}} = D_\star(\boldsymbol{u} - \boldsymbol{v}),$$

where $D_\star$ is a given constant drag coefficient. This is the formula that we will consider in this thesis. The drag force is a force that is common in most fluid-kinetic models and is often the driving mechanism of the dynamics of the system.

- An additional force arising from Archimedes' principle, specific to thick sprays within fluid-kinetic models, appears in the force field:

$$\mathbf{F}_{\text{press}} = -\frac{m_\star}{\rho_p}\nabla_x p(t, \boldsymbol{x}).$$

Since the total volume occupied by the particles is no longer negligible, this force becomes comparable to the drag force. In two-fluid models, it is common to consider a system where the two phases share a common pressure. This same concept underlies the emergence of this term, and it allows to formally recover a two-fluid model from (1.9), by considering the limit $\kappa \to +\infty$ (see [46]).

Finally, in this thesis, we consider a force field $\boldsymbol{\Gamma}$ that writes (in a system of units where $\rho_p = 1$):

$$m_\star \boldsymbol{\Gamma}(t,\boldsymbol{x}, \boldsymbol{v}) = -m_\star \nabla_x p(t,\boldsymbol{x}) - D_\star(\boldsymbol{v} - \boldsymbol{u}(t,\boldsymbol{x})).$$

The retroaction of this force is present in the momentum equation of the fluid in (1.9). In our case, it writes

$$-m_\star \int_{\mathbf{R}^3} \boldsymbol{\Gamma} f \, \mathrm{d}v = m_\star \nabla_x p \int_{\mathbf{R}^3} f \, \mathrm{d}v + D_\star \int_{\mathbf{R}^3} (\boldsymbol{v} - \boldsymbol{u}) f \, \mathrm{d}v.$$

Notice that by substracting the first term of the right-hand-side from the momentum equation yields

$$\partial_t(\alpha\varrho\boldsymbol{u}) + \nabla_x \cdot (\alpha\varrho\boldsymbol{u} \otimes \boldsymbol{u}) + \alpha\nabla_x p - \nu\mathcal{A}\boldsymbol{u} = D_\star \int_{\mathbf{R}^3} (\boldsymbol{v} - \boldsymbol{u}) f \, \mathrm{d}v. \tag{1.10}$$

The right hand side is the retroaction of the drag force on the fluid, sometimes called the *Brinkman force*.

In this manuscript, we consider several simplifications:

- First, we neglect fragmentation and coalescence in the operator $\mathcal{Q}(f,f)$. According to Dukowicz [49], this implies that the particles are sufficiently far apart, allowing us to disregard the collisions between them. Ultimately, this leads to setting $\kappa = 0$. It is worth noting that, while it seems that in numerous test cases, the presence of a collision operator appears to have minimal impact on the macroscopic physical outputs of a numerical simulation (as observed by Benjelloun, Desvillettes, Ghidaglia and Nielsen [17]), this term remains important for linking the fluid-kinetic system (1.9) to the corresponding bifluid model [46].

- We neglect any diffusion process in the system and we set $\nu = 0$. This is a simplification that is commonly found in the physics literature due to the industrial context in which this kind of systems is used, such as the injection of liquid sprays into an ambient gas (see [49, 97]). For an analysis of the system (1.9) with diffusion, we refer to the work of Ertzbischoff and Han-Kwan [53], as well as the PhD thesis of Ertzbischoff [52].
- In this work, we primarily focus on the barotropic case where the pressure depends solely on the density of the fluid $p := p(\varrho)$. This implies that the equation for the internal energy is not needed and can be discarded from the system. Specifically, we assume that $p(\varrho) = \varrho^\gamma$, where $\gamma > 1$ is the adiabatic index.

To conclude this section, let us write the final thick spray model that is used in most of this work

$$\begin{cases} \partial_t(\alpha\varrho) + \nabla_x \cdot (\alpha\varrho\boldsymbol{u}) = 0 \\ \partial_t(\alpha\varrho\boldsymbol{u}) + \nabla_x \cdot (\alpha\varrho\boldsymbol{u}\otimes\boldsymbol{u}) + \nabla_x p(\varrho) = -m_\star \displaystyle\int_{\mathbf{R}^3} \boldsymbol{\Gamma} f \,\mathrm{d}v \\ \partial_t f + \boldsymbol{v}\cdot\nabla_x f + \nabla_v\cdot(\boldsymbol{\Gamma} f) = 0 \\ \alpha = 1 - m_\star \displaystyle\int_{\mathbf{R}^3} f \,\mathrm{d}v \\ m_\star\boldsymbol{\Gamma} = -m_\star\nabla_x p(\varrho) - D_\star(\boldsymbol{v}-\boldsymbol{u}). \end{cases} \tag{1.11}$$

1.1.3.3 Preliminary remarks

Like for most systems describing complex flows, we verify that fundamental conservation properties hold. First, the mass of each phase is preserved since one has

$$\partial_t(\alpha\varrho) + \nabla_x\cdot(\alpha\varrho\boldsymbol{u}) = 0, \quad \partial_t f + \nabla_x\cdot(\boldsymbol{v} f) + \nabla_v\cdot(\boldsymbol{\Gamma} f) = 0.$$

By multiplying the Vlasov equation by $m_\star\boldsymbol{v}$ and integrating with respect to $\boldsymbol{v}$, one obtains the momentum equations for the dispersed phase.

$$\partial_t\left(m_\star\int_{\mathbf{R}^3}\boldsymbol{v} f\,\mathrm{d}v\right) + \nabla_x\cdot\left(\int_{\mathbf{R}^3}\boldsymbol{v}\otimes\boldsymbol{v} f\,\mathrm{d}v\right) = m_\star\int_{\mathbf{R}^3}\boldsymbol{\Gamma} f\,\mathrm{d}v.$$

Then, by adding this equation to the balance equation for the momentum of the fluid, one obtains that the total momentum is preserved

$$\partial_t\left(\alpha\varrho\boldsymbol{u} + m_\star\int_{\mathbf{R}^3} f\boldsymbol{v}\,\mathrm{d}v\right) + \nabla_x\cdot\left(\alpha\varrho\boldsymbol{u}\otimes\boldsymbol{u} + m_\star\int_{\mathbf{R}^3} f\boldsymbol{v}\otimes\boldsymbol{v}\,\mathrm{d}v\right) + \nabla_x p = 0.$$

Multiplying by $\boldsymbol{u}$ the momentum balance law of the fluid, one obtains the balance law for the kinetic energy of the fluid

$$\partial_t\left(\alpha\varrho\frac{|\boldsymbol{u}|^2}{2}\right) + \nabla_x\cdot\left(\alpha\varrho\frac{|\boldsymbol{u}|^2}{2}\boldsymbol{u}\right) + \alpha\boldsymbol{u}\cdot\nabla_x p = D_\star\boldsymbol{u}\cdot\int_{\mathbf{R}^3}(\boldsymbol{v}-\boldsymbol{u}) f\,\mathrm{d}v. \tag{1.12}$$

Then, the balance law for the kinetic energy of the particles writes

$$\partial_t\left(m_\star\int_{\mathbf{R}^3}\frac{|\boldsymbol{v}|^2}{2} f\,\mathrm{d}v\right) + \nabla_x\cdot\left(m_\star\int_{\mathbf{R}^3}\frac{|\boldsymbol{v}|^2}{2}\boldsymbol{v} f\,\mathrm{d}v\right) = \int_{\mathbf{R}^3} m_\star\boldsymbol{v}\cdot\boldsymbol{\Gamma} f\,\mathrm{d}v$$

Then, one sees that the total energy is preserved

$$\partial_t \left(\alpha \varrho E + m_\star \int_{\mathbf{R}^3} f \frac{|\boldsymbol{v}|^2}{2} \, \mathrm{d}v \right) + \nabla_x \cdot \left(\alpha \varrho \boldsymbol{u} E + m_\star \int_{\mathbf{R}^3} f \boldsymbol{v} \frac{|\boldsymbol{v}|^2}{2} \, \mathrm{d}v + \alpha \boldsymbol{u} p + m_\star p \int_{\mathbf{R}^3} f \boldsymbol{v} \, \mathrm{d}v \right) = 0.$$

where $E = e + \frac{|\boldsymbol{u}|^2}{2}$ is the total energy of the fluid.

1.2 Construction of solutions

In this section we introduce the content of the Chapter 2. It is dedicated to the local in time well-posedness for strong solutions of a modified thick spray model, where the terms specific to thick spray are regularized by mean of a convolution with a kernel of bounded variation.

1.2.1 Mathematical difficulties for thick spray

The mathematical study of (1.9) is still in its very early stages. For instance, no local Cauchy theory has been established for this system. In the case $\nu > 0$, meaning diffusion is reintroduced into the fluid phase, a significant advancement in the understanding of thick spray equations has been made by Ertzbichoff and Han-Kwan in [53], where they proved the existence and uniqueness of local-in-time strong solutions with high Sobolev regularity. As explained in [53], standard energy estimates seem to result in a loss of several derivatives, which make this system a singular coupling between the kinetic phase and the fluid phase. For the case without viscosity $\nu = 0$, Baranger and Desvillettes [12] conjectured that the system (1.11) might be ill-posed, by analogy with the corresponding two-fluid model [46]. Additionally, constructing global weak solutions for (1.11) seems to be a difficult problem. Standard frameworks [3] require that the gradient of the pressure $\nabla_x p(t)$ be at least in $W^{1,1}_x$ or in BV_x, which is unlikely. As a nonlinear system of conservation law, the fluid part of (1.9) is expected to generate discontinuous solutions (shock waves) in finite time. In particular, $p(t)$ is expected to belong at most to BV_x in the presence of shock waves in the fluid.

There seems to be a need for a system that accurately describes thick sprays while offering improved mathematical properties. To meet this need, we propose a new system that is locally well-posed in time and preserves key conservation properties. The main idea is to reintroduce the radius of the particle in the system and to regularize the terms in (1.11) which are specific to thick sprays.

1.2.2 Heuristics for a regularization of the thick spray model

Consider a single spherical particle with radius $r_p > 0$ located at the coordinate $\boldsymbol{x}_\star$. In the surrounding gas characterized by a pressure field p. If we neglect the friction, the gas exerts a force on the particle given by

$$F = -\int_{\mathbf{S}^2(\boldsymbol{x}_\star, r_p)} p \boldsymbol{n} \, \mathrm{d}x.$$

Assuming that the pressure is differentiable in the particle, one obtains using Stokes's theorem

$$F = -\int_{\mathbf{S}^3(\boldsymbol{x}_\star, r_p)} \nabla_x p(\boldsymbol{x}) \, \mathrm{d}x = -m_\star \int_{\mathbf{R}^3} w(\boldsymbol{x} - \boldsymbol{x}_\star) \nabla_x p(\boldsymbol{x}) \, \mathrm{d}x = m_\star (w \star \nabla_x p)(\boldsymbol{x}_\star),$$

where the convolution kernel is

$$w(\boldsymbol{y}) = \frac{1}{m_\star}\mathbf{1}_{|y|<r}(\boldsymbol{y}).$$

Using the notation $\langle\cdot\rangle = w \star \cdot$ for the convolution operator, the force is rewritten as

$$m_\star \boldsymbol{\Gamma} = -m_\star \langle \nabla_x p\rangle.$$

It seems then to be natural to replace the term $\nabla_x p \cdot \nabla_v f$ in the Vlasov equation by $\langle \nabla_x p\rangle \cdot \nabla_v f$, and obtain

$$\partial_t f + \boldsymbol{v}\cdot\nabla_x f - \langle\nabla_x p\rangle\cdot\nabla_v f = 0. \tag{1.13}$$

However, it seems that if we only modify this term, we lose the conservation of total momentum and total energy. Indeed, because of this modificaiton, the total momentum equation is also modified and one has

$$\partial_t \int_{\mathbf{R}^3}\left(\alpha\varrho\boldsymbol{u} + m_\star\int_{\mathbf{R}^3} f\boldsymbol{v}\,\mathrm{d}v\right)\mathrm{d}x = m_\star\int_{\mathbf{R}^3}\left(\nabla_x p\int_{\mathbf{R}^3} f\,\mathrm{d}v - \langle\nabla_x p\rangle\int_{\mathbf{R}^3} f\,\mathrm{d}v\right)\mathrm{d}x. \tag{1.14}$$

The right hand side is a priori non zero, so the total momentum is not conserved. It appears then that the regularisation of the pressure in the Vlasov equation requires that we also modify some terms in the fluid equations to recover conservation of important physical quantities.

At this point, there are multiple choices that lead to the conservation of thoses quantities.

For instance, a possible choice to recover the conservation of total momentum, is to modify the right hand side of the second equation of (1.11) and regularise the gradient of the pressure $\nabla_x p$ on the right hand side

$$\partial_t(\alpha\varrho\boldsymbol{u}) + \nabla_x\cdot(\alpha\varrho\boldsymbol{u}\otimes\boldsymbol{u}) + \nabla_x p = m_\star\langle\nabla_x p\rangle\int_{\mathbf{R}^3} f\,\mathrm{d}v + D_\star\int_{\mathbf{R}^3}(\boldsymbol{v}-\boldsymbol{u})f\,\mathrm{d}v,$$

and we obtain the conservation of the total momentum. However, because we have

$$\langle\nabla_x p\rangle\int_{\mathbf{R}^3} f\,\mathrm{d}v = (1-\alpha)\langle\nabla_x p\rangle$$

we are then not able to write the balance law like in (1.10), which implies that we lose the relation (1.12) and we lose the total conservation of energy.

A simpler choice, that leads to the conservation of both the total momentum and the total energy, is to regularise the volume fraction α and to writes

$$\alpha = 1 - m_\star\int_{\mathbf{R}^3}\langle f\rangle\,\mathrm{d}v.$$

By doing so, one recovers immediatly the relations of the Subsection 1.1.3.3. For the sake of simplicity, this is the choice that we have made. In retrospective, it is also the choice that seems the wisest consedering the loss of regularity of the system (1.11), which is due to the presence of the volume fraction term in the fluid equations, and to the gradient of the pressure in the Vlasov equation.

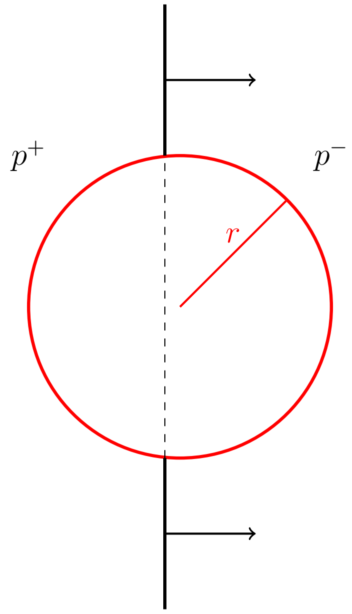

Fig. 1.1: Shock wave passing through a particle.

The last step is to reintroduce the friction in the system, which is done without modification as those terms do not imply any added difficulty.

In the end, we propose the following thick spray model with regularisation

$$\begin{cases} \partial_t(\alpha\varrho) + \nabla_x \cdot (\alpha\varrho\boldsymbol{u}) = 0 \\ \partial_t(\alpha\varrho\boldsymbol{u}) + \nabla_x \cdot (\alpha\varrho\boldsymbol{u} \otimes \boldsymbol{u}) + \nabla_x p = m_\star \nabla_x p \int_{\mathbf{R}^3} \langle f \rangle \,\mathrm{d}v + D_\star \int_{\mathbf{R}^3} (\boldsymbol{v} - \boldsymbol{u}) f \,\mathrm{d}v \\ \partial_t f + \boldsymbol{v} \cdot \nabla_x f + \nabla_v \cdot (\boldsymbol{\Gamma} f) = 0 \\ \alpha = 1 - m_\star \int_{\mathbf{R}^3} \langle f \rangle \,\mathrm{d}v \\ m_\star \boldsymbol{\Gamma} = -m_\star \langle \nabla_x p \rangle - D_\star (\boldsymbol{v} - \boldsymbol{u}). \end{cases} \tag{1.15}$$

We will show that the presence of this convolution, with a kernel $\omega \in \mathrm{BV}$ is sufficient to obtain the local-in-time well posedness of smooth solutions. Extension to the full Euler system is straightforward as it does not require any modification.

1.2.3 Local in time well-posedness for an averaged thick spray model.

The main result of Chapter 2 is the local in time well-posedness for the regularized thick spray model (1.15) in the class of Sobolev initial data.

Theorem 1.2.1. *Let $\Omega = (0, +\infty) \times \mathbf{R}^3$, $s \in \mathbf{N}$ such that $s > 3/2 + 1$ and Ω_1, Ω_2 two open sets of Ω such that $\overline{\Omega}_1 \subset \Omega_2$ and Ω_1 and Ω_2 are relatively compact in Ω. Let $(\varrho_0, \varrho_0\boldsymbol{u}_0) : \mathbf{R}^3 \to \Omega_1$ satisfying $\varrho_0 - 1 \in H^s(\mathbf{R}^3)$ and $\boldsymbol{u}_0 \in H^s(\mathbf{R}^3)$. Let $f_0 : \mathbf{R}^3 \times \mathbf{R}^3 \to \mathbf{R}_+$ be a function in $\mathscr{C}_c^1(\mathbf{R}^3 \times \mathbf{R}^3) \cap H^s(\mathbf{R}^3 \times \mathbf{R}^3)$ satisfying*

$$\|f_0\|_{L^\infty} < \frac{1}{2^4 \|w\|_{L^1} V_M(0)^3}.$$

with $V_M(0) = \sup_{(\boldsymbol{x},\boldsymbol{v})\in\mathbf{R}^3\times\mathbf{R}^3, f_0(\boldsymbol{x},\boldsymbol{v})>0} |\boldsymbol{v}|$.

Then, one can find $T \in (0,1)$ *such that there exists a solution* $(\varrho, \varrho\boldsymbol{u}, f)$ *of the system* (1.15) *belonging to* $\mathscr{C}^1([0,T]\times\mathbf{R}^3,\Omega_2)\times\mathscr{C}^1_c([0,T]\times\mathbf{R}^3\times\mathbf{R}^3,\mathbf{R}_+)$. *Moreover, this solution is unique and it satisfies*

$$C \le \alpha(t,\boldsymbol{x}) \le 1, \quad t\in[0,T], \quad \boldsymbol{x}\in\mathbf{R}^3.$$

The initial bound on f_0, which is propagated for small time, ensures that the volume fraction stays positive. The strategy of the proof is to follow the ideas of Baranger, Desvillettes [12] and Mathiaud [92] and to invoke the general theory of symmetrisable hyperbolic systems of conservation laws(see the book of Majda [87]), by treating the terms that lose derivatives in the original system (1.9) as terms of order 0. Let us notice that the time of existence in Theorem 2.1.5 depends on the radius of the particles $r_p > 0$ and it is not possible to use this strategy to construct classical solutions for the original system (1.9) by taking the limit $r_p \to 0$.

1.2.3.1 Strategy of the proof.

Let us detail briefly the strategy and main steps of the proof of Theorem 2.1.5. First, it is sufficient to only consider the system without friction. After normalizing the constants to 1, it writes

$$\begin{cases} \partial_t(\alpha\varrho) + \nabla_x\cdot(\alpha\varrho\boldsymbol{u}) = 0 \\ \partial_t(\alpha\varrho\boldsymbol{u}) + \nabla_x\cdot(\alpha\varrho\boldsymbol{u}\otimes\boldsymbol{u}) + \nabla_x p = \nabla_x p\displaystyle\int_{\mathbf{R}^3}\langle f\rangle\,\mathrm{d}v \\ \partial_t f + \boldsymbol{v}\cdot\nabla_x f - \langle\nabla_x p\rangle\cdot\nabla_v f = 0 \\ \alpha = 1 - \displaystyle\int_{\mathbf{R}^3}\langle f\rangle\,\mathrm{d}v \\ p = p(\varrho) = \varrho^\gamma. \end{cases} \tag{1.16}$$

The idea is then to adapt the strategy developed by Baranger and Desvillettes [12] (see also the work of Mathiaud [92]) based on the theory of local-in-time solutions for a symmetrisable hyperbolic system of conservation laws.

We explain now the main steps of this strategy.

The principle of the method is to combine the theory of hyperbolic symmetrisable system of conservation laws (see for instance the book of Majda [87]) for the fluid part, and the characteristics method with the control of the support of the phase space distribution f for the Vlasov equation [102].

The first step of such strategies is to symmetrise the fluid part of the system. However, because of the presence of the volume fraction α, The fluid part of (1.16) is not trivial to symmetrize. The idea is to expand the derivative on the left-hand-side of the fluid part, and to treat the terms containing derivatives of α as source term. Let us remark immediatly that such a strategy cannot work for the original system (1.9) because of the loss of regularity mentioned earlier. However, the convolution kernel, despite being only in BV, allows us to compensate the lost derivatives and to construct local in time classical solutions for (1.16). We want to emphasize that this gives a time of existence that depends of the radius of the particles $r_p > 0$, and this does not allow us to construct solutions to (1.9) by taking the limit $r_p \to 0$ because the bounds we obtain during the proof degenerate. We also note that using the same strategy for the thick spray model without regularisation (1.11) will not work because of the mentionned loss of regularity.

1.3 Analog of Landau damping in thick sprays

In this section, we present the results of Chapter 3. In 1946, Landau shocked the physics community by predicting that collisionless electrostatic plasmas can exhibit wave damping. Landau formally solved the linearized equations by means of Fourier and Laplace transforms, and after a study of singularities in the complex planes, concluded that the electric field must decay exponentially fast (see the original paper of Landau [81]. Today, Landau damping is considered as a cornerstone of plasma physics [26, 107, 113]. The mathematically rigourous theory of the linear Landau damping was pioneered by Backus [8] and Penrose [99]. It was latter analyzed in depth by many mathematicians [40, 89]. We refer to the work of Mouhot and Villani [96] and the references therein for a review of Landau damping.

In Chapter 3, we show that the structure of the linearized thick spray model around an homogeneous (in x) "one bump" equilibrium is reminiscent of the structure of the linearized (around a suitable equilibrium) of the Vlasov-Poisson equations (1.5). In particular, we show that the linearized equations exhibits an analog of Linear Landau damping. This effect will be illustrated by numerical simulations. Nonlinear Landau damping [16, 96], however, is beyond the scope of this work and will not be addressed.

1.3.1 Linearization of thick spray equations

We explain how we linearize the thick spray model (1.11), following [27]. The first is to determine an equilibrium of the system. We start from the initial condition

$$\begin{cases} \varrho(0,\boldsymbol{x}) = \varrho_0, \\ \boldsymbol{u}(0,\boldsymbol{x}) = 0, \\ f(0,\boldsymbol{x},\boldsymbol{v}) = f_0(t,\boldsymbol{v}) := n_0 F\left(\frac{|\boldsymbol{v}|^2}{2}\right). \end{cases} \tag{1.17}$$

Where $\varrho_0 > 0$, $n_0 > 0$, $d_\star = D_\star/m_\star$ and $F : \mathbf{R}_+ \to \mathbf{R}_+$ is a smooth strictly decreasing function $F' < 0$. The case of a Maxwellian corresponds to $F(w) = e^{-w}$. Then, a solution of the system (1.11) writes, for $t > 0$

$$\begin{cases} \varrho(t,\boldsymbol{x}) = \varrho_0, \\ \boldsymbol{u}(t,\boldsymbol{x}) = 0, \\ f(t,\boldsymbol{x},\boldsymbol{v}) = e^{3d_\star t} n_0 F\left(\frac{e^{2d_\star t}|\boldsymbol{v}|^2}{2}\right). \end{cases} \tag{1.18}$$

We then linearize the thick spray model (1.11) around the equilibrium (1.18)

$$\begin{aligned} \varrho(t,\boldsymbol{x}) &= \varrho_0 + \varepsilon \varrho_1(t,\boldsymbol{x}) + O(\varepsilon^2), \\ \boldsymbol{u}(t,\boldsymbol{x}) &= \varepsilon \boldsymbol{u}_1(t,\boldsymbol{x}) + O(\varepsilon^2), \\ f(t,\boldsymbol{x},\boldsymbol{v}) &= f_0(t,\boldsymbol{v}) + \varepsilon \sqrt{f_0(t,\boldsymbol{v})} f_1(t,\boldsymbol{x},\boldsymbol{v}) + O(\varepsilon^2). \end{aligned}$$

Notice the scaling by $\sqrt{f_0(t,v)}$, it is not necessary for the linearization, however it will be useful after. We also introduce the linearization of the volume fraction $\alpha(t,x) = \alpha_0 + \varepsilon\alpha_1(t,\boldsymbol{x}) + O(\varepsilon)$. The linearization of the fluid mass equation writes

$$\alpha_0\partial_t\varrho_1 + \varrho_0\partial_t\alpha_1 + \alpha_0\varrho_0\nabla_x \cdot \boldsymbol{u}_1 = 0.$$

It is then natural to introduce the linearized specific volume $\tau_1 = -\varrho_1/\varrho_0^2$. Then the linearization of the fluid mass equation writes

$$\begin{aligned}
\alpha_0\varrho_0\partial_t\tau_1 &= \alpha_0\nabla_x \cdot \boldsymbol{u}_1 + \partial_t\alpha_1 \\
&= \alpha_0\nabla_x \cdot \boldsymbol{u}_1 - m_\star\partial_t\left(\int_{\mathbf{R}^3}\sqrt{f_0}e^{d_\star t}f_1\,\mathrm{d}v\right) \\
&= \alpha_0\nabla_x \cdot \boldsymbol{u}_1 + m_\star\nabla_x \cdot \left(\int_{\mathbf{R}^3}\sqrt{f_0}e^{d_\star t}f_1\boldsymbol{v}\,\mathrm{d}v\right).
\end{aligned}$$

Where we used the linearization of the mass conservation of the dispersed phase

$$\partial_t\left(m_\star\int_{\mathbf{R}^3}\sqrt{f_0}e^{d_\star t}f_1\,\mathrm{d}v\right) + \nabla_x \cdot \left(m_\star\int_{\mathbf{R}^3}\sqrt{f_0}e^{d_\star t}f_1\boldsymbol{v}\,\mathrm{d}v\right) = 0.$$

Defining the speed of sound $c_0 = \sqrt{p'(\varrho_0)}$, one has

$$p(\varrho) = p(\varrho_0 + \varepsilon\varrho_1 + O(\varepsilon^2)) = p(\varrho_0) + \varepsilon\varrho_1 p'(\varrho_0) + O(\varepsilon^2)$$

and $\varrho_1 p'(\varrho_0) = -\varrho_0^2c_0^2\tau_1$ and the linearization of the momentum equation can be written under the form

$$\alpha_0\varrho_0\partial_t\boldsymbol{u}_1 = \alpha_0\varrho_0^2c_0^2\nabla_x\tau_1 + m_\star d_\star\int_{\mathbf{R}^3}\boldsymbol{v}\sqrt{f_0}e^{d_\star t}f_1\,\mathrm{d}v - m_\star d_\star\boldsymbol{u}_1\int_{\mathbf{R}^3}f_0\,\mathrm{d}v.$$

We now turn to the linearisation of the Vlasov equation. One has

$$\begin{aligned}
\sqrt{f_0(t,\boldsymbol{v})}e^{d_\star t}\partial_t f_1 + f_1\partial_t(\sqrt{f_0(t,\boldsymbol{v})}e^{d_\star t}) &+ \sqrt{f_0(t,\boldsymbol{v})}e^{d_\star t}\boldsymbol{v}\cdot\nabla_x f_1 \\
&+ \nabla_v \cdot \left(\boldsymbol{\Gamma}_0\sqrt{f_0(t,\boldsymbol{v})}e^{d_\star t}f_1 + \boldsymbol{\Gamma}_1 f_0(t,\boldsymbol{v})\right) = 0,
\end{aligned}$$

where $\boldsymbol{\Gamma}_0 = -d_\star\boldsymbol{v}$ and $\boldsymbol{\Gamma}_1 = -\nabla_x(p'(\varrho_0)\varrho_1) + d_\star\boldsymbol{u}_1 = \varrho_0^2c_0^2\nabla\tau_1 + d_\star\boldsymbol{u}_1$. So

$$\begin{aligned}
&\partial_t f_1 + \boldsymbol{v}\cdot\nabla_x f_1 + (\sqrt{f_0(t,\boldsymbol{v})}e^{d_\star t})^{-1}\left(\varrho_0^2c_0^2\nabla\tau_1\cdot\nabla_v f_0\right) \\
&\quad = (\sqrt{f_0(t,\boldsymbol{v})}e^{d_\star t})^{-1}\left[-f_1\partial_t(\sqrt{f_0(t,\boldsymbol{v})}e^{d_\star t}) - \nabla_v\cdot\left(\boldsymbol{\Gamma}_0\sqrt{f_0(t,\boldsymbol{v})}e^{d_\star t}f_1\right) - d_\star\boldsymbol{u}_1\cdot\nabla_v f_0(t,\boldsymbol{v})\right].
\end{aligned}$$

One has the following formula for f_0

$$\nabla_v f_0(t,|\boldsymbol{v}|) = -\boldsymbol{v}e^{2d_\star t}\left(-\frac{F'}{F}\right)\left(\frac{e^{2d_\star t}|\boldsymbol{v}|^2}{2}\right)f_0(t,\boldsymbol{v}),$$

which yields the identity

$$(\sqrt{f_0(t,\boldsymbol{v})}e^{d_\star t})^{-1}\nabla_v f_0(t,\boldsymbol{v}) = -\boldsymbol{v}\sqrt{f_0(t,\boldsymbol{v})}e^{d_\star t}\left(-\frac{F'}{F}\right)\left(\frac{e^{2d_\star t}|\boldsymbol{v}|^2}{2}\right). \tag{1.19}$$

One gets

$$\begin{aligned}
&\partial_t f_1 + \boldsymbol{v}\cdot\nabla_x f_1 - \varrho_0^2 c_0^2 \sqrt{f_0(t,\boldsymbol{v})} e^{d_\star t} \boldsymbol{v}\cdot\nabla\tau_1 \left(-\frac{F'}{F}\right)\left(\frac{e^{2d_\star t}|\boldsymbol{v}|^2}{2}\right)\\
&\qquad = d_\star \sqrt{f_0(t,\boldsymbol{v})} e^{d_\star t} \boldsymbol{v}\cdot\boldsymbol{u}_1 \left(-\frac{F'}{F}\right)\left(\frac{e^{2d_\star t}|\boldsymbol{v}|^2}{2}\right)\\
&\qquad\quad - (\sqrt{f_0(t,\boldsymbol{v})} e^{d_\star t})^{-1}\left[f_1\partial_t(\sqrt{f_0(t,\boldsymbol{v})} e^{d_\star t}) + \nabla_v\cdot\left(\boldsymbol{\Gamma}_0\sqrt{f_0(t,\boldsymbol{v})} e^{d_\star t} f_1\right)\right].
\end{aligned}$$

The opposite of the last term in the right-hand side is

$$\begin{aligned}
&(\sqrt{f_0(t,\boldsymbol{v})} e^{d_\star t})^{-1}\left[f_1\partial_t(\sqrt{f_0(t,\boldsymbol{v})} e^{d_\star t}) + \nabla_v\cdot\left(\boldsymbol{\Gamma}_0\sqrt{f_0(t,\boldsymbol{v})} e^{d_\star t} f_1\right)\right]\\
&\qquad = (\sqrt{f_0(t,\boldsymbol{v})} e^{d_\star t})^{-1}\left[\partial_t(\sqrt{f_0(t,\boldsymbol{v})} e^{d_\star t}) + \nabla_v\cdot\left(\boldsymbol{\Gamma}_0\sqrt{f_0(t,\boldsymbol{v})} e^{d_\star t}\right)\right] f_1\\
&\qquad\quad + \boldsymbol{\Gamma}_0\cdot\nabla_v f_1\\
&\qquad = (\sqrt{f_0(t,\boldsymbol{v})} e^{d_\star t})^{-1}\left[\partial_t(\sqrt{f_0(t,\boldsymbol{v})} e^{d_\star t}) + \nabla_v\cdot\left(\boldsymbol{\Gamma}_0\sqrt{f_0(t,\boldsymbol{v})} e^{d_\star t}\right)\right] f_1\\
&\qquad\quad - \frac{1}{2}\left[\nabla_v\cdot\boldsymbol{\Gamma}_0\right](\sqrt{f_0(t,\boldsymbol{v})} e^{d_\star t}) f_1 + \frac{1}{f_1}\nabla_v\cdot\left(\frac{1}{2}\boldsymbol{\Gamma}_0 f_1^2\right).
\end{aligned}$$

The term in front of f_1 is

$$\begin{aligned}
&(\sqrt{f_0(t,\boldsymbol{v})} e^{d_\star t})^{-1}\left[\partial_t(\sqrt{f_0(t,\boldsymbol{v})} e^{d_\star t}) + \nabla_v\cdot\left(\boldsymbol{\Gamma}_0\sqrt{f_0(t,\boldsymbol{v})} e^{d_\star t}\right) - \frac{1}{2}\left[\nabla_v\cdot\boldsymbol{\Gamma}_0\right](\sqrt{f_0(t,\boldsymbol{v})} e^{d_\star t})\right]\\
&\qquad = (\sqrt{f_0(t,\boldsymbol{v})})^{-1}\left[\partial_t\sqrt{f_0(t,\boldsymbol{v})} + \boldsymbol{\Gamma}_0\cdot\nabla_v\sqrt{f_0(t,\boldsymbol{v})}\right] + \left(d_\star + \frac{1}{2}\nabla_v\cdot\boldsymbol{\Gamma}_0\right)\\
&\qquad = (2f_0(t,\boldsymbol{v}))^{-1}\left[\partial_t f_0(t,\boldsymbol{v}) + \boldsymbol{\Gamma}_0\cdot\nabla_v f_0(t,\boldsymbol{v})\right] + \left(d_\star + \frac{1}{2}\nabla_v\cdot\boldsymbol{\Gamma}_0\right)\\
&\qquad = -\frac{1}{2}\nabla_v\cdot\boldsymbol{\Gamma}_0 + \left(d_\star + \frac{1}{2}\nabla_v\cdot\boldsymbol{\Gamma}_0\right) = d_\star.
\end{aligned}$$

because f_0 satisfies

$$\partial_t f_0(t,\boldsymbol{v}) + \boldsymbol{\Gamma}_0\cdot\nabla_v f_0(t,\boldsymbol{v}) + f_0(t,\boldsymbol{v})\boldsymbol{\Gamma}_0 = 0.$$

One gets

$$\begin{aligned}
&\partial_t f_1 + \boldsymbol{v}\cdot\nabla_x f_1 - \varrho_0^2 c_0^2 \sqrt{f_0(t,\boldsymbol{v})} e^{d_\star t} \boldsymbol{v}\cdot\nabla\tau_1 \left(-\frac{F'}{F}\right)\left(\frac{e^{2d_\star t}|\boldsymbol{v}|^2}{2}\right)\\
&\qquad = d_\star \sqrt{f_0(t,\boldsymbol{v})} e^{d_\star t} \boldsymbol{v}\cdot\boldsymbol{u}_1 \left(-\frac{F'}{F}\right)\left(\frac{e^{2d_\star t}|\boldsymbol{v}|^2}{2}\right) - d_\star f_1 - \frac{1}{f_1}\nabla_v\cdot\left(\frac{1}{2}\boldsymbol{\Gamma}_0 f_1^2\right).
\end{aligned}$$

In the end, one obtains the linearized thick spray equations

$$\begin{cases}\alpha_0\varrho_0\partial_t\tau_1 = \alpha_0\nabla_x\cdot\boldsymbol{u}_1 + m_\star\nabla_x\cdot\int_{\mathbf{R}^3}\sqrt{f_0}e^{d_\star t}f_1\boldsymbol{v}\,\mathrm{d}v\\ \alpha_0\varrho_0\partial_t\boldsymbol{u}_1 = \alpha_0\varrho_0c_0^2\nabla_x\tau_1 + m_\star d_\star\int_{\mathbf{R}^3}\boldsymbol{v}\sqrt{f_0}e^{d_\star t}f_1\,\mathrm{d}v - m_\star d_\star\boldsymbol{u}_1\int_{\mathbf{R}^3}f_0\,\mathrm{d}v\\ \partial_t f_1 + \boldsymbol{v}\cdot\nabla_x f_1 - \varrho_0^2c_0^2\sqrt{f_0}e^{d_\star t}\boldsymbol{v}\cdot\nabla_x\tau_1\left(-\frac{F'}{F}\right)\left(\frac{e^{2d_\star t}|\boldsymbol{v}|^2}{2}\right)\\ = d_\star\sqrt{f_0}e^{d_\star t}\boldsymbol{v}\cdot\boldsymbol{u}_1\left(-\frac{F'}{F}\right)\left(\frac{e^{2d_\star t}|\boldsymbol{v}|^2}{2}\right) - d_\star g_1 + \frac{d_\star}{g_1}\nabla_v\cdot\left(\frac{1}{2}\boldsymbol{v}g_1^2\right).\end{cases} \tag{1.20}$$

The main goal of Chapter 3 is to prove that in the case with no friction, $D_\star = 0$, one has a linear damping result in the same fashion as the Landau damping of Vlasov-Poisson equations. Our approach is to use the framework of spectral theory [79, 84].

1.3.2 Parallel between the thick spray model and Vlasov-Poisson equations

In Chapter 2, our strategy is based on a recent study of the linear Vlasov-Ampère equation using the point of view of abstract scattering theory. (see [43, 44]).

Consider the linearized Vlasov-Poisson equation for one species of negatively charged particle (electrons) in a plasma.

$$\begin{cases}\dfrac{\partial f}{\partial t} + v\partial_x f + \partial_x\phi f_0'(v) = 0,\\ \partial_x^2\phi = \displaystyle\int_{\mathbf{R}^3} f\,\mathrm{d}v.\end{cases} \tag{1.21}$$

- The spectral properties of the Vlasov-Poisson equation have been studied by Degond in [40]. The main result is that the electric potential ϕ admits an asymptotic expansion of the form
$$\phi(t,x) = \sum_{s=1}^{S} c_s e^{\lambda_s t + i n_s x} + O(e^{rt}), \quad r < \min_{1\le s\le S}\Re\lambda_s.$$
The main tools used are the Dunford formula and an analytic continuation of the resolvent. The λ_s are then no longer eigenvalues of the linearized Vlasov-Poisson operator.

- Another approach done by Després in [43, 44] is to rewrite the linearized Vlasov-Poisson equation (1.21) as a linear Vlasov-Ampère equation. Indeed, one has the identity
$$\partial_x(\partial_t E - \int_{\mathbf{R}^3} fv\,\mathrm{d}v) = \partial_t\partial_x E - \partial_x\int_{\mathbf{R}^3} fv\,\mathrm{d}v = -\partial_t\int_{\mathbf{R}^3} f\,\mathrm{d}v - \partial_x\int_{\mathbf{R}^3} fv\,\mathrm{d}v = 0$$
So one can write the Ampère law under the form
$$\partial_t E = 1^\star\int_{\mathbf{R}^3} fv\,\mathrm{d}v$$
where $1^\star = L^2(\mathbf{T}) \to L_0^2(\mathbf{T})$ is the projection operator
$$1^\star g = g - \int_{\mathbf{T}} g(x)\,\mathrm{d}x.$$

Then, the linearized Vlasov-Poisson equations (1.21) are equivalent to the linearized Vlasov-Ampère equations

$$\begin{cases} \partial_t f + v\partial_x f - E f_0'(v) = 0, \\ \partial_t E = 1^\star \int_{\mathbf{R}^3} f v \, \mathrm{d}v \end{cases} \tag{1.22}$$

The main result is that the linearized operator associated to (1.22) is self-adjoint, and a careful study of the spectrum of this operator yields linear Landau damping. This approach has the advantage that it is capable to also deal with the inhomogeneous (in x) case.

1.3.3 Linear damping in thick sprays

For simplicity, we present the results in 1D, but our result is true in any dimension $d \in \mathbf{N}^*$. Setting a null friction $D_\star = 0$ and normalizing the other coefficients, the linearized equations (1.20) write

$$\begin{cases} \partial_t \tau_1 = \partial_x u_1 + \partial_x \int_{\mathbf{R}} \sqrt{f_0} f_1 v \, \mathrm{d}v \\ \partial_t u_1 = \partial_x \tau_1 \\ \partial_t f_1 + v\partial_x f_1 - \sqrt{f_0} v \partial_x \tau_1 \left(-\frac{F'}{F}\right)\left(\frac{|v|^2}{2}\right) = 0. \end{cases} \tag{1.23}$$

Then we rewrite the system (1.23) in the framework of spectral theory

$$\partial_t \mathbf{U}(t) = iH\mathbf{U} \tag{1.24}$$

where $\mathbf{U} = (\tau, u, f)$ and H is an operator formally defined by

$$iH = \begin{pmatrix} 0 & \partial_x & \partial_x \int_{\mathbf{R}} v\sqrt{f^0(v)} \cdot \mathrm{d}v \\ \partial_x & 0 & 0 \\ v\sqrt{f^0(v)}\left(-\frac{F'}{F}\right)\partial_x & 0 & -v\partial_x \end{pmatrix}.$$

Denote

$$L^2_0(\mathbf{T}) = \left\{ u \in L^2(\mathbf{T}), \quad \int_{\mathbf{T}} u \, \mathrm{d}x = 0 \right\},$$

and let $X = L^2_0(\mathbf{T}) \times L^2_0(\mathbf{T}) \times L^2_0(\mathbf{T} \times \mathbf{R})$ be equipped with the natural scalar product of L^2. If the equilibrium profile for the particles is a Maxwellian $f_0(v) = e^{-v^2/2}$, the operator H rewrites as a symmetric operator in X

$$iH = \begin{pmatrix} 0 & \partial_x & \partial_x \int_{\mathbf{R}} v\sqrt{f^0(v)} \cdot \mathrm{d}v \\ \partial_x & 0 & 0 \\ v\sqrt{f^0(v)}\partial_x & 0 & -v\partial_x \end{pmatrix}. \tag{1.25}$$

We now write the main result of Chapter 3:

Theorem 1.3.1. *If $f_0(v) = e^{-v^2/2}$, then the operator H restricted to $X := L^2_0(\mathbf{T}) \times L^2_0(\mathbf{T}) \times L^2_0(\mathbf{T} \times \mathbf{R})$ with domain $D[H] = \{\mathbf{U} \in X, \quad H\mathbf{U} \in X\}$ is self-adjoint and one has the decomposition*

$$X = X^{\mathrm{ac}}.$$

As a consequence, a solution $(\tau(t,\cdot),u(t,\cdot),f(t,\cdot,\cdot))$ of (1.24) weakly converges in X to 0 as $t \to \infty$. One also has convergence of the acoustic energy $\|\tau(t)\|^2_{L^2} + \|\boldsymbol{u}(t)\|^2_{L^2}$ to 0 as $t \to +\infty$.

1.3.4 Strategy of the proof

We present here the general idea of the proof of Theorem 1.3.1.

The first step is to show that the operator H restricted to $X := L^2_0(\mathbf{T}) \times L^2_0(\mathbf{T}) \times L^2_0(\mathbf{T} \times \mathbf{R})$ with domain $D[H] = \{\mathbf{U} \in X, \quad H\mathbf{U} \in X\}$ is self-adjoint. At this point, one can apply the full arsernal of scattering theory for self-adjoint operators. A general result from scattering theory [14,78,84,106,119] states that a self-adjoint operator induces an orthogonal decomposition of the Hilbert space on which it acts in terms of measure theory. The decomposition reads

$$X = X^{\mathrm{ac}} \oplus X^{\mathrm{sc}} \oplus X^{\mathrm{pp}}.$$

The "pure point" subspace X^{pp} corresponds to the subset of the spectrum made of the eigenvalues of H, and is spanned by the classical eigenvectors

$$X^{\mathrm{pp}} = \mathrm{Span}\{\varphi \in X,\ H\varphi = \lambda\varphi \text{ for some } \lambda \in \mathbf{R}\}.$$

The "absolutely continuous" subspace X^{ac} corresponds to the so-called pseudo eigenvectors. A usefull characterisation of this space that was proved by Gustafson and Johnson [71] reads

$$X^{\mathrm{ac}} = \overline{\left\{\varphi \in X,\ \|(H - \lambda - i\varepsilon)\,\varphi\|_X = O\left(\frac{1}{\varepsilon}\right)\right\}}. \tag{1.26}$$

Finally the subspace X^{sc} corresponds to the "singular continuous part" of the spectrum. In most operators coming from the physics, one usually expects that singular continuous part is absent, that is $X^{\mathrm{sc}} = \{0\}$.

An analysis of the spectrum of H shows that it is entirely composed of absolutely continuous spectrum, meaning $X = X^{\mathrm{ac}}$. It is then a classical fact of scattering theory [79,84] that, denoting e^{itH} the semigroup associated with H, the solution $U(t) = (\tau(t), u(t), f(t)) = e^{itH}(\tau_{ini}, u_{ini}, f_{ini})$ weakly converges to 0 in X as $t \to \infty$. Finally, using the conservation of the quadratic norm, one can show that $\tau(t)$ and $u(t)$ strongly converge in 0 in L^2_0 as $t \to \infty$.

We obtain then, in the same spirit as in [44], a linear damping property of the acoustic energy $\|\tau(t)\|^2_{L^2} + \|\boldsymbol{u}(t)\|^2_{L^2}$ of the gas. In view of the conservation of the total quadratic energy $\|(\tau,u,f)\|_{L^2}(t)$, the Theorem 1.3.1 implies that all the quadratic energy of the system is eventually absorbed by the particles. In the numerical simulations, this effect is visible via the formation of filamentation in the velocity variable of the particles distribution f.

Remark 1.3.2.
- *It is a priori complicated to obtain a similar expansion like in [40], because the operator H does not write as a compact perturbation of a simpler operator.*

- *As in [43, 44], Theorem 1.3.1 does not give any insights on the rate of convergence. It also does not give any information on the convergence of the density of the particles* $\varrho_f := \int f \,\mathrm{d}v$.
- *One can extend this result to a general "one bump" function of the form*
$$f_0(v) = F(v^2/2)$$
where $F : \mathbf{R} \to \mathbf{R}_+$ *is a strictly decreasing function. Then, the operator* H *is a symmetric operator in the weighted space* $X_R = L^2_0(\mathbf{T}) \times L^2_0(\mathbf{T}) \times L^2_0(\mathbf{T} \times \mathbf{R})$*, equipped with the scalar product*
$$\langle (\tau,u,f),(\sigma,w,g)\rangle_{X_R} = \int_{\mathbf{T}} \tau(x)\sigma(x)\,\mathrm{d}x + \int_{\mathbf{T}} u(x)w(x)\,\mathrm{d}x + \iint_{\mathbf{T}\times\mathbf{R}} f(x,v)g(x,v)\,R(v)\mathrm{d}x\mathrm{d}v$$
and $R(v) = -(F/F')(v^2/2)$ *is the Lyapunov function introduced in [27]. Then, adapting the proof of Theorem 1.3.1 is straightforward.*

1.4 A coupled Finite Volume/semi-Lagrangian method for thick sprays

In this section, we present the results of Chapter 4. We present a numerical scheme for the discretisation of the thick spray equations (1.9) based on a semi-Lagrangian scheme for the Vlasov equation, and a Finite Volume Scheme for the Euler equations. We also present two ways to deal with close-packing limit in such flows. The first way is a correction procedure on the particle distribution function, inspired by works by Maury and his collaborators [94, 108]. The second way is to modify the Vlasov equation, to incorporate a pressure term that explicitly prevents the particle density from exceeding a given threshold.

We begin by giving a brief overview of congestion phenomena in fluid equations, then we turn to the problem of close-packing limit in thick spray models. Then, we describe the numerical methods used.

1.4.1 Congestion in fluid equations

The problem of congestion phenomena in fluid equations has received a lot of attention in the past decades [19,22,41,42,74,83,100,101]. The applications stem from traffic flow, granular media, crowd motion, high-density regimes. In these types of problems, fluid mechanics equations are used to describe the density of a population, or particles. In most of theses applications, the density (e.g. the density of an animal crowd) cannot cross a given critical density ρ^*, which corresponds to a maximal packing constraint, that is the non-overlap constraint on the microscopic components. Standard fluid mechanics equations like the Euler system (1.7) or the Navier-Stokes equations do not take into account such maximal density constraints. Several different models have been proposed. An important number of these models are variants of the following toy model

$$\begin{cases} \partial_t \rho + \nabla_x \cdot (\rho \boldsymbol{u}) = 0 \\ \partial_t (\rho \boldsymbol{u}) + \nabla_x \cdot (\rho \boldsymbol{u} \otimes \boldsymbol{u}) + \nabla_x p = 0 \\ 0 \leq \rho \leq \rho^*, \ \operatorname{supp} p \subset \{\rho = \rho^*\}, \ p \geq 0 \end{cases} \tag{1.27}$$

In the literature, such system are sometimes called *hard congestion models*, because the dynamics is free of any constraint, until the density enters the maximal density zone $\rho = \rho^*$, then the constraint is imposed by a sudden activation of the pressure p. The system (4.7) is then a free boundary problem, between the free phase where $\rho < \rho^\star$ and $p = 0$ and the congested zone where $\rho = \rho^*$ and $p > 0$. The dynamics of the free boundary between these two regimes is not explicitely given by the system. The lack of regularity of the pressure is an important obstacle for a rigourous study of the system. From a numerical point of view, the implicit nature of the pressure (no explicit formula is given) is also an important obstacle in the construction of numerical schemes. Because of these issues, another approach is sometimes given in the literature. It consists of replacing the hard congestion constraint $(\rho^* - \rho)p = 0$ by an explicit formula of the pressure, which blows up when $\rho \to \rho^*$:

$$\begin{cases} \partial_t \rho + \nabla_x \cdot (\rho \boldsymbol{u}) = 0 \\ \partial_t (\rho \boldsymbol{u}) + \nabla_x \cdot (\rho \boldsymbol{u} \otimes \boldsymbol{u}) + \nabla_x p = 0 \\ 0 \le \rho \le \rho^*, p_\varepsilon(\rho) \to +\infty \text{ as } \rho \to \rho^* \end{cases} \tag{1.28}$$

The singular pressure p can be interpreted as a repulsive force between the particles. A commonly cited formula in the literature is given by:

$$p_\varepsilon(\rho) = \varepsilon \left(\frac{\rho}{\rho^* - \rho} \right)^\beta, \beta > 1. \tag{1.29}$$

and one has formally $p_\varepsilon \to p$ as $\varepsilon \to 0$. Such model are sometimes called *soft congestion models* [100].

1.4.2 Close-packing limit in thick sprays

In some applications, the model (1.9) is used for small fluid volume fractions [6, 20, 49]. There is a need for the developement of model and methods for thick sprays which preserve this maximum principle. This is the subject of Chapter 4 where we propose two ways to deal with this issue. The first way is to do a numerical correction of the solution by adapting a method developed by Maury, Roudneff-Chupin, Santambrogio and Venel [94] in the context of crowd motion. A second way is to modify the system (1.9) and to add an additionnal pressure in the kinetic equation, which modelises the inability of the particles to overlap.

Consider the thick spray model, with the addition of a constraint on the fluid volume fraction α,

$$\begin{cases} \partial_t (\alpha \varrho) + \nabla_x \cdot (\alpha \varrho \boldsymbol{u}) = 0 \\ \partial_t (\alpha \varrho \boldsymbol{u}) + \nabla_x \cdot (\alpha \varrho \boldsymbol{u} \otimes \boldsymbol{u}) + \alpha \nabla_x p = D_\star \displaystyle\int_{\mathbf{R}^3} (\boldsymbol{v} - \boldsymbol{u}) f \, \mathrm{d}v \\ \partial_t f + \boldsymbol{v} \cdot \nabla_x f + \nabla_v \cdot (\boldsymbol{\Gamma} f) = 0 \\ \alpha = 1 - m_\star \displaystyle\int_{\mathbf{R}^3} f \, \mathrm{d}v \\ m_\star \boldsymbol{\Gamma} = -m_\star \nabla_x p - D_\star (\boldsymbol{v} - \boldsymbol{u}) \\ \alpha(t,x) \ge \alpha_{\min} > 0. \end{cases} \tag{1.30}$$

Without modification of the system, it is not expected that an initial condition $(\varrho_{\text{ini}}, \boldsymbol{u}_{\text{ini}}, f_{\text{ini}})$, satisfying $\alpha_{\text{ini}} = 1 - \frac{4}{3}\pi r_p^3 \int f_{\text{ini}}\,\mathrm{d}v \geq \alpha_{\min}$ will propagate in time. To fix this, we propose the following two alternatives.

Random Repair Algorithm. Our first idea was to numerically impose the constraint $\alpha \geq \alpha_{\min}$. We adapted an algorithm developed by Maury and his collaborators [94, 108] for the modelling of crowd motion. The idea of the algorithm is to redistribute the exceeding mass of a saturated cell using a random walk. For now, this method is purely a numerical correction and it is not clear what is the actual set of equations that this method solves.

Addition of an explicit singular pressure term Another idea we proposed is to modify the model (4.1), and by taking inspiration from the literature on congestion phenomena [100], to add a pressure that can deal with packing effects. The model writes

$$\begin{cases} \partial_t(\alpha\varrho) + \nabla_x \cdot (\alpha\varrho\boldsymbol{u}) = 0 \\ \partial_t(\alpha\varrho\boldsymbol{u}) + \nabla_x \cdot (\alpha\varrho\boldsymbol{u} \otimes \boldsymbol{u}) + \alpha\nabla_x p_{\text{gas}}(\varrho) = D_\star \displaystyle\int_{\mathbf{R}^3} (\boldsymbol{v} - \boldsymbol{u}) f\,\mathrm{d}v \\ \partial_t f + \nabla_x \cdot [(\boldsymbol{v} - \nabla_x p_{\text{packing}}) f] + \nabla_v \cdot (\Gamma f) = 0 \\ \alpha = 1 - \dfrac{4}{3}\pi r_p^3 \displaystyle\int_{\mathbf{R}^3} f\,\mathrm{d}v \\ m_\star\Gamma = -\dfrac{4}{3}\pi r_p^3 \nabla_x p_{\text{gas}}(\varrho) - D_\star(\boldsymbol{v} - \boldsymbol{u}) \\ \alpha \geq \alpha_{\min}, \quad (\alpha - \alpha_{\min})\, p_{\text{packing}} = 0. \end{cases} \tag{1.31}$$

However, the direct numerical discretization of the system (4.7) is not obvious, because we do not know how to compute the pressure p_{packing} when the packing limit $\alpha = \alpha_{\min}$ is achieved. We then proposed to relax the relation $(\alpha - \alpha_{\min})\, p_{\text{packing}} = 0$, and to replace p_{packing} by another explicit singular pressure

$$p^{\varepsilon}_{\text{packing}}(\alpha) = \varepsilon \left(\frac{1 - \alpha}{\alpha - \alpha_{\min}} \right)^{\beta}, \quad \beta > 1$$

where $\varepsilon > 0$ is a small parameter. Formally, the pressure $p^{\varepsilon}_{\text{packing}}(\alpha)$ tends to p_{packing}.

1.4.3 Numerical discretization

The numerical simulation of a fluid-kinetic system, such as (1.11), presents several key challenges. First, consider the fluid part. Discretizing this part aligns with the methods used for hyperbolic conservation laws [68], which is a complex field due to the nonlinear nature of such systems and the frequent emergence of discontinuities in the solutions. Accurately capturing these discontinuities is challenging, and critical to obtain convergence to the correct weak solution. Second, there is the kinetic equation, which brings additional difficulties due to its high dimensionality [35, 51, 59]. For realistic simulations, the entire 6-dimensional phase space must be discretized. This requires a grid with $O(n^6)$ points, where n represents the number of grid points in each direction, resulting in a substantial computational cost.

Another characteristic difficulty in solving kinetic equations is the phenomenon known as filamentation. To illustrate, consider the free transport equation:

$$\partial_t f(t,x,v) + v\partial_x f(t,x,v) = 0 \tag{1.32}$$
$$f(t=0,x,v) = f_0(x,v). \tag{1.33}$$

This equation is a linear transport equation, and its solution can be computed explicitly as $f(t,x,v) = f_0(x - vt, v)$. However, despite its simplicity, filamentation introduces computational challenges. For example, with an initial condition $f_0(x,v) = \cos(kx)e^{-v^2/2}$ for some $k \in \mathbb{R}$, the solution evolves as:

$$f(t,x,v) = \cos(k(x - vt))e^{-v^2/2}.$$

Over time, we observe that $\|\partial_v^m f(t,\cdot,\cdot)\| \propto (kt)^m$, indicating that increasingly fine-scale structures emerge in phase space even as the solution remains smooth (see Figure 1.2). This filamentation effect necessitates the use of very fine grids to accurately capture these small-scale structures, which are essential for producing physically meaningful results.

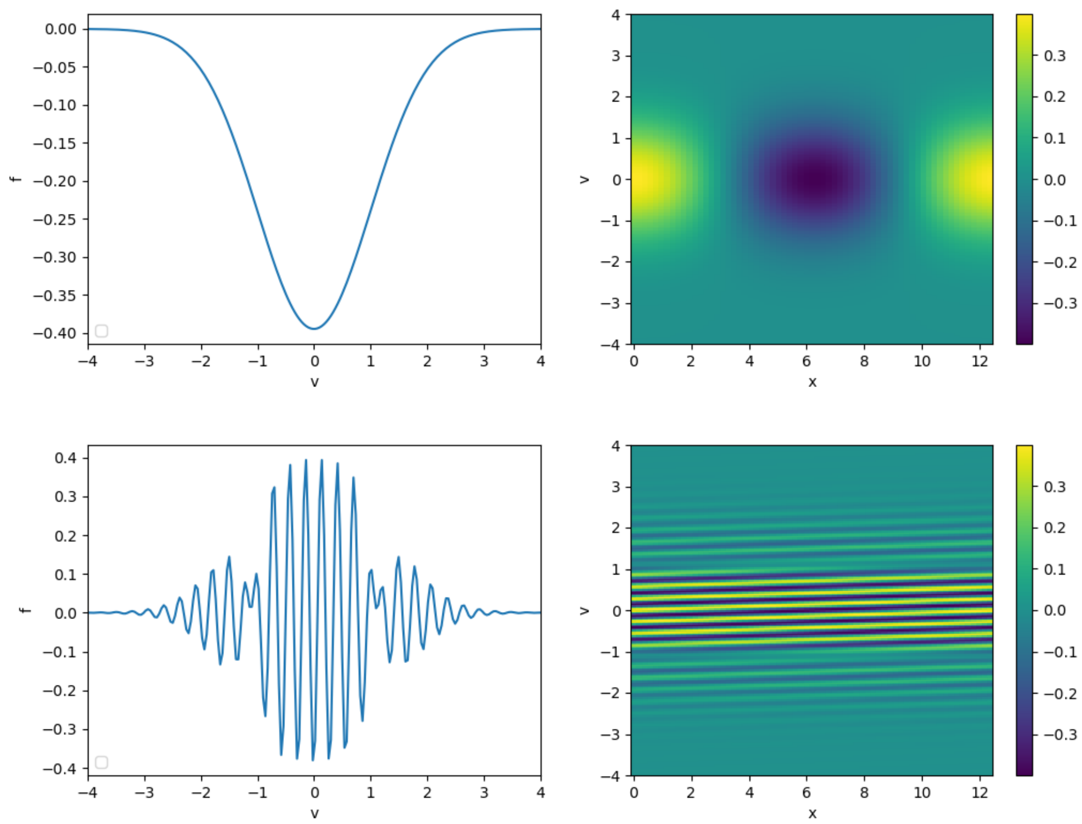

Fig. 1.2: Filamention of the particle distribution in the phase space

1.4.4 Methods used in this thesis

We restrict ourselves to one dimensional problems. In this section, we describe the numerical methods that are used in this thesis. All the numerical results presented are done using a code in Python.

The first step involves reformulating the fluid equations. In (1.9), the momentum equation contains a nonconservative product, $\alpha\nabla_x p$, which can pose challenges, particularly in the presence of shocks. To address this, we instead consider the total momentum equation for the spray, resulting in the fluid equations as:

$$\begin{cases} \partial_t(\alpha\varrho) + \partial_x(\alpha\varrho u) = 0 \\ \partial_t\left(\alpha\varrho u + m_\star \int_{\mathbf{R}} vf \,\mathrm{d}v\right) + \partial_x\left(\alpha\varrho u^2 + m_\star \int_{\mathbf{R}} fv^2 \,\mathrm{d}v\right) + \partial_x p = 0. \end{cases}$$

Denoting the vector of conserved variables

$$\mathbf{U} = \begin{pmatrix} n \\ q \end{pmatrix} := \begin{pmatrix} \alpha\varrho \\ \alpha\varrho\boldsymbol{u} + m_\star \int \boldsymbol{v} f \,\mathrm{d}v \end{pmatrix},$$

and the flux

$$\mathbf{F}(\mathbf{U},f) = \begin{pmatrix} \alpha\varrho u \\ \alpha\varrho u^2 + p + m_\star \int_{\mathbf{R}} fv^2 \,\mathrm{d}v \end{pmatrix} = \begin{pmatrix} q - \frac{4}{3}\pi r_p^3 \int_{\mathbf{R}} fv \,\mathrm{d}v \\ \frac{(q - m_\star \int_{\mathbf{R}} fv \,\mathrm{d}v)^2}{n} + \frac{n^\gamma}{\alpha^\gamma} + \int_{\mathbf{R}} fv^2 \,\mathrm{d}v \end{pmatrix},$$

we can write the governing equation as

$$\partial_t \mathbf{U} + \partial_x \mathbf{F}(\mathbf{U},f) = 0.$$

The idea is then to discretize this this conservation law with a Finite Volume scheme. In this study, we restrict ourselve to a simple Rusanov scheme [68].

For the Vlasov equation, we use a semi-Lagrangian scheme. Usually, particles method such as the PIC method are used for this kind of system [5, 6, 76]. Such method have a lot of drawback such as the presence of numerical noise. Moreover, particle methods are known to struggle to capture correctly the distribution function when the density of particles is very low [50,112]. Semi-Lagrangian methods have been rarely used for thick sprays in our knownledge (see nevertheless some recent works [18,47]). We main focus of this study was the discretization of the dispersed phase. We will use two scheme for the dispersed phase, the first one is a semi-Lagrangian scheme based on cubic B-Spline (BPSL) [112]. The other will be a conservative semi-Lagrangian scheme known as the Positive Flux Conservative (PFC) scheme [59].

For the time discretization, we use the following time splitting. The time-splitting is done in a Strang fashion, at it is classical in plasma physics [35, 112].

- **Transport in the direction x.**

  Particles are transported along their velocities in the x-direction for half a time step.

- **Correction of the particle distribution.** In this step, we correct the transport of the particle by taking into account the close packing constraint.

- **Transport of the fluid.**

  The fluid variables are updated through a Finite Volume scheme with a full time step.

- **Transport in the direction v.**

  The particles are accelerated with a full time step.

- **Transport of the particles with velocity v the direction x.**

  The particles undergo a final transport in the x-direction, again for half a time step.

- **Correction of the particle distribution.** A final correction step is applied to ensure the particle distribution satisfies the close-packing limit.

An important remark regarding the time stepping: A formal computation of the Jacobian $A(\mathbf{U},f)$ of $\mathbf{F}(\mathbf{U},f)$ with respect to $\mathbf{U}$ reveals that the eigenvalues of the fluid phase are

$$\lambda_{\pm} = u \pm \sqrt{\frac{p'(\varrho)}{\alpha}}.$$

So small volume fraction α will lead to very small timestep. We will give more detail on the choice of the time step in the Chapter 4.

Chapter 2

Construction of solutions

Summary

The main part of this chapter corresponds to a joint work with Christophe Buet and Bruno Després and has been published in *Kinetic and Related Models* [63].

We propose a new system for the modelling of thick sprays. We prove that this system verifies conservation properties together with a maximum principle regarding the volume fraction of the gas. Our main result is that the barotropic version of this system is locally in time well-posed in H^s. We also discuss the problems associated to the construction of weak solutions.

2.1 Local-in-time existence of strong solutions to an averaged thick spray model

2.1.1 Introduction

Sprays are defined as dispersed liquid (such as droplets) or solid (such as dust) phase evolving in an underlying gas. Such models are usually presented as a coupling between a kinetic equation (for example, a Vlasov equation or a Vlasov-Boltzmann equation) and an hyperbolic (or Navier-Stokes) system and were introduced in [29, 118]. A classification of different types of sprays have been proposed in [97]. See [45] for a recent review of the different ways to model sprays.

One type of sprays are the so-called *thin sprays*, in which the total volume occupied by the particles is negligible compared to the volume occupied by the gas. In this case, the coupling is usually made through a drag force, sometimes called the *Brinkman force*. Such models have been heavily studied in the purely hyperbolic setting [12, 92] and in the Navier-Stokes setting, that is, with parabolic terms (see [7, 54, 73] and the references therein).

In this work, we are interested in so-called *thick spray* models, in which the total volume occupied by the particles is no longer negligible compared to the volume of the gas. On the mathematical side, less is known about thick spray models compared to thin spray models. We refer to [23, 27] for recent works on thick sprays.

Hereafter the gas is described with a system of compressible Euler equations, for which the variables are the density $\varrho := \varrho(t,\boldsymbol{x}) \geq 0$, the velocity $\boldsymbol{u} := \boldsymbol{u}(t,\boldsymbol{x}) \in \mathbf{R}^3$ and the internal energy $e := (t,\boldsymbol{x}) \geq 0$. The particles are described with a phase space density $f := f(t,\boldsymbol{x},\boldsymbol{v}) \geq 0$ following a Vlasov equation. It is also possible to use a Vlasov-Boltzmann equation, but numerical results may suggest that adding a collision operator is not necessary for accurate simulations [17]. Various other effects such as coalescence and fragmentation can also be taken into account, we chose here to neglect all these effects. The force acting on the particles, that shall be denoted $m_\star\boldsymbol{\Gamma}$, is usually decomposed in two parts: one related to drag or friction between the particles and the gas. The other one is related, since the total volume of the particles is not negligible, to the pressure of the gas:

$$m_\star\boldsymbol{\Gamma} = -m_\star\nabla_x p - D_\star(\boldsymbol{v} - \boldsymbol{u}).$$

The presence of the term $-\nabla_x p$ is a specific feature of thick sprays models, and it is formally linked to bifluid equations (see [46]). Depending of the modelisation, the coefficient $D_\star$ can be treated as a constant or as a function of $\boldsymbol{v} - \boldsymbol{u}$. We shall limit ourselves to the constant case.

The constant $m_\star$ can be interpreted as the mass of the particles and is linked to their radius r by the formula (we assume here that the particles have a density equal to 1)

$$m_\star = \frac{4}{3}\pi r^3.$$

The spray is assumed to be monodisperse, meaning that all particles have the same radius. With those hypotheses, a possible thick spray model [23] can be written as

$$\begin{cases} \partial_t(\alpha\varrho) + \nabla_x \cdot (\alpha\varrho\boldsymbol{u}) = 0 \\ \partial_t(\alpha\varrho\boldsymbol{u}) + \nabla_x \cdot (\alpha\varrho\boldsymbol{u}\otimes\boldsymbol{u}) + \nabla_x p = m_\star \nabla_x p \displaystyle\int_{\mathbf{R}^3} f \,\mathrm{d}v + D_\star \int_{\mathbf{R}^3} (\boldsymbol{v}-\boldsymbol{u}) f \,\mathrm{d}v \\ \partial_t(\alpha\varrho e) + \nabla_x \cdot (\alpha\varrho e\boldsymbol{u}) + p(\partial_t\alpha + \nabla_x\cdot(\alpha\boldsymbol{u})) = D_\star \displaystyle\int_{\mathbf{R}^3} |\boldsymbol{v}-\boldsymbol{u}|^2 f \,\mathrm{d}v \\ \partial_t f + \boldsymbol{v}\cdot\nabla_x f + \nabla_v \cdot (\boldsymbol{\Gamma} f) = 0 \\ \alpha = 1 - m_\star \displaystyle\int_{\mathbf{R}^3} f \,\mathrm{d}v \\ m_\star \boldsymbol{\Gamma} = -m_\star \nabla_x p - D_\star(\boldsymbol{v}-\boldsymbol{u}). \end{cases} \tag{2.1}$$

This model can be used to describe various physical phenomena at different length scales, such as aerosols for medical use [24,25], the combustion in engines [5], aerosols in the atmosphere [90], and also in astrophysics for the modelling of gas giants and exoplanets [66].

In the thin spray case, the volume fraction α is absent from the equations. One of the simplest examples of thin spray models is the so-called (compressible, barotropic) Euler-Vlasov system, which writes

$$\begin{cases} \partial_t\varrho + \nabla_x \cdot (\varrho\boldsymbol{u}) = 0 \\ \partial_t(\varrho\boldsymbol{u}) + \nabla_x \cdot (\varrho\boldsymbol{u}\otimes\boldsymbol{u}) + \nabla_x p = D_\star \displaystyle\int_{\mathbf{R}^3} (\boldsymbol{v}-\boldsymbol{u}) f \,\mathrm{d}v \\ \partial_t f + \boldsymbol{v}\cdot\nabla_x f + \nabla_v \cdot \left(\frac{D_\star}{m_\star}(\boldsymbol{u}-\boldsymbol{v}) f\right) = 0. \end{cases} \tag{2.2}$$

One remarks that taking the formal limit $\alpha \to 1$ in (4.1) does not yield (2.2), because the term $-\nabla_x p$ does not vanish. Indeed, to the best of our knowledge, there is no well established hierarchy between the two regimes. One formal way to recover (2.2) from (4.1) is to take the limit $m_\star \to 0$ (which means that the radius of the particles $r_\star$ goes to 0). Then $\alpha \to 1$, and $\frac{D_\star}{m_\star} \to +\infty$. In the end the term $\nabla_x p$ in the force acting on the particles becomes negligible compared to the friction force, and one obtains the system (2.2).

The system (4.1) suffers from some mathematical issues. It displays losses of regularity, and therefore standard techniques to prove a local-in-time well posedness result fail. Typically, the term $\nabla_x p \cdot \nabla_v f$ in the Vlasov equation cannot be treated within standard theory for weak solutions of such systems. To the best of our knowledge, even local-in-time well-posedness result is lacking. It is even conjectured in [12] that the system (4.1) is ill-posed locally in time. All those reasons motivate us to modify the model, with regularisation-convolution of certain terms specific to thick spray models. We propose the following thick spray model with regularisation

$$
\begin{cases}
\partial_t(\alpha\varrho) + \nabla_x \cdot (\alpha\varrho\boldsymbol{u}) = 0 \\
\partial_t(\alpha\varrho\boldsymbol{u}) + \nabla_x \cdot (\alpha\varrho\boldsymbol{u}\otimes\boldsymbol{u}) + \nabla_x p = m_\star \nabla_x p \int_{\mathbf{R}^3} \langle f \rangle \,\mathrm{d}v + D_\star \int_{\mathbf{R}^3} (\boldsymbol{v}-\boldsymbol{u}) f \,\mathrm{d}v \\
\partial_t(\alpha\varrho e) + \nabla_x \cdot (\alpha\varrho e\boldsymbol{u}) + p(\partial_t\alpha + \nabla_x \cdot (\alpha\boldsymbol{u})) = D_\star \int_{\mathbf{R}^3} |\boldsymbol{v}-\boldsymbol{u}|^2 f \,\mathrm{d}v \\
\partial_t f + \boldsymbol{v}\cdot\nabla_x f + \nabla_v \cdot (\boldsymbol{\Gamma} f) = 0 \\
\alpha = 1 - m_\star \int_{\mathbf{R}^3} \langle f \rangle \,\mathrm{d}v \\
m_\star \boldsymbol{\Gamma} = -m_\star \langle \nabla_x p \rangle - D_\star(\boldsymbol{v}-\boldsymbol{u}).
\end{cases}
\tag{2.3}
$$

where the convolution operator $\langle\cdot\rangle$ is introduced in the second, fifth and sixth line of the initial model (4.1). A possible "physical" form of the convolution operator is justified in subsection 2.1.2. This convolution operator preserves the conservation of mass, momentum, total energy and still produces entropy. We will show that it is enough to to obtain the local-in-time well posedness of smooth solutions.

This work is organized as follows. In subsection 2.1.2, we justify the convolution operator and explain the modifications of the usual thick spray equations leading to (4.4). In subsection 2.1.3, we show that the system verifies conservation properties for the total mass, the total momentum, and the total energy of the system, and is equipped with an entropy balance law. We also show that under reasonable assumptions, the volume fraction α stays in (0,1] for all times, provided that the initial condition verifies this property. Finally, in subsection 2.1.5, we prove the main result of this work on the local-in-time well-posedness in H^s of the barotropic version of (4.4).

2.1.2 Justification of the convolution operator

The idea of a convolution operator is easy to conceive on the equation that defines the force $m_\star\boldsymbol{\Gamma}$, ignoring the friction force. Let us consider a single spherical particle of radius $r > 0$ with center coordinate $\boldsymbol{x}_\star$. In a surrounding gas with a pressure field p, the gas acts on the particle with the force

$$F = -\int_{\mathbf{S}^2(\boldsymbol{x}_\star, r)} p\boldsymbol{n} \,\mathrm{d}x.$$

In a thought experiment, the pressure can be extended inside the particle. Assuming that the pressure is differentiable in the particle, one obtains using Stokes's theorem

$$F = -\int_{\mathbf{S}^3(\boldsymbol{x}_\star, r)} \nabla_x p(\boldsymbol{x}) \,\mathrm{d}x = -m_\star \int_{\mathbf{R}^3} w(\boldsymbol{x}-\boldsymbol{x}_\star) \nabla_x p(\boldsymbol{x}) \,\mathrm{d}x = m_\star (w \star \nabla_x p)(\boldsymbol{x}_\star),$$

where the convolution kernel is

$$w(\boldsymbol{y}) = \frac{1}{m_\star} \mathbf{1}_{|\boldsymbol{y}|<r}(\boldsymbol{y}).$$

Using the notation $\langle\cdot\rangle = w \star \cdot$ for the convolution operator, the force is rewritten as

$$m_\star\boldsymbol{\Gamma} = -m_\star \langle \nabla_x p \rangle.$$

This formula is valid independently of the extension of p inside the particle, provided it is differentiable. We recall the definition [56] of the total variation of a function

$$\mathrm{TV}(f) := \sup\left(\int_{\mathbf{R}^3} f \,\mathrm{div}\,\varphi \,\mathrm{d}x, \quad \varphi \in \mathscr{C}^1_c(\mathbf{R}^3; \mathbf{R}^n), \|\varphi\|_{L^\infty} \le 1 \right),$$

Lemma 2.1.1. *The kernel w verifies $w \in \mathrm{BV}(\mathbf{R}^3)$, $\|w\|_{L^1} = 1$ and $\mathrm{TV}(w) = \frac{3}{r}$.*

Proof. Since w is the indicator function of a sphere, then $w \in \mathrm{BV}(\mathbf{R}^3)$. The kernel w has unit L^1-norm because $m_\star = \frac{4}{3}\pi r^3$. Finally the total variation of an indicator function is the perimeter of its support, therefore $\mathrm{TV}(w) = \frac{4\pi r^2}{m_\star} = \frac{3}{r}$. □

In order to introduce this principle in the original system (4.1), one needs to reintroduce the friction in the force $m_\star \mathbf{\Gamma}$ and to modify other equations in a way that preserve the global conservation properties. Considering additionally that the modifications should be kept to the minimum, we are led to propose the following system

$$\begin{cases} \partial_t(\alpha\varrho) + \nabla_x \cdot (\alpha\varrho\boldsymbol{u}) = 0 & (2.4)\\ \partial_t(\alpha\varrho\boldsymbol{u}) + \nabla_x \cdot (\alpha\varrho\boldsymbol{u}\otimes\boldsymbol{u}) + \nabla_x p = m_\star \nabla_x p \displaystyle\int_{\mathbf{R}^3} \langle f\rangle \,\mathrm{d}v + D_\star \int_{\mathbf{R}^3} (\boldsymbol{v}-\boldsymbol{u}) f \,\mathrm{d}v & (2.5)\\ \partial_t(\alpha\varrho e) + \nabla_x \cdot (\alpha\varrho e\boldsymbol{u}) + p(\partial_t\alpha + \nabla_x\cdot(\alpha\boldsymbol{u})) = D_\star \displaystyle\int_{\mathbf{R}^3} |\boldsymbol{v}-\boldsymbol{u}|^2 f \,\mathrm{d}v & (2.6)\\ \partial_t f + \boldsymbol{v}\cdot\nabla_x f + \nabla_v \cdot (\mathbf{\Gamma} f) = 0 & (2.7)\\ \alpha = 1 - m_\star \displaystyle\int_{\mathbf{R}^3} \langle f\rangle \,\mathrm{d}v & (2.8)\\ m_\star \mathbf{\Gamma} = -m_\star\langle\nabla_x p\rangle - D_\star(\boldsymbol{v}-\boldsymbol{u}). & (2.9)\end{cases}$$

Let us comment in more details the equations (2.4)-(2.9). Equations (2.4), (2.6) and (2.7) are unchanged. Equation (2.5) is modified with the convolution kernel on the right-hand-side since we found that it is a way to recover the conservation of the total momentum, as justified in Proposition 2.1.2. Equation (2.8) is also modified by compatibility with the conservation of the total energy. In the last equation (2.9), the friction is reintroduced without a convolution because there is no conservation issue related to this term. Notice that when the size of the support of w goes to 0 (ignoring the fact that $m_\star$ is dependent of the size of the particle r), meaning that w converges to a Dirac mass, one recovers the system (4.1). To close the system, we assume that p follows a perfect gas law

$$p = (\gamma - 1)\varrho e, \quad \gamma > 1 \tag{2.10}$$

and the energy law

$$e = C_v T, \tag{2.11}$$

with $T > 0$ the temperature and $C_v > 0$ is a constant.

2.1.3 Properties of the system

In this section, we present basic properties of the new model (4.4).

2.1.3.1 Conservation properties

To obtain the conservation properties, we will make use of the classical formula: let f,g be two functions and let w be even, then

$$\int_{\mathbf{R}^d} (f\star w) g \,\mathrm{d}x = \int_{\mathbf{R}^d} f (g\star w) \,\mathrm{d}x, \tag{2.12}$$

which is easily shown using a change of variable and the fact that w is even.

Proposition 2.1.2. *Formally, the following holds:*

(i)

$$\frac{\mathrm{d}}{\mathrm{d}t}\int_{\mathbf{R}^3}\alpha\varrho\,\mathrm{d}x = 0, \qquad \frac{\mathrm{d}}{\mathrm{d}t}\iint_{\mathbf{R}^3\times\mathbf{R}^3} f\,\mathrm{d}x\mathrm{d}v = 0,$$

(ii)

$$\frac{\mathrm{d}}{\mathrm{d}t}\left(\int_{\mathbf{R}^3}\alpha\varrho\boldsymbol{u}\,\mathrm{d}x + \iint_{\mathbf{R}^3\times\mathbf{R}^3} f\boldsymbol{v}\,\mathrm{d}x\mathrm{d}v\right) = 0,$$

(iii)

$$\frac{\mathrm{d}}{\mathrm{d}t}\left(\frac{1}{2}\int_{\mathbf{R}^3}\alpha\varrho|\boldsymbol{u}|^2\,\mathrm{d}x + \frac{1}{2}\iint_{\mathbf{R}^3\times\mathbf{R}^3}|\boldsymbol{v}|^2 f\,\mathrm{d}x\mathrm{d}v + \int_{\mathbf{R}^3}\alpha\varrho e\,\mathrm{d}x\right) = 0.$$

Proof. By formally we mean that all functions are smooth and integrable. The proof of (i) is obvious because the equations are already in divergence form.

To obtain (ii) one multiplies the Vlasov equation (2.7) by $\boldsymbol{v}$. Integration yields

$$m_\star\partial_t\int_{\mathbf{R}^3} f\boldsymbol{v}\,\mathrm{d}v + m_\star\nabla_x\cdot\int_{\mathbf{R}^3} f\boldsymbol{v}\otimes\boldsymbol{v}\,\mathrm{d}v = -m_\star\langle\nabla_x p\rangle\int_{\mathbf{R}^3} f\,\mathrm{d}v - D_\star\int_{\mathbf{R}^3}(\boldsymbol{v}-\boldsymbol{u})f\,\mathrm{d}v.$$

Summing with the fluid momentum equation (2.5), one gets

$$\partial_t\left(\alpha\varrho\boldsymbol{u} + m_\star\int_{\mathbf{R}^3} f\boldsymbol{v}\,\mathrm{d}v\right) + \nabla_x\cdot\left(\alpha\varrho\boldsymbol{u}\otimes\boldsymbol{u} + m_\star\int_{\mathbf{R}^3} f\boldsymbol{v}\otimes\boldsymbol{v}\,\mathrm{d}v\right) + \nabla_x p \tag{2.13}$$

$$= m_\star\left(\nabla_x p\int_{\mathbf{R}^3}\langle f\rangle\,\mathrm{d}v - \langle\nabla_x p\rangle\int_{\mathbf{R}^3} f\,\mathrm{d}v\right). \tag{2.14}$$

Using formula (2.12), one has $\int_{\mathbf{R}^3}\left(\nabla_x p\int_{\mathbf{R}^3}\langle f\rangle\,\mathrm{d}v - \langle\nabla_x p\rangle\int_{\mathbf{R}^3} f\,\mathrm{d}v\right)\,\mathrm{d}x = 0$, so integrating (2.14) in x yields (ii).

To obtain (iii) one multiplies the momentum equation (2.5) by $\boldsymbol{u}$. One obtains

$$\partial_t\left(\alpha\varrho\frac{|\boldsymbol{u}|^2}{2}\right) + \nabla_x\cdot\left(\alpha\varrho\boldsymbol{u}\frac{|\boldsymbol{u}|^2}{2}\right) + \boldsymbol{u}\cdot\nabla_x p$$
$$= m_\star\boldsymbol{u}\cdot\nabla_x p\cdot\int_{\mathbf{R}^3}\langle f\rangle\,\mathrm{d}v + D_\star\int_{\mathbf{R}^3}\boldsymbol{u}\cdot(\boldsymbol{v}-\boldsymbol{u})f\,\mathrm{d}v.$$

Multiplying the Vlasov equation (2.7) by $m_\star\frac{|\boldsymbol{v}|^2}{2}$ and integrating, one gets

$$m_\star\partial_t\left(\int_{\mathbf{R}^3} f\frac{|\boldsymbol{v}|^2}{2}\,\mathrm{d}v\right) + m_\star\nabla_x\cdot\left(\int_{\mathbf{R}^3} f\boldsymbol{v}\frac{|\boldsymbol{v}|^2}{2}\,\mathrm{d}v\right)$$
$$= -m_\star\langle\nabla_x p\rangle\cdot\int_{\mathbf{R}^3} f\boldsymbol{v}\,\mathrm{d}v - D_\star\int_{\mathbf{R}^3}\boldsymbol{v}\cdot(\boldsymbol{v}-\boldsymbol{u})f\,\mathrm{d}v.$$

Then, addition of these equations to the internal energy equation (2.6) yields

$$\begin{aligned}
A &:= \partial_t \left(\alpha\varrho \frac{|\boldsymbol{u}|^2}{2} + m_\star \int_{\mathbf{R}^3} f \frac{|\boldsymbol{v}|^2}{2} \,\mathrm{d}v + \alpha\varrho e \right) \\
&\quad + \nabla_x \cdot \left(\alpha\varrho\boldsymbol{u} \frac{|\boldsymbol{u}|^2}{2} + m_\star \int_{\mathbf{R}^3} f\boldsymbol{v} \frac{|\boldsymbol{v}|^2}{2} \,\mathrm{d}v + \alpha\varrho e\boldsymbol{u} \right) \\
&= -p\partial_t\alpha - p\nabla_x \cdot (\alpha\boldsymbol{u}) - \boldsymbol{u}\cdot\nabla_x p - m_\star \boldsymbol{u}\cdot\nabla_x p \int_{\mathbf{R}^3} \langle f\rangle \,\mathrm{d}v - m_\star \langle\nabla_x p\rangle \cdot \int_{\mathbf{R}^3} f\boldsymbol{v}\,\mathrm{d}v \\
&\quad + D_\star \int_{\mathbf{R}^3} \boldsymbol{u}\cdot(\boldsymbol{v}-\boldsymbol{u}) f \,\mathrm{d}v - D_\star \int_{\mathbf{R}^3} \boldsymbol{v}\cdot(\boldsymbol{v}-\boldsymbol{u}) f\,\mathrm{d}v + D_\star \int_{\mathbf{R}^3} |\boldsymbol{v}-\boldsymbol{u}|^2 f\,\mathrm{d}v \\
&= -p\partial_t\alpha - p\nabla_x \cdot (\alpha\boldsymbol{u}) - \boldsymbol{u}\cdot\nabla_x p + m_\star \boldsymbol{u}\cdot\nabla_x p \int_{\mathbf{R}^3} \langle f\rangle \,\mathrm{d}v - m_\star \langle\nabla_x p\rangle \cdot \int_{\mathbf{R}^3} f\boldsymbol{v}\,\mathrm{d}v.
\end{aligned}$$

Then, using $1-\alpha = m_\star \int_{\mathbf{R}^3} \langle f\rangle \,\mathrm{d}v$, one has $m_\star \boldsymbol{u}\cdot\nabla_x p \int_{\mathbf{R}^3} \langle f\rangle\,\mathrm{d}v = (1-\alpha)\boldsymbol{u}\cdot\nabla_x p$,

$$\begin{aligned}
A &= -p\partial_t\alpha - p\nabla_x\cdot(\alpha\boldsymbol{u}) - \boldsymbol{u}\cdot\nabla_x p + (1-\alpha)\boldsymbol{u}\cdot\nabla_x p - m_\star\langle\nabla_x p\rangle \cdot \int_{\mathbf{R}^3} f\boldsymbol{v}\,\mathrm{d}v \\
&= -p\partial_t\alpha - p\nabla_x\cdot(\alpha\boldsymbol{u}) - \alpha\boldsymbol{u}\cdot\nabla_x p - m_\star\langle\nabla_x p\rangle \cdot \int_{\mathbf{R}^3} f\boldsymbol{v}\,\mathrm{d}v.
\end{aligned}$$

One writes $p\nabla_x\cdot(\alpha\boldsymbol{u}) + \alpha\boldsymbol{u}\ \cdot\nabla_x p = \nabla_x\cdot(\alpha\boldsymbol{u}p)$ and $\partial_t\alpha = m_\star\nabla_x\cdot\int_{\mathbf{R}^3}\langle f\rangle v\,\mathrm{d}v$ to obtain

$$\begin{aligned}
A &= -\nabla_x\cdot(\alpha\boldsymbol{u}p) - p\partial_t\alpha - m_\star\langle\nabla_x p\rangle\cdot\int_{\mathbf{R}^3} f\boldsymbol{v}\,\mathrm{d}v \\
&= -\nabla_x\cdot(\alpha\boldsymbol{u}p) - m_\star p\nabla_x\cdot\int_{\mathbf{R}^3}\langle f\rangle\boldsymbol{v}\,\mathrm{d}v - m_\star\langle\nabla_x p\rangle\cdot\int_{\mathbf{R}^3} f\boldsymbol{v}\,\mathrm{d}v \\
&= -\nabla_x\cdot(\alpha\boldsymbol{u}p) - m_\star p\nabla_x\cdot\int_{\mathbf{R}^3}\langle f\rangle\boldsymbol{v}\,\mathrm{d}v - m_\star\nabla_x p\cdot\int_{\mathbf{R}^3}\langle f\rangle\boldsymbol{v}\,\mathrm{d}v \\
&\quad + m_\star\left(\nabla_x p\cdot\int_{\mathbf{R}^3}\langle f\rangle\boldsymbol{v}\,\mathrm{d}v - \langle\nabla_x p\rangle\cdot\int_{\mathbf{R}^3} f\boldsymbol{v}\,\mathrm{d}v\right) \\
&= -\nabla_x\cdot(\alpha\boldsymbol{u}p) - m_\star\nabla_x\cdot\left(p\int_{\mathbf{R}^3}\langle f\rangle\boldsymbol{v}\,\mathrm{d}v\right) \\
&\quad + m_\star\left(\nabla_x p\int_{\mathbf{R}^3}\langle f\rangle\boldsymbol{v}\,\mathrm{d}v - \langle\nabla_x p\rangle\int_{\mathbf{R}^3} f\boldsymbol{v}\,\mathrm{d}v\right).
\end{aligned}$$

Using again formula (2.12), we have $\int_{\mathbf{R}^3}\left(\nabla_x p\int_{\mathbf{R}^3}\langle f\rangle\boldsymbol{v}\,\mathrm{d}v - \langle\nabla_x p\rangle\int_{\mathbf{R}^3} f\boldsymbol{v}\,\mathrm{d}v\right)\mathrm{d}x = 0$, so integrating in x yields (*iii*). □

2.1.3.2 Entropy property

Following the analysis made in [27], we show that the system (2.4)-(2.9) closed by the equation of state (2.10) is equipped with an entropy inequality.

Proposition 2.1.3. *Formally, one has the entropy inequality*

$$\partial_t(\alpha\varrho S) + \nabla_x\cdot(\alpha\varrho S\boldsymbol{u}) = \frac{D_\star}{T}\int_{\mathbf{R}^3}|\boldsymbol{v}-\boldsymbol{u}|^2 f\,\mathrm{d}v \geq 0. \tag{2.15}$$

Proof. The density equation (2.4) yields

$$\varrho(\partial_t \alpha + \nabla_x \cdot (\alpha \boldsymbol{u})) + \alpha \mathrm{D}_t \varrho = 0 \iff \partial_t \alpha + \nabla_x \cdot (\alpha \boldsymbol{u}) = \alpha \varrho \mathrm{D}_t \tau,$$

with $\tau = 1/\varrho > 0$ the specific volume, and $\mathrm{D}_t = \partial_t + \boldsymbol{u} \cdot \nabla_x$. The internal energy equation (2.6) can be rewritten as

$$\alpha \varrho (\mathrm{D}_t e + p \mathrm{D}_t \tau) = D_\star \int_{\mathbf{R}^3} |\boldsymbol{v} - \boldsymbol{u}|^2 f \, \mathrm{d}v.$$

With the perfect gas pressure law (2.10) and the energy law (2.11), the entropy S is

$$S = C_v \ln(e \varrho^{1-\gamma}).$$

The second principle of thermodynamics writes

$$T \mathrm{d}S = \mathrm{d}e + p \mathrm{d}\tau,$$

so that

$$\alpha \varrho \mathrm{D}_t S = \frac{D_\star}{T} \int_{\mathbf{R}^3} |\boldsymbol{v} - \boldsymbol{u}|^2 f \, \mathrm{d}v,$$

which is rewritten as (2.15). □

2.1.4 Positivity of the volume fraction of the gas for smooth solutions

In this section, we study the positivity of the volume fraction α, which is that if $0 < \alpha \leq 1$ at time $t = 0$, then the inequality stays true for all times $t > 0$. Although it is clear that $\alpha \leq 1$ (due to the fact that $f \geq 0$ is propagated by the characteristic curves), it is less immediate to prove that $\alpha > 0$. In [27], the authors proved that this property holds for thick spray equations (4.1) under reasonable assumptions. We prove here the same result for (4.4) under similar assumptions.

Proposition 2.1.4. *We assume that a solution of the system (4.4) is defined on the whole space $\mathbf{R}^3$ and is smooth on $[0,T_{\mathrm{end}})$ for some $T_{\mathrm{end}} > 0$. We assume that*

- *For all $(\boldsymbol{x},\boldsymbol{v}) \in \mathbf{R}^3 \times \mathbf{R}^3$, $\quad f(0,\boldsymbol{x},\boldsymbol{v}) > 0$.*
- *One has $0 < \varrho_- = \inf_{\boldsymbol{x} \in \mathbf{R}^3} \varrho(0,\boldsymbol{x}) \leq \varrho_+ = \sup_{\boldsymbol{x} \in \mathbf{R}^3} \varrho(0,\boldsymbol{x}) < +\infty$.*
- *One has $-\infty < S_- = \inf_{\boldsymbol{x} \in \mathbf{R}^3} S(0,\boldsymbol{x})$.*
- *One has $0 < \alpha_- = \inf_{\boldsymbol{x} \in \mathbf{R}^3} \alpha(0,\boldsymbol{x}) \leq 1$.*

We assume the following regularity of the velocity variables

$$\boldsymbol{u} \in W^{1,\infty}([0,T_{\mathrm{end}}) \times \mathbf{R}^3), \quad \frac{\int_{\mathbf{R}^3} f \boldsymbol{v} \, \mathrm{d}v}{\int_{\mathbf{R}^3} \langle f \rangle \, \mathrm{d}v} \in L^\infty([0,T_{\mathrm{end}}) \times \mathbf{R}^3).$$

We finally assume that the pressure vanishes at infinity, that is for all $\varepsilon > 0$, there exists $A > 0$ such that

$$0 < p(t,\boldsymbol{x}) = (\gamma - 1)\varrho(t,\boldsymbol{x}) e(t,\boldsymbol{x}) < \varepsilon, \quad \text{for } 0 \leq t < T_{end} \text{ and } |\boldsymbol{x}| > A.$$

Then there exists a constant $C > 0$ depending on T_{end}, ϱ_+, ϱ_-, α_-, S_-, A (corresponding to $\varepsilon = 1$), $\|\boldsymbol{u}\|_{W^{1,\infty}([0,T_{\text{end}}[\times\mathbf{R}^3)}$ and $\left\|\frac{\int f\boldsymbol{v}\,\mathrm{d}v}{\int\langle f\rangle\,\mathrm{d}v}\right\|_{L^\infty([0,T_{\text{end}}[\times\mathbf{R}^3)}$ so that the following estimate holds :

$$0 < C \leq \alpha(t,\boldsymbol{x}) \leq 1, \quad t \in [0,T_{\text{end}}[, \quad \boldsymbol{x} \in \mathbf{R}^3.$$

Proof. The momentum equation (2.5) can be rewritten as

$$\alpha\nabla_x p = -\alpha\varrho \mathrm{D}_t\boldsymbol{u} + D_\star\frac{1-\alpha}{m_\star}\left(\frac{\int_{\mathbf{R}^3} f\boldsymbol{v}\,\mathrm{d}v}{\int_{\mathbf{R}^3}\langle f\rangle\,\mathrm{d}v} - \boldsymbol{u}\frac{\int_{\mathbf{R}^3} f\,\mathrm{d}v}{\int_{\mathbf{R}^3}\langle f\rangle\,\mathrm{d}v}\right),$$

with $\mathrm{D}_t = \partial_t + \boldsymbol{u}\cdot\nabla_x$. Using the regularity $\boldsymbol{u} \in W^{1,\infty}$ and the assumptions above, we find

$$\|\alpha\nabla_x p\|_{L^\infty} \leq C\left(1 + \|1-\alpha\|_{L^\infty}\right).$$

Following the fact that p follows a perfect gas law, we have the identity

$$\alpha\nabla_x p = \left[(\gamma-1)^{1/\gamma}e^{S/C_v\gamma}\alpha\varrho\right]\frac{1}{p^{1/\gamma}}\nabla_x p = \left[\frac{(\gamma-1)^{1/\gamma}e^{S/(C_v\gamma)}}{1-1/\gamma}\alpha\varrho\right]\nabla_x(p^{1-1/\gamma}).$$

Now, using again $\boldsymbol{u} \in W^{1,\infty}$ and a classical treatment of the characteristic curves of the continuity equation, we obtain for some $C_-, C_+ > 0$,

$$C_- = \inf_{\boldsymbol{x}\in\mathbf{R}^3}(\alpha\varrho)(t,\boldsymbol{x}) \leq \sup_{\boldsymbol{x}\in\mathbf{R}^3}(\alpha\varrho)(t,\boldsymbol{x}) = C_+, \quad 0 \leq t < T_{\text{end}}. \tag{2.16}$$

Therefore, because S is lower bounded.

$$\|\nabla_x(p^{1-1/\gamma})\|_{L^\infty} \leq C\left(1 + \|1-\alpha\|_{L^\infty}\right).$$

We then use the fact that the pressure vanishes at infinity

$$\|p^{1-1/\gamma}\|_{L^\infty} \leq C\left(1 + \|1-\alpha\|_{L^\infty}\right).$$

We then obtain that the density ϱ is bounded, using the perfect gas law for the pressure and the boundedness of the entropy S,

$$\|\varrho^{\gamma-1}\|_{L^\infty} \leq C\left(1 + \|1-\alpha\|_{L^\infty}\right).$$

Finally, using (2.16)

$$\left\|\frac{1}{\alpha}\right\|_{L^\infty} \leq C\left(1 + \|1-\alpha\|_{L^\infty}^{1/(\gamma-1)}\right) \leq C.$$

□

2.1.5 Local in time well-posedness

In this section, we consider the barotropic version of system (4.4), meaning that we suppose that the pressure depends only on the density of the fluid ϱ, that is

$$p = \varrho^\gamma, \quad \gamma > 1,$$

so that the energy equation (2.6) is not needed. We also assume, without loss of generality, that $D_\star = 0$ and $m_\star = 1$. The treatment of the friction term presents no difficulty because it does not contain any derivatives, so the treatment of this term is very similar to what is done in [12]. The barotropic system writes

$$\begin{cases} \partial_t(\alpha\varrho) + \nabla_x \cdot (\alpha\varrho\boldsymbol{u}) = 0 \\ \partial_t(\alpha\varrho\boldsymbol{u}) + \nabla_x \cdot (\alpha\varrho\boldsymbol{u}\otimes\boldsymbol{u}) + \nabla_x p = \nabla_x p \displaystyle\int_{\mathbf{R}^3} \langle f\rangle \,\mathrm{d}v \\ \partial_t f + \boldsymbol{v}\cdot\nabla_x f - \langle\nabla_x p\rangle \cdot \nabla_v f = 0 \\ \alpha = 1 - \displaystyle\int_{\mathbf{R}^3} \langle f\rangle \,\mathrm{d}v \\ p = p(\varrho) = \varrho^\gamma. \end{cases} \tag{2.17}$$

The goal of this section is to prove the following theorem:

Theorem 2.1.5. *Let $\Omega = (0,+\infty)\times\mathbf{R}^3$, $s \in \mathbf{N}$ such that $s > 3/2+1$ and Ω_1,Ω_2 two open sets of Ω such that $\overline{\Omega}_1 \subset \Omega_2$ and Ω_1 and Ω_2 are relatively compact in Ω. Let $(\varrho_0, \varrho_0\boldsymbol{u}_0) : \mathbf{R}^3 \to \Omega_1$ satisfying $\varrho_0 - 1 \in H^s(\mathbf{R}^3)$ and $\boldsymbol{u}_0 \in H^s(\mathbf{R}^3)$. Let $f_0 : \mathbf{R}^3\times\mathbf{R}^3 \to \mathbf{R}_+$ be a function in $\mathscr{C}^1_c(\mathbf{R}^3\times\mathbf{R}^3) \cap H^s(\mathbf{R}^3\times\mathbf{R}^3)$ satisfying*

$$\|f_0\|_{L^\infty} < \frac{1}{2^4\|w\|_{L^1} V_M(0)^3}.$$

with $V_M(0) = \sup\limits_{(\boldsymbol{x},\boldsymbol{v})\in\mathbf{R}^3\times\mathbf{R}^3, f_0(\boldsymbol{x},\boldsymbol{v})>0} |\boldsymbol{v}|$.

Then, one can find $T \in]0,1[$ such that there exists a solution $(\varrho, \varrho\boldsymbol{u}, f)$ of the system (2.17) belonging to $\mathscr{C}^1([0,T]\times\mathbf{R}^3,\Omega_2)\times\mathscr{C}^1_c([0,T]\times\mathbf{R}^3\times\mathbf{R}^3,\mathbf{R}_+)$. Moreover this solution is unique and it satisfies

$$C \le \alpha(t,\boldsymbol{x}) \le 1, \quad t\in[0,T], \quad \boldsymbol{x}\in\mathbf{R}^3.$$

.

Remark 2.1.6. *This result could be extended to the whole system (4.4) with an energy equation. It could also be extended if p a sufficiently well-behaved function [12] not necessarily a power function of ϱ. For example, it works for $p \in \mathscr{C}(\mathbf{R}^+)\cap\mathscr{C}^\infty(\mathbf{R}^+\setminus\{0\})$. It is also true if w is a non-negative convolution kernel in* $\mathrm{BV}(\mathbf{R}^3)$.

The proof is based on the following idea. We want to combine classical theory of local-in-time solutions for symmetrisable hyperbolic systems of conservation laws (see [87]) and the theory of characteristics for the control of H^s norms of f and its support (like for the Vlasov-Poisson system [102]). This idea has already been used in [12, 92]. Finding appropriate symmetrisers for the system (2.17) is not obvious. Our strategy is to expand the derivatives on the left-hand-side of the equations, then to treat the terms containing derivatives of α as source terms. The left-hand-side then becomes the well-known Euler equations of gas dynamics for which a symmetriser is classical. To apply the proof [87], the source term needs to be of degree 0, that is, no derivative. An issue is that the initial thick sprays equations (4.1) contains derivatives in the source term. This is an asset of the convolution operator in systems (4.4) and (2.17), because it avoids the loss of regularity in the source term in the original thick spray equations (4.1).

Proposition 2.1.7. *The system (2.17) is equivalent, for strong solution verifying $\alpha > 0$, to*

$$\begin{cases} \partial_t \mathbf{U} + \nabla_x \cdot \mathbf{F}(\mathbf{U}) = b(\mathbf{U}, f) \\ \partial_t f + \boldsymbol{v} \cdot \nabla_x f - \langle \nabla_x p \rangle \cdot \nabla_v f = 0, \end{cases}$$

with

$$\mathbf{U} = \begin{pmatrix} \varrho \\ \varrho \boldsymbol{u} \end{pmatrix}, \quad \mathbf{F}(\mathbf{U}) = \begin{pmatrix} \varrho \boldsymbol{u} \\ \varrho \boldsymbol{u} \otimes \boldsymbol{u} + p\mathrm{Id} \end{pmatrix},$$

$$\text{and } b(\mathbf{U}, f) = \begin{pmatrix} \dfrac{\varrho \boldsymbol{u} \cdot \nabla_x \int_{\mathbf{R}^3} \langle f \rangle \,\mathrm{d}v}{1 - \int_{\mathbf{R}^3} \langle f \rangle \,\mathrm{d}v} - \dfrac{\varrho \nabla_x \cdot \int_{\mathbf{R}^3} \langle f \rangle \boldsymbol{v} \,\mathrm{d}v}{1 - \int_{\mathbf{R}^3} \langle f \rangle \,\mathrm{d}v} \\ \dfrac{\varrho \boldsymbol{u} \otimes \boldsymbol{u} \int_{\mathbf{R}^3} \nabla_x \langle f \rangle \,\mathrm{d}v}{1 - \int_{\mathbf{R}^3} \langle f \rangle \,\mathrm{d}v} - \dfrac{\varrho \boldsymbol{u} \nabla_x \cdot \int_{\mathbf{R}^3} \langle f \rangle \boldsymbol{v} \,\mathrm{d}v}{1 - \int_{\mathbf{R}^3} \langle f \rangle \,\mathrm{d}v} \end{pmatrix}.$$

Furthermore, the hyperbolic part of the system can be symmetrized as

$$S(\mathbf{U}) \partial_t \mathbf{U} + \sum_{i=1}^{3} (SA_i)(\mathbf{U}) \partial_{x_i} \mathbf{U} = S(\mathbf{U}) b(\mathbf{U}, f),$$

with

$$S(\mathbf{U}) = \begin{pmatrix} p'(\varrho) + |\boldsymbol{u}|^2 & -\boldsymbol{u}^T \\ -\boldsymbol{u} & \mathrm{Id} \end{pmatrix}.$$

See [12] for the expression of the matrices A_i. Moreover, the symmetric positive definite matrix $S(\mathbf{U})$ is a smooth function of $\mathbf{U}$. For all relatively compact set Ω_1, there exists a constant $c > 0$ such that $\forall \mathbf{U} \in \Omega_1$

$$c\mathrm{Id} \leq S(\mathbf{U}) \leq c^{-1}\mathrm{Id}.$$

Finally, the matrices $SA_i(\mathbf{U})$ are symmetric.

Proof. First, notice that from the Vlasov equation in (2.17), one has, by first applying the convolution operator $\langle \cdot \rangle$ and integrating in v

$$\partial_t \alpha = \nabla_x \cdot \int_{\mathbf{R}^3} \langle f \rangle \boldsymbol{v} \,\mathrm{d}v.$$

Taking the first equation of (2.17), one has

$$\varrho \partial_t \alpha + \alpha \partial_t \varrho + \alpha \nabla_x \cdot (\varrho \boldsymbol{u}) + \varrho \boldsymbol{u} \cdot \nabla_x \alpha = 0,$$

then, by moving to the right-hand-side the terms containing derivatives of α, and dividing by $\alpha = 1 - \int_{\mathbf{R}^3} \langle f \rangle \,\mathrm{d}v$, one obtains

$$\partial_t \varrho + \nabla_x \cdot (\varrho \boldsymbol{u}) = \frac{\varrho \boldsymbol{u} \cdot \nabla_x \int_{\mathbf{R}^3} \langle f \rangle \,\mathrm{d}v}{1 - \int_{\mathbf{R}^3} \langle f \rangle \,\mathrm{d}v} - \frac{\varrho \nabla_x \cdot \int_{\mathbf{R}^3} \langle f \rangle \boldsymbol{v} \,\mathrm{d}v}{1 - \int_{\mathbf{R}^3} \langle f \rangle \,\mathrm{d}v}.$$

Then, first writting the second equation of (2.17) as

$$\partial_t (\alpha \varrho \boldsymbol{u}) + \nabla_x \cdot (\alpha \varrho \boldsymbol{u} \otimes \boldsymbol{u}) + \alpha \nabla_x p = 0,$$

and by using similar computations as before, one is led to

$$\partial_t (\varrho \boldsymbol{u}) + \nabla_x \cdot (\varrho \boldsymbol{u} \otimes \boldsymbol{u}) + \nabla_x p = \frac{\varrho \boldsymbol{u} \otimes \boldsymbol{u} \int_{\mathbf{R}^3} \nabla_x \langle f \rangle \,\mathrm{d}v}{1 - \int_{\mathbf{R}^3} \langle f \rangle \,\mathrm{d}v} - \frac{\varrho \boldsymbol{u} \nabla_x \cdot \int_{\mathbf{R}^3} \langle f \rangle \boldsymbol{v} \,\mathrm{d}v}{1 - \int_{\mathbf{R}^3} \langle f \rangle \,\mathrm{d}v}.$$

For the symmetrisation of the system, we refer to [12]. $\square$

We now introduce some notations. Let ϱ be a smooth enough function, then the Vlasov equation in (2.17) is a linear transport equation

$$\partial_t f + \boldsymbol{v} \cdot \nabla_x f - \langle \nabla_x \varrho^\gamma \rangle \cdot \nabla_v f = 0.$$

It has a unique solution, computed by the method of characteristics

$$f(t,\boldsymbol{x},\boldsymbol{v}) = f_0(\mathbf{X}(0;\boldsymbol{x},\boldsymbol{v},t),\mathbf{V}(0;\boldsymbol{x},\boldsymbol{v},t)),$$

where the characteristic curves are defined by

$$\begin{aligned}
\frac{\mathrm{d}\mathbf{X}}{\mathrm{d}t}(t;\boldsymbol{x},\boldsymbol{v},s) &= \mathbf{V}(t;\boldsymbol{x},\boldsymbol{v},s),\\
\mathbf{X}(s;\boldsymbol{x},\boldsymbol{v},s) &= \boldsymbol{x},\\
\frac{\mathrm{d}\mathbf{V}}{\mathrm{d}t}(t;\boldsymbol{x},\boldsymbol{v},s) &= -\langle \nabla_x \varrho^\gamma(\mathbf{X}(t;\boldsymbol{x},\boldsymbol{v},s),t)\rangle,\\
\mathbf{V}(s;\boldsymbol{x},\boldsymbol{v},s) &= \boldsymbol{v}.
\end{aligned}$$

If f_0 has a compact support, then $f(t,\cdot,\cdot)$ also has a compact support for all t. We denote

$$X_M(t) = \sup_{(\boldsymbol{x},\boldsymbol{v})\in\mathbf{R}^3\times\mathbf{R}^3, f(t,\boldsymbol{x},\boldsymbol{v})>0} |\boldsymbol{x}|,$$

and

$$V_M(t) = \sup_{(\boldsymbol{x},\boldsymbol{v})\in\mathbf{R}^3\times\mathbf{R}^3, f(t,\boldsymbol{x},\boldsymbol{v})>0} |\boldsymbol{v}|.$$

Then the following holds: $\operatorname{supp} f(t,\cdot,\cdot) \subset B(0,X_M(t)) \times B(0,V_M(t))$.

In the following, we will use the following notations ($s \in \mathbf{N}$, $T > 0$, and α is a multi-index):

$$\begin{aligned}
\|h\|_{H^s} = \sum_{|\alpha|\le s} \|\partial^\alpha h\|_{L^2} &= \sum_{|\alpha|\le s} \sqrt{\int_{\mathbf{R}^3} |\partial^\alpha h(\boldsymbol{x})|^2 \,\mathrm{d}x},\\
\|h\|_{H^s,T} &= \sup_{t\in[0,T]} \|h\|_{H^s}(t),\\
\|h\|_{L^2,T} &= \sup_{t\in[0,T]} \|h\|_{L^2}(t).
\end{aligned}$$

In particular, the notation ∂^α will always denote a derivative in the x variable. Those notations will sometimes be used for function $h = h(x,v)$, and in this case the norms are always on both variables.

2.1.6 Iterative approximation scheme

We explain here the main steps of the proof of Theorem 2.1.5. We fix $s \in \mathbf{N}$ an integer such that $s > 3/2 + 1$. Constructing a solution of the system (2.17) is equivalent to constructing a solution to the symmetrised quasi-linear system

$$\begin{cases}
S(\mathbf{U})\partial_t \mathbf{U} + \displaystyle\sum_{i=1}^{3} (SA_i)(\mathbf{U})\partial_{x_i}\mathbf{U} &= S(\mathbf{U})b(\mathbf{U},f),\\
\partial_t f + \boldsymbol{v}\cdot\nabla_x f - \langle \nabla_x p\rangle \cdot \nabla_v f &= 0.
\end{cases} \tag{2.18}$$

The proof follows a classical iterarive scheme. We first work with smooth and compactly supported initial data

$$\varrho_0 - 1 \in \mathcal{D}(\mathbf{R}^3), \quad \boldsymbol{u}_0 \in \mathcal{D}(\mathbf{R}^3), \quad f_0 \in \mathcal{D}(\mathbf{R}^3 \times \mathbf{R}^3). \tag{2.19}$$

Later, we use a mollification process to prove the case of all initial data in H^s. We require that f_0 is small, more precisely, we assume

$$\|f_0\|_{L^\infty} < \frac{1}{2^4 \|w\|_{L^1} V_M(0)^3}. \tag{2.20}$$

We denote $\Omega = (0, +\infty) \times \mathbf{R}^3$ and Ω_1 a relatively compact open set of Ω such that

$$\mathbf{U}_0 := \begin{pmatrix} \varrho_0 \\ \varrho_0 \boldsymbol{u}_0 \end{pmatrix} \in \Omega_1.$$

We will construct the solution of (2.18) through the following iterative process: for $k = 0$, one sets $\theta_0 = +\infty$ and $(\mathbf{U}^0(t), f^0(t)) = (\mathbf{U}_0, f_0)$. Then, given $\theta_k > 0$, and functions $\mathbf{U}^k$ and f^k that live on the time interval $[0, \theta_k)$, one defines $(\mathbf{U}^{k+1}, f^{k+1})$ as the solution of the linear system

$$S(\mathbf{U}^k)\partial_t \mathbf{U}^{k+1} + \sum_{i=1}^{3} (SA_i)(\mathbf{U}^k)\partial_{x_i} \mathbf{U}^{k+1} = S(\mathbf{U}^k) b(\mathbf{U}^k, f^k), \tag{2.21}$$

$$\mathbf{U}^{k+1}(\boldsymbol{x}, 0) = \mathbf{U}_0(\boldsymbol{x}), \tag{2.22}$$

$$\partial_t f^{k+1} + \boldsymbol{v} \cdot \nabla_x f^{k+1} - \langle \nabla_x p^k \rangle \cdot \nabla_v f^{k+1} = 0, \tag{2.23}$$

$$f^{k+1}(\boldsymbol{x}, \boldsymbol{v}, 0) = f_0(\boldsymbol{x}, \boldsymbol{v}). \tag{2.24}$$

For now, it is not obvious that the sequence $(\mathbf{U}^k, f^k)_{k \in \mathbf{N}}$ is well-defined.

Let Ω_2 a relatively compact open subset of $\mathbf{R}^3$ such that $\overline{\Omega_1} \subset \Omega_2$. From the Sobolev embedding for $s > 3/2 + 1$, $H^s(\mathbf{R}^3) \hookrightarrow L^\infty(\mathbf{R}^3)$, there exists a constant $R > 0$ depending on Ω_1, Ω_2 and s, such that, if $\|\mathbf{U} - \mathbf{U}_0\|_{H^s} \leq R$, then $\mathbf{U} \in \Omega_2$. Then, one defines θ_{k+1} as the supremum of times $\theta < \theta_k$ such that $\|\mathbf{U}^{k+1} - \mathbf{U}_0\|_{H^s, \theta} \leq R$.

The system (2.21) is linear in $\mathbf{U}^{k+1}$, symmetric and has smooth coefficients on $[0, \theta_k)$, therefore it admits a smooth solution on $[0, \theta_k)$ [87]. For equation (2.23), since it is a linear transport equation with smooth coefficients on $[0, \theta_k)$, it admits a smooth solution that can be explicitly computed by the method of characteristics. Finally, $\theta_{k+1} > 0$ since $\mathbf{U}^{k+1}$ is smooth, and $\mathbf{U}_0 \in \Omega_1$. The sequence $(\mathbf{U}^k, f^k)_{k \in \mathbf{N}}$ is then well-defined.

We will restrict further the lifetime of the solution. One defines T_k as the supremum of times $T \in [0, \theta_k)$ such that

$$\|\mathbf{U}^k - \mathbf{U}_0\|_{H^s, T} \leq R, \tag{2.25}$$

$$\forall t \in [0, T], \quad X_M^k(t) \leq 2X_M(0), \tag{2.26}$$

$$\forall t \in [0, T], \quad V_M^k(t) \leq 2V_M(0), \tag{2.27}$$

$$\left\| \int_{\mathbf{R}^3} \langle f^k \rangle \, \mathrm{d}v \right\|_{L^\infty, T} \leq 2^4 \|w\|_{L^1} V_M(0)^3 \|f_0\|_{L^\infty}, \tag{2.28}$$

and such that $T_{k+1} \leq T_k$. In particular,

$$\left\| \frac{1}{1 - \int_{\mathbf{R}^3} \langle f^k \rangle \, \mathrm{d}v} \right\|_{L^\infty} \leq \left\| \frac{1}{1 - 2^4 \|w\|_{L^1} V_M(0)^3 f_0} \right\|_{L^\infty}, \tag{2.29}$$

and one considers the sequence $(\mathbf{U}^k, f^k)_{k\in\mathbf{N}}$ on the time interval $[0, T_k)$. Note that the right-hand-side of (2.29) is finite thanks to the hypothesis (2.20). We emphasize that the number 2 in the inequalities (2.26)-(2.28) serves only a cosmetic purpose. One could replace the number 2 by any $a > 1$ and it would not change the proof.

The proof is then made of three parts:

- First, we prove that there exists a time $T_\star > 0$ such that $T_k \geq T_\star$ for all $k \in \mathbf{N}$. This is the subject of the Proposition 2.1.16, for which we will need lemmas 2.1.13, 2.1.14 and 2.1.15. Note that, without this result, the sequence of lifespan $(T_k)_{k\in\mathbf{N}}$ could converge to 0. This is the subject of Section 2.1.7
- Next, we prove in Proposition 2.1.17 that the sequence $(\mathbf{U}^k, f^k)_{k\in\mathbf{N}}$ converges in the space $L^\infty(0, T_{\star\star}; L^2(\mathbf{R}^3)) \times L^\infty(0, T_{\star\star}; L^2(\mathbf{R}^3 \times \mathbf{R}^3))$, where $0 < T_{\star\star} \leq T_\star$. The proof of this Proposition is found in Section 2.1.8
- Finally, we conclude the proof of Theorem 2.1.5 and we prove that the limit $(\mathbf{U}, f)$ is a solution of (2.18) in $\mathscr{C}^1([0,T] \times \mathbf{R}^3, \Omega_2) \times \mathscr{C}^1_c([0,T] \times \mathbf{R}^3 \times \mathbf{R}^3, \mathbf{R}_+)$ and the solution is unique. We also explain why the proof works in the case of all initial data in H^s.

2.1.7 Preliminary lemmas and a priori estimates

2.1.7.1 Preliminary lemmas

We write some preliminary lemmas which we use in this work.

Lemma 2.1.8. *Let $S, A_i \in \mathscr{C}^1([0,T) \times \mathbf{R}^3, \mathcal{M}_3(\mathbf{R}))$ be smooth matrices such that S and SA_i are symmetric, We suppose moreover that there exists $c > 0$ such that $c\mathrm{Id} \leq S(t, \boldsymbol{x}) \leq c^{-1}\mathrm{Id}$. Then, all smooth and compactly supported vectors $\mathbf{W}$ and $\mathbf{F}$ satisfying the equation $S\partial_t \mathbf{W} + \sum_i SA_i \partial_{x_i} \mathbf{W} = \mathbf{F}$ with the initial data $\mathbf{W}(0, \boldsymbol{x}) = \mathbf{W}_0(\boldsymbol{x})$ verify the energy estimate*

$$\|\mathbf{W}\|_{L^2} \leq c^{-1} \Bigg(\|\mathbf{W}_0\|_{L^2} + \frac{1}{2} \left\| \partial_t S + \sum_i \partial_{x_i}(SA_i) \right\|_{L^\infty, T} \int_0^t \|\mathbf{W}\|_{L^2}(\tau) \, \mathrm{d}\tau + \int_0^t \|\mathbf{F}\|_{L^2}(\tau) \, \mathrm{d}\tau \Bigg). \tag{2.30}$$

Proof. By multiplying by $\mathbf{W}^T$ and integrating, one has

$$\frac{1}{2}\partial_t \int_{\mathbf{R}^3} \mathbf{W}^T S \mathbf{W} \, \mathrm{d}x = \frac{1}{2} \int_{\mathbf{R}^3} \mathbf{W}^T (\partial_t S + \sum_i \partial_{x_i}(SA_i)) \mathbf{W} \, \mathrm{d}x + \int_{\mathbf{R}^3} \mathbf{W}^T \mathbf{F} \, \mathrm{d}x,$$

then one integrates with respect to t and uses the estimate $\mathbf{W}^T S \mathbf{W} \geq c \mathbf{W}^T \mathbf{W}$. □

Lemma 2.1.9 (See [87]). *Let $\boldsymbol{g} : \Omega \subset \mathbf{R}^3 \to \mathbf{R}^3$ a smooth vector-valued function, $\boldsymbol{u} : \mathbf{R}^3 \to \Omega_1 \subset \Omega$ with Ω_1 relatively compact in Ω. Assume that $\boldsymbol{u} \in H^s(\mathbf{R}^3) \cap L^\infty(\mathbf{R}^3)$. Then for $|\alpha| \leq s$, one has the inequality*

$$\|\partial^\alpha \boldsymbol{g}(\boldsymbol{u})\|_{L^2} \leq C(s) \sup_{\boldsymbol{v}\in\Omega_1} \left(\sup_{|\beta|\leq s-1} |\partial^\beta \boldsymbol{g}(\boldsymbol{v})| \right) \|\boldsymbol{u}\|_{L^\infty}^{s-1} \|\boldsymbol{u}\|_{H^s}.$$

Lemma 2.1.10 (See [87]). *Let $f,g \in H^s(\mathbf{R}^3) \cap L^\infty(\mathbf{R}^3)$, one has the inequality*

$$\|\partial^\alpha (fg)\|_{L^2} \leq C(s)(\|f\|_{L^\infty}\|g\|_{H^s} + \|f\|_{H^s}\|g\|_{L^\infty}).$$

Lemma 2.1.11. *Let $f \in H^s(\mathbf{R}^3)$ and $g \in \mathrm{BV}(\mathbf{R}^3)$. Then*

$$\|\nabla (f \star g)\|_{H^s} \leq \|f\|_{H^s}\mathrm{TV}(g)$$

and

$$\|\nabla (f \star g)\|_{L^\infty} \leq \|f\|_{L^\infty}\mathrm{TV}(g).$$

Proof. The proof is done via an approximation argument. The function g belongs to $\mathrm{BV}(\mathbf{R}^3)$, therefore [56] (Theorem 5.3), there exists a sequence $(g_k)_{k\in\mathbf{N}} \in \mathrm{BV}(\mathbf{R}^3) \cap \mathscr{C}^\infty(\mathbf{R}^3)$ such that $g_k \xrightarrow{L^1} g$ and $\mathrm{TV}(g_k) \to \mathrm{TV}(g)$. In particular, $g_k \in W^{1,1}(\mathbf{R}^3)$ for all k, and $\mathrm{TV}(g_k) = \|\nabla g_k\|_{L^1} \to \mathrm{TV}(g)$. Applying Young's convolution inequality to f and g_k, we obtain $\|\nabla (f \star g_k)\|_{L^2} \leq \|f\|_{L^2}\|\nabla g_k\|_{L^1}$, passing to the limit we obtain $\|\nabla (f \star g)\|_{L^2} \leq \|f\|_{L^2}\mathrm{TV}(g)$. Replacing f by $\partial^\alpha f$ with $|\alpha| \leq s$ in the previous inequality, we obtain $\|\nabla (f \star g)\|_{H^s} \leq \|f\|_{H^s}\mathrm{TV}(g)$. The second inequality follow directly from the definition of the total variation.

□

Lemma 2.1.12 (See [87]). *Let $h \in H^s(\mathbf{R}^3)$, $\nabla h \in L^\infty(\mathbf{R}^3)$, $g \in H^{s-1}(\mathbf{R}^3) \cap L^\infty(\mathbf{R}^3)$ and $|\alpha| \leq s$, then*

$$\|\partial^\alpha (hg) - h\partial^\alpha g\|_{L^2} \leq C(s)\left(\|\nabla h\|_{L^\infty}\|g\|_{H^{s-1}} + \|g\|_{L^\infty}\|h\|_{H^s}\right).$$

2.1.7.2 A priori estimates

The goal is to prove that the sequence $(T_k)_{k\in\mathbf{N}}$ has a strictly positive lower bound $T_\star$. In all this section, one considers initial data such that (2.19)-(2.20) hold and define the sequences θ_k, $\mathbf{U}^k$, f^k by (2.21)-(2.24) and T_k by (2.25)-(2.27).

Lemma 2.1.13. *For all $k \geq 0$,*

$$\|\partial_t \mathbf{U}^{k+1}\|_{H^{s-1},T_{k+1}} \leq C(s,f_0,\mathbf{U}_0,\Omega_2,R,w)\mathrm{TV}(w). \tag{2.31}$$

Proof. Let $t \in [0, T_{k+1})$, then

$$\|\partial_t \mathbf{U}^{k+1}\|_{H^{s-1}}(t) \le \sum_i \|A_i(\mathbf{U}^k)\partial_{x_i}\mathbf{U}^{k+1}\|_{H^{s-1},T_{k+1}} + \|b(\mathbf{U}^k,f^k)\|_{H^{s-1},T_{k+1}}.$$

One has to control each term, let's start with b. One has,

$$\|b(\mathbf{U}^k,f^k)\|_{H^{s-1},T_{k+1}} = \sum_{|\alpha|\le s-1} \left\| \begin{pmatrix} \partial^\alpha \left(\dfrac{\varrho^k \int_{\mathbf{R}^3}(\boldsymbol{u}^k - \boldsymbol{v})\cdot\nabla_x\langle f^k\rangle \,\mathrm{d}v}{1-\int_{\mathbf{R}^3}\langle f^k\rangle \,\mathrm{d}v} \right) \\ \partial^\alpha \left(\dfrac{\varrho^k \boldsymbol{u}^k \int_{\mathbf{R}^3}(\boldsymbol{u}^k - \boldsymbol{v})\cdot\nabla_x\langle f^k\rangle \,\mathrm{d}v}{1-\int_{\mathbf{R}^3}\langle f^k\rangle \,\mathrm{d}v} \right) \end{pmatrix} \right\|_{L^2,T_{k+1}}.$$

Applying lemma 2.1.10 for $|\alpha| \le s-1$,

$$\begin{aligned} \left\| \partial^\alpha \left(\frac{\varrho^k \boldsymbol{u}^k \cdot \int_{\mathbf{R}^3}\nabla_x\langle f^k\rangle \,\mathrm{d}v}{1-\int_{\mathbf{R}^3}\langle f^k\rangle \,\mathrm{d}v} \right)\right\|_{L^2} \le C(s) \Bigg(&\|\varrho^k\boldsymbol{u}^k\|_{H^{s-1}} \left\| \frac{\int_{\mathbf{R}^3}\nabla_x\langle f^k\rangle \,\mathrm{d}v}{1-\int_{\mathbf{R}^3}\langle f^k\rangle \,\mathrm{d}v}\right\|_{L^\infty} \\ &+ \|\varrho^k\boldsymbol{u}^k\|_{L^\infty} \left\| \frac{\int_{\mathbf{R}^3}\nabla_x\langle f^k\rangle \,\mathrm{d}v}{1-\int_{\mathbf{R}^3}\langle f^k\rangle \,\mathrm{d}v}\right\|_{H^{s-1}} \Bigg). \end{aligned} \tag{2.32}$$

Thanks to (2.25), one has

$$\|\varrho^k\boldsymbol{u}^k\|_{H^{s-1}} \le \|\mathbf{U}^k\|_{H^{s-1}} \le \|\mathbf{U}_0\|_{H^{s-1}} + \|\mathbf{U}^k - \mathbf{U}_0\|_{H^{s-1}} \le C(\mathbf{U}_0,R).$$

Thanks to the Sobolev embedding $H^{s-1}(\mathbf{R}^3) \hookrightarrow L^\infty(\mathbf{R}^3)$, one has

$$\|\varrho^k\boldsymbol{u}^k\|_{L^\infty} \le C(\Omega_2)\|\varrho^k\boldsymbol{u}^k\|_{H^{s-1}} \le C(\Omega_2,\mathbf{U}_0,R).$$

Thanks to (2.25)-(2.28) and lemma 2.1.11, one has

$$\begin{aligned} \left\| \int_{\mathbf{R}^3} \nabla_x\langle f^k\rangle \,\mathrm{d}v\right\|_{L^\infty} &\le \mathrm{TV}(w) \left\| \int_{\mathbf{R}^3} f^k \,\mathrm{d}v \right\|_{L^\infty} \\ &\le \mathrm{TV}(w) 2^3 (V_M^k)^3 \|f^k\|_{L^\infty} \\ &\le \mathrm{TV}(w) 2^3 (V_M^k)^3 \|f_0\|_{L^\infty} \\ &\le C(f_0)\mathrm{TV}(w). \end{aligned}$$

So that, using (2.20), (2.29) and the previous inequality

$$\left\| \frac{\int_{\mathbf{R}^3}\nabla_x\langle f^k\rangle \,\mathrm{d}v}{1-\int_{\mathbf{R}^3}\langle f^k\rangle \,\mathrm{d}v}\right\|_{L^\infty} \le C(f_0,w)\mathrm{TV}(w).$$

It remains to bound the last term in (2.32) $\left\| \frac{\int_{\mathbf{R}^3}\nabla_x\langle f^k\rangle \,\mathrm{d}v}{1-\int_{\mathbf{R}^3}\langle f^k\rangle \,\mathrm{d}v}\right\|_{H^{s-1}}$. Again applying lemma 2.1.10 and lemma 2.1.11, one has for $|\alpha| \le s-1$:

$$\begin{aligned} &\left\| \partial^\alpha \left(\frac{\int_{\mathbf{R}^3}\nabla_x\langle f^k\rangle \,\mathrm{d}v}{1-\int_{\mathbf{R}^3}\langle f^k\rangle \,\mathrm{d}v}\right)\right\|_{L^2} \\ &\le C(s) \left(\left\| \int_{\mathbf{R}^3}\nabla_x\langle f^k\rangle \,\mathrm{d}v \right\|_{H^{s-1}} \left\| \frac{1}{1-\int_{\mathbf{R}^3}\langle f^k\rangle \,\mathrm{d}v}\right\|_{L^\infty} + \left\| \int_{\mathbf{R}^3}\nabla_x\langle f^k\rangle \,\mathrm{d}v \right\|_{L^\infty} \left\| \frac{1}{1-\int_{\mathbf{R}^3}\langle f^k\rangle \,\mathrm{d}v}\right\|_{H^{s-1}} \right) \\ &\le C(s) \left(C(f_0,w)\mathrm{TV}(w) + C(f_0)\mathrm{TV}(w) \left\| \frac{1}{1-\int_{\mathbf{R}^3}\langle f^k\rangle \,\mathrm{d}v}\right\|_{H^{s-1}} \right). \end{aligned}$$

For the term $\left\|\frac{1}{1-\int_{\mathbf{R}^3}\langle f^k\rangle\,\mathrm{d}v}\right\|_{H^{s-1}}$, one has

$$\begin{aligned}\left\|\frac{1}{1-\int_{\mathbf{R}^3}\langle f^k\rangle\,\mathrm{d}v}\right\|_{H^{s-1}} &= \sum_{|\alpha|\le s-1}\left\|\partial^\alpha\left(\frac{1}{1-\int_{\mathbf{R}^3}\langle f^k\rangle\,\mathrm{d}v}\right)\right\|_{L^2}\\ &= \sum_{|\alpha|\le s-1}\left\|\frac{P_\alpha}{(1-\int_{\mathbf{R}^3}\langle f^k\rangle\,\mathrm{d}v)^{q(\alpha)}}\right\|_{L^2},\end{aligned}$$

where P_α is a polynomial in $\partial^\alpha(1-\int_{\mathbf{R}^3}\langle f^k\rangle\,\mathrm{d}v)$, and $q(\alpha)$ is an integer that depends on α. One can bound the numerator P_α thanks to the inequality

$$\begin{aligned}\left\|\int_{\mathbf{R}^3}\langle f^k\rangle\,\mathrm{d}v\right\|_{H^s} &\le (V_M^k)^{3/2}\|\langle f^k\rangle\|_{H^s}\\ &\le \mathrm{TV}(w)C(f_0),\end{aligned}$$

where we used lemma 2.1.11, and the denominator is bounded thanks to (2.28). As a consequence, one obtains

$$\left\|\partial^\alpha\left(\frac{\varrho^k\boldsymbol{u}^k\cdot\int_{\mathbf{R}^3}\nabla_x\langle f^k\rangle\,\mathrm{d}v}{1-\int_{\mathbf{R}^3}\langle f^k\rangle\,\mathrm{d}v}\right)\right\|_{L^2}\le C(\mathbf{U}_0,f_0,\Omega_2,R,w)\mathrm{TV}(w). \tag{2.33}$$

Next, one has the term

$$\begin{aligned}\left\|\partial^\alpha\left(\frac{\varrho^k\int_{\mathbf{R}^3}\boldsymbol{v}\cdot\nabla_x\langle f^k\rangle\,\mathrm{d}v}{1-\int_{\mathbf{R}^3}\langle f^k\rangle\,\mathrm{d}v}\right)\right\|_{L^2} \le& C(s)\left(\|\varrho^k\|_{H^{s-1}}\left\|\frac{\int_{\mathbf{R}^3}\boldsymbol{v}\cdot\nabla_x\langle f^k\rangle\,\mathrm{d}v}{1-\int_{\mathbf{R}^3}\langle f^k\rangle\,\mathrm{d}v}\right\|_{L^\infty}\right.\\ &\left.+\|\varrho^k\|_{L^\infty}\left\|\frac{\int_{\mathbf{R}^3}\boldsymbol{v}\cdot\nabla_x\langle f^k\rangle\,\mathrm{d}v}{1-\int_{\mathbf{R}^3}\langle f^k\rangle\,\mathrm{d}v}\right\|_{H^{s-1}}\right).\end{aligned}$$

We have, using lemma 2.1.11

$$\left\|\int_{\mathbf{R}^3}\boldsymbol{v}\cdot\nabla_x\langle f^k\rangle\,\mathrm{d}v\right\|_{L^\infty}\le 2^3\|f^k\|_{L^\infty}(V_M^k)^4\mathrm{TV}(w)\le C(f_0,w)\mathrm{TV}(w),$$

and,

$$\left\|\int_{\mathbf{R}^3}\boldsymbol{v}\cdot\nabla_x\langle f^k\rangle\,\mathrm{d}v\right\|_{H^{s-1}}\le C(V_M)\left\|\int_{\mathbf{R}^3}\nabla_x\langle f^k\rangle\,\mathrm{d}v\right\|_{H^{s-1}}\le C(f_0)\mathrm{TV}(w),$$

so

$$\left\|\partial^\alpha\left(\frac{\varrho^k\int_{\mathbf{R}^3}\boldsymbol{v}\cdot\nabla_x\langle f^k\rangle\,\mathrm{d}v}{1-\int_{\mathbf{R}^3}\langle f^k\rangle\,\mathrm{d}v}\right)\right\|_{L^2}\le C(\mathbf{U}_0,f_0,\Omega_2,R,w)\mathrm{TV}(w). \tag{2.34}$$

It is clear thanks to the previous inequalities that we have the bound

$$\left\|\frac{\varrho^k\boldsymbol{u}^k\left(\int_{\mathbf{R}^3}\boldsymbol{v}\cdot\nabla_x\langle f^k\rangle\,\mathrm{d}v\right)}{1-\int_{\mathbf{R}^3}\langle f^k\rangle\,\mathrm{d}v}\right\|_{H^{s-1}}\le C(s,f_0,R,\mathbf{U}_0,\Omega_2,w)\mathrm{TV}(w). \tag{2.35}$$

For the term

$$\left\|\frac{\varrho^k\boldsymbol{u}^k\otimes\boldsymbol{u}^k\int_{\mathbf{R}^3}\nabla_x\langle f^k\rangle\,\mathrm{d}v}{1-\int_{\mathbf{R}^3}\langle f^k\rangle\,\mathrm{d}v}\right\|_{H^{s-1}}=\left\|\frac{\varrho^k\boldsymbol{u}^k\left(\boldsymbol{u}^k\cdot\int_{\mathbf{R}^3}\nabla_x\langle f^k\rangle\,\mathrm{d}v\right)}{1-\int_{\mathbf{R}^3}\langle f^k\rangle\,\mathrm{d}v}\right\|_{H^{s-1}},$$

we use the fact that Ω_2 is relatively compact and so ϱ^k is bounded from below by a constant that depends only on Ω_2. Writing

$$\begin{aligned}\left\|\partial^\alpha\left(\frac{\varrho^k\boldsymbol{u}^k\left(\boldsymbol{u}^k\cdot\int_{\mathbf{R}^3}\nabla_x\langle f^k\rangle\,\mathrm{d}v\right)}{1-\int_{\mathbf{R}^3}\langle f^k\rangle\,\mathrm{d}v}\right)\right\|_{L^2}\\
\leq C(s)\Bigg(\|\varrho^k\boldsymbol{u}^k\|_{H^{s-1}}\left\|\frac{\boldsymbol{u}^k\cdot\int_{\mathbf{R}^3}\nabla_x\langle f^k\rangle\,\mathrm{d}v}{1-\int_{\mathbf{R}^3}\langle f^k\rangle\,\mathrm{d}v}\right\|_{L^\infty}\\
+\|\varrho^k\boldsymbol{u}^k\|_{L^\infty}\left\|\frac{\boldsymbol{u}^k\cdot\int_{\mathbf{R}^3}\nabla_x\langle f^k\rangle\,\mathrm{d}v}{1-\int_{\mathbf{R}^3}\langle f^k\rangle\,\mathrm{d}v}\right\|_{H^{s-1}}\Bigg),\end{aligned}$$

and

$$\|\boldsymbol{u}^k\|_{L^\infty}=\left\|\frac{\varrho^k\boldsymbol{u}^k}{\varrho^k}\right\|_{L^\infty}\leq C(\Omega_2)\|\varrho^k\boldsymbol{u}^k\|_{L^\infty},$$

one obtains

$$\left\|\frac{\boldsymbol{u}^k\cdot\int_{\mathbf{R}^3}\nabla_x\langle f^k\rangle\,\mathrm{d}v}{1-\int_{\mathbf{R}^3}\langle f^k\rangle\,\mathrm{d}v}\right\|_{L^\infty}\leq C(s,\mathbf{U}_0,f_0,R,\Omega_2,w)\mathrm{TV}(w).$$

Therefore

$$\begin{aligned}\left\|\partial^\alpha\left(\frac{\boldsymbol{u}^k\cdot\int_{\mathbf{R}^3}\nabla_x\langle f^k\rangle\,\mathrm{d}v}{1-\int_{\mathbf{R}^3}\langle f^k\rangle\,\mathrm{d}v}\right)\right\|_{L^2}\leq C(s)\Bigg(\|\boldsymbol{u}^k\|_{H^{s-1}}\left\|\frac{\int_{\mathbf{R}^3}\nabla_x\langle f^k\rangle\,\mathrm{d}v}{1-\int_{\mathbf{R}^3}\langle f^k\rangle\,\mathrm{d}v}\right\|_{L^\infty}\\
+\|\boldsymbol{u}^k\|_{L^\infty}\left\|\frac{\int_{\mathbf{R}^3}\nabla_x\langle f^k\rangle\,\mathrm{d}v}{1-\int_{\mathbf{R}^3}\langle f^k\rangle\,\mathrm{d}v}\right\|_{H^{s-1}}\Bigg).\end{aligned}$$

Writing

$$\|\partial^\alpha\boldsymbol{u}^k\|_{L^2}\leq C(s)\left(\|\varrho^k\boldsymbol{u}^k\|_{H^{s-1}}\left\|\frac{1}{\varrho^k}\right\|_{L^\infty}+\|\varrho^k\boldsymbol{u}^k\|_{L^\infty}\left\|\frac{1}{\varrho^k}\right\|_{H^{s-1}}\right),$$

one notices that

$$\begin{aligned}\left\|\partial^\alpha\left(\frac{1}{\varrho^k}\right)\right\|_{L^2}&=\left\|\frac{P_\alpha(\partial^\alpha\varrho^k)}{(\varrho^k)^{q(\alpha)}}\right\|_{L^2}\\
&\leq\frac{1}{\|\,(\varrho^k)^{q(\alpha)}\,\|_{L^\infty}}\|P_\alpha(\partial^\alpha\varrho^k)\|_{L^2}\\
&\leq C(\Omega_2,R,\mathbf{U}_0),\end{aligned}$$

where P_α is a polynomial in $\partial^\alpha(\varrho^k)$ and $q(\alpha)$ an integer depending on α. One gets

$$\left\|\frac{\varrho^k\boldsymbol{u}^k\left(\boldsymbol{u}\cdot\int_{\mathbf{R}^3}\nabla_x\langle f^k\rangle\,\mathrm{d}v\right)}{1-\int_{\mathbf{R}^3}\langle f^k\rangle\,\mathrm{d}v}\right\|_{H^{s-1}}\leq C(s,f_0,R,\mathbf{U}_0,\Omega_2,w)\mathrm{TV}(w).\tag{2.36}$$

In the end, combining the inequalities (2.33)-(2.36)

$$\|b(\mathbf{U}^k,f^k)\|_{H^{s-1},T_{k+1}}\leq C(s,\mathbf{U}_0,f_0,w,R,\Omega_2)\mathrm{TV}(w).$$

We turn to the term

$$\|A_i(\mathbf{U}^k)\partial_{x_i}\mathbf{U}^{k+1}\|_{H^{s-1},T_{k+1}}=\sum_{|\alpha|\leq s-1}\|\partial^\alpha(A_i(\mathbf{U}^k)\partial_{x_i}\mathbf{U}^{k+1})\|_{L^2,T_{k+1}}.$$

Using lemma 2.1.9 and the Sobolev embedding $H^s(\mathbf{R}^3) \hookrightarrow L^\infty(\mathbf{R}^3)$, one has for $|\alpha| \leq s-1$,

$$\begin{aligned}\|\partial^\alpha(A_i(\mathbf{U}^k)\partial_{x_i}\mathbf{U}^{k+1})\|_{L^2,T_{k+1}} \leq & \|\partial^\alpha((A_i(\mathbf{U}^k)-A_i(\overline{\mathbf{U}_0}))\partial_{x_i}\mathbf{U}^{k+1})\|_{L^2,T_{k+1}} \\ & + \|A_i(\overline{\mathbf{U}_0})\partial^\alpha(\partial_{x_i}\mathbf{U}^{k+1})\|_{L^2,T_{k+1}} \\ \leq & C(s)(\|A_i(\mathbf{U}^k)-A_i(\overline{\mathbf{U}_0})\|_{H^s,T_{k+1}}\|\partial_{x_i}\mathbf{U}^{k+1}\|_{L^\infty,T_{k+1}} \\ & + \|A_I(\overline{\mathbf{U}_0})\|_{L^\infty,T_{k+1}}\|\partial_{x_i}\mathbf{U}^{k+1}\|_{H^{s-1},T_{k+1}}) \\ \leq & C(s,\Omega_2,R,\mathbf{U}_0).\end{aligned}$$

This completes the proof. □

Lemma 2.1.14. *For all $k \geq 0$ and $T \in [0,\inf(1,T_{k+1}))$*

$$\sup_{t\in[0,T]} \|\mathbf{U}^{k+1}-\mathbf{U}_0\|_{H^s}(t) \leq TC(s,R,\Omega_2,\mathbf{U}_0,f_0,w,\mathrm{TV}(w))e^{C(s,R,f_0,\mathbf{U}_0,\Omega_2,w,\mathrm{TV}(w))T}. \tag{2.37}$$

Proof. The function $\mathbf{W}^{k+1} = \mathbf{U}^{k+1}-\mathbf{U}_0$ satisfies

$$S(\mathbf{U}^k)\partial_t\mathbf{W}^{k+1} + \sum_i (SA_i)(\mathbf{U}^k)\partial_{x_i}\mathbf{W}^{k+1} = S(\mathbf{U}^k)b(\mathbf{U}^k,f^k) + \mathbf{H}^k,$$
$$\mathbf{W}^{k+1}(x,0) = 0,$$

with $\mathbf{H}^k = -\sum_i (SA_i)(\mathbf{U}^k)\partial_{x_i}\mathbf{U}_0$. We look for a bound in H^s of $\mathbf{W}^{k+1}$. The function $\partial^\alpha\mathbf{W}^{k+1}$satifies

$$\begin{aligned}&S(\mathbf{U}^k)\partial_t\partial^\alpha\mathbf{W}^{k+1} + \sum_i (SA_i)(\mathbf{U}^k)\partial_{x_i}\partial^\alpha\mathbf{W}^{k+1} \\ &= S(\mathbf{U}^k)\partial^\alpha(S^{-1}(\mathbf{U}^k)\mathbf{H}^k + b(\mathbf{U}^k,f^k)) + \mathbf{F}_\alpha,\end{aligned}$$

with $\mathbf{F}_\alpha = S(\mathbf{U}^k)\sum_i \left(A_i(\mathbf{U}^k)\partial_{x_i}\partial^\alpha\mathbf{W}^{k+1} - \partial^\alpha(A_i(\mathbf{U}^k)\partial_{x_i}\mathbf{W}^{k+1})\right)$. Moreover, one has

$$\begin{aligned}&\frac{1}{2}\partial_t\int_{\mathbf{R}^3}(\partial^\alpha\mathbf{W}^{k+1})^T S(\mathbf{U}^k)\partial^\alpha\mathbf{W}^{k+1}\,\mathrm{d}x \\ &\quad=\frac{1}{2}\int_{\mathbf{R}^3}(\partial^\alpha\mathbf{W}^{k+1})^T\left(\partial_t S(\mathbf{U}^k) + \sum_i \partial_{x_i}(SA_i)(\mathbf{U}^k)\right)\partial^\alpha\mathbf{W}^{k+1}\,\mathrm{d}x \\ &\quad\quad+\int_{\mathbf{R}^3}(\partial^\alpha\mathbf{W}^{k+1})^T S(\mathbf{U}^k)\partial^\alpha(S^{-1}(\mathbf{U}^k)\mathbf{H}^k \\ &\quad\quad+ b(\mathbf{U}^k,f^k))\,\mathrm{d}x + \int_{\mathbf{R}^3}(\partial^\alpha\mathbf{W}^{k+1})^T\mathbf{F}_\alpha\,\mathrm{d}x.\end{aligned}$$

Up to time T_k, $\mathbf{U}^k$ takes its values in Ω_2 on which S and SA_i are smooth. One can bound the derivatives of S and SA_i at any order by a constant that depends on Ω_2. One also uses the Sobolev embedding $H^{s-1}(\mathbf{R}^3) \hookrightarrow L^\infty(\mathbf{R}^3)$ and lemma 2.1.13 to obtain the estimates

$$\|\partial_t\mathbf{U}^k\|_{L^\infty,T_k} \leq C(s)\|\partial_t\mathbf{U}^k\|_{H^{s-1},T_k} \leq C(s,\Omega_2,R,\mathbf{U}_0,f_0,w)\mathrm{TV}(w),$$

$$\begin{aligned}\|\partial_{x_i}\mathbf{U}^k\|_{L^\infty,T_k} &\leq C(s)\|\partial_{x_i}\mathbf{U}^k\|_{H^{s-1},T_k} \\ &\leq C(s)\left(\|\mathbf{U}^k-\mathbf{U}_0\|_{H^s,T_k} + \|\mathbf{U}_0-\bar{\mathbf{U}}_0\|_{H^s,T_k}\right) \leq C(s,R,\mathbf{U}_0).\end{aligned}$$

So that

$$\left\|\partial_t S(\mathbf{U}^k)+\sum_i \partial_{x_i}(SA_i)(\mathbf{U}^k)\right\|_{L^\infty,T_{k+1}} \leq C(s,\Omega_2,R,\mathbf{U}_0,f_0,w,\mathrm{TV}(w)).$$

One now uses lemma 2.1.12 to obtain, for $|\alpha|\leq s$

$$\begin{aligned}&A_i(\mathbf{U}^k)\partial_{x_i}\partial^\alpha\mathbf{W}^{k+1}-\partial^\alpha\left(A_i(\mathbf{U}^k)\partial_{x_i}\mathbf{W}^{k+1}\right)\\&=\left((A_i\ \left(\mathbf{U}^k\right)-A_i\left(\bar{\mathbf{U}}_0\right)\right)\partial^\alpha\partial_{x_i}\mathbf{W}^{k+1}-\partial^\alpha\left(\left(A_i\left(\mathbf{U}^k\right)-A_i\left(\bar{\mathbf{U}}_0\right)\right)\partial_{x_i}\mathbf{W}^{k+1}\right).\end{aligned}$$

According to the previous inequality, one has

$$\begin{aligned}\|\mathbf{F}_\alpha\|_{L^2,T_{k+1}}\leq&\|S(\mathbf{U}^k)\|_{L^\infty,T_{k+1}}C(s)\sum_i\Big(\|\partial^\alpha(A_i(\mathbf{U}^k)-A_i(\bar{\mathbf{U}}_0))\|_{L^\infty,T_{k+1}}\\&\times\|\partial_{x_i}\mathbf{W}^{k+1}\|_{H^{s-1},T_{k+1}}\\&+\|\partial_{x_i}\mathbf{W}^{k+1}\|_{L^\infty,T_{k+1}}\|A_i(\mathbf{U}^k)-A_i(\bar{\mathbf{U}}_0)\|_{H^s,T_{k+1}}\Big)\\\leq&C(s,\Omega_2,R,\mathbf{U}_0).\end{aligned}$$

One has using lemma 2.1.10

$$\begin{aligned}&\left\|S(\mathbf{U}^k)\partial^\alpha(S^{-1}(\mathbf{U}^k)\mathbf{H}^k\right\|_{L^2,T_{k+1}}\\&\leq\|S(\mathbf{U}^k)\|_{L^\infty,T_k}\sum_i\|\partial^\alpha(A_i(\mathbf{U}^k)\partial_{x_i}\mathbf{U}_0)\|_{L^2,T_k}\\&\leq C(s,\Omega_2)\sum_i\|A_i(\mathbf{U}^k)-A_i(\bar{\mathbf{U}}_0)\|_{L^\infty,T_k}\|\partial_{x_i}\mathbf{U}_0\|_{H^s,T_k}\\&\quad+\sum_i\|\partial_{x_i}\mathbf{U}_0\|_{L^\infty,T_k}\|A_i(\mathbf{U}^k)-A_i(\bar{\mathbf{U}}_0)\|_{H^s,T_k}+C\|\partial_{x_i}\mathbf{U}_0\|_{H^s,T_k}\\&\leq C(s,\Omega_2,R,\mathbf{U}_0).\end{aligned}$$

It yields

$$\|S(\mathbf{U}^k)\partial^\alpha(b(\mathbf{U}^k,f^k))\|_{L^2,T_{k+1}}\leq C(s,R,f_0,\Omega_2,w,\mathrm{TV}(w)).$$

One now uses the estimate (2.30). For $t\in[0,T_{k+1}]$, one obtains

$$\begin{aligned}&\|\partial^\alpha\mathbf{W}^{k+1}\|_{L^2}(t)\\&\leq C(\Omega_2)[\|\partial^\alpha\mathbf{W}^{k+1}\|_{L^2}(0)+\frac{1}{2}\|\partial_t S+\sum_i\partial_{x_i}(SA_i)\|_{L^\infty,T_{k+1}}\int_0^t\|\partial^\alpha\mathbf{W}^{k+1}\|_{L^2}(\tau)\,\mathrm{d}\tau\\&\quad+\int_0^t\Big(\|\mathbf{F}_\alpha\|_{L^2}+\|S(\mathbf{U}^k)\partial^\alpha(S^{-1}(\mathbf{U}^k)\mathbf{H}^k)\|_{L^2}+\|S(\mathbf{U}^k)\partial^\alpha(b(\mathbf{U}^k,f^k))\|_{L^2}\Big)\,\mathrm{d}\tau.\end{aligned}$$

Then one gets

$$\begin{aligned}&\|\partial^\alpha\ \mathbf{W}^{k+1}\|_{L^2}(t)\\&\leq\|\partial^\alpha\mathbf{W}^{k+1}\|_{L^2}(0)+C(s,\Omega_2,R,\mathbf{U}_0,f_0)\int_0^t\|\partial^\alpha\mathbf{W}^{k+1}\|_{L^2}(\tau)\,\mathrm{d}\tau\\&\quad+\int_0^t(C(s,\Omega_2,R,\mathbf{U}_0)+C(s,\Omega_2,R,\mathbf{U}_0)+C(s,\mathbf{U}_0,f_0,w,\mathrm{TV}(w),R,\Omega_2))\,\mathrm{d}\tau.\end{aligned}$$

Summing for all $|\alpha| \leq s$ these estimates, one ends up with

$$
\begin{aligned}
&\|\mathbf{W}^{k+1}\|_{H^s}(t) \\
&\leq C(\Omega_2)\left(\|\mathbf{W}^{k+1}\|_{H^s}(0) + C(s,\Omega_2,R,\mathbf{U}_0,f_0)\int_0^t \|\mathbf{W}^{k+1}\|_{H^s}(\tau)\,\mathrm{d}\tau\right) \\
&\quad + tC(s,R,\Omega_2,\mathbf{U}_0,f_0,w,\mathrm{TV}(w)).
\end{aligned}
$$

Thanks to Gronwall's lemma, one has for all $t \in [0,T]$ with $T \leq T_{k+1}$

$$
\begin{aligned}
&\|\mathbf{W}^{k+1}\|_{H^s}(t) \\
&\leq C(\Omega_2)\left(\|\mathbf{W}^{k+1}\|_{H^s}(0) + TC(s,R,\Omega_2,\mathbf{U}_0,f_0,w,\mathrm{TV}(w))\right)e^{C(s,R,f_0,\mathbf{U}_0,\Omega_2,w,\mathrm{TV}(w))T}.
\end{aligned}
$$

Choosing $T \leq 1$, and since $\mathbf{W}^{k+1}(x,0) = 0$, one obtains the claim. □

Lemma 2.1.15. *The following inequalities hold for all* $T \in [0, \inf(1,T_{k+1}))$

$$
\sup_{t\in[0,T]} V_M^{k+1}(t) \leq V_M(0) + C(\Omega_2,w,\gamma,\mathbf{U}_0)\mathrm{TV}(w)T, \tag{2.38}
$$

$$
\sup_{t\in[0,T]} X_M^{k+1}(t) \leq X_M(0) + C(f_0,\Omega_2,w,\gamma,\mathbf{U}_0)\mathrm{TV}(w)T, \tag{2.39}
$$

$$
\left\|\int_{\mathbf{R}^3}\langle f^{k+1}\rangle\,\mathrm{d}v\right\|_{L^\infty,T} \leq 2^3\|w\|_{L^1}\|f_0\|_{L^\infty}(V_M(0) + C(\Omega_2,w,\gamma,\mathbf{U}_0)T)^3. \tag{2.40}
$$

Proof. Recall the characteristic curves of the Vlasov equation

$$
\frac{\mathrm{d}\mathbf{X}^{k+1}}{\mathrm{d}t}(t;\boldsymbol{x},\boldsymbol{v},s) = \mathbf{V}^{k+1}(t;\boldsymbol{x},\boldsymbol{v},s), \tag{2.41}
$$

$$
\mathbf{X}^{k+1}(s;\boldsymbol{x},\boldsymbol{v},s) = \boldsymbol{x}, \tag{2.42}
$$

$$
\frac{\mathrm{d}\mathbf{V}^{k+1}}{\mathrm{d}t}(t;\boldsymbol{x},\boldsymbol{v},s) = -\langle\nabla_x p(\mathbf{X}^{k+1}(t;\boldsymbol{x},\boldsymbol{v},s),t)\rangle, \tag{2.43}
$$

$$
\mathbf{V}^{k+1}(s;\boldsymbol{x},\boldsymbol{v},s) = \boldsymbol{v}. \tag{2.44}
$$

One has, writting implicitly the equations (2.41) and (2.43),

$$
\mathbf{X}^{k+1}(t;\boldsymbol{x},\boldsymbol{v},s) = \boldsymbol{x} + \int_s^t \mathbf{V}^{k+1}(\tau;\boldsymbol{x},\boldsymbol{v},s)\,\mathrm{d}\tau, \tag{2.45}
$$

$$
\mathbf{V}^{k+1}(t;\boldsymbol{x},\boldsymbol{v},s) = \boldsymbol{v} - \int_s^t \langle\nabla_x p^k(\mathbf{X}^{k+1}(\tau,\boldsymbol{x},\boldsymbol{v},s),\tau)\rangle\,\mathrm{d}\tau. \tag{2.46}
$$

We recall the notations

$$
X_M^{k+1}(t) = \sup_{(\boldsymbol{x},\boldsymbol{v})\in\mathbf{R}^3\times\mathbf{R}^3, f^{k+1}(t,\boldsymbol{x},\boldsymbol{v})>0} |\boldsymbol{x}|,
$$

$$
V_M^{k+1}(t) = \sup_{(\boldsymbol{x},\boldsymbol{v})\in\mathbf{R}^3\times\mathbf{R}^3, f^{k+1}(t,\boldsymbol{x},\boldsymbol{v})>0} |\boldsymbol{v}|.
$$

Then

$$
\mathbf{V}^{k+1}(0;\boldsymbol{x},\boldsymbol{v},t) = \boldsymbol{v} - \int_t^0 \langle\nabla p^k(\mathbf{X}^{k+1}(\tau;\boldsymbol{x},\boldsymbol{v},t),\tau)\rangle\,\mathrm{d}\tau,
$$

and

$$|\boldsymbol{v}| \le \mathbf{V}^{k+1}(0;\boldsymbol{x},\boldsymbol{v},t) + \int_0^t \|p^k\|_{L^\infty}\mathrm{TV}(w)\,\mathrm{d}\tau.$$

One obtains

$$V_M^{k+1}(t) \le V_M(0) + \int_0^t \|p^k\|_{L^\infty}(\tau)\mathrm{TV}(w)\,\mathrm{d}\tau.$$

And it yields (2.38). One proceeds similarly for X_M^{k+1}. Using the formula (2.46), one has

$$\begin{aligned}\boldsymbol{x} &= \mathbf{X}^{k+1}(0;\boldsymbol{x},\boldsymbol{v},t) + \int_0^t \mathbf{V}^{k+1}(\tau;\boldsymbol{x},\boldsymbol{v},t)\,\mathrm{d}\tau \\ &= \mathbf{X}^{k+1}(0;\boldsymbol{x},\boldsymbol{v},t) + \boldsymbol{v}\int_0^t \mathrm{d}\tau - \int_0^t \int_t^\tau \langle \nabla_x p^k(\mathbf{X}^{k+1}(\tilde\tau;\boldsymbol{x},\boldsymbol{v},t),\tilde\tau)\rangle\,\mathrm{d}\tilde\tau\,\mathrm{d}\tau,\end{aligned}$$

so, using lemma 2.1.11

$$X_M^{k+1}(t) \le X_M(0) + V_M(0)t + \int_0^t \int_\tau^t \|p^k\|_{L^\infty}(\tilde\tau)\mathrm{TV}(w)\,\mathrm{d}\tilde\tau\,\mathrm{d}\tau.$$

And one obtains (2.39).

Moreover, one has, with lemma 2.1.11

$$\begin{aligned}\left\|\int_{\mathbf{R}^3}\langle f^{k+1}\rangle\,\mathrm{d}v\right\|_{L^\infty,T} &\le \|w\|_{L^1}\left\|\int_{\mathbf{R}^3} f^{k+1}\,\mathrm{d}v\right\|_{L^\infty,T} \\ &\le 2^3\|w\|_{L^1}\|f^{k+1}\|_{L^\infty,T}(V_M^{k+1})^3 \\ &\le 2^3\|w\|_{L^1}\|f_0\|_{L^\infty}(V_M(0)+C(\Omega_2,w,\gamma,\mathbf{U}_0)\mathrm{TV}(w)T)^3.\end{aligned}$$

□

We then obtain the main Proposition of this section:

Proposition 2.1.16. *There exists $T_\star \in (0,1]$ which depends only on Ω_1, Ω_2, s, $\mathbf{U}_0$, w and f_0 such that, for all $k\in\mathbf{N}$, $T_k \ge T_\star$.*

Proof. From lemma 2.1.14, one has

$$\sup_{t\in[0,T]}\|\mathbf{U}^{k+1}-\mathbf{U}_0\|_{H^s}(t) \le TC(s,R,\Omega_2,\mathbf{U}_0,f_0,w,\mathrm{TV}(w))e^{C(s,R,f_0,\mathbf{U}_0,\Omega_2,w,\mathrm{TV}(w))T}.$$

The right-hand-side of this inequality defines a continuous function of T independent of k, with value 0 if $T=0$. Therefore, for all k there exists $T_k > T_1 > 0$ such that

$$\begin{aligned}\sup_{t\in[0,T]}\|\mathbf{U}^{k+1}-\mathbf{U}_0\|_{H^s}(t) &\le T_1C(s,R,\Omega_2,\mathbf{U}_0,f_0,w,\mathrm{TV}(w))e^{C(s,R,f_0,\mathbf{U}_0,\Omega_2,w,\mathrm{TV}(w))T_1} \\ &\le R.\end{aligned}$$

For the same reasons, using lemma 2.1.15, for all k there exists T_2, T_3 and T_4 in $]0,T_k)$ such that

$$\begin{aligned}\sup_{t\in[0,T]} V_M^{k+1}(t) &\le V_M(0) + C(\Omega_2,w,\gamma,\mathbf{U}_0)\mathrm{TV}(w)T_2 \le 2V_M(0), \\ \sup_{t\in[0,T]} X_M^{k+1}(t) &\le X_M(0) + C(f_0,\Omega_2,w,\gamma,\mathbf{U}_0)\mathrm{TV}(w)T_3 \le 2X_M(0), \\ \left\|\int_{\mathbf{R}^3}\langle f^{k+1}\rangle\,\mathrm{d}v\right\|_{L^\infty,T} &\le 2^3\|w\|_{L^1}\|f_0\|_{L^\infty}(V_M(0)+C(\Omega_2,w,\gamma,\mathbf{U}_0)T_4)^3 \\ &\le 2^4\|w\|_{L^1}\|f_0\|_{L^\infty}V_M(0)^3.\end{aligned}$$

Let $T_\star = \min(T_1,T_2,T_3,T_4)$ then for all $k\in\mathbf{N}$, $T_k \ge T_\star > 0$ and the bounds (2.25)-(2.28) are verified. □

2.1.8 Convergence of the iterative process

The goal of this section is to prove

Proposition 2.1.17. *We consider initial data such that (2.19)-(2.20) hold and the associated sequences* $\mathbf{U}^k$*,* f^k *defined by (2.21)-(2.24). Let* $T_\star$ *given by Proposition 2.1.16.*

Then one can find $T_{\star\star} \in (0,T_\star)$ *such that, for* $k \geq 2$*,*

$$\|\mathbf{U}^{k+1} - \mathbf{U}^k\|_{L^2,T_{\star\star}} \leq \frac{1}{4}\|\mathbf{U}^k - \mathbf{U}^{k-1}\|_{L^2,T_{\star\star}} + \frac{1}{4}\|\mathbf{U}^{k-1} - \mathbf{U}^{k-2}\|_{L^2,T_{\star\star}}, \tag{2.47}$$

$$\|f^k - f^{k-1}\|_{L^2,T_{\star\star}} \leq C(f_0,\Omega_2,\gamma)\mathrm{TV}(w)\|\mathbf{U}^{k-1} - \mathbf{U}^{k-2}\|_{L^2,T_{\star\star}}. \tag{2.48}$$

Proof. Let $k \geq 2$. The function $\mathbf{U}^{k+1} - \mathbf{U}^k$ is solution of the system

$$\begin{aligned} S(\mathbf{U}^k)\partial_t(\mathbf{U}^{k+1} - \mathbf{U}^k) + \sum_{i=1}^{3}((SA_i(\mathbf{U}^{k-1}) - (SA_i)(\mathbf{U}^k)\partial_{x_i}(\mathbf{U}^{k+1} - \mathbf{U}^k) \\ = b(\mathbf{U}^k, f^k) - b(\mathbf{U}^{k-1}, f^{k-1}) + \mathbf{F}_k, \end{aligned}$$

with

$$\mathbf{F}_k = (S(\mathbf{U}^{k-1}) - S(\mathbf{U}^k))\partial_t \mathbf{U}^k + \sum_{i=1}^{3}((SA_i(\mathbf{U}^{k-1}) - (SA_i)(\mathbf{U}^k))\partial_{x_i}\mathbf{U}^k.$$

Thanks to lemma 2.1.8, one can write

$$\begin{aligned} &\|\mathbf{U}^{k+1} - \mathbf{U}^k\|_{L^2}(t) \\ \leq& C(\frac{1}{2}\|\partial_t S(\mathbf{U}^k) + \sum_i \partial_{x_i}(SA_i)(\mathbf{U}^k)\|_{L^\infty,T_\star}\int_0^t \|\mathbf{U}^{k+1} - \mathbf{U}^k\|_{L^2}(\tau)\,\mathrm{d}\tau \\ &+ \int_0^t (\|\mathbf{F}_k\|_{L^2}(\tau) + \|b(\mathbf{U}^k,f^k) - b(\mathbf{U}^{k-1}, f^{k-1})\|_{L^2}(\tau))\,\mathrm{d}\tau). \end{aligned}$$

Then, by Gronwall's lemma, inequalities (2.25)-(2.31) and the fact that S and SA_i are smooth on $\overline{\Omega_2}$ which is compact, one has

$$\begin{aligned} \|\mathbf{U}^{k+1} - \mathbf{U}^k\|_{L^2}(t) \leq& Ce^{\left(C(\Omega_2)\|\partial_t S(\mathbf{U}^k) + \sum_i \partial_{x_i}(SA_i)(\mathbf{U}^k)\|_{L^\infty,T_\star}\right)T_\star} \\ &\times \int_0^t (\|\mathbf{F}_k\|_{L^2}(\tau) + \|b(\mathbf{U}^k, f^k) - b(\mathbf{U}^{k-1}, f^{k-1})\|_{L^2}(\tau)\,\mathrm{d}\tau \\ \leq& C(\Omega_2)e^{C(s,\Omega_2,R,\mathbf{U}_0,f_0)T_\star}T_\star \\ &\times (\|\mathbf{F}_k\|_{L^2,T_\star} + \|b(\mathbf{U}^k,f^k) - b(\mathbf{U}^{k-1},f^{k-1})\|_{L^2,T_\star}). \end{aligned}$$

The goal is then to obtain inequality (2.47).

To bound to right-hand-side of this inequality, one first notices that the first term verifies $\|\mathbf{F}_k\|_{L^2} \leq C(s,\Omega_2,R,\mathbf{U}_0,\mathrm{TV}(w))\|\mathbf{U}^k - \mathbf{U}^{k-1}\|_{L^2,T_\star}$. It remains to bound the term

$$\begin{aligned} &\|b(\mathbf{U}^k,f^k) - b(\mathbf{U}^{k-1},f^{k-1})\|_{L^2,T_\star} \\ =& \left\| \begin{pmatrix} \dfrac{\varrho^k \int_{\mathbf{R}^3}(\boldsymbol{u}^k - \boldsymbol{v}) \cdot \nabla_x\langle f^k\rangle\,\mathrm{d}v}{1 - \int_{\mathbf{R}^3}\langle f^k\rangle\,\mathrm{d}v} - \dfrac{\varrho^{k-1} \int_{\mathbf{R}^3}(\boldsymbol{u}^{k-1} - \boldsymbol{v}) \cdot \nabla_x\langle f^{k-1}\rangle\,\mathrm{d}v}{1 - \int_{\mathbf{R}^3}\langle f^{k-1}\rangle\,\mathrm{d}v} \\ \dfrac{\varrho^k \boldsymbol{u}^k \int_{\mathbf{R}^3}(\boldsymbol{u}^k - \boldsymbol{v}) \cdot \nabla_x\langle f^k\rangle\,\mathrm{d}v}{1 - \int_{\mathbf{R}^3}\langle f^k\rangle\,\mathrm{d}v} - \dfrac{\varrho^{k-1}\boldsymbol{u}^{k-1} \int_{\mathbf{R}^3}(\boldsymbol{u}^{k-1} - \boldsymbol{v}) \cdot \nabla_x\langle f^{k-1}\rangle\,\mathrm{d}v}{1 - \int_{\mathbf{R}^3}\langle f^{k-1}\rangle\,\mathrm{d}v} \end{pmatrix} \right\|_{L^2,T_\star}. \end{aligned}$$

One has, making use of lemma 2.1.11

$$\begin{aligned}
&\left\| \frac{\varrho^k \boldsymbol{u}^k \cdot \int_{\mathbf{R}^3} \nabla_x \langle f^k \rangle \,\mathrm{d}v}{1 - \int_{\mathbf{R}^3} \langle f^k \rangle \,\mathrm{d}v} - \frac{\varrho^{k-1} \boldsymbol{u}^{k-1} \cdot \int_{\mathbf{R}^3} \nabla_x \langle f^{k-1} \rangle \,\mathrm{d}v}{1 - \int_{\mathbf{R}^3} \langle f^{k-1} \rangle \,\mathrm{d}v} \right\|_{L^2,T_\star} \\
&\leq \left\| (\varrho^k \boldsymbol{u}^k - \varrho^{k-1} \boldsymbol{u}^{k-1}) \cdot \frac{\int_{\mathbf{R}^3} \nabla_x \langle f^k \rangle \,\mathrm{d}v}{1 - \int_{\mathbf{R}^3} \langle f^k \rangle \,\mathrm{d}v} \right\|_{L^2,T_\star} \\
&\quad + \left\| \varrho^{k-1} \boldsymbol{u}^{k-1} \cdot \left(\frac{\int_{\mathbf{R}^3} \nabla_x \langle f^k \rangle \,\mathrm{d}v}{1 - \int_{\mathbf{R}^3} \langle f^k \rangle \,\mathrm{d}v} - \frac{\int_{\mathbf{R}^3} \nabla_x \langle f^{k-1} \rangle \,\mathrm{d}v}{1 - \int_{\mathbf{R}^3} \langle f^{k-1} \rangle \,\mathrm{d}v} \right) \right\|_{L^2,T_\star} \\
&\leq \| \varrho^k \boldsymbol{u}^k - \varrho^{k-1} \boldsymbol{u}^{k-1} \|_{L^2,T_\star} \left\| \frac{\int_{\mathbf{R}^3} \nabla_x \langle f^k \rangle \,\mathrm{d}v}{1 - \int_{\mathbf{R}^3} \langle f^k \rangle \,\mathrm{d}v} \right\|_{L^\infty,T_\star} \\
&\quad + \| \varrho^{k-1} \boldsymbol{u}^{k-1} \|_{L^\infty} \left\| \frac{1}{1 - 2^4 \|w\|_{L^1} V_M(0)^3 f_0} \right\|_{L^\infty} \left\| \int_{\mathbf{R}^3} \nabla_x \langle f^k - f^{k-1} \rangle \,\mathrm{d}v \right\|_{L^2,T_\star} \\
&\leq C(f_0) \mathrm{TV}(w) \left\| \frac{1}{1 - 2^4 \|w\|_{L^1} V_M(0)^3 f_0} \right\|_{L^\infty} \| \mathbf{U}^k - \mathbf{U}^{k-1} \|_{L^2,T_\star} \\
&\quad + C(f_0,R) \mathrm{TV}(w) \left\| \frac{1}{1 - 2^4 \|w\|_{L^1} V_M(0)^3 f_0} \right\|_{L^\infty} \| f^k - f^{k-1} \|_{L^2,T_\star} \\
&\leq C(f_0,w) \mathrm{TV}(w) \| \mathbf{U}^k - \mathbf{U}^{k-1} \|_{L^2,T_\star} \\
&\quad + C(f_0,R,w) \mathrm{TV}(w) \| f^k - f^{k-1} \|_{L^2,T_\star}.
\end{aligned}$$

Similarly, because of the inequality

$$\left\| \int_{\mathbf{R}^3} (f^k - f^{k-1}) \boldsymbol{v} \,\mathrm{d}v \right\|_{L^2,T_\star} \leq C(f_0) \| f^k - f^{k-1} \|_{L^2,T_\star},$$

one has

$$\begin{aligned}
&\left\| \frac{\varrho^k \int_{\mathbf{R}^3} \boldsymbol{v} \cdot \nabla_x \langle f^k \rangle \,\mathrm{d}v}{1 - \int_{\mathbf{R}^3} \langle f^k \rangle \,\mathrm{d}v} - \frac{\varrho^{k-1} \int_{\mathbf{R}^3} \boldsymbol{v} \cdot \nabla_x \langle f^{k-1} \rangle \,\mathrm{d}v}{1 - \int_{\mathbf{R}^3} \langle f^{k-1} \rangle \,\mathrm{d}v} \right\|_{L^2,T_\star} \\
&\leq C(f_0) \mathrm{TV}(w) \left\| \frac{1}{1 - 2^4 \|w\|_{L^1} V_M(0)^3 f_0} \right\|_{L^\infty} \| \mathbf{U}^k - \mathbf{U}^{k-1} \|_{L^2,T_\star} \\
&\quad + C(f_0,R) \mathrm{TV}(w) \left\| \frac{1}{1 - 2^4 \|w\|_{L^1} V_M(0)^3 f_0} \right\|_{L^\infty} \| f^k - f^{k-1} \|_{L^2,T_\star} \\
&\leq C(f_0,w) \mathrm{TV}(w) \| \mathbf{U}^k - \mathbf{U}^{k-1} \|_{L^2,T_\star} + C(f_0,R,w) \| f^k - f^{k-1} \|_{L^2,T_\star}.
\end{aligned}$$

In the same way

$$\begin{aligned}
&\left\| \frac{\varrho^k \boldsymbol{u}^k \int_{\mathbf{R}^3} \boldsymbol{v} \cdot \nabla_x \langle f^k \rangle \,\mathrm{d}v}{1 - \int_{\mathbf{R}^3} \langle f^k \rangle \,\mathrm{d}v} - \frac{\varrho^{k-1} \boldsymbol{u}^{k-1} \int_{\mathbf{R}^3} \boldsymbol{v} \cdot \nabla_x \langle f^{k-1} \rangle \,\mathrm{d}v}{1 - \int_{\mathbf{R}^3} \langle f^{k-1} \rangle \,\mathrm{d}v} \right\|_{L^2,T_\star} \\
&\leq C(f_0) \mathrm{TV}(w) \left\| \frac{1}{1 - 2^4 \|w\|_{L^1} V_M(0)^3 f_0} \right\|_{L^\infty} \| \mathbf{U}^k - \mathbf{U}^{k-1} \|_{L^2,T_\star} \\
&\quad + C(f_0,R) \mathrm{TV}(w) \left\| \frac{1}{1 - 2^4 \|w\|_{L^1} V_M(0)^3 f_0} \right\|_{L^\infty} \| f^k - f^{k-1} \|_{L^2,T_\star} \\
&\leq C(f_0,w) \mathrm{TV}(w) \| \mathbf{U}^k - \mathbf{U}^{k-1} \|_{L^2,T_\star} + C(f_0,R,w) \| f^k - f^{k-1} \|_{L^2,T_\star}.
\end{aligned}$$

For the final term, one notices that

$$\begin{aligned}
&\left\| \frac{\varrho^k \boldsymbol{u}^k \int_{\mathbf{R}^3} \boldsymbol{u}^k \cdot \nabla_x \langle f^k \rangle \,\mathrm{d}v}{1 - \int_{\mathbf{R}^3} \langle f^k \rangle \,\mathrm{d}v} - \frac{\varrho^{k-1} \boldsymbol{u}^{k-1} \int_{\mathbf{R}^3} \boldsymbol{u}^{k-1} \cdot \nabla_x \langle f^{k-1} \rangle \,\mathrm{d}v}{1 - \int_{\mathbf{R}^3} \langle f^{k-1} \rangle \,\mathrm{d}v} \right\|_{L^2, T_\star} \\
\leq & \|\varrho^k \boldsymbol{u}^k - \varrho^{k-1} \boldsymbol{u}^{k-1}\|_{L^2, T_\star} \left\| \frac{\int_{\mathbf{R}^3} \nabla_x \langle f^k \rangle \,\mathrm{d}v}{1 - \int_{\mathbf{R}^3} \langle f^k \rangle \,\mathrm{d}v} \right\|_{L^\infty, T_\star} \|\boldsymbol{u}^k\|_{L^\infty, T_\star} \\
&+ \|\varrho^{k-1} \boldsymbol{u}^{k-1}\|_{L^\infty} \left\| \frac{1}{1 - 2^4 \|w\|_{L^1} V_M(0)^3 f_0} \right\|_{L^\infty} \\
&\times \max(\|\boldsymbol{u}^k\|_{L^\infty, T_\star}, \|\boldsymbol{u}^{k-1}\|_{L^\infty, T_\star}) \left\| \int_{\mathbf{R}^3} \nabla_x \langle f^k - f^{k-1} \rangle \,\mathrm{d}v \right\|_{L^2, T_\star}.
\end{aligned}$$

Moreover, because that for all k, $\mathbf{U}^k \in \Omega_2$ which is relatively compact in $(0, +\infty) \times \mathbf{R}^3$, the quantity ϱ^k is bounded from below for all k by a constant that depends only on Ω_2. So that one has, for all $k \geq 2$

$$\|\boldsymbol{u}^k\|_{L^\infty} = \left\| \frac{\varrho^k \boldsymbol{u}^k}{\varrho^k} \right\|_{L^\infty} \leq C(\Omega_2) \|\varrho^k \boldsymbol{u}^k\|_{L^\infty}.$$

So

$$\begin{aligned}
&\left\| \frac{\varrho^k \boldsymbol{u}^k \int_{\mathbf{R}^3} \boldsymbol{u}^k \cdot \nabla_x \langle f^k \rangle \,\mathrm{d}v}{1 - \int_{\mathbf{R}^3} \langle f^k \rangle \,\mathrm{d}v} - \frac{\varrho^{k-1} \boldsymbol{u}^{k-1} \int_{\mathbf{R}^3} \boldsymbol{u}^{k-1} \cdot \nabla_x \langle f^{k-1} \rangle \,\mathrm{d}v}{1 - \int_{\mathbf{R}^3} \langle f^{k-1} \rangle \,\mathrm{d}v} \right\|_{L^2, T_\star} \\
&\leq C(f_0, w, \Omega_2) \mathrm{TV}(w) \|\mathbf{U}^k - \mathbf{U}^{k-1}\|_{L^2, T_\star} + C(f_0, R, w, \Omega_2) \mathrm{TV}(w) \|f^k - f^{k-1}\|_{L^2, T_\star}.
\end{aligned}$$

In the end

$$\begin{aligned}
&\|b(\mathbf{U}^k, f^k) - b(\mathbf{U}^{k-1}, f^{k-1})\|_{L^2, T_\star} \\
&\leq C(f_0, w, \Omega_2) \mathrm{TV}(w) \|\mathbf{U}^k - \mathbf{U}^{k-1}\|_{L^2, T_\star} + C(f_0, R, w, \Omega_2) \mathrm{TV}(w) \|f^k - f^{k-1}\|_{L^2, T_\star}.
\end{aligned} \tag{2.49}$$

The goal is then to control the term $\|f^k - f^{k-1}\|_{L^2, T_\star}$ by $\|\mathbf{U}^{k-1} - \mathbf{U}^{k-2}\|_{L^2, T_\star}$.

The function $f^k - f^{k-1}$ verifies

$$\begin{aligned}
&\partial_t (f^k - f^{k-1}) + \boldsymbol{v} \cdot \nabla_x (f^k - f^{k-1}) - \langle \nabla p^{k-1} \rangle \cdot \nabla_v (f^k - f^{k-1}) \\
&= (\langle \nabla p^{k-1} \rangle - \langle \nabla p^{k-2} \rangle) \cdot \nabla_v f^{k-1}.
\end{aligned}$$

Moreover $f^k(\boldsymbol{x}, \boldsymbol{v}, 0) - f^{k-1}(\boldsymbol{x}, \boldsymbol{v}, 0) = 0$, so

$$(f^k - f^{k-1})(\boldsymbol{x}, \boldsymbol{v}, t) = \int_0^t B(\mathbf{X}^{k-1}(\tau; \boldsymbol{x}, \boldsymbol{v}, t), \mathbf{V}^{k-1}(\tau; \boldsymbol{x}, \boldsymbol{v}, t), \tau) \,\mathrm{d}\tau,$$

with

$$B = (\langle \nabla p^{k-1} \rangle - \langle \nabla p^{k-2} \rangle) \cdot \nabla_v f^{k-1}.$$

One writes

$$\|f^k - f^{k-1}\|_{L^2}(t) \leq \int_0^t \|B\|_{L^2}(\tau) \,\mathrm{d}\tau,$$

then one has, using lemma 2.1.11, the following for B in the L^2-norm,

$$\begin{aligned}\|B\|_{L^2} &\leq \|\nabla_v f^{k-1}\|_{L^\infty}\|\langle\nabla p^{k-1}\rangle - \langle\nabla p^{k-2}\rangle\|_{L^2}\\ &\leq \|\nabla_v f^{k-1}\|_{L^\infty}\mathrm{TV}(w)\|(\varrho^{k-1})^\gamma - (\varrho^{k-2})^\gamma\|_{L^2}.\end{aligned}$$

One needs to bound $\nabla_v f^k$ in L^∞. The function $\nabla_v f^k$ verifies

$$\partial_t(\nabla_v f^k) + \boldsymbol{v}\cdot\nabla_x\nabla_v f^k - \langle\nabla_x p^{k-1}\rangle\cdot\nabla_v\nabla_v f^k = -\nabla_x f,$$

where $\cdot$ is understood as a matrix-vector product. Therefore, the characteristic method yields the formula

$$\begin{aligned}\nabla_v f^k(\boldsymbol{x},\boldsymbol{v},t) =& \nabla_v f_0(\mathbf{X}^{k-1}(0;\boldsymbol{x},\boldsymbol{v},t),\mathbf{V}^{k-1}(0;\boldsymbol{x},\boldsymbol{v},t))\\ &- \int_0^t \nabla_x f^k(\mathbf{X}^{k-1}(\tau;\boldsymbol{x},\boldsymbol{v},t),\mathbf{V}^{k-1}(\tau;\boldsymbol{x},\boldsymbol{v},t),\tau)\,\mathrm{d}\tau,\end{aligned}$$

which yields, for $t\in[0,T_\star)$

$$\|\nabla_v f^k\|_{L^\infty}(t) \leq \|\nabla_v f_0\|_{L^\infty} + \int_0^t \|\nabla_x f^k\|_{L^\infty}(\tau)\,\mathrm{d}\tau.$$

Similarly, the function $\nabla_x f^k$ verifies

$$\partial_t(\nabla_x f^k) + \boldsymbol{v}\cdot\nabla_x\nabla_x f^k - \langle\nabla_x p^{k-1}\rangle\cdot\nabla_v\nabla_x f^k = \langle\nabla_x\nabla_x p^{k-1}\rangle\cdot\nabla_v f^k.$$

Again, applying the method of characteristics

$$\begin{aligned}\nabla_x f^k(\boldsymbol{x},\boldsymbol{v},t) &= \nabla_x f_0(\mathbf{X}^{k-1}(0;\boldsymbol{x},\boldsymbol{v},t),\mathbf{V}^{k-1}(0;\boldsymbol{x},\boldsymbol{v},t))\\ &+ \int_0^t \Big\langle\nabla_x\nabla_x p^{k-1}(\mathbf{X}^{k-1}(\tau;\boldsymbol{x},\boldsymbol{v},t),\tau)\Big\rangle\nabla_v f^k(\mathbf{X}^{k-1}(\tau;\boldsymbol{x},\boldsymbol{v},t),\mathbf{V}^{k-1}(\tau;\boldsymbol{x},\boldsymbol{v},t),\tau)\,\mathrm{d}\tau,\end{aligned}$$

and, with lemma 2.1.11

$$\begin{aligned}\|\nabla_x f^k\|_{L^\infty}(t) &\leq \|\nabla_x f_0\|_{L^\infty} + \int_0^t \Big\|\langle\nabla_x\nabla_x p^{k-1}\rangle\Big\|_{L^\infty}(\tau)\|\nabla_v f^k\|_{L^\infty}(\tau)\,\mathrm{d}\tau\\ &\leq \|\nabla_x f_0\|_{L^\infty} + C(s,\gamma,R,\Omega_2,U_0\mathrm{TV}(w))\int_0^t \|\nabla_v f^k\|_{L^\infty}(\tau)\,\mathrm{d}\tau.\end{aligned}$$

It is a consequence of Gronwall's lemma that for $t\in[0,T_\star[$

$$\|\nabla_x f^k\|_{L^\infty}(t) + \|\nabla_v f^k\|_{L^\infty}(t) \leq C(s,R,f_0,\Omega_2,\gamma,\mathrm{TV}(w)).$$

Then, applying the mean value theorem to $z\mapsto z^\gamma$ and using the fact that Ω_2 is relatively compact in Ω yields

$$\begin{aligned}\|B\|_{L^2}(t) &\leq \|\nabla_v f^{k-1}\|_{L^\infty}(t)\mathrm{TV}(w)\sup_z\|\gamma z^{\gamma-1}\|_{L^\infty}\|\varrho^{k-1}-\varrho^{k-2}\|_{L^2}(t)\\ &\leq C(s,R,f_0,\Omega_2,\gamma,\mathrm{TV}(w))\mathrm{TV}(w)\|\mathbf{U}^{k-1}-\mathbf{U}^{k-2}\|_{L^2,T_\star},\end{aligned}$$

and

$$\|f^k - f^{k-1}\|_{L^2}(t) \leq tC(s,R,f_0,\Omega_2,\gamma,\mathrm{TV}(w))\mathrm{TV}(w)\|\mathbf{U}^{k-1}-\mathbf{U}^{k-2}\|_{L^2}(t).$$

Finally, using the inequality $T_\star \leq 1$,

$$\begin{aligned}
&\|b(\mathbf{U}^k,f^k) - b(\mathbf{U}^{k-1},f^{k-1})\|_{L^2,T_\star} \\
&\leq C(f_0,w,\Omega_2)\mathrm{TV}(w)\|\mathbf{U}^k - \mathbf{U}^{k-1}\|_{L^2,T_\star} \\
&\quad + C(s,R,f_0,\Omega_2,\gamma,\mathrm{TV}(w))\mathrm{TV}(w)\|\mathbf{U}^{k-1} - \mathbf{U}^{k-2}\|_{L^2,T_\star}.
\end{aligned}$$

So that one obtains for all $t \in [0,T_\star)$

$$\begin{aligned}
&\|\mathbf{U}^{k-1} - \mathbf{U}^k\|_{L^2}(t) \\
&\leq C(R,f_0,\mathbf{U}_0,\Omega_2,w,\mathrm{TV}(w),\gamma)T_\star\left(\|\mathbf{U}^k - \mathbf{U}^{k-1}\|_{L^2,T_\star} + \|\mathbf{U}^{k-1} - \mathbf{U}^{k-2}\|_{L^2,T_\star}\right).
\end{aligned}$$

This inequality is also valid if one replaces $T_\star$ by $T_{\star\star} \in (0,T_\star)$. In particular, one can chose $T_{\star\star}$ such that

$$C(R,f_0,\mathbf{U}_0,\Omega_2,w,\mathrm{TV}(w),\gamma)T_{\star\star} < \frac{1}{4}.$$

This concludes the proof. □

2.1.9 Proof of Theorem 2.1.5

The proof of Theorem 2.1.5 is divided into three parts. First we prove the existence in the case of smooth compactly supported initial data. Then we treat the uniqueness in this case. Finally we explain how to modify the proof to obtain the result for general initial data.

Proof of Theorem 2.1.5.
1) Existence for smooth compactly supported initial data. From Proposition 2.1.17, one has

$$\sum_{k\in\mathbf{N}} \|\mathbf{U}^{k+1} - \mathbf{U}^k\|_{L^2,T_{\star\star}} < +\infty.$$

Then the sequence $(\mathbf{U}^k)_k$ is a Cauchy sequence and converges in $L^\infty(0,T_{\star\star};L^2(\mathbf{R}^3))$ to $\mathbf{U}$. Since $\mathbf{U}^k$ is smooth for all k, we have $\mathbf{U} \in \mathscr{C}(0,T_{\star\star};L^2(\mathbf{R}^3))$. In the same way,

$$\sum_{k\in\mathbf{N}} \|f^{k+1} - f^k\|_{L^2,T_{\star\star}} < +\infty.$$

Then the sequence $(f^k)_k$ is a Cauchy sequence and converges in $L^\infty(0,T_{\star\star};L^2(\mathbf{R}^3\times\mathbf{R}^3))$ to f. Since f^k is smooth for all k, we have $f \in \mathscr{C}(0,T_{\star\star};L^2(\mathbf{R}^3\times\mathbf{R}^3))$. Thanks to the inequality (2.25), one has $\|\mathbf{U}-\mathbf{U}_0\|_{H^s,T_{\star\star}} \leq R$ and $\mathbf{U} \in L^\infty(0,T_{\star\star};H^s(\mathbf{R}^3))$. In particular, thanks to the Sobolev embedding $H^s(\mathbf{R}^3) \hookrightarrow \mathscr{C}^1(\mathbf{R}^3)$ (remember that $s > 3/2+1$), one has that $\mathbf{U} \in L^\infty(0,T_{\star\star};\mathscr{C}^1(\mathbf{R}^3))$ takes its values in Ω_2. For the same reasons, $f \in L^\infty(0,T_{\star\star};H^s(\mathbf{R}^3\times\mathbf{R}^3))$.

We emphasize however, that we do not yet have $\mathbf{U}^k \overset{\mathscr{C}(0,T_{\star\star};H^s(\mathbf{R}^3))}{\longrightarrow} \mathbf{U}$. To get the convergence in $\mathscr{C}(0,T_{\star\star};\mathscr{C}^1(\mathbf{R}^3))$, we use an interpolation argument. By interpolation inequality between Sobolev spaces, we have for all $s' \in (3/2+1,s)$:

$$\begin{aligned}
\|\mathbf{U}^{k+1} - \mathbf{U}^k\|_{H^{s'},T_{\star\star}} &\leq C(s)\|\mathbf{U}^{k+1} - \mathbf{U}^k\|_{H^s,T_{\star\star}}^{s'/s}\|\mathbf{U}^{k+1} - \mathbf{U}^k\|_{L^2,T_{\star\star}}^{1-s'/s} \\
&\leq C(s)\left(\|\mathbf{U}^{k+1} - \mathbf{U}_0\|_{H^s,T_{\star\star}}^{s'/s} + \|\mathbf{U}^k - \mathbf{U}_0\|_{H^s,T_{\star\star}}^{s'/s}\right) \\
&\quad \times \|\mathbf{U}^{k+1} - \mathbf{U}^k\|_{L^2,T_{\star\star}}^{1-s'/s} \\
&\leq C(s)2R^{s'/s}\|\mathbf{U}^{k+1} - \mathbf{U}^k\|_{L^2,T_{\star\star}}^{1-s'/s}.
\end{aligned}$$

So $(\mathbf{U}^k)_k$ converges to $\mathbf{U}$ in $\mathscr{C}(0,T_{\star\star}; H^{s'}(\mathbf{R}^3))$ for $s' \in (3/2+1,s)$. By the Sobolev embedding $H^{s'}(\mathbf{R}^3) \hookrightarrow \mathscr{C}^1(\mathbf{R}^3)$, we conclude that

$$\mathbf{U}^k \overset{\mathscr{C}(0,T_{\star\star};\mathscr{C}^1(\mathbf{R}^3))}{\longrightarrow} \mathbf{U}.$$

Then $\left(\partial_{x_i}\mathbf{U}^k\right)_k$ converges to $\partial_{x_i}\mathbf{U}$ in $\mathscr{C}([0,T_{\star\star}]\times\mathbf{R}^3)$. The same is true for $\left(\sum_i A_i(\mathbf{U}^{k+1})\partial_{x_i}\mathbf{U}^k\right)_k$ because the A_i are smooth. We now turn to the convergence of

$$b(\mathbf{U}^k,f^k) = \begin{pmatrix} \dfrac{\varrho^k \int_{\mathbf{R}^3}(\boldsymbol{u}^k-\boldsymbol{v})\cdot\nabla_x\langle f^k\rangle\,\mathrm{d}v}{1-\int_{\mathbf{R}^3}\langle f^k\rangle\,\mathrm{d}v} \\ \dfrac{\varrho^k\boldsymbol{u}^k \int_{\mathbf{R}^3}(\boldsymbol{u}^k-\boldsymbol{v})\cdot\nabla_x\langle f^k\rangle\,\mathrm{d}v}{1-\int_{\mathbf{R}^3}\langle f^k\rangle\,\mathrm{d}v}\end{pmatrix}.$$

The support in v of f^k is uniformly bounded for all k, therefore, using that (f^k) converges in $L^\infty(0,T_{\star\star}; L^2(\mathbf{R}^3\times\mathbf{R}^3))$ towards f and a Cauchy-Schwarz inequality, the sequences $\left(\int_{\mathbf{R}^3} f^k\,\mathrm{d}v\right)_k$ and $\left(\int_{\mathbf{R}^3}\boldsymbol{v}f^k\right)_k$ converge in $L^\infty(0,T_{\star\star}; L^2(\mathbf{R}^3))$ towards $\int_{\mathbf{R}^3} f\,\mathrm{d}v$ and $\int_{\mathbf{R}^3}\boldsymbol{v}f\,\mathrm{d}v$. Then, using the inequality

$$\left\|\nabla_x\int_{\mathbf{R}^3}\langle f^k\rangle\,\mathrm{d}v\right\|_{H^s} \leq \mathrm{TV}(w)\left\|\int_{\mathbf{R}^3} f^k\,\mathrm{d}v\right\|_{H^s},$$

we get that the sequences $\left(\int_{\mathbf{R}^3}\nabla_x\langle f^k\rangle\,\mathrm{d}v\right)_k$ and $\left(\int_{\mathbf{R}^3}\boldsymbol{v}\cdot\nabla_x\langle f^k\rangle\,\mathrm{d}v\right)_k$ converge in $L^\infty(0,T_{\star\star}; L^2(\mathbf{R}^3))$. Using again the interpolation inequality between Sobolev spaces, we obtain that $\left(\int_{\mathbf{R}^3}\nabla_x\langle f^k\rangle\,\mathrm{d}v\right)_k$ and $\left(\int_{\mathbf{R}^3}\boldsymbol{v}\cdot\nabla_x\langle f^k\rangle\,\mathrm{d}v\right)_k$ converge in $L^\infty(0,T_{\star\star}; H^{s'}(\mathbf{R}^3))$ towards $\int_{\mathbf{R}^3}\nabla_x\langle f\rangle\,\mathrm{d}v$ and $\int_{\mathbf{R}^3}\boldsymbol{v}\cdot\nabla_x\langle f\rangle\,\mathrm{d}v$ and therefore in $\mathscr{C}([0,T_{\star\star}]\times\mathbf{R}^3)$. Furthermore, since $\int_{\mathbf{R}^3}\langle f^k\rangle\,\mathrm{d}v$ converges to $\int_{\mathbf{R}^3}\langle f\rangle\,\mathrm{d}v$ in $\mathscr{C}([0,T_{\star\star}]\times\mathbf{R}^3)$ (again using an interpolation argument) and using the inequality (2.28) we obtain that

$$\left\|\frac{1}{1-\int_{\mathbf{R}^3}\langle f\rangle\,\mathrm{d}v}\right\|_{L^\infty} < +\infty,$$

and $\left(\frac{1}{1-\int_{\mathbf{R}^3}\langle f^k\rangle\,\mathrm{d}v}\right)_k$ converges to $\frac{1}{1-\int_{\mathbf{R}^3}\langle f\rangle\,\mathrm{d}v}$ in $\mathscr{C}([0,T_{\star\star}]\times\mathbf{R}^3)$. Finally $b(\mathbf{U}^k,f^k)$ converges towards $b(\mathbf{U},f)$ in $\mathscr{C}([0,T_{\star\star}]\times\mathbf{R}^3)$. We now prove that

$$\partial_t\mathbf{U}^k \overset{\mathscr{C}(0,T_{\star\star};\mathscr{C}^1(\mathbf{R}^3))}{\longrightarrow} \partial_t\mathbf{U}.$$

Passing to the limit in $\mathcal{D}'$ in the equation

$$\partial_t\mathbf{U}^k = -\sum_{i=1}^3 A_i(\mathbf{U}^k)\partial_{x_i}\mathbf{U}^{k+1} + b(\mathbf{U}^k,f^k),$$

we obtain that $\mathbf{U}$ solves

$$\partial_t\mathbf{U} = -\sum_{i=1}^3 A_i(\mathbf{U})\partial_{x_i}\mathbf{U} + b(\mathbf{U},f), \tag{2.50}$$

in $\mathcal{D}'$. Since the right-hand-side defines a function in $\mathscr{C}([0,T_{\star\star}]\times\mathbf{R}^3)$, we have $\partial_t\mathbf{U} \in \mathscr{C}([0,T_{\star\star}]\times\mathbf{R}^3)$ and $\mathbf{U}$ solves (2.50) in the classical sense.

We now turn to the Vlasov equation. We pass to the limit in $\mathcal{D}'$ in

$$\partial_t f^{k+1} + \boldsymbol{v} \cdot \nabla_x f^{k+1} - \nabla_x \langle (\varrho^k)^\gamma \rangle \cdot \nabla_v f^{k+1} = 0.$$

We already know that $(\varrho^k)_k$ converges to ϱ in $\mathscr{C}([0,T_{\star\star}] \times \mathbf{R}^3)$, so does $\left((\varrho^k)^\gamma\right)_k$ towards ϱ^γ, finally we have $\nabla_x \langle (\varrho^k)^\gamma \rangle$ converges towards $\nabla_x \langle \varrho^\gamma \rangle$ in $\mathscr{C}([0,T_{\star\star}] \times \mathbf{R}^3)$. So we can pass to the limit in the sense of distribution and f is a solution in $\mathcal{D}'$ of

$$\partial_t f + \boldsymbol{v} \cdot \nabla_x f - \nabla_x \langle \varrho^\gamma \rangle \cdot \nabla_v f = 0. \tag{2.51}$$

Now, using the fact that the characteristic curves of f are $\mathscr{C}^1$ because $\mathbf{U}$ is $\mathscr{C}^1$, we obtain that $f \in \mathscr{C}^1_c([0,T_{\star\star}\,] \times \mathbf{R}^3 \times \mathbf{R}^3)$ and f is a solution of (2.51) in the classical sense. This concludes the proof in the case where the initial data are smooth with compact support.

2) Uniqueness. For the uniqueness, we consider two solutions $(\varrho^1, \varrho^1\boldsymbol{u}^1, f^1)$ and $(\varrho^2, \varrho^2\boldsymbol{u}^2, f^2)$ which are smooth in $[0,T]$. Then, using the same algebra as in Proposition 2.1.17, one has for some $T_{\star\star} \in (0,T)$,

$$\|\mathbf{U}^1 - \mathbf{U}^2\|_{L^2,T_{\star\star}} \leq \frac{1}{4}\|\mathbf{U}^1 - \mathbf{U}^2\|_{L^2,T_{\star\star}} + \frac{1}{4}\|\mathbf{U}^1 - \mathbf{U}^2\|_{L^2,T_{\star\star}},$$

$$\|f^1 - f^2\|_{L^2,T_{\star\star}} \leq C(\Omega_2,s,R,f_0)\|\mathbf{U}^1 - \mathbf{U}^2\|_{L^2,T_{\star\star}}.$$

As a consequence, $\mathbf{U}^1 = \mathbf{U}^2$ and $f^1 = f^2$.

3) General initial data. We turn to the case where $\varrho_0 - 1 \in H^s(\mathbf{R}^3)$, $\boldsymbol{u} \in H^s(\mathbf{R}^3)$ and $f_0 \in \mathscr{C}^1_c(\mathbf{R}^3 \times \mathbf{R}^3) \cap H^s(\mathbf{R}^3 \times \mathbf{R}^3)$. We introduce an approximation of the identity φ_{ε_k} with $\varepsilon_k = 2^{-k}\varepsilon_0$, with ε_0 small enough. Then we define $\mathbf{U}_0^k = \varphi_{\varepsilon_k} \star \mathbf{U}_0$ and $f_0^k = (\varphi_{\varepsilon_k} \otimes \varphi_{\varepsilon_k}) \star f_0$, where the convolution and tensor products are in (x,v). With such a choice, one has (see [110])

$$\sum_{k\in\mathbf{N}} \|\mathbf{U}_0^{k+1} - \mathbf{U}_0^k\|_{L^2} < +\infty, \qquad \sum_{k\in\mathbf{N}} \|f_0^{k+1} - f_0^k\|_{L^2} < +\infty.$$

The solution is then obtained by the same approximation scheme but we replace the initial data by $\mathbf{U}_0^{k+1}$ and f_0^{k+1}. The proof is then similar, except for two small modifications. Firstly, one has to prove estimates on $\mathbf{U}^k - \mathbf{U}_0^0$ instead of $\mathbf{U}^k - \mathbf{U}_0$, this is where we need to chose ε_0 small enough. Secondly, the estimates (2.47)-(2.48) are replaced by

$$\|\mathbf{U}^{k+1} - \mathbf{U}^k\|_{L^2,T_{\star\star}} \leq \frac{1}{4}\|\mathbf{U}^k - \mathbf{U}^{k-1}\|_{L^2,T_{\star\star}} + \frac{1}{4}\|\mathbf{U}^{k-1} - \mathbf{U}^{k-2}\|_{L^2,T_{\star\star}} + C\|\mathbf{U}_0^{k+1} - \mathbf{U}_0^k\|_{L^2},$$

and

$$\|f^k - f^{k-1}\|_{L^2,T_{\star\star}} \leq C(f_0,\Omega_2,\mathrm{TV}(w),\gamma)\|\mathbf{U}^{k-1} - \mathbf{U}^{k-2}\|_{L^2,T_{\star\star}} + \|f_0^k - f_0^{k-1}\|_{L^2}.$$

□

2.2 Weak solutions

The construction of weak solutions for the thick spray model discussed in this thesis presents different difficulties compared to the construction of strong solutions. Below, we briefly discuss two axis of research for the construction of weak solutions. For now, the construction of weak solutions is a problem that appears too challenging for these techniques.

2.2.1 Construction of weak solutions for the regularized thick spray model

In the introduction of this Chapter, we mentioned that in the original thick spray equations (4.1), the presence of the term $\nabla_x p \cdot \nabla_v f$ makes the construction of weak solutions a challenging problem, because the standard theory can at most handle a force field in BV [3,4].

A natural question after introducing the system (4.4) is: Is it possible to construct weak solutions of this system? Let's have a look at the following Vlasov equation in 1D:

$$\partial_t f + v\partial_x f - \langle \partial_x p \rangle \partial_v f = 0.$$

Now, if for all t, $p(t,\cdot)$ is in $\mathrm{BV} \cap \mathscr{C}^\infty$, one has

$$\begin{aligned}\langle \partial_x p \rangle (x) &= \int_{\mathbf{R}} w(x-y)\partial_x p(y)\,\mathrm{d}y \\ &= \int_{x-r_p}^{x+r_p} \partial_x p(y)\mathrm{d}y \\ &= p(x+r_p) - p(x-r_p).\end{aligned}$$

Then if $p(t,\cdot)$ is in BV, we define the term $\langle \partial_x p \rangle$ by

$$\langle \partial_x p \rangle := \tau_{r_p} p - \tau_{-r_p} p$$

where τ_y is the translation by y. Then one can write the Vlasov equation as

$$\partial_t f + v\partial_x f - \left(\tau_{r_p} p - \tau_{-r_p} p\right)\partial_v f = 0.$$

In principle, one could then construct a weak solution of this equation, following [3].

2.2.2 Weak solutions for the thick spray model

Let us make some comments about the construction of weak solution for the thick spray model without regularization (4.1). From the point of view of the applications, it is highly desirable to be able to simulate shock waves in flows described by the thick spray system [64].

If $f = 0$, then (4.1) become the isentropic Euler equations, and then shock waves (that is, solutions that are piecewise smooth with discontinuities) are described by weak solutions in the sense of distribution [68].

If f is a given function, then the fluid part, which writes

$$\begin{cases}\partial_t(\alpha\varrho) + \partial_x(\alpha\varrho u) = 0\\ \partial_t(\alpha\varrho u) + \partial_x(\alpha\varrho u^2) + \alpha\partial_x p = 0\end{cases}$$

is the same equations as the isentropic Euler equations for a single fluid in a nozzle of section α [68]. Weak solutions in the sense of distribution are not appropriate for this system. Indeed, the problem comes from the presence of the nonconservative product $\alpha\partial_x p$. In the case where

α and p are discontinuous, this product makes no sense in the framework of distributions. Dal Masot, Le Floch and Murat proposed a theory to give a sense to such product [39]. This led to numerical schemes specificly designed to tackle this kind of problems [1, 30, 33, 75, 98]. In the following, we present some exploration work on how to define weak solutions for the thick spray system and if the theory developed in [39] is suitable to handle this kind of problem.

Let us give a brief presentation of the theory developed in [39] for nonconservative product. Typically, such nonconservative products are of the form $g(u)\partial_x u$, where g is a continuous function and u a piecewise smooth function. Formally, the aim is to give a definition to products of the type $H\delta$ where H is the heaviside function and δ is the dirac Delta distribution.

Let ϕ be a lipschitz continuous map $\phi : [0,1] \times \mathbf{R} \times \mathbf{R} \to \mathbf{R}$ satisfying the following properties

- $\forall p^-,p^+ \in \mathbf{R}, \forall s \in [0,1],\ \phi(0,p^-,p^+) = p^-, \quad \phi(1,p^-,p^+) = p^+,$
- $\exists k > 0,\ \forall p^-,p^+ \in \mathbf{R},\ \forall s \in [0,1], |\partial_s \phi(s,p^-,p^+)| \leq k|p^- - p^+|$.

Then, the following definition of nonconservative products is based on this family ϕ

Definition 2.2.1. *Let $u : \mathbf{R} \to \mathbf{R}$ be a function of bounded variation, so that its derivative $\frac{du}{dx}$ defines a Radon measure, and $g : \mathbf{R} \to \mathbf{R}$ be a continuous function. Then, there exists a unique real-valued bounded Borel measure μ on $\mathbf{R}$ characterized by the following properties :*

1. *If u is continuous on a Borel set $B \subset \mathbf{R}$, then*
$$\mu(B) = \int_B g(u)\frac{du}{dx}\,\mathrm{d}x.$$
2. *If u is discontinuous at a point x_0, then*
$$\mu(\{x_0\}) = \int_0^1 g(\Phi(s; u(x_0-), u(x_0+)))\partial_s\Phi(s; u(x_0-), u(x_0+))ds.$$

We say that μ is the nonconservative product of $g(u)$ by $\frac{du}{dx}$ and we denote
$$\mu = \left[g(u)\frac{du}{dx}\right]_\phi .$$

In the fluid part of the thick spray system (4.1), there is actually a way to get rid of the product $\alpha\partial_x p$. One possibility is to replace this equation by the conservation law of the total momentum, then the fluid part writes in 1D

$$\partial_t n + \partial_x q = 0, \tag{2.52}$$
$$\partial_t q + \partial_x \left(\frac{(q - \int fv\,\mathrm{d}v)^2}{n} + m_\star \int fv^2\,\mathrm{d}v\right) + \partial_x p\left(\frac{n^\gamma}{\alpha^\gamma}\right) = 0, \tag{2.53}$$

with $n = \alpha\varrho$ and $q = \alpha\varrho u + m_\star \int fv\,\mathrm{d}v$. If f is a given smooth function, this system is conservative and it is possible to define weak solutions in the sense of distribution (with regularity in BV). However, there is still a problem for the Vlasov equation, which writes (ignoring the friction which does not cause any issue)

$$\partial_t f + v\partial_x f - \partial_x p \partial_v f = 0. \tag{2.54}$$

The problem with the Vlasov equation seems to be even more difficult because f could have discontinuities in x and v. In this case the product $\partial_x p \partial_v f$ is a nonconservative product and the standard theory of distributions is not adapted to deal with this kind of products. In the rest of this section, we investigate if the Definition 2.2.1 of a nonconservative product given by [39] is a good tool to define weak solution for the system (4.1).

We propose the following definition of weak solution for the equation (2.54)

Definition 2.2.2. *Let ϕ be a Lipschitz continuous path and $p \in L^\infty(0,+\infty;\mathrm{BV}(\mathbf{R}))$. We say that $f \in L^\infty(0,+\infty;L^1_{x,v} \cap L^\infty_{x,v} \cap \mathrm{BV}_x)$ is a weak solution of the Vlasov equation*

$$\partial_t f + v\partial_x f - \partial_x p \partial_v f = 0,$$

if, for every $\zeta \in \mathcal{D}((0,+\infty) \times \mathbf{R}_x \times \mathbf{R}_v)$,

$$\int_0^{+\infty}\int_{\mathbf{R}_x}\int_{\mathbf{R}_v} \left(\partial_t\zeta(t,x,v) + v\partial_x\zeta(t,x,v)\right) f(t,x,v)\mathrm{d}v\mathrm{d}x\mathrm{d}t - \int_0^{+\infty}\int_{\mathbf{R}_x}\int_{\mathbf{R}_v} \left[\partial_x p f\right]_\phi \partial_v\zeta(t,x,v)\mathrm{d}v\mathrm{d}x\mathrm{d}t = 0$$

A natural scenario that we would like to capture with the Definition 2.2.2 is the following: A stream of particles hitting a shock wave, without enough kinetic energy to pass through it, so the particles will bounce on the shock wave. Another similar situation is a stream of particles accelerated by a shock wave catching it up. A prototype solution would be like this

$$f(t,x,v) = \mathbf{1}_{[\sigma t,+\infty[\times[v_{1,+}-\sigma, v_{2,+}-\sigma]}(x,v) + \mathbf{1}_{[\sigma t,+\infty[\times[v_{1,-}-\sigma, v_{2,-}-\sigma]}(x,v).$$

It turns out that Definition 2.2.2 does not include such profiles. This is the subject of the following lemma:

Lemma 2.2.3. *Let ϕ be a Lipschitz continuous path. Let f be a function of the form*

$$f(x,v,t) = \mathbf{1}_{[\sigma t,+\infty[\times[v_{1,+}-\sigma, v_{2,+}-\sigma]}(x,v) + \mathbf{1}_{[\sigma t,+\infty[\times[v_{1,-}-\sigma, v_{2,-}-\sigma]}(x,v).$$

There exist $\zeta \in \mathcal{D}(\mathbf{R}^3)$ such that

$$\int_{\mathbf{R}^3} \left(\partial_t\zeta(t,x,v) + v\partial_x\zeta(t,x,v)\right) f(t,x,v)dxdvdt - \int_{\mathbf{R}^3} \left[\partial_x p f\right]_\phi \partial_v\zeta(t,x,v)dxdvdt \neq 0.$$

Proof. Let $\zeta \in \mathcal{D}(\mathbf{R}^3)$, we write, thanks to the change of variable $y = x - \sigma t$, $w = v - \sigma$:

$$\int_{\mathbf{R}^3} \left(\partial_t\zeta(t,x,v) + v\partial_x\zeta(t,x,v)\right) f(t,x,v)dxdvdt - \int_{\mathbf{R}^3} \left[\partial_x p f\right]_\phi \partial_v\zeta(t,x,v)dvdt \tag{2.55}$$

$$= \int_{\mathbf{R}^3} \left(\partial_t\tilde{\zeta}(t,y,w) + v\partial_y\tilde{\zeta}(t,y,w)\right) g(y,w)dydwdt - \int_{\mathbf{R}^2} \left(\int_0^1 f(\phi(s),v,t)\phi'(s)ds\right) \partial_v\tilde{\zeta}(t,0+,v-\sigma)dvdt. \tag{2.56}$$

The first term yield

$$\int_{\mathbf{R}^3} \partial_t\tilde{\varphi}(t,y,w)g(y,w)dydwdt = -\int_{\mathbf{R}^2} \tilde{\varphi}(0,y,w)g(y,w)dydw = 0$$

and

$$\int_{\mathbf{R}^3} w\partial_y\tilde{\varphi}(t,y,w)g(y,w)dydwdt = -\int_{\mathbf{R}^2} w\tilde{\varphi}(t,0,w)g(0+,w)dwdt.$$

For the second term :

$$\int_{\mathbf{R}^2}\left(\int_0^1 f(\phi(s),v,t)\phi'(s)ds\right)\partial_v\tilde{\zeta}(t,0+,v-\sigma)dvdt \tag{2.57}$$

$$= \int_{\mathbf{R}}\sum_i\left(\int_0^1 f(\phi(s),v_i,t)\phi'(s)ds\right)\tilde{\zeta}(t,0+,v_i-\sigma)dt \tag{2.58}$$

We then choose $\tilde{\zeta}$ so that only $\tilde{\zeta}(t,0,v-\sigma)$ for $v_{1,+} < v < v_{2,+}$ is positive, which is always possible. Then we have

$$\int_{\mathbf{R}^3}\left(\partial_t\zeta(t,x,v) + v\partial_x\zeta(t,x,v)\right)f(t,x,v)dxdvdt - \int_{\mathbf{R}^3}\left[\partial_x pf\right]_\phi\partial_v\zeta(t,x,v)dxdvdt \tag{2.59}$$

$$= -\int_{\mathbf{R}^2} w\tilde{\zeta}(t,0,w)g(0+,w)dwdt < 0. \tag{2.60}$$

□

This result can be extended if we replace f by a regularized version in v. From this result, it seems that Definition 2.2.2 is not adequate to work with this kind of problem.

Chapter 3

Analogy between the thick spray system and plasma physics: Linear Landau damping and instabilities

Summary

The aim of this chapter to study a linearized thick sprays model. We show analogy at the linear level between the thick spray system (4.4) and the Vlasov Poisson equations of plasma physics.

This chapter is divided in two part. The first part corresponds to a joint work with Christophe Buet and Bruno Després accepted in *Communications in Mathematical Sciences* [28]. We recast the system as a linear Schrödinger equation and we prove that the corresponding operator only has absolutely continuous spectrum. This proves that the system display an analog of the Landau damping and one observes a decay of the acoustic energy. We also present numerical illustration showing such effect.

The second part is based on the proceeding [62] accepted in *ESAIM: Proceedings and Surveys*. The goal is to discuss instability properties of the linear thick spray model without friction, still taking the Vlasov Poisson system as a guide for the analysis. We also present numerical illustrations inspired by typical plasma physics test case.

3.1 Introduction

Collisionless motion of an electrostatic plasma is well-described by the Vlasov-Poisson system

$$\begin{cases} \partial_t f + \boldsymbol{v}\cdot\nabla_x f + \mathbf{E}\cdot\nabla_v f = 0 \\ \mathbf{E} = \nabla\Delta^{-1}\left(\int_{\mathbf{R}} f \mathrm{d}v\right). \end{cases} \tag{3.1}$$

It is known since the seminal work of Landau [81] that such model can exhibit a decay of the electric field for large times. This property of plasma, known today as *Landau damping*, has received a lot of interest since then and there exists an extensive literature on the linear Landau damping and more recently on the nonlinear Landau damping. See for example [40, 96, 113] and the reference therein. See also [15, 69, 70] for similar effect in other systems.

In this work, we present new results of linear damping properties of solutions of a multiphase model describing suspensions of particles in a underlying gas. Such complex flow is usually refered to as a *spray* [45]. A typical system which describes this kind of spray writes

$$\begin{cases} \partial_t f + \boldsymbol{v}\cdot\nabla_x f + \nabla_v\cdot(\boldsymbol{\Gamma} f) = 0 \\ \partial_t(\alpha\varrho) + \nabla_x\cdot(\alpha\varrho\boldsymbol{u}) = 0 \\ \partial_t(\alpha\varrho\boldsymbol{u}) + \nabla_x\cdot(\alpha\varrho\boldsymbol{u}\otimes\boldsymbol{u}) + \alpha\nabla_x p(\varrho) = D_\star\int_{\mathbf{R}^3}(\boldsymbol{v}-\boldsymbol{u})f\,\mathrm{d}v. \end{cases} \tag{3.2}$$

In (4.4), the first equation is a Vlasov-type equation and it describes the evolution of the particles through a distribution function $f = f(t,\boldsymbol{x},\boldsymbol{v}) \geq 0$ in the phase space $\mathbf{T}^3\times\mathbf{R}^3$ for times $t > 0$. The second and third equations of (4.4) are the barotropic compressible Euler equations and they describe the evolution of the density $\varrho = \varrho(t,\boldsymbol{x}) \geq 0$ and the velocity $\boldsymbol{u} = \boldsymbol{u}(t,\boldsymbol{x}) \in \mathbf{R}^3$ of the fluid, for times $t > 0$ and $\boldsymbol{x} \in \mathbf{T}^3$. The system (4.4) describes the so-called *thick* sprays regime, in which the total volume occupied by the particles is not negligible compared to the one of the fluid. This has the consequence that the fluid and the particles are coupled through the following quantities. The first quantity is the volume fraction of the fluid $\alpha = \alpha(t,\boldsymbol{x})$. It is linked to the f by the formula

$$\alpha(t,\boldsymbol{x}) = 1 - \frac{4}{3}\pi r_p^3 \int_{\mathbf{R}^3} f(t,\boldsymbol{x},\boldsymbol{v})\,\mathrm{d}v.$$

Here, we assume that $\alpha(t,\boldsymbol{x}) \in [0,1]$. This is in strong contrast with the *thin* sprays regime where this quantity is assumed to be very closed to 1 and is therefore absent from the equations [12]. The radius of the particles $r_p > 0$ is a constant in this work. The force field acting on the particles $\boldsymbol{\Gamma} := \boldsymbol{\Gamma}(t,\boldsymbol{x},\boldsymbol{v})$ is given by

$$\boldsymbol{\Gamma}(t,\boldsymbol{x},\boldsymbol{v}) = -\nabla_x p(\varrho) - \frac{D_\star}{\frac{4}{3}\pi r_p^3}(\boldsymbol{v} - \boldsymbol{u}).$$

It is composed of two terms. The term $-\nabla_x p(\varrho)$ is a specific feature of thick sprays (it is absent in the thin sprays regime). The term $D_\star(v-u)$ is a drag force exerted on the particles by the fluid. The retroaction of the drag force on the fluid appears in the third equation of (4.4) through the term $D_\star \int_{\mathbf{R}^3}(\boldsymbol{v}-\boldsymbol{u})f\,\mathrm{d}v$ and is sometimes refered to as the *Brinkman force*. The drag coefficient $D_\star \geq 0$ is usually given in a semi-empirical manner.

This model can be used to describe various physical phenomena at different length scales, such as aerosols for medical use [24,25], the combustion in engines [5], aerosols in the atmosphere [90], and also in astrophysics for the modelling of gas giants and exoplanets [66]. See also [17,23,46,53,63,97,118].

In parallel with the system (3.25) where collisions are neglected, we neglect the drag force in (4.4). Thus, $D_\star = 0$ and the model problem that we will use in most of this work writes

$$\begin{cases} \partial_t f + \boldsymbol{v}\cdot\nabla_x f - \nabla_x p(\varrho)\cdot\nabla_v f = 0 \\ \partial_t(\alpha\varrho) + \nabla_x\cdot(\alpha\varrho\boldsymbol{u}) = 0 \\ \partial_t(\alpha\varrho\boldsymbol{u}) + \nabla_x\cdot(\alpha\varrho\boldsymbol{u}\otimes\boldsymbol{u}) + \alpha\nabla_x p(\varrho) = 0. \end{cases} \tag{3.3}$$

A description of our main results is the following.

(i) The first result investigates damping properties of small perturbations of homogenous profiles at the linear level. It is described in the Theorem 3.2.1 below. We linearize the system (3.3) around a reference solution and we analyze the decay of the perturbation in L^2 norm. We adapt ideas from plasma physics [34, 43, 44] and exploit the scattering structure of the linearized system, rewriting it as a linear Schrödinger equation of the form

$$\frac{\mathrm{d}}{\mathrm{d}t}\mathbf{U} = iH\mathbf{U}.$$

The analysis is based on a careful analysis of the spectrum of the unbounded operator H. The main difficulty is that the system at stakes is more complex than the Vlasov-Poisson system, making the computations more tedious.

(ii) The second result is the computation of the rate of decay of the perturbation of the linearized equations for analytic initial data. Mimicking computations done by Landau [81] for the Vlasov-Poisson system, we obtain the dispersion relation of the linearized system. This function is written as the sum of the dispersion relation of the Vlasov-Poisson equation and an additional term which is specific to the model (3.3). The computation of the dispersion relation is done in the Proposition 3.2.5 below. Then, we formally derive an expansion for the perturbation of the density.

(iii) Finally we show numerical simulation illustrating the damping investigated in this paper. We present schemes for the linearized and the nonlinear equations. The schemes are derived from classical methods. It shows that the damping predicted by the linear equations is observed in the linear and the nonlinear simulations. We also present preliminary formal and numerical results for the case with nonzero friction $D_\star > 0$.

Overview of the Chapter. This chapter is organized as follows. In section 3.2.2, we prove Theorem 3.2.1. In section 3.2.3, we show formal computation leading to the dispersion relation. In section 3.3, we show numerical results illustrating Theorem 3.2.1, and we show that the computation done in section 3.2.3 are verified numerically. Finally in section 3.4, we discuss remaining open questions about this work.

3.2 Linear Damping

In this section, our aim is to analyze the damping properties of the system (3.3) in the linear regime. We follow a classical approach where we linearize the equations around gaussian equilibrium. In contrast with plasma physics, the physical validity of such equilibrium is questionable for thick sprays, and should be justified. Another possibility is to use a more general class of equilibrium as in [27]. In this work we limit ourselves to gaussian equilibrium since it simplifies the equations and already brings valuable insight on the mathematical structure of the system.

3.2.1 The linear thick spray model

We consider the following homogeneous solution of (3.3)

$$\begin{cases} \varrho(t,\boldsymbol{x}) = \varrho_0 > 0, \\ \boldsymbol{u}(t,\boldsymbol{x}) = 0, \\ f(t,\boldsymbol{x},\boldsymbol{v}) = f^0(\boldsymbol{v}) := \frac{n_0}{\sqrt{2\pi}} e^{-|\boldsymbol{v}|^2/2}, \end{cases}$$

where the density $n_0 = \int_{\mathbf{R}^3} f^0 \, \mathrm{d}v$ is related to the volume fraction α_0 by

$$1 - \frac{4}{3}\pi r_p^3 n_0 = \alpha_0 \in (0,1). \tag{3.4}$$

Following [27], we perform the linearization

$$\begin{cases} \varrho(t,\boldsymbol{x}) = \varrho_0 + \varepsilon \varrho_1(t,\boldsymbol{x}) + O(\varepsilon^2) \\ \boldsymbol{u}(t,\boldsymbol{x}) = \varepsilon \boldsymbol{u}_1(t,\boldsymbol{x}) + O(\varepsilon^2) \\ f(t,\boldsymbol{x},\boldsymbol{v}) = f^0(\boldsymbol{v}) + \varepsilon\sqrt{f^0(\boldsymbol{v})} f_1(t,\boldsymbol{x},\boldsymbol{v}) + O(\varepsilon^2). \end{cases}$$

Dropping the quadratic terms and the subscripts, one obtains the following linear thick sprays equations with $\tau(t,\boldsymbol{x}) = -\varrho_1(t,\boldsymbol{x})/\varrho_0^2$ and $c_0 = \sqrt{p'(\varrho_0)}$

$$\begin{cases} \alpha_0\varrho_0\partial_t\tau = \alpha_0\nabla_x \cdot \boldsymbol{u} + \dfrac{4}{3}\pi r_p^3 \nabla_x \cdot \displaystyle\int_{\mathbf{R}^3} \boldsymbol{v}\sqrt{f^0} f \, \mathrm{d}v \\ \alpha_0\varrho_0\partial_t\boldsymbol{u} = \alpha_0\varrho_0^2 c_0^2 \nabla_x\tau \\ \partial_t f + \boldsymbol{v}\cdot\nabla_x f - \varrho_0^2 c_0^2 \sqrt{f^0(v)}\boldsymbol{v}\cdot\nabla_x\tau = 0. \end{cases} \tag{3.5}$$

3.2.2 Spectral theory for linear thick sprays

The main result of this section is the following.

Theorem 3.2.1. *Let $f^0 = f^0(v)$ satisfies (3.4), and initial condition $(\tau_{\rm ini},\boldsymbol{u}_{\rm ini},f_{\rm ini}) \in L^2(\mathbf{T}^3) \times (L^2(\mathbf{T}^3))^3 \times L^2(\mathbf{T}^3 \times \mathbf{R}^3)$ such that*

$$\iint_{\mathbf{T}^3\times\mathbf{R}^3} f_{\rm ini}(\boldsymbol{x},\boldsymbol{v})\,\mathrm{d}v\mathrm{d}x = 0, \qquad \int_{\mathbf{T}^3} \tau_{\rm ini}(\boldsymbol{x})\,\mathrm{d}x = 0, \qquad \int_{\mathbf{T}^3} \boldsymbol{u}_{\rm ini}(\boldsymbol{x})\,\mathrm{d}x = 0.$$

Then as $t \to +\infty$ the solution $(\tau(t,\cdot),u(t,\cdot),f(t,\cdot,\cdot))$ of the linearized thick sprays equations (3.5) with initial data $(\tau_{\rm ini},u_{\rm ini},f_{\rm ini})$ verifies

$$\|\tau(t)\|_{L^2} + \|\boldsymbol{u}(t)\|_{L^2} \to 0,$$

and $f(t,\cdot,\cdot)$ converges weakly to 0 in $L^2(\mathbf{T}^3 \times \mathbf{R}^3)$.

Remark 3.2.2. *As the quadratic energy $\int_{\mathbf{T}^3\times\mathbf{R}^3} |f|^2\,\mathrm{d}x\mathrm{d}v + \int_{\mathbf{R}^3} |\tau|^2 + |\boldsymbol{u}|^2\,\mathrm{d}x$ is conserved, Theorem 3.2.1 implies that all the acoustic energy is transferred to the particles. It will be visible in Figure 3.3 where fast oscillations show up in the velocity variable. It is known in the plasma community as filamentation.*

The proof of Theorem 3.2.1 is done using tools from spectral theory [79, 84]. For the sake of simplicity of the notations, we place ourselves in 1D, but the proof is valid in dimension $d \in \mathbf{N}^*$. After setting all constants to 1, the system (3.5) rewrites

$$\begin{cases} \partial_t \tau = \partial_x u + \partial_x \displaystyle\int_{\mathbf{R}} v\sqrt{f^0} f\,\mathrm{d}v \\ \partial_t u = \partial_x \tau \\ \partial_t f + v\partial_x f - \sqrt{f^0(v)}v\partial_x \tau = 0. \end{cases} \tag{3.6}$$

We start from initial data $(\tau_{\rm ini}, u_{\rm ini}, f_{\rm ini})$ satisfying

$$\iint_{\mathbf{T}\times\mathbf{R}} f_{\rm ini}(x,v)\,\mathrm{d}v\mathrm{d}x = 0, \qquad \int_{\mathbf{T}} \tau_{\rm ini}(x)\,\mathrm{d}x = 0, \qquad \int_{\mathbf{T}} u_{\rm ini}(x)\,\mathrm{d}x = 0.$$

One can show that solutions of (3.6) conserve the quadratic energy

$$\frac{\mathrm{d}}{\mathrm{d}t}\left(\iint_{\mathbf{T}\times\mathbf{R}} |f|^2\,\mathrm{d}v\mathrm{d}x + \int_{\mathbf{T}} |\tau|^2 + |u|^2\,\mathrm{d}x\right) = 0. \tag{3.7}$$

Functional setting We define the following functional spaces

$$L^2_0(\mathbf{T}) = \left\{u \in L^2(\mathbf{T}), \quad \int_{\mathbf{T}} u(x)\,\mathrm{d}x = 0\right\},$$

and

$$L^2_0(\mathbf{T}\times\mathbf{R}) = \left\{f \in L^2(\mathbf{T}\times\mathbf{R}), \quad \iint_{\mathbf{T}\times\mathbf{R}} f(x,v)\,\mathrm{d}x\mathrm{d}v = 0\right\},$$

and

$$\ell^2_0(\mathbf{Z}) = \left\{u \in \ell^2(\mathbf{Z}), \quad u_0 = 0\right\},$$

and the unbounded operator $H : L^2_0(\mathbf{T}) \times L^2_0(\mathbf{T}) \times L^2_0(\mathbf{T}\times\mathbf{R}) \longrightarrow L^2_0(\mathbf{T}) \times L^2_0(\mathbf{T}) \times L^2_0(\mathbf{T}\times\mathbf{R})$, by

$$iH = \begin{pmatrix} 0 & \partial_x & \partial_x \int_{\mathbf{R}} v\sqrt{f^0(v)} \cdot \,\mathrm{d}v \\ \partial_x & 0 & 0 \\ v\sqrt{f^0(v)}\partial_x & 0 & -v\partial_x \end{pmatrix},$$

with domain

$$D[H] = \{(\tau,u,f) \in L^2_0(\mathbf{T})\times L^2_0(\mathbf{T})\times L^2_0(\mathbf{T}\times\mathbf{R}), \text{ such that } \partial_x\tau \in L^2(\mathbf{T}), \partial_x u \in L^2(\mathbf{T}), v\partial_x f \in L^2(\mathbf{T}\times\mathbf{R})\}.$$

The system (3.6) rewrites as a linear Schrödinger equation

$$\frac{\mathrm{d}}{\mathrm{d}t}\mathbf{U} = iH\mathbf{U}, \quad \mathbf{U} = (\tau,u,f).$$

To study the operator H, we introduce the Fourier transform $\mathcal{F} : L^2_0(\mathbf{T}) \longrightarrow \ell^2_0(\mathbf{Z})$ defined by

$$\mathcal{F}(f)(k) = f_k := \int_{\mathbf{T}} e^{-ikx} f(x)\,\mathrm{d}x, \quad \forall k \in \mathbf{Z}.$$

In this context, the Fourier inverse $\mathcal{F}^{-1} : \ell^2_0(\mathbf{Z}) \longrightarrow L^2_0(\mathbf{T})$ is well-defined and $\mathcal{F}$ is a unitary operator. Denote $\ell^2_k L^2_v = \mathcal{F}(L^2_0(\mathbf{T}\times\mathbf{R}))$. We work in the Hilbert space

$$X = \ell^2_0(\mathbf{Z}) \times \ell^2_0(\mathbf{Z}) \times \ell^2_k L^2_v,$$

equipped with the hermitian product

$$\langle(\tau,u,f),(\sigma,w,g)\rangle_X = \sum_{k\in\mathbf{Z}} \tau_k\overline{\sigma_k} + \sum_{k\in\mathbf{Z}} u_k\overline{w_k} + \sum_{k\in\mathbf{Z}} \int_{\mathbf{R}} f_k(v)\overline{g_k(v)}\,\mathrm{d}v.$$

We introduce $\mathbf{k}$ the operator defined by $(\mathbf{k}\tau)_k = k\tau_k$ for all $k \in \mathbf{Z}$. Let $\mathcal{H} : X \longrightarrow X$ the operator defined by

$$i\mathcal{H} = i\mathbf{k}\begin{pmatrix} 0 & 1 & \int_{\mathbf{R}} v\sqrt{f^0(v)} \cdot \,\mathrm{d}v \\ 1 & 0 & 0 \\ v\sqrt{f^0(v)}\cdot & 0 & -v \end{pmatrix},$$

with domain

$$D[\mathcal{H}] = \Big\{(\tau,u,f) \in X, \text{ such that } \quad \mathbf{k}\tau \in \ell^2(\mathbf{Z}),\ \mathbf{k}u \in \ell^2(\mathbf{Z}),\ \mathbf{k}vf \in \ell^2_k L^2_v\Big\}.$$

By construction, H and $\mathcal{H}$ are unitarily equivalent. The system (3.6) rewrites in the Fourier space, as

$$\frac{\mathrm{d}}{\mathrm{d}t}\mathbf{U} = i\mathcal{H}\mathbf{U}.$$

Proposition 3.2.3. *The operators H and $\mathcal{H}$ are self adjoint.*

Proof. Let us write $\mathcal{H} = \mathcal{H}_0 + \mathcal{K}$, with

$$\mathcal{H}_0 = \mathbf{k}\begin{pmatrix} 0 & 1 & 0 \\ 1 & 0 & 0 \\ 0 & 0 & -v \end{pmatrix}, \quad \mathcal{K} = \mathbf{k}\begin{pmatrix} 0 & 0 & \int_{\mathbf{R}} v\sqrt{f^0(v)} \cdot \,\mathrm{d}v \\ 0 & 0 & 0 \\ v\sqrt{f^0(v)}\cdot & 0 & 0 \end{pmatrix},$$

with domain

$$D[\mathcal{H}_0] = D[\mathcal{H}],$$

$$D[\mathcal{K}] = \left\{(\tau,u,f) \in X, \quad \mathbf{k}\int_{\mathbf{R}} v\sqrt{f^0(v)}f \,\mathrm{d}v \in \ell^2(\mathbf{Z}),\ \ \mathbf{k}v\sqrt{f^0(v)}\tau \in \ell^2_k L^2_v\right\}.$$

Let us show that $(\mathcal{H}_0, D[\mathcal{H}_0])$ is self-adjoint. A simple computation show that $\mathcal{H}_0$ is symmetric, $\langle \mathcal{H}_0 U,V\rangle_X = \langle U,\mathcal{H}_0 V\rangle_X$ for all U, $V \in D[\mathcal{H}_0]$. It remains to show that $D[\mathcal{H}_0^*] \subset D[\mathcal{H}_0]$. Let $(\sigma,w,g) \in D[\mathcal{H}_0^*]$. By definition of the adjoint, for every $(\tau,u,f) \in D[\mathcal{H}_0]$, there exists $(s,\omega,h) \in X$ such that

$$\langle \mathcal{H}(\tau,u,f),(\sigma,w,g)\rangle = \langle (\tau,u,f),(s,\omega,h)\rangle.$$

In particular, for

$$(\tau,u,f) = \mathbf{k}\begin{pmatrix} w\mathbf{1}_{[\![-n,n]\!]} \\ \sigma\mathbf{1}_{[\![-n,n]\!]} \\ -vg\mathbf{1}_{[\![-n,n]\!]\times[-m,m]}\end{pmatrix},$$

one has

$$\begin{aligned}\langle \mathcal{H}_0(\tau,u,f),(\sigma,w,g)\rangle &= \sum_{k=-n}^{n} k^2\left|w_k\right|^2 + \sum_{k=-n}^{n} k^2|\sigma_k|^2 + \sum_{k=-n}^{n}\int_{-m}^{m} k^2v^2\left|g_k\right|^2\,\mathrm{d}v \\ &= \langle (\tau,u,f),(s,\omega,h)\rangle_X \\ &\le \|\tau,u,f\|_X\|s,\omega,h\|_X \\ &= \left[\sum_{k=-n}^{n} k^2\left|w_k\right|^2 + \sum_{k=-n}^{n} k^2|\sigma_k|^2 + \sum_{k=-n}^{n}\int_{-m}^{m} k^2v^2\left|g_k(v)\right|^2\,\mathrm{d}v\right]^{1/2}\|s,\omega,h\|_X.\end{aligned}$$

So

$$\left[\sum_{k=-n}^{n} k^2\left|w_k\right|^2 + \sum_{k=-n}^{n} k^2|\sigma_k|^2 + \sum_{k=-n}^{n}\int_{-m}^{m} k^2v^2\left|g_k(v)\right|^2\,\mathrm{d}v\right]^{1/2} \le \|s,\omega,h\|_X,$$

and, taking the limit $m,n \to \infty$, it yields

$$\mathbf{k}w \in \ell^2(\mathbf{Z}),$$

$$\mathbf{k}\sigma \in \ell^2(\mathbf{Z}),$$

$$-\mathbf{k}vg \in \ell^2_k L^2_v.$$

This show that $\mathcal{H}_0$ is self adjoint. Moreover, the operator $\mathcal{K}$ is clearly symmetric, and $D[\mathcal{H}_0] \subset D[\mathcal{K}]$. Furthermore

$$\begin{aligned}\|\mathcal{K}(\tau,u,f)\|_X^2 &= \sum_{k\in\mathbf{Z}} k^2\int_{\mathbf{R}} v^2 f^0(v)|\tau_k|^2\,\mathrm{d}v + \sum_{k\in\mathbf{Z}} k^2\left|\int_{\mathbf{R}} v\sqrt{f^0(v)}f_k(v)\,\mathrm{d}v\right|^2 \\ &\le \int_{\mathbf{R}} v^2 f^0(v)\,\mathrm{d}v\sum_{k\in\mathbf{Z}} k^2|\tau_k|^2 + n_0\sum_{k\in\mathbf{Z}} k^2|u_k|^2 + \int_{\mathbf{R}} f^0(v)\,\mathrm{d}v\sum_{k\in\mathbf{Z}}\int_{\mathbf{R}} v^2k^2|f_k(v)|^2\,\mathrm{d}v \\ &\le n_0\|\mathcal{H}_0(\tau,u,f)\|_X^2.\end{aligned}$$

So the operator $\mathcal{K}$ is $\mathcal{H}_0$-bounded. Thanks to the hypothesis (3.4), $n_0 < 1$ and the Kato-Rellich theorem applies. One concludes that $\mathcal{H}$ is self adjoint on $D[\mathcal{H}] = D[\mathcal{H}_0]$. Since H is unitary equivalent to $\mathcal{H}$, the operator $(H, D[H])$ is self adjoint. $\square$

Since the operators H and $\mathcal{H}$ are self-adjoint, their spectrums can be decomposed in terms of theory of measure [79, 84]. It yields the following decomposition

$$X = X^{\mathrm{ac}} \oplus X^{\mathrm{sc}} \oplus X^{\mathrm{pp}}.$$

where X^{ac} (resp. X^{sc}, resp. X^{pp}) corresponds to the absolutely continuous (resp. singular continuous, resp. pure point) part of the spectrum. The pure point subspace X^{pp} is spanned by the eigenvectors

$$X^{\mathrm{pp}} = \mathrm{Span}\{\varphi \in X,\ \mathcal{H}\varphi = \lambda\varphi \text{ for some } \lambda \in \mathbf{R}\}.$$

On the other hand, the subspace X^{ac} is characterized [71, 78, 105] by the existence of a dense subset $A \subset X^{\mathrm{ac}}$ such that

$$\varphi \in A \Rightarrow \left\| (\mathcal{H} - \lambda - i\varepsilon)^{-1} \varphi \right\|_X = O\left(\frac{1}{\sqrt{\varepsilon}}\right). \tag{3.8}$$

This characterisation is known as the Christensen criterion. Before moving on, we recall the so-called Plemelj formula,

$$\lim_{\varepsilon \to 0} \frac{1}{x + i\varepsilon} = \mathrm{P.V}\left(\frac{1}{x}\right) - i\pi\delta_0, \quad \text{in } \mathcal{D}'.$$

Theorem 3.2.4. *The operator H only has absolutely continuous spectrum.*

Proof. Since H is unitary equivalent to $\mathcal{H}$, if $\mathcal{H}$ only has absolutely continuous spectrum, then the same statement holds for H. We verify the criterion (3.8) by means of a series of elementary calculations.

Let A be the set of triplet of function (τ,u,f) such that $\tau,\ u \in \ell^2_0(\mathbf{Z})$ with finite support and $f \in \ell^2_k L^2_v$ with finite support in k, and bounded in v. The set A is dense in X. Let us compute $(\mathcal{H} - (\lambda + i\varepsilon))^{-1}(\tau,u,f)$ by solving for $(\sigma,w,g) \in X$ the equation $(\mathcal{H} - (\lambda + i\varepsilon)(\sigma,w,g) = (\tau,u,f)$ which writes, for all $k \neq 0$, $v \in \mathbf{R}$

$$\begin{cases} kw_k + k\int_{\mathbf{R}} v\sqrt{f^0(v)}g_k(v)\,\mathrm{d}v - (\lambda + i\varepsilon)\sigma_k = \tau_k \\ k\sigma_k - (\lambda + i\varepsilon)w_k = u_k \\ -vkg_k(v) + kv\sqrt{f^0(v)}\sigma_k - (\lambda + i\varepsilon)g_k(v) = f_k(v). \end{cases}$$

Taking the third equation, one has

$$g_k(v) = \frac{kv\sqrt{f^0(v)}}{\lambda + i\varepsilon + vk}\sigma_k - \frac{f_k(v)}{\lambda + i\varepsilon + vk}. \tag{3.9}$$

The second equation gives

$$w_k = \frac{1}{\lambda + i\varepsilon}(k\sigma_k - u_k). \tag{3.10}$$

Then, the first equation gives

$$\frac{k^2}{\lambda + i\varepsilon}\sigma_k - \frac{k}{\lambda + i\varepsilon}u_k + k\int_{\mathbf{R}} v\sqrt{f^0(v)}g_k(v)\,\mathrm{d}v - (\lambda + i\varepsilon)\sigma_k = \tau_k.$$

Using (3.9) and (3.10)

$$\frac{k^2}{(\lambda+i\varepsilon)^2}\sigma_k + \frac{k^2}{\lambda+i\varepsilon}\sigma_k \int_{\mathbf{R}} \frac{v^2 f^0(v)}{\lambda+i\varepsilon+vk}\,\mathrm{d}v - \sigma_k$$
$$= \frac{k}{(\lambda+i\varepsilon)^2}u_k + \frac{1}{\lambda+i\varepsilon}\tau_k + \frac{k}{\lambda+i\varepsilon}\int_{\mathbf{R}} \frac{v\sqrt{f^0(v)}f_k(v)}{\lambda+i\varepsilon+vk}\,\mathrm{d}v.$$

Finally

$$\sigma_k = \frac{-1}{1-\frac{k^2}{(\lambda+i\varepsilon)^2}-\frac{k^2}{\lambda+i\varepsilon}\int_{\mathbf{R}}\frac{v^2 f^0(v)}{\lambda+i\varepsilon+vk}\,\mathrm{d}v} \tag{3.11}$$
$$\times\left(\frac{\tau_k}{\lambda+i\varepsilon}+\frac{k}{(\lambda+i\varepsilon)^2}u_k+\frac{k}{\lambda+i\varepsilon}\int_{\mathbf{R}}\frac{v\sqrt{f^0(v)}f_k(v)}{\lambda+i\varepsilon+vk}\,\mathrm{d}v\right)$$
$$= -\frac{(\lambda+i\varepsilon)^2}{(\lambda+i\varepsilon)^2-k^2-k^2(\lambda+i\varepsilon)\int_{\mathbf{R}}\frac{v^2 f^0(v)}{\lambda+i\varepsilon+vk}\,\mathrm{d}v} \tag{3.12}$$
$$\times\left(\frac{\tau_k}{\lambda+i\varepsilon}+\frac{k}{(\lambda+i\varepsilon)^2}u_k+\frac{k}{\lambda+i\varepsilon}\int_{\mathbf{R}}\frac{v\sqrt{f^0(v)}f_k(v)}{\lambda+i\varepsilon+vk}\,\mathrm{d}v\right)$$
$$= -\frac{(\lambda+i\varepsilon)\tau_k+ku_k+k(\lambda+i\varepsilon)\int_{\mathbf{R}}\frac{v\sqrt{f^0(v)}f_k(v)}{\lambda+i\varepsilon+vk}\,\mathrm{d}v}{(\lambda+i\varepsilon)^2-k^2-k(\lambda+i\varepsilon)\int_{\mathbf{R}}\frac{v^2 f^0(v)}{\lambda+i\varepsilon+vk}\,\mathrm{d}v}. \tag{3.13}$$

To satisfy the criterion (3.8), it is enough, from the formula (3.9)-(3.10), to bound σ and w in ℓ^∞. One obtains using Plemelj formula

$$\sigma_k = -\frac{(\lambda+i\varepsilon)\tau_k+ku_k+k(\lambda+i\varepsilon)\int_{\mathbf{R}}\frac{v\sqrt{f^0(v)}f_k(v)}{\lambda+i\varepsilon+vk}\,\mathrm{d}v}{(\lambda+i\varepsilon)^2-k^2-k(\lambda+i\varepsilon)\int_{\mathbf{R}}\frac{v^2 f^0(v)}{\lambda+i\varepsilon+vk}\,\mathrm{d}v}$$
$$\xrightarrow[\varepsilon\to 0]{} -\frac{\lambda\tau_k+ku_k+k\lambda\left[\mathrm{P.V}\int_{\mathbf{R}}\frac{v\sqrt{f^0(v)}f_k(v)}{\lambda+vk}\,\mathrm{d}v+i\pi\lambda\sqrt{f^0(\lambda)}f_k(\lambda)\right]}{\lambda^2-k^2-k\lambda\left[\mathrm{P.V}\int_{\mathbf{R}}\frac{v^2 f^0(v)}{\lambda+vk}\,\mathrm{d}v+i\pi\lambda^2 f^0(\lambda)\right]}.$$

So σ is uniformly bounded in ε in $\ell^\infty(\mathbf{Z})$. In the same way, from (3.10)

$$\begin{aligned}
w_k &= \frac{1}{\lambda+i\varepsilon}\left(-\frac{k(\lambda+i\varepsilon)\tau_k+k^2u_k+k^2(\lambda+i\varepsilon)\int_{\mathbf{R}}\frac{v\sqrt{f^0(v)}f_k(v)}{\lambda+i\varepsilon+vk}\,\mathrm{d}v}{(\lambda+i\varepsilon)^2-k^2-k(\lambda+i\varepsilon)\int_{\mathbf{R}}\frac{v^2f^0(v)}{\lambda+i\varepsilon+vk}\,\mathrm{d}v}-u_k\right)\\
&= -\frac{k\tau_k+k^2\int_{\mathbf{R}}\frac{v\sqrt{f^0(v)}f_k(v)}{\lambda+i\varepsilon+vk}\,\mathrm{d}v}{(\lambda+i\varepsilon)^2-k^2-k(\lambda+i\varepsilon)\int_{\mathbf{R}}\frac{v^2f^0(v)}{\lambda+i\varepsilon+vk}\,\mathrm{d}v}\\
&\quad-\frac{k^2\frac{u_k}{\lambda+i\varepsilon}}{(\lambda+i\varepsilon)^2-k^2-k(\lambda+i\varepsilon)\int_{\mathbf{R}}\frac{v^2f^0(v)}{\lambda+i\varepsilon+vk}}-\frac{u_k}{\lambda+i\varepsilon}\\
&= -\frac{k\tau_k+k^2\int_{\mathbf{R}}\frac{v\sqrt{f^0(v)}f_k(v)}{\lambda+i\varepsilon+vk}\,\mathrm{d}v}{(\lambda+i\varepsilon)^2-k^2-k(\lambda+i\varepsilon)\int_{\mathbf{R}}\frac{v^2f^0(v)}{\lambda+i\varepsilon+vk}\,\mathrm{d}v}\\
&\quad-\frac{u_k}{\lambda+i\varepsilon}\left[1+\frac{k^2}{(\lambda+i\varepsilon)^2-k^2-k(\lambda+i\varepsilon)\int_{\mathbf{R}}\frac{v^2f^0(v)}{\lambda+i\varepsilon+vk}\,\mathrm{d}v}\right]\\
&= -\frac{k\tau_k+k^2\int_{\mathbf{R}}\frac{v\sqrt{f^0(v)}f_k(v)}{\lambda+i\varepsilon+vk}\,\mathrm{d}v}{(\lambda+i\varepsilon)^2-k^2-k(\lambda+i\varepsilon)\int_{\mathbf{R}}\frac{v^2f^0(v)}{\lambda+i\varepsilon+vk}\,\mathrm{d}v}\\
&\quad-\frac{u_k}{\lambda+i\varepsilon}\left[\frac{(\lambda+i\varepsilon)^2-k(\lambda+i\varepsilon)\int_{\mathbf{R}}\frac{v^2f^0(v)}{\lambda+i\varepsilon+vk}\,\mathrm{d}v}{(\lambda+i\varepsilon)^2-k^2-k(\lambda+i\varepsilon)\int_{\mathbf{R}}\frac{v^2f^0(v)}{\lambda+i\varepsilon+vk}\,\mathrm{d}v}\right]\\
&= -\frac{k\tau_k+k^2\int_{\mathbf{R}}\frac{v\sqrt{f^0(v)}f_k(v)}{\lambda+i\varepsilon+vk}\,\mathrm{d}v}{(\lambda+i\varepsilon)^2-k^2-k(\lambda+i\varepsilon)\int_{\mathbf{R}}\frac{v^2f^0(v)}{\lambda+i\varepsilon+vk}\,\mathrm{d}v}\\
&\quad-u_k\left[\frac{(\lambda+i\varepsilon)-k\int_{\mathbf{R}}\frac{v^2f^0(v)}{\lambda+i\varepsilon+vk}\,\mathrm{d}v}{(\lambda+i\varepsilon)^2-k^2-k(\lambda+i\varepsilon)\int_{\mathbf{R}}\frac{v^2f^0(v)}{\lambda+i\varepsilon+vk}\,\mathrm{d}v}\right]\\
&= -\frac{k\tau_k+k^2\int_{\mathbf{R}}\frac{v\sqrt{f^0(v)}f_k(v)}{\lambda+i\varepsilon+vk}\,\mathrm{d}v+u_k\left[(\lambda+i\varepsilon)-k\int_{\mathbf{R}}\frac{v^2f^0(v)}{\lambda+i\varepsilon+vk}\,\mathrm{d}v\right]}{(\lambda+i\varepsilon)^2-k^2-k(\lambda+i\varepsilon)\int_{\mathbf{R}}\frac{v^2f^0(v)}{\lambda+i\varepsilon+vk}\,\mathrm{d}v}.
\end{aligned}$$

Then one concludes using again Plemelj formula that

$$w_k \underset{\varepsilon\to 0}{\longrightarrow} -\frac{k\tau_k+\mathrm{P.V}\int_{\mathbf{R}}\frac{v\sqrt{f^0(v)}f_k(v)}{\lambda+vk}\,\mathrm{d}v+i\pi\lambda\sqrt{f^0(\lambda)}f_k(\lambda)+u_k\left[\lambda-k\mathrm{P.V}\int_{\mathbf{R}}\frac{v^2f^0(v)}{\lambda+vk}\,\mathrm{d}v-i\pi k\lambda^2f^0(\lambda)\right]}{\lambda^2-k^2-k\mathrm{P.V}\int_{\mathbf{R}}\frac{v^2f^0(v)}{\lambda+vk}\,\mathrm{d}v-i\pi k\lambda^2f^0(\lambda)}.$$

In the end, one obtains that w is uniformly bounded in ε in $\ell^\infty(\mathbf{Z})$. We then turn to an estimate of g in $\ell^2_kL^2_v$. The triangle inequality yields

$$\|g\|_{\ell^2_kL^2_v}\le\left\|\frac{kv\sqrt{f^0}\sigma}{\lambda+i\varepsilon+vk}\right\|_{\ell^2_kL^2_v}+\left\|\frac{f}{\lambda+i\varepsilon+vk}\right\|_{\ell^2_kL^2_v}.$$

One has

$$\begin{aligned}\left\|\frac{kv\sqrt{f^0}\sigma}{\lambda+i\varepsilon+vk}\right\|^2_{\ell^2_k L^2_v} &= \sum_{k\in\mathbf{Z}}\int_{v\in\mathbf{R}}\left|\frac{kv\sqrt{f^0}\sigma_k}{\lambda+i\varepsilon+vk}\right|^2 \mathrm{d}v\\ &= \sum_{k\in\mathbf{Z}\setminus\{0\}} k^2\sigma_k^2\int_{v\in\mathbf{R}}\frac{v^2 f^0}{(\lambda+vk)^2+\varepsilon^2}\,\mathrm{d}v\\ &\leq \|v^2f^0\|_{L^\infty_v}\sum_{k\in\mathbf{Z}\setminus\{0\}}\frac{k^2\sigma_k^2}{k\varepsilon}\\ &\leq \frac{\|v^2f^0\|_{L^\infty_v}\|\mathbf{k}\sigma\|^2_{\ell^2}}{\varepsilon},\end{aligned}$$

and

$$\begin{aligned}\left\|\frac{f}{\lambda+i\varepsilon+vk}\right\|^2_{\ell^2_k L^2_v} &= \sum_{k\in\mathbf{Z}\setminus\{0\}}\int_{v\in\mathbf{R}}\frac{|f_k(v)|^2}{(\lambda+vk)^2+\varepsilon^2}\,\mathrm{d}v\\ &\leq \sum_{k\in\mathbf{Z}\setminus\{0\}}\int_{v\in\mathbf{R}}\frac{\|f_k\|^2_{L^\infty_v}}{(\lambda+vk)^2+\varepsilon^2}\,\mathrm{d}v\\ &\leq \frac{C}{\varepsilon}\left\|\mathbf{k}^{-1}f\mathbf{1}_{k\neq 0}\right\|^2_{\ell^2_k L^\infty_v}.\end{aligned}$$

Finally, it yields for ε small enough,

$$\forall(\tau,u,f)\in A,\quad \|(\mathcal{H}-(\lambda+i\varepsilon))^{-1}(\tau,u,f)\|_X \leq \frac{C_{\lambda,\tau,u,f}}{\sqrt{\varepsilon}}.$$

With $C_{\tau,u,f,\lambda}$ a constant that depends only on τ,u,f,λ. One concludes that $\mathcal{H}$ only has absolutely continuous spectrum. □

We can then conclude this section and prove Theorem 3.2.1.

Proof of Theorem 3.2.1. Since the operator H has absolutely continuous spectrum and does not have pure point and singular spectrum, it is a standard consequence of scattering theory [79,84] that the solution $(\tau(t),u(t),f(t)) = e^{-itH}(\tau_{\text{ini}},u_{\text{ini}},f_{\text{ini}})$ converges weakly to 0. Furthermore it is easy to see that

$$\forall k,\quad \tau_k(t)\to 0,\quad u_k(t)\to 0.$$

Using the conservation of energy, one has

$$\begin{aligned}\sum_{k\in\mathbf{Z}}\left(|\tau_k(t)|^2+|u_k(t)|^2\right) &\leq \sum_{k\in\mathbf{Z}}\left(|\tau_k(t)|^2+|u_k(t)|^2+\int_{\mathbf{R}}|f_k(t,v)|^2\,\mathrm{d}v\right)\\ &= \sum_{k\in\mathbf{Z}}\left(|\tau_k(0)|^2+|u_k(0)|^2+\int_{\mathbf{R}}|f_k(0,v)|^2\,\mathrm{d}v\right).\end{aligned}$$

Let $\varepsilon>0$, then there exists $N>0$ such that

$$\sum_{|k|>N}\left(|\tau_k(0)|^2+|u_k(0)|^2+\int_{\mathbf{R}}|f_k(0,v)|^2\,\mathrm{d}v\right)<\varepsilon.$$

Then one writes

$$\sum_{k\in\mathbf{Z}} \left(|\tau_k(t)|^2 + |u_k(t)|^2\right) = \sum_{|k|\le N} \left(|\tau_k(t)|^2 + |u_k(t)|^2\right) + \sum_{|k|>N} \left(|\tau_k(t)|^2 + |u_k(t)|^2\right)$$
$$< \sum_{|k|\le N} \left(|\tau_k(t)|^2 + |u_k(t)|^2\right) + \varepsilon.$$

Taking $t \to +\infty$,

$$\lim_{t\to+\infty} \sum_{k\in\mathbf{Z}} \left(|\tau_k(t)|^2 + |u_k(t)|^2\right) \le \varepsilon, \quad \forall \varepsilon > 0.$$

One concludes by Plancherel identity. □

3.2.3 Dispersion relation

In this section, we perform a more quantitative analysis than in the previous section by assuming that the initial data are analytic functions. For simplicity of the notations we take $n_0 = 1$. The conclusion (3.17) is that the damping is a combination of a decreasing exponential part and an oscillatory part. This behaviour is qualitatively the same to the linear Landau damping in plasma physics for the Vlasov-Poisson system, even if the physical nature of the force that acts on the particles is different.

For a function $\tau \in L^\infty(\mathbf{R}_+; L^2(\mathbf{T}))$, we define the Laplace-Fourier transform as

$$\tilde{\tau}_k(\omega) := \int_0^{+\infty} \int_{\mathbf{T}} e^{i\omega t} e^{-ikx} \tau(t,x)\, \mathrm{d}x\mathrm{d}t, \quad \Im(\omega) > 0.$$

Proposition 3.2.5. *Let (τ,u,f) solutions of the linearized system (3.6), and $\tilde{\tau}_k$ be the Fourier-Laplace transform of τ. Then one has, for $\Im(\omega) > 0$*

$$\tilde{\tau}_k(\omega) = \frac{\mathcal{N}(\omega,k)}{\mathcal{D}(\omega,k)},$$

with

$$\mathcal{N}(\omega,k) = \frac{i}{\omega}\left(\tau_k(0) - \frac{k}{\omega}u_k(0) + \int_{\mathbf{R}} \frac{v\sqrt{f^0(v)}f_k(0,v)}{v - \frac{\omega}{k}}\,\mathrm{d}v\right),$$

and

$$\mathcal{D}(\omega,k) = 1 - \frac{k^2}{\omega^2} + \left[1 + \frac{\omega}{\sqrt{2\pi}k}\int_{\mathbf{R}} \frac{e^{-v^2/2}}{v - \frac{\omega}{k}}\,\mathrm{d}v\right].$$

The function $\mathcal{D}$ is the dispersion relation of the linear system.

Remark 3.2.6. *It is interesting to compare $\mathcal{D}$ to the dispersion relation of the linear Vlasov-Poisson system*

$$\mathcal{D}_{\mathrm{VP}}(\omega,k) = 1 + \frac{1}{k^2}\left[1 + \frac{\omega}{\sqrt{2\pi}k}\int_{\mathbf{R}} \frac{e^{-v^2/2}}{v - \frac{\omega}{k}}\,\mathrm{d}v\right].$$

We remark that

$$\mathcal{D}(\omega,k) = 1 - \frac{k^2}{\omega^2} + k^2(\mathcal{D}_{\mathrm{VP}}(\omega,k) - 1) = 1 - k^2 - \frac{k^2}{\omega^2} + k^2\mathcal{D}_{\mathrm{VP}}(\omega,k).$$

Proof. We consider the system (3.6) written for Fourier modes $k \neq 0$.

$$\begin{cases} \partial_t \tau_k(t) = iku_k(t) + ik \int_{\mathbf{R}} \sqrt{f^0} f_k(t,v) v \,\mathrm{d}v \\ \partial_t u_k(t) = ik\tau_k(t) \\ \partial_t f_k(t,v) + ikv f_k(t,v) - ikv\sqrt{f^0}\tau_k(t) = 0. \end{cases} \tag{3.14}$$

For bounded solutions of (3.14), the following Fourier-Laplace transforms are well-defined

$$\widetilde{\tau}_k(\omega) = \int_0^{+\infty} e^{i\omega t}\tau_k(t)\,\mathrm{d}t, \quad \Im(\omega) > 0,$$

$$\widetilde{u}_k(\omega) = \int_0^{+\infty} e^{i\omega t}u_k(t)\,\mathrm{d}t, \quad \Im(\omega) > 0,$$

$$\widetilde{f}_k(\omega,v) = \int_0^{+\infty} e^{i\omega t}f_k(t,v)\,\mathrm{d}t, \quad \Im(\omega) > 0, \quad v \in \mathbf{R}.$$

Multiplying the Vlasov equation by $e^{i\omega t}$ and integrating in t, (3.14) writes

$$\begin{cases} -i\omega\widetilde{\tau}_k(\omega) = ik\widetilde{u}_k(\omega) + ik \int_{\mathbf{R}} v\sqrt{f^0(v)}\widetilde{f}_k(\omega,v)\,\mathrm{d}v + \tau_k(0) \\ -i\omega\widetilde{u}_k(\omega) = ik\widetilde{\tau}_k(\omega) + u_k(0) \\ (-i\omega + ikv)\widetilde{f}_k(\omega,v) - ikv\sqrt{f^0}\widetilde{\tau}_k(\omega) = f_k(0,v). \end{cases}$$

Then one has

$$\begin{aligned} -i\omega\widetilde{\tau}_k(\omega) =& ik\widetilde{u}_k(\omega) + ik\int_{\mathbf{R}} v\sqrt{f^0(v)}\widetilde{f}_k(\omega,v)\,\mathrm{d}v + \tau_k(0) \\ =& ik\left(-\frac{ik\widetilde{\tau}_k(\omega) + u_k(0)}{i\omega}\right) + ik\int_{\mathbf{R}} v\sqrt{f^0(v)}\widetilde{f}(\omega,v)\,\mathrm{d}v + \tau_k(0) \\ =& -i\frac{k^2}{\omega}\widetilde{\tau}_k(\omega) + ik\int_{\mathbf{R}} v\sqrt{f^0(v)}\widetilde{f}_k(\omega,v)\,\mathrm{d}v + \tau_k(0) - \frac{k}{\omega}u_k(0) \\ =& -i\frac{k^2}{\omega}\widetilde{\tau}_k(\omega) + ik\int_{\mathbf{R}} v\sqrt{f^0(v)}\left(\frac{f_k(0,v) + ikv\sqrt{f^0(v)}\widetilde{\tau}_k(\omega)}{-i\omega + ikv}\right)\mathrm{d}v \\ &+ \tau_k(0) - \frac{k}{\omega}u_k(0) \\ =& -i\frac{k^2}{\omega}\widetilde{\tau}_k(\omega) + ik\widetilde{\tau}_k(\omega)\int_{\mathbf{R}} \frac{ikv^2 f^0(v)}{-i\omega + ikv}\,\mathrm{d}v \\ &+ \tau_k(0) - \frac{k}{\omega}u_k(0) + ik\int_{\mathbf{R}} \frac{v\sqrt{f^0(v)}f_k(0,v)}{-i\omega + ikv}\,\mathrm{d}v. \end{aligned}$$

Then one has

$$\widetilde{\tau}_k(\omega) = \left(\frac{k^2}{\omega^2} - \frac{k}{\omega}\int_{\mathbf{R}} \frac{v^2 f^0(v)}{v - \frac{\omega}{k}}\,\mathrm{d}v\right)\widetilde{\tau}_k(\omega) + \frac{i}{\omega}\left(\tau_k(0) - \frac{k}{\omega}u_k(0) + \int_{\mathbf{R}} \frac{v\sqrt{f^0(v)}f_k(0,v)}{v - \frac{\omega}{k}}\,\mathrm{d}v\right),$$

which rewrites

$$\widetilde{\tau}_k(\omega) = \frac{\mathcal{N}(\omega,k)}{\mathcal{D}(\omega,k)} \tag{3.15}$$

with

$$\mathcal{N}(\omega,k) = \frac{i}{\omega}\left(\hat{\tau}(0,k) - \frac{k}{\omega}\hat{u}(0,k) + \int_{\mathbf{R}} \frac{v\sqrt{f^0(v)}\hat{f}_0(k,v)}{v-\frac{\omega}{k}}\,\mathrm{d}v\right)$$

and

$$\mathcal{D}(\omega,k) = 1 - \frac{k^2}{\omega^2} + \frac{k}{\omega}\int_{\mathbf{R}} \frac{v^2 f^0(v)}{v-\frac{\omega}{k}}\,\mathrm{d}v.$$

Furthermore, since

$$\int_{\mathbf{R}} \frac{v^2 e^{-v^2/2}}{v-\frac{\omega}{k}}\,\mathrm{d}v = \int_{\mathbf{R}} \frac{v(v-\frac{\omega}{k})e^{-v^2/2}}{v-\frac{\omega}{k}}\,\mathrm{d}v + \frac{\omega}{k}\int_{\mathbf{R}} \frac{v e^{-v^2/2}}{v-\frac{\omega}{k}}\,\mathrm{d}v = \frac{\omega}{k}\int_{\mathbf{R}} \frac{v e^{-v^2/2}}{v-\frac{\omega}{k}}\,\mathrm{d}v$$

and

$$\begin{aligned}\int_{\mathbf{R}} \frac{v e^{-v^2/2}}{v-\frac{\omega}{k}}\,\mathrm{d}v &= \int_{\mathbf{R}} \frac{(v-\frac{\omega}{k})e^{-v^2/2}}{v-\frac{\omega}{k}}\,\mathrm{d}v + \frac{\omega}{k}\int_{\mathbf{R}} \frac{e^{-v^2/2}}{v-\frac{\omega}{k}}\,\mathrm{d}v \\ &= \sqrt{2\pi} + \frac{\omega}{k}\int_{\mathbf{R}} \frac{e^{-v^2/2}}{v-\frac{\omega}{k}}\,\mathrm{d}v.\end{aligned}$$

One obtains that $\mathcal{D}$ writes

$$\mathcal{D}(\omega,k) = 1 - \frac{k^2}{\omega^2} + \left[1 + \frac{\omega}{\sqrt{2\pi}k}\int_{\mathbf{R}} \frac{e^{-v^2/2}}{v-\frac{\omega}{k}}\,\mathrm{d}v\right].$$

□

For all $k \neq 0$, the function $\mathcal{D}(\cdot,k)$ is analytic on the half-space $\Im(\omega) > 0$. One can define an analytic continuation of $\mathcal{D}$ on $\mathbf{C}^*$. Let Z be a function defined on $\mathbf{C}$ by

$$Z(\zeta) = \sqrt{\pi}e^{-\zeta^2}\left(i - \frac{2}{\sqrt{\pi}}\int_0^{\zeta} e^{t^2}\,\mathrm{d}t\right).$$

Then Z is analytic on $\mathbf{C}$ and $\forall \Im(\zeta) > 0$,

$$Z(\zeta) = \frac{1}{\sqrt{\pi}}\int_{\mathbf{R}} \frac{e^{-v^2}}{v-\zeta}\,\mathrm{d}v.$$

Therefore, one can do an analytic continuation of $\zeta \mapsto \int_{\mathbf{R}} \frac{e^{-v^2}}{v-\zeta}\,\mathrm{d}v$ on $\mathbf{C}$. Then, the function $\mathcal{D}(\omega,k)$ can also be continued analytically on $\mathbf{C}^*$ by the formula

$$\mathcal{D}(\omega,k) = 1 - \frac{k^2}{\omega^2} + \left[1 + \frac{\sqrt{\pi}}{\sqrt{2}}\frac{\omega}{k}e^{-\frac{\omega^2}{2k^2}}\left(i - \frac{2}{\sqrt{\pi}}\int_0^{\frac{\omega}{\sqrt{2}k}} e^{t^2}\,\mathrm{d}t\right)\right].$$

The function $\mathcal{N}$ can also be continued analytically in the same manner, and then $\tilde{\tau}_k(\omega)$ is continued analytically on $\mathbf{C}^*$. At this point, we follow what is classically done in the plasma physics community [111, 113] for the Vlasov-Poisson system and we assume that $\mathcal{D}$ only has finitely many zeros (which seems reasonable to prove) and that they are all simple (a proof of this fact seems much more difficult). So that the Laplace inversion theorem applies and one has

$$\tau_k(t) = \frac{1}{2i\pi}\int_{-\infty+i\gamma}^{+\infty+i\gamma} e^{-i\omega t}\tilde{\tau}_k(\omega)\,\mathrm{d}\omega.$$

One can use the residue Theorem to compute this integral. One obtains the following expansion

$$\tau_k(t) = \sum_{\omega_j} \mathrm{Res}(\widetilde{\tau}_k, \omega_j) e^{-i\omega_j t}. \tag{3.16}$$

where the ω_j are the roots of $\mathcal{D}$, which is a finite set, and $\mathrm{Res}(\widetilde{\tau}_k, \omega_j)$ is the residue of $\widetilde{\tau}_k$ at ω_j. We then obtain that the dominant term of this expansion decay exponentially. The expression of $\mathcal{D}$ when the constant are not normalized to 1 (one must redo the computation of the section 3.2.3 with the system (3.5)) is

$$\mathcal{D}(\omega,k) = 1 - c_0^2 \frac{k^2}{\omega^2} + \frac{4\pi r_p^3 \varrho_0 c_0^2}{3\alpha_0} \left[1 + \frac{\sqrt{\pi}\omega}{\sqrt{2}k} e^{-\frac{\omega^2}{2k^2}} \left(i - \frac{2}{\sqrt{\pi}} \int_0^{\frac{\omega}{\sqrt{2}k}} e^{t^2} \, \mathrm{d}t \right) \right].$$

The ω_j are the solutions of $\mathcal{D}(\omega,k) = 0$ for a given k. As all the terms in the sum (3.16) decay exponentially fast, only the term corresponding to the ω_j with the largest imaginary part will remain for large time , and the others will quickly become negligible. Denote $\omega_r = \Re(\omega_j)$, $\omega_i = \Im(\omega_j)$, and $\mathrm{Res}(\widetilde{\tau}_k, \omega_j) = re^{i\varphi}$, one notices that there is alway a root of the form $\omega_r + i\omega_j$ associated to $re^{i\varphi}$ and one of the form $-\omega_r + i\omega_i$ associated to $re^{-i\varphi}$. Therefore, by considering only the two roots with the largest ω_i, one has

$$\tau_k(t) \approx re^{i\varphi} e^{-(\omega_r + i\omega_i)t} + re^{-i\varphi} e^{(-\omega_r + i\omega_i)t} = 2re^{\omega_i t} \cos(\omega_r t - \varphi). \tag{3.17}$$

To compute the two roots with the largest imaginary part of $\mathcal{D}$, we use a standard numerical method such as a Newton's scheme from the python library SCIPY. For example with $\frac{4}{3}\pi r_p^3 = 0.3$, $\varrho_0 = 1$ and $k = 0.5$, one obtains that the two roots with the largest imaginary part are

$$\omega \approx \pm 0.4969 - 0.1295i.$$

3.3 Numerical illustrations

In this section, we illustrate the results of Theorem 3.2.1 in dimension $1+1$. We show results on the linear and nonlinear equations. We consider a uniform discretisation of the phase space $\mathbf{T} \times \mathbf{R}$, with steps Δx, $\mathrm{d}v$. In all the numerical results, we chose r_p so that $\frac{4}{3}\pi r_p^3 = 0.3$.

3.3.1 Numerical methods

We describe here the numerical schemes used in the next section for the purpose of illustration. We present two schemes. The first one is for the nonlinear problem, which is the most interesting one in view of possible physical applications. The second one is for the linearized problem because it is a direct illustration of the theoretical results.

3.3.1.1 Nonlinear equations

We start with the nonlinear equations

$$\begin{cases} \partial_t f + v\partial_x f - \partial_x p \partial_v f = 0 \\ \partial_t(\alpha\varrho) + \partial_x(\alpha\varrho u) = 0 \\ \partial_t(\alpha\varrho u) + \partial_x(\alpha\varrho u^2) + \alpha\partial_x p = 0 \\ p(\varrho) = \varrho^\gamma, \gamma = 1.4. \end{cases} \tag{3.18}$$

We use a semi-Lagrangian method for the Vlasov equation and a Lax-Wendroff scheme for the fluid part. Multiplying the Vlasov equation in (3.18) by v and integrating in v, then summing with the momentum equation of the fluid, one sees that the fluid part of the equation can be written in a conservative form

$$\begin{cases} \partial_t(\alpha\varrho) + \partial_x(\alpha\varrho u) = 0 \\ \partial_t\left(\alpha\varrho u + \dfrac{4}{3}\pi r_p^3 \displaystyle\int_{\mathbf{R}} f v \,\mathrm{d}v\right) + \partial_x(\alpha\varrho u^2) + \partial_x p + \partial_x\left(\dfrac{4}{3}\pi r_p^3 \displaystyle\int_{\mathbf{R}} v^2 f \,\mathrm{d}v\right) = 0 \\ \partial_t f + v\partial_x f - \partial_x p \partial_v f = 0. \end{cases}$$

It writes

$$\partial_t \mathbf{U} + \partial_x \mathbf{F}(\mathbf{U}, f) = 0$$

with

$$\mathbf{U} = \begin{pmatrix} U_1 \\ U_2 \end{pmatrix} := \begin{pmatrix} \alpha\varrho \\ \alpha\varrho u + \frac{4}{3}\pi r_p^3 \int_{\mathbf{R}} f v \,\mathrm{d}v \end{pmatrix}$$

and

$$\mathbf{F}(\mathbf{U}, f) = \begin{pmatrix} \alpha\varrho u \\ \alpha\varrho u^2 + p + \frac{4}{3}\pi r_p^3 \int_{\mathbf{R}} f v^2 \,\mathrm{d}v \end{pmatrix} = \begin{pmatrix} U_2 - m_\star \int_{\mathbf{R}} f v \,\mathrm{d}v \\ \frac{(U_2 - \frac{4}{3}\pi r_p^3 \int_{\mathbf{R}} f v \,\mathrm{d}v)^2}{U_1} + \frac{U_1^\gamma}{\alpha^\gamma} + \int_{\mathbf{R}} f v^2 \,\mathrm{d}v \end{pmatrix}.$$

The jacobian matrix of $\mathbf{F}$ with respect to $\mathbf{U}$ is

$$\mathbf{A}(\mathbf{U}, f) := \boldsymbol{\nabla}_{\mathbf{U}} \mathbf{F}(\mathbf{U}, f) = \begin{pmatrix} 0 & 1 \\ \frac{-(U_2 - \frac{4}{3}\pi r_p^3 \int_{\mathbf{R}} f v \,\mathrm{d}v)^2}{U_1^2} + \frac{\gamma U_1^{\gamma-1}}{\alpha^\gamma} & \frac{2(U_2 - \frac{4}{3}\pi r_p^3 \int_{\mathbf{R}} f v \,\mathrm{d}v)}{U_1} \end{pmatrix}. \tag{3.19}$$

Proposition 3.3.1. *The eigenvalues of the Jacobian $A(\mathbf{U}, f)$ are*

$$\lambda_\pm = u \pm \sqrt{\frac{p'(\varrho)}{\alpha}}. \tag{3.20}$$

Proof. It suffices to notice that $A(\mathbf{U}, f)$ writes

$$A(\mathbf{U}, f) = \begin{pmatrix} 0 & 1 \\ c^2 - u^2 & 2u \end{pmatrix}$$

with $u = \dfrac{(U_2 - \frac{4}{3}\pi r_p^3 \int_{\mathbf{R}} f v \,\mathrm{d}v)}{U_1}$ and $c^2 = \dfrac{\gamma U_1^{\gamma-1}}{\alpha^\gamma}$. A simple standard computation shows the desired result. Moreover, one has

$$c^2 = \frac{\gamma U_1^{\gamma-1}}{\alpha^\gamma} = \frac{\gamma(\alpha\varrho)^{\gamma-1}}{\alpha^\gamma} = \frac{\gamma\varrho^{\gamma-1}}{\alpha} = \frac{p'(\varrho)}{\alpha}.$$

□

This allows us to use a classical hyperbolic numerical scheme to discretize the fluid part, and to immediately obtain a scheme preserving the mass and the total momentum.

The numerical method to discretize the system (3.18) is described as follow: Given $(\mathbf{U}^n, f^n)$ at a given time t^n.

- Compute f^* by solving the free transport $\partial_t f + v\partial_x f = 0$ with a semi-lagrangian scheme during a timestep Δt with initial condition f^n.
- Compute f^{n+1} by solving $\partial_t f - \partial_x p \partial_v f = 0$ with a semi-lagrangian scheme during a timestep Δt with initial condition f^*.
- Compute $\mathbf{U}^{n+1}$ by solving $\partial_t \mathbf{U} + \partial_x \mathbf{F}(\mathbf{U}, f) = 0$ with a Lax-Wendroff scheme during a timestep Δt with initial condition $(\mathbf{U}^n, f^{n+1})$.

The semi-Lagrangian method [35,112] is a classical method to discretize transport equations, so we do not describe it here, only the Lax-Wendroff scheme used here is somehow non standard and we describe it hereafter.

Given initial data $(\mathbf{U}^n, f^{n+1})$, the quantity $\mathbf{U}^{n+1}$ is computed by the Lax-Wendroff scheme [68]:

$$\begin{aligned}
&\mathbf{U}_j^{n+1} = \mathbf{U}_j^n - \frac{\Delta t}{2\Delta x}(\mathbf{F}(\mathbf{U}_{j+1}^n, f_{j+1}^{n+1}) - \mathbf{F}(\mathbf{U}_{j-1}^n, f_{j-1}^{n+1})) \\
&+ \frac{\Delta t^2}{2\Delta x^2}\left(\mathbf{A}_{j+1/2}^n(\mathbf{F}(\mathbf{U}_{j+1}^n, f_{j+1}^{n+1}) - \mathbf{F}(\mathbf{U}_j^n, f_j^{n+1})) - \mathbf{A}_{j-1/2}^n(\mathbf{F}(\mathbf{U}_j^n, f_j^{n+1}) - \mathbf{F}(\mathbf{U}_{j-1}^n, f_{j-1}^{n+1}))\right),
\end{aligned}$$

where $\mathbf{A}_{j+1/2}^n$ is the jacobian (4.9) evaluated at some average state:

$$\mathbf{A}_{j+1/2}^n = \mathbf{A}\left(\frac{\mathbf{U}_{j+1}^n + \mathbf{U}_j^n}{2}, \frac{f_{j+1}^{n+1} + f_j^{n+1}}{2}\right).$$

As it is classically done in the hyperbolic community, we impose a CFL condition:

$$\lambda_\pm \frac{\Delta t}{\Delta x} \leq \frac{1}{2}.$$

The dependency of λ with respect to α is $\lambda = O\left(\frac{1}{\sqrt{\alpha}}\right)$ as visible in Proposition 3.3.1. If α is small, it could trigger very small time steps. Notice that λ is in $1/\alpha$ so small value of α could lead very small time step Δt.

3.3.1.2 Linear equations

We start with the linearized equations

$$\begin{cases}
\alpha_0\varrho_0\partial_t\tau = \alpha_0\partial_x u + \dfrac{4}{3}\pi r_p^3\partial_x \displaystyle\int_{\mathbf{R}} v\sqrt{f^0} f \,\mathrm{d}v \\
\alpha_0\varrho_0\partial_t u = \alpha_0\varrho_0^2 c_0^2\partial_x\tau \\
\partial_t f + v\partial_x f - \varrho_0^2 c_0^2\sqrt{f^0(v)}v\partial_x\tau = 0.
\end{cases} \tag{3.21}$$

One notices that the variable v only acts as a parameter. A discretization in v yields

$$\begin{cases} \alpha_0\varrho_0\partial_t\tau = \alpha_0\partial_x u + \dfrac{4}{3}\pi r_p^3\partial_x \displaystyle\sum_k v_k\sqrt{f^0}(v_k)f(t,x,v_k)\mathrm{d}v \\ \alpha_0\varrho_0\partial_t u = \alpha_0\varrho_0^2c_0^2\partial_x\tau \\ \partial_t f(t,x,v_k) + v_k\partial_x f(t,x,v_k) - \varrho_0^2c_0^2\sqrt{f^0(v_k)}v_k\partial_x\tau = 0, \quad \forall k \in [\![0,N]\!] \end{cases}$$

It can be recast as a linear system of conservations laws

$$\partial_t\mathbf{W} + A\partial_x\mathbf{W} = 0,$$

with

$$\mathbf{W} = \begin{pmatrix} \alpha_0\varrho_0\tau \\ \alpha_0\varrho_0 u \\ f(\cdot,\cdot,v_0) \\ \vdots \\ f(\cdot,\cdot,v_N) \end{pmatrix}$$

and A a constant matrix. We use a Lax-Wendroff scheme under the form [68]

$$\mathbf{W}_j^{n+1} = \mathbf{W}_j^n - \frac{\Delta t}{2\Delta x}A\left(\mathbf{W}_{j+1}^n - \mathbf{W}_{j-1}^n\right) + \frac{\Delta t^2}{2\Delta x^2}A^2\left(\mathbf{W}_{j+1}^n - 2\mathbf{W}_j^n + \mathbf{W}_{j-1}^n\right).$$

3.3.2 Numerical results

In this section we consider the nonlinear system (3.18) with initial data

$$\begin{cases} \varrho(t=0,x) = 1, \\ u(t=0,x) = 0, \\ f(t=0,x,v) = \frac{1}{\sqrt{2\pi}}(1+\varepsilon\cos(kx)\sqrt{f^0(v)})e^{-v^2/2}, \end{cases}$$

and the linear system (3.21),

$$\begin{cases} \tau(t=0,x) = 0, \\ u(t=0,x) = 0, \\ f(t=0,x,v) = \frac{1}{\sqrt{2\pi}}\cos(kx)e^{-v^2/2}. \end{cases}$$

The coefficient are $\varepsilon = 0.001$ and $k = 0.5$. The domain of computation $[0,4\pi]\times[-10,10]$ with periodic boundary condition. Using (3.17), an approximation of $\tau(t,x)$ writes

$$\tau(t,x) \approx 4re^{\omega_i t}\sin(kx)\cos(\omega_r t - \varphi).$$

As it is done in plasma physics [111, 113], this allows in our case to write the following family of reference solutions

$$\tau_{\text{ref}}(t,x) = 4re^{-0.1295t}\sin(0.5x)\cos(0.4969t - \varphi),$$

where $r \in \mathbf{R}$ is the amplitude and $\varphi \in \mathbf{R}$ is the phase.

The numerical results obtained with the schemes described in section 3.3.1 are visible in Figure 3.1 for the nonlinear case and in Figure 3.2 for the linear case for $r = -6.5$ and $\varphi = 4$. One notices that the numerical solutions computed by both schemes are of the form predicted by the linear theory. Moreover the expected rate of decay is observed with great accuracy, both in the linear and nonlinear case. This indicates that the linear damping effect survives the nonlinear effect of the nonlinear system. In Figure 3.3, one can see the strong oscillations in the v-variable. This is a typical effect seen in plasma physics and it is usually called *filamentation*. It is also an illustration of the weak convergence of the perturbation of the distribution function to 0.

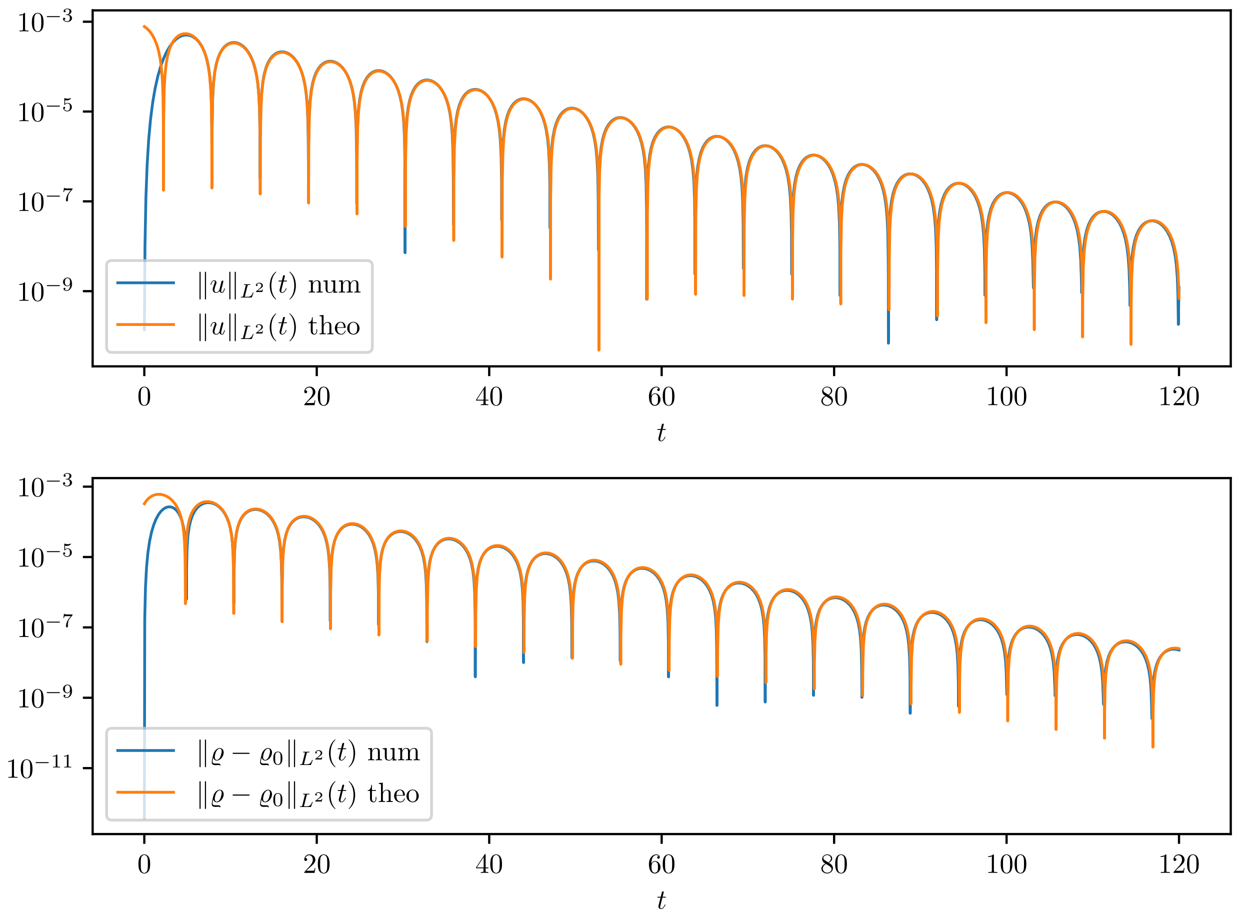

Fig. 3.1: Decay of the acoustic energy computed with the nonlinear equations. In blue, the numerical solution and in orange the solution predicted by the linear theory.

3.4 The case with friction

The introduction of a nonzero friction $D_\star > 0$ is important in view of physical applications [27]. It introduces an explicit dissipation mechanism in the equations. Since there is no such mechanism in the Vlasov-Poisson equations, the way to generalise the mathematical analysis is not obvious. In what follows, we present preliminary results on the problem for small friction.

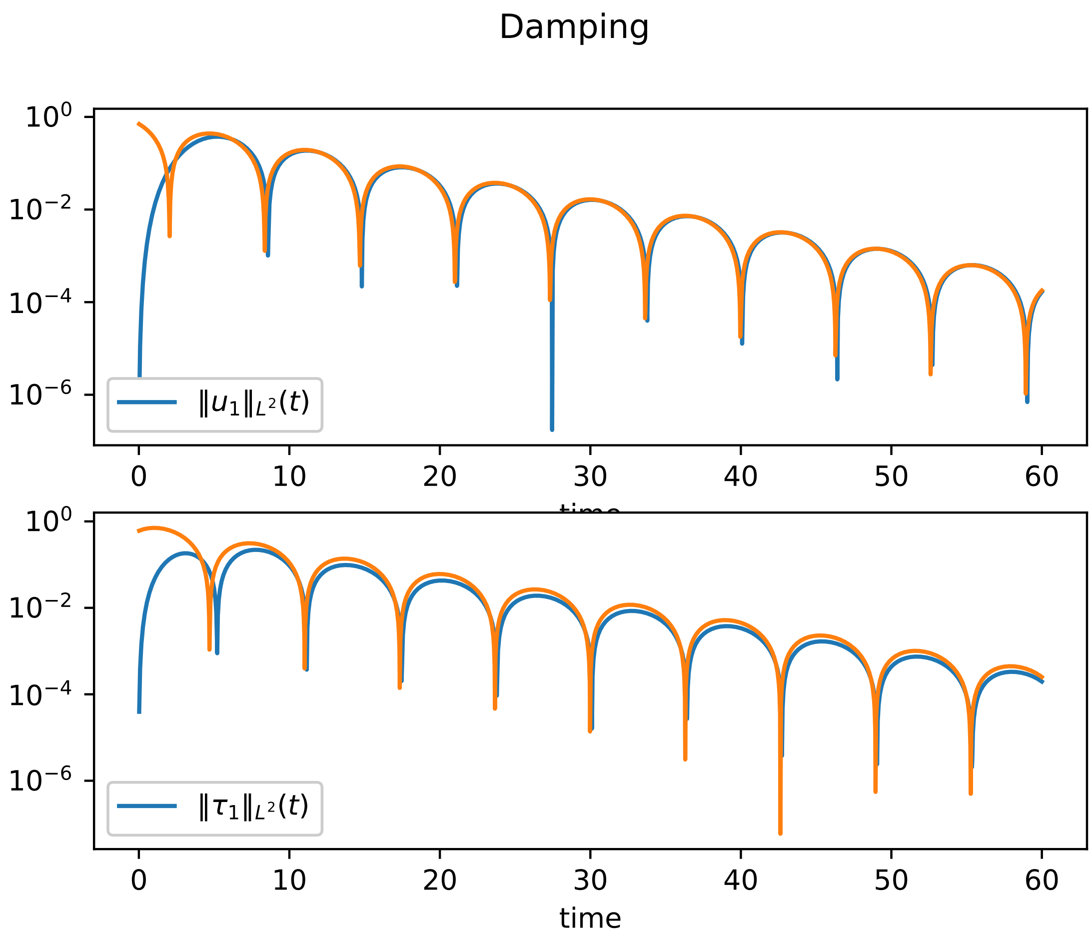

Fig. 3.2: Decay of the acoustic energy computed with the linear equations. In blue, the numerical solution and in orange the solution predicted by the linear theory.

Following [27], the linearization of the system (4.4) with friction $d_\star = \frac{D_\star}{\frac{4}{3}\pi r_p^3} > 0$ yields

$$\begin{cases} \partial_t \tau = \partial_x u + \partial_x \int_{\mathbf{R}} \sqrt{f^0} e^{d_\star t} f v \,\mathrm{d}v \\ \partial_t u = \partial_x \tau + d_\star \int_{\mathbf{R}} v \sqrt{f^0} e^{d_\star t} g \,\mathrm{d}v - d_\star u \int_{\mathbf{R}} f^0 \,\mathrm{d}v \\ \partial_t f + v \partial_x f - \sqrt{f^0} e^{d_\star t} v \partial_x \tau = d_\star \sqrt{f^0} e^{d_\star t} v u - d_\star f + d_\star \partial_v (v f). \end{cases}$$

Applying the Fourier-Laplace transform, one gets

$$\begin{cases} -i\omega \widetilde{\tau}_k(\omega) = ik \widetilde{u}_k(\omega) + ik \displaystyle\int_{\mathbf{R}} v \sqrt{f^0} \widetilde{f}_k(\omega - i d_\star) \,\mathrm{d}v + \tau_k(0) \\ -i\omega \widetilde{u}_k(\omega) = ik \widetilde{\tau}_k(\omega) + d_\star \displaystyle\int_{\mathbf{R}} v \sqrt{f^0} \widetilde{f}_k(\omega - i d_\star) \,\mathrm{d}v - d_\star \widetilde{u}_k(\omega) \displaystyle\int_{\mathbf{R}} f^0 \,\mathrm{d}v + u_k(0) \\ (-i\omega + ikv) \widetilde{f}_k(\omega, v) = ikv \sqrt{f^0} \widetilde{\tau}_k(\omega - i d_\star) + d_\star \widetilde{u}_k(\omega - i d_\star) v \sqrt{f^0} + d_\star v \partial_v \widetilde{f}_k(\omega, v) + f_k(0, v). \end{cases}$$

If one assumes that the coefficient $d_\star$ is small, another linearization procedure based on a Taylor expansion with respect to $d_\star$ yields

$$\widetilde{\tau}_k(\omega - i d_\star) = \tau_k(\omega) - i d_\star \partial_\omega \tau_k(\omega) + O(d_\star^2),$$

with similar formula for $\widetilde{u}_k$ and $\widetilde{f}_k$. Injecting those expansions and dropping the quadratic terms in $d_\star$, it yields

$$\begin{cases}-i\omega\widetilde{\tau}_k(\omega) = ik\widetilde{u}_k(\omega) + ik\int_{\mathbf{R}} v\sqrt{f^0}\widetilde{f}_k(\omega)\,\mathrm{d}v + d_\star k\int_{\mathbf{R}} v\sqrt{f^0}\partial_\omega\widetilde{f}_k(\omega) + \tau_k(0)\\ -i\omega\widetilde{u}_k(\omega) = ik\widetilde{\tau}_k(\omega) + d_\star\int_{\mathbf{R}} v\sqrt{f^0}\widetilde{f}_k(\omega)\,\mathrm{d}v - d_\star\widetilde{u}_k(\omega)\int_{\mathbf{R}} f^0\,\mathrm{d}v + u_k(0)\\ (-i\omega+ikv)\widetilde{f}_k(\omega,v) = ikv\sqrt{f^0}\widetilde{\tau}_k(\omega) - d_\star v\sqrt{f^0}\partial_\omega\widetilde{\tau}_k(\omega) + d_\star\widetilde{u}_k(\omega)v\sqrt{f^0} + d_\star v\partial_v\widetilde{f}_k(\omega,v) + f_k(0,v).\end{cases}$$

One obtains

$$\begin{aligned}\widetilde{f}_k(\omega,v) =& \frac{ikv\sqrt{f^0}\widetilde{\tau}_k(\omega)}{ikv-i\omega} + \frac{f_k(0,v)}{ikv-i\omega}\\ &+ \frac{d_\star}{ikv-i\omega}\left[\widetilde{u}_k(\omega)v\sqrt{f^0} + v\partial_v\widetilde{f}_k(\omega,v) - v\sqrt{f^0}\partial_w\widetilde{\tau}_k(\omega)\right],\end{aligned}$$

and

$$\begin{aligned}\widetilde{u}_k(\omega) &= \frac{-\frac{k}{\omega}\widetilde{\tau}_k(\omega) + \frac{i}{\omega}u_k(0) - \frac{id_\star}{\omega}\int_{\mathbf{R}} v\sqrt{f^0}\widetilde{f}_k(\omega)\,\mathrm{d}v}{1 - \frac{id_\star\int_{\mathbf{R}} f^0\,\mathrm{d}v}{\omega}}\\ &= \frac{-k\widetilde{\tau}_k(\omega) + iu_k(0) - id_\star\int_{\mathbf{R}} v\sqrt{f^0}\widetilde{f}_k(\omega)\,\mathrm{d}v}{\omega - id_\star\int_{\mathbf{R}} f^0\,\mathrm{d}v}.\end{aligned}$$

Then $\widetilde{f_k}(\omega,v)$ writes (dropping quadratic terms in $d_\star$)

$$\begin{aligned}\widetilde{f_k}(\omega,v) =& \frac{ikv\sqrt{f^0}\widetilde{\tau}_k(\omega)}{ikv-i\omega} + \frac{f_k(0,v)}{ikv-i\omega}\\ &+ \frac{d_\star}{ikv-i\omega}\frac{v\sqrt{f^0}}{\omega - id_\star\int_{\mathbf{R}} f^0\,\mathrm{d}v}\left[-k\widetilde{\tau}_k(\omega) + iu_k(0)\right]\\ &+ \frac{d_\star}{ikv-i\omega}\left[v\partial_v\widetilde{f}_k(\omega,v) - v\sqrt{f^0}\partial_w\widetilde{\tau}_k(\omega)\right].\end{aligned}$$

For $\widetilde{u}_k$, one has

$$\widetilde{u}_k(\omega) = \frac{-k\widetilde{\tau}_k(\omega) + iu_k(0) + d_\star k\int_{\mathbf{R}}\frac{v^2f^0}{ikv-i\omega}\,\mathrm{d}v\widetilde{\tau}_k(\omega) - id_\star\int_{\mathbf{R}}\frac{v\sqrt{f^0}f_k(0,v)}{ikv-i\omega}\,\mathrm{d}v}{\omega - id_\star\int_{\mathbf{R}} f^0\,\mathrm{d}v}.$$

For $\widetilde{\tau}_k$, one has

$$\begin{aligned}-i\omega\widetilde{\tau}_k(\omega) =& \frac{-k\widetilde{\tau}_k(\omega) + iu_k(0) + d_\star k\int_{\mathbf{R}}\frac{v^2f^0}{ikv-i\omega}\,\mathrm{d}v\widetilde{\tau}_k(\omega) - id_\star\int_{\mathbf{R}}\frac{v\sqrt{f^0}f_k(0,v)}{ikv-i\omega}\,\mathrm{d}v}{\omega - id_\star\int_{\mathbf{R}} f^0\,\mathrm{d}v}\\ &+ ik\int_{\mathbf{R}}\frac{v^2f^0}{ikv-i\omega}\,\mathrm{d}v\widetilde{\tau}_k(\omega) + \int_{\mathbf{R}}\frac{v\sqrt{f^0}f_k(0,v)}{ikv-i\omega}\,\mathrm{d}v\\ &+ \frac{d_\star ik}{w - id_\star\int_{\mathbf{R}} f^0\,\mathrm{d}v}\int_{\mathbf{R}}\frac{v^2f^0}{ikv-i\omega}\,\mathrm{d}v\left[-k\widetilde{\tau}_k(\omega) + iu_k(0)\right]\\ &+ id_\star k\int_{\mathbf{R}}\frac{v^2\sqrt{f^0}\partial_v\widetilde{f}_k(\omega,v)}{ikv-i\omega}\,\mathrm{d}v - id_\star k\int_{\mathbf{R}}\frac{v^2f^0}{ikv-i\omega}\,\mathrm{d}v\partial_\omega\widetilde{\tau}_k(\omega)\\ &+ ikd_\star\frac{\partial}{\partial\omega}\int_{\mathbf{R}}\frac{v^2f^0\widetilde{\tau}_k(\omega)}{ikv-i\omega}\,\mathrm{d}v + d_\star k\frac{\partial}{\partial\omega}\int_{\mathbf{R}}\frac{f_k(0,v)}{ikv-i\omega}\,\mathrm{d}v\\ &+ \tau_k(0).\end{aligned}$$

Rewriting this equation, one gets a differential equation of the form

$$d_\star A(\omega)\partial_w \widetilde{\tau}_k + B(\omega,d_\star)\widetilde{\tau}_k + C(\omega,d_\star) = 0,$$

where A,B,C are functions of ω. If $d_\star = 0$, one recovers equation (3.15). One would need to study this equation to see how the friction interacts with the damping mechanism. This is left for further research.

We nevertheless show numerical illustration for small value of $d_\star$. The results have been obtained with the nonlinear equations. We observe that for sufficiently small value of $d_\star$, the behaviour of the numerical solution is similar to the previous results, see Figure 3.4. But, with larger value of $d_\star$, we observe initially a damping phenomenon, which is replaced by the purely oscillatory phenomenon, see Figure 3.5. For even larger value of $d_\star$, we observe an oscillatory phenomenon, see Figure 3.6. The interpretation of those results with respect to the Lyapunov functional constructed in [27] remains to be done.

3.5 Instabilities of the linearized system

This section is based on the proceeding [62] published in *ESAIM: proceedings and surveys*

3.5.1 The dispersion relation.

As in the Vlasov-Poisson system, we can characterize the linearly instable particle profiles by the dispersion relation of the system. We look for exponentially growing modes of (3.5), i.e. solutions of the form

$$f(t,x,v) = \alpha(v)e^{-i\omega t}e^{ikx}, \quad \tau(t,x) = \beta e^{-i\omega t}e^{ikx}, \quad u(t,x) = \gamma e^{-i\omega t}e^{ikx}, \tag{3.22}$$

with $k \in \mathbf{Z}$, $\omega \in \mathbf{C}$ with $\Im m(\omega) > 0$, $\alpha \in L^\infty(\mathbf{R})$, β and $\gamma \in \mathbf{R}$. Injecting this ansatz into (3.5), one gets

$$\begin{cases} -i\omega\beta = ik\gamma + i\displaystyle\int kv\sqrt{f_0(v)}\alpha(v)\,\mathrm{d}v \\ -i\omega\gamma = ik\beta \\ (-i\omega + ikv)\alpha(v) = -i\beta\dfrac{kf_0'(v)}{\sqrt{f_0(v)}} \end{cases}$$

Then one obtains

$$\alpha(v) = \frac{-\beta k}{-\omega + kv}\frac{f_0'(v)}{\sqrt{f_0(v)}}, \quad \gamma = -\frac{\beta}{\omega}k, \tag{3.23}$$

and

$$-i\omega\beta = -ik^2\frac{\beta}{\omega} - i\beta\int\frac{k^2 v\partial_v f_0(v)}{kv-\omega}\,\mathrm{d}v.$$

In particular, one has the dispersion relation

$$\frac{k^2}{\omega^2} + \int\frac{f_0'(v)}{v-\omega/k}\,\mathrm{d}v = 1. \tag{3.24}$$

Conversevely, if (3.24) holds for some $k \in \mathbf{Z}$ and $\omega \in \mathbf{C}$ with $\Im m(\omega) > 0$, then the modes (3.22) with α and γ given by (3.23) are solutions of (3.5). We proved the following proposition

Proposition 3.5.1. *The linearized equations (3.5) have exponentially growing modes if and only if there exists $k \in \mathbf{Z}$ and $\omega \in \mathbf{C}$ with $\Im m(\omega) > 0$ satisfying (3.24). In that case, α and γ are given by (3.23) for any $\beta \in \mathbf{R}$.*

Dispersion relation in other kinetic equations. This situation is similar to the case of the Vlasov-Poisson system [40, 96, 113]

$$\begin{cases} \partial_t f + \boldsymbol{v} \cdot \nabla_x f - \nabla_x \varphi \cdot \nabla_v f = 0 \\ -\Delta_x \varphi = \int_{\mathbf{R}} f \mathrm{d}v - 1. \end{cases} \tag{3.25}$$

Applying the same strategy to the linearized Vlasov-Poisson equations, one founds the dispersion relation

$$Z\left(\frac{\omega}{k}\right) := \int \frac{f_0'(v)}{v - \omega/k} \,\mathrm{d}v = k^2 \tag{3.26}$$

Denoting $\Im_+$ the upper half plane, a solution $\omega(k)$ of (3.26) exists if and only if $Z(\Im_+)$ constains a positive real number k^2. The set $Z(\Im_+)$ is bounded and its boundary is the curve

$$x \mapsto PV \int \frac{f_0'(v)}{v - x} \,\mathrm{d}v + i\pi f_0'(x)$$

and this curve is bounded, starting and ending at the origin, and for k large enough, the equation (3.26) has no solution. Therefore, in the case where the profile f_0 leads to a solution $\omega \in \Im_+$ of (3.26), there is a finite number of exponentially growing modes. For the system (3.5), the situation is quite different since the equation (3.24) can be rewritten as

$$\zeta(z) := \frac{1}{z^2} + \int \frac{f_0'(v)}{v - z} \,\mathrm{d}v = 1, \quad z \in \mathbf{C},$$

with $z = \omega/k$. Therefore, if $z = \omega/k \in \Im_+$ is a solution, then so is $z = (n\omega)/(kn)$, with $n \in \mathbf{N}^*$. This situation also happen in other singular kinetic equations such as the Vlasov-Benney equation (see [13])

$$\begin{cases} \partial_t f + v \partial_x f - \partial_x V \partial_v f = 0 \\ V = \int_{\mathbf{R}} f \,\mathrm{d}v, \end{cases} \tag{3.27}$$

for which the dispersion relation writes

$$\int \frac{f_0'(v)}{v - \omega/k} \,\mathrm{d}v = 1,$$

or this equation, which can be seen as a kinetic version of the incompressible Euler equation (see [10, 72])

$$\begin{cases} \partial_t f + v \partial_x f - \partial_x V \partial_v f = 0 \\ \int_{\mathbf{R}} f \,\mathrm{d}v = 1. \end{cases} \tag{3.28}$$

for which the dispersion relation writes

$$\int \frac{f_0'(v)}{v - \omega/k} \,\mathrm{d}v = 0.$$

3.5.2 Numerical illustrations

In this section, we show examples unstable equilibrium f_0. The numerical illustrations are done again by discretizing the nonlinear equations (3.3) with the method described in Section 3.3.1. For the initial conditions, we take

$$\begin{cases} \varrho(t=0,x) = \varrho_0 \\ u(t=0,x) = 0 \\ f(t=0,x,v) = (1+\varepsilon\cos(kx))f_0(v). \end{cases}$$

with $\varrho_0 = 1$, $k = 0.5$ and $\varepsilon = 0.001$.

All the initial conditions are inspired by typical plasma physics test case [50,51,59,112]. We present analogy of two stream instability, bump on tail instability, weak and strong damping with and without friction.

3.5.3 Two-stream instability

We consider here the case where

$$f(t=0,x,v) = \frac{1}{2\sqrt{2\pi}}\left(e^{\frac{-(v-v_0)^2}{2}} + e^{\frac{-(v+v_0)^2}{2}}\right)(1+\varepsilon\cos(kx)), \quad v_0 = 2.5.$$

The computational domain is $[0,4\pi]\times[-6,6]$. We impose both in the x- and v- direction periodic boundary conditions. We take $N = 256$ grid point on the x and v direction. By analogy with plasma physics [38,61], we call this test "two-stream instability". The evolution of $\|\varrho-\varrho_0\|_{L^2}$ and $\|u\|_{L^2}$ in time is plotted in Figure 3.10. One observes that at first,the quantities $\|\varrho-\varrho_0\|_{L^2}$ and $\|u\|_{L^2}$ increase exponentially, as predicted by the linear theory. At some later time saturation sets in and the solution enters the nonlinear regime. It seems that the nature of the linear regime is that it is just a numerical artifact. Indeed, as the mesh is refined, the system enters the nonlinear regime earlier. This is due to the fact that the scheme is able to capture higher frequency mode earlier.

In Figure 3.9, one can see the apparition of vortex in the phase space distribution at $t = 55$. Eventually, the vortex get bigger and bigger and this lead to the apparition of shock waves in the fluid. The particles are then transported by the shock waves, which is visibled at $t = 73$. At $t = 75$ two shock waves collide this leads to the merge of the two streams. At this point there is a significant filamentation of the phase space distribution. The dispersion relation is illustrated in Figure 3.8 for Vlasov-Poisson and the system (3.5). It appears that the set $\zeta(\Im_+)$ is the whole complex plane.

3.5.4 Bump on tail instability

By analogy with plasma physics [50], we consider the case where

$$f(t=0,x,v) = \frac{1}{\sqrt{2\pi}}\left(0.8e^{-v^2/2} + 0.2e^{-4(v-3)^2}(1+0.1\cos x)\right),$$

on the domain $[0,4\pi]\times[-6,6]$. We impose both in the x- and v- direction periodic boundary conditions. There $N = 512$ grid point on the x and v direction.

This corresponds to the situation where there is a uniform cloud of droplet, where 80% of the mass is concentrated. Then a smaller beam of droplets of average velocity $v_0 = 3$ enters. As in the Vlasov-Poisson equations, this situation is an equilibrium of the system. However this equilibrium is unstable, and there is a growth of the acoustic energy, resulting in the apparition of small vortex with differents size in the particle phase space distribution. After this period of increase, the acoustic energy apppears to stay constant afterwards. See Figure 3.12 and Figure 3.11.

3.5.5 Strong damping

We consider here the case where the initial condition for the particle density is

$$f(t=0,x,v) = \frac{1}{\sqrt{2\pi}} e^{-v^2/2}(1 + \varepsilon \cos kx)$$

with $\varepsilon = 0.5$. The purpose of this test is to investigate the damping effect with a strong enough perturbation so that the nonlinear effects comes into play. The result is in the Figure 3.13. At first, one still observes damping of the acoustic energy. After some time, the nonlinear effects kick in and the acoustic energy goes back up, followed by oscillations.

3.6 Perspective

Several remarks can be made about future works

- The proof of a nonlinear damping result seems extremely difficult. The tools used in [15, 96] are not suitable to deal with the loss of regularity of the system.
- Regarding the instabilities, one can think on generalizing the analysis done in [13] to the linear thick spray model.
- It should be noticed that the result of this chapter are physically questionnable, because the friction force is still the driving mechanism of most fluid-particles flow. However, those result are still usefull from a numerical point of view to validate a numerical code.

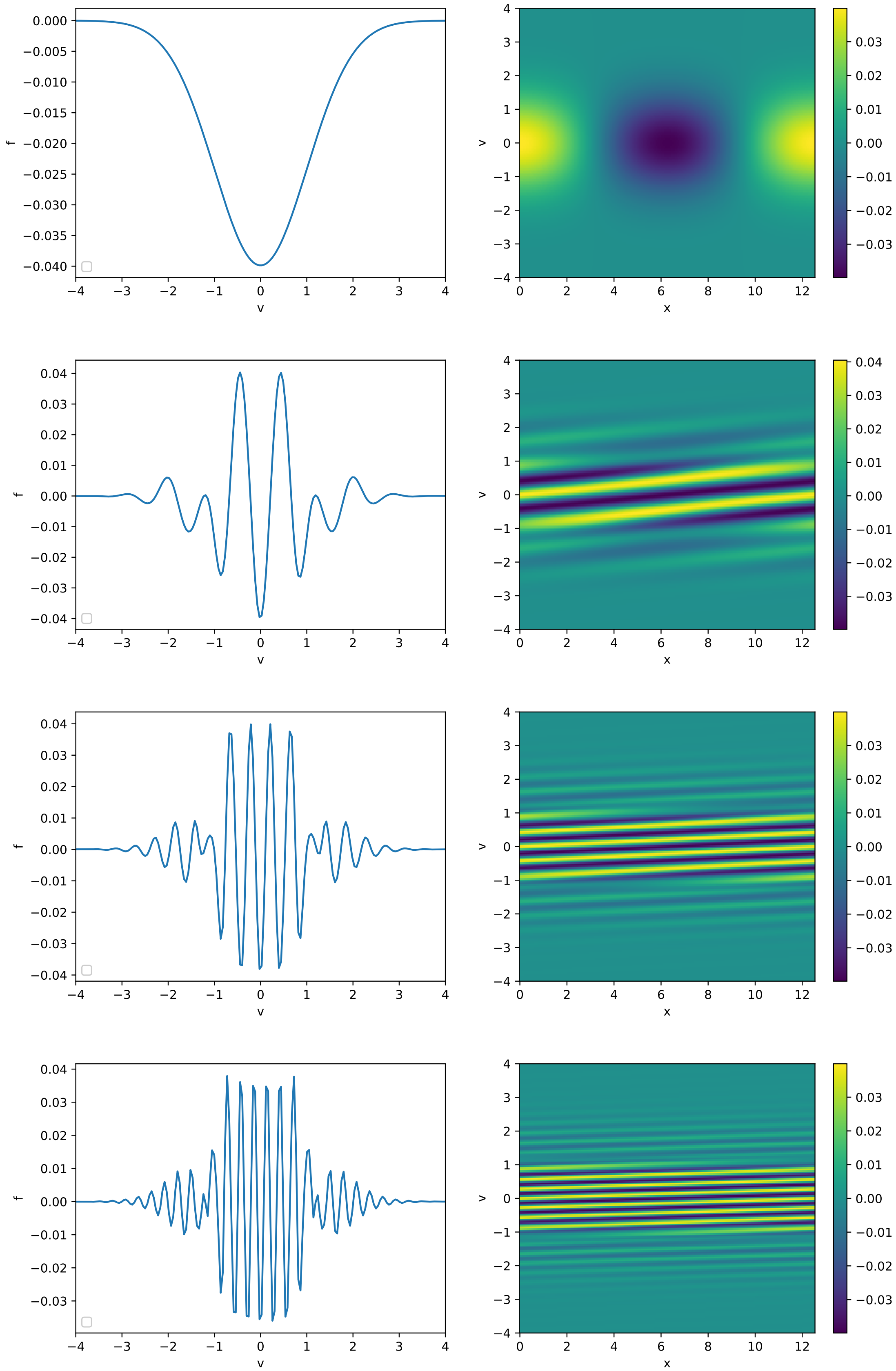

Fig. 3.3: Filamention or weak convergence of $f - f^0$ in the nonlinear equations for different times. In descending order, $t = 0$, $t = 15$, $t = 30$, $t = 45$.

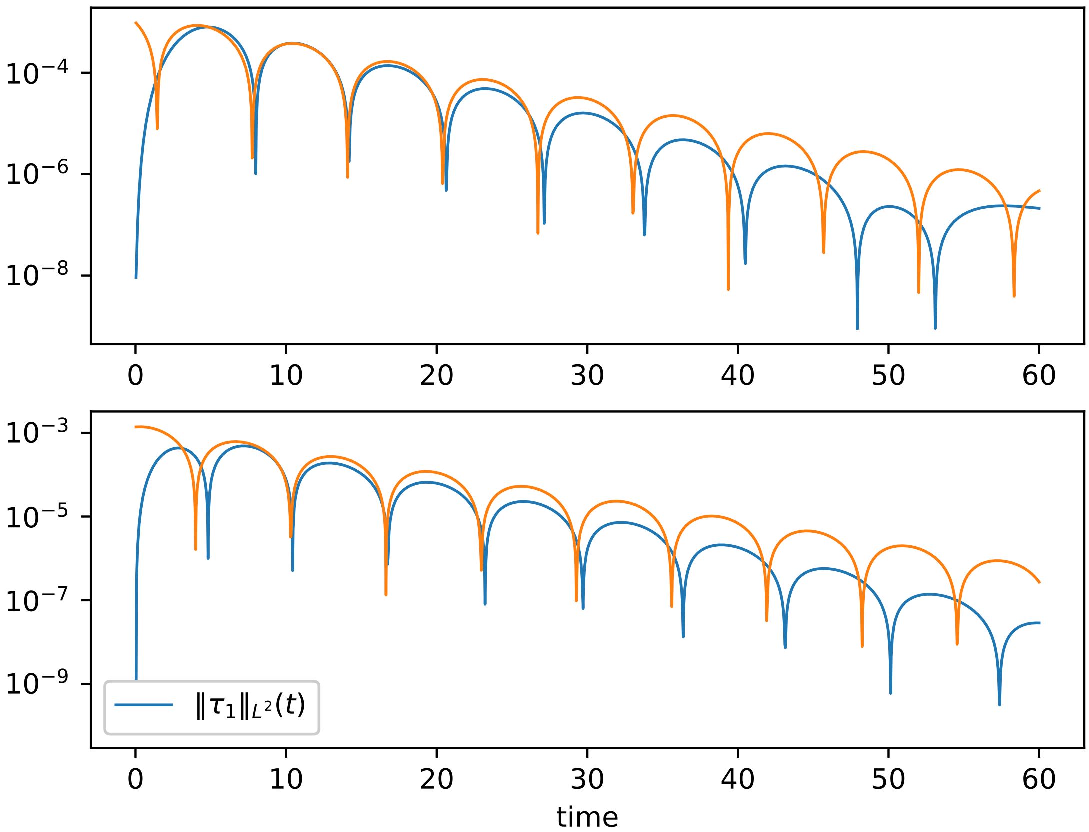

Fig. 3.4: Decay of the acoustic energy with friction for the nonlinear equations for $D_\star = 10^{-3}$. In blue, the numerical solution and in orange, the solution in the case with no friction

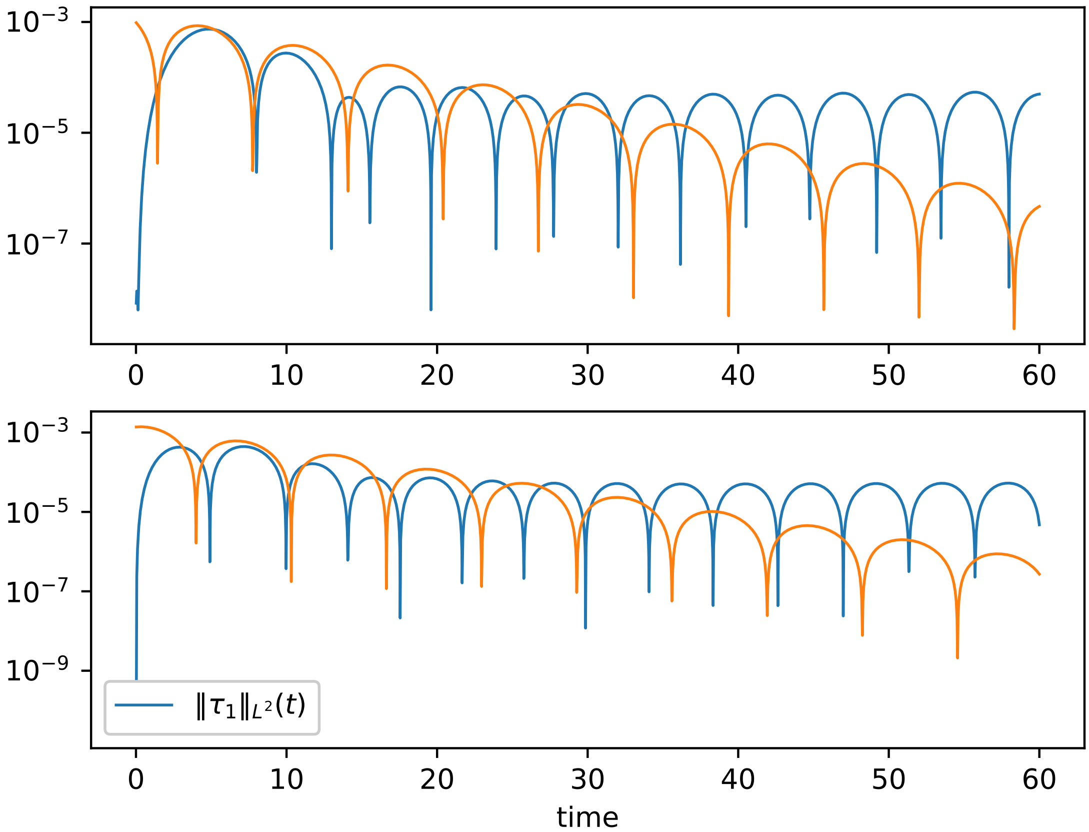

Fig. 3.5: Decay of the acoustic energy with friction for the nonlinear equations for $D_\star = 10^{-2}$. In blue, the numerical solution and in orange, the solution in the case with no friction

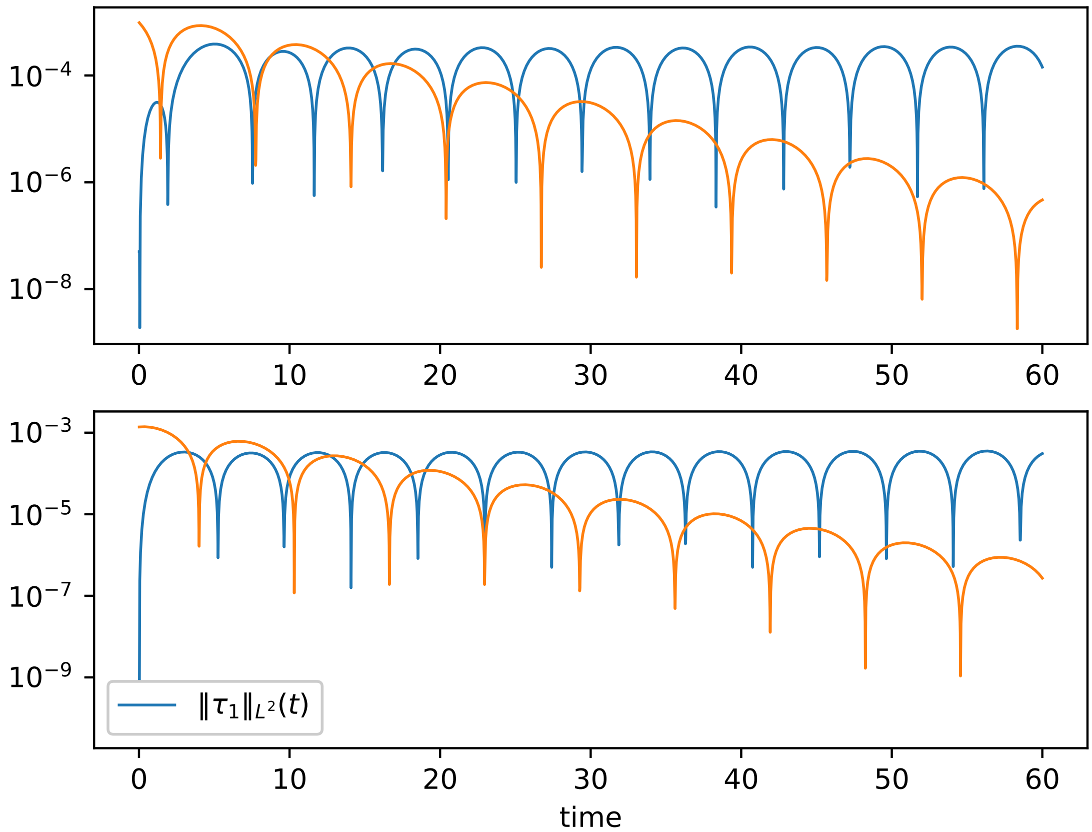

Fig. 3.6: Decay of the acoustic energy with friction for the nonlinear equations for $D_\star = 10^{-1}$. In blue, the numerical solution and in orange, the solution in the case with no friction

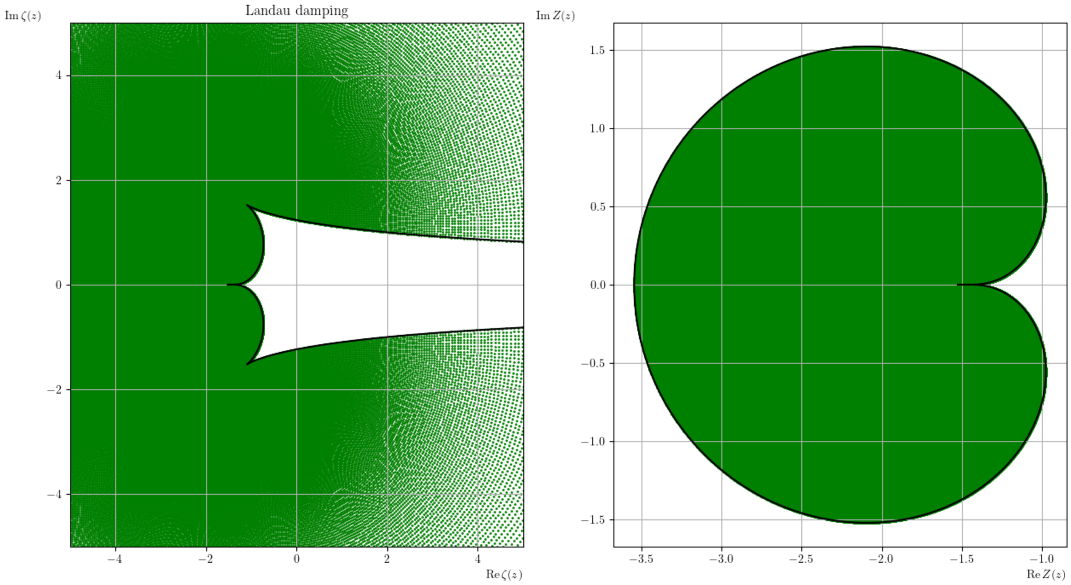

Fig. 3.7: Plot of the functions $\zeta(s)$ (left) and $Z(s)$ in the case where $f_0(v) = \left(\sqrt{2\pi}\right)^{-1} e^{-v^2/2}$. The image of the upper half complex plane is in green, and the image of the real line is the black curve. Notice how 1 is not in the image of ζ.

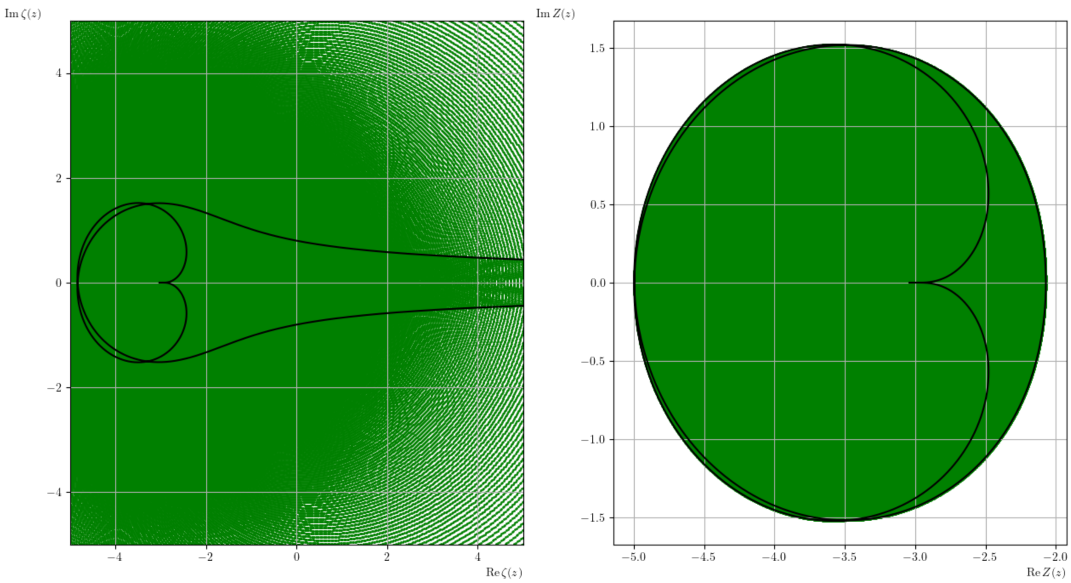

Fig. 3.8: Plot of the functions $\zeta(s)$ (left) and $Z(s)$ in the case where $f_0(v) = \left(2\sqrt{2\pi}\right)^{-1} \left(e^{-(v-v_0)^2/2} + e^{(-v+v_0)^2/2}\right)$ with $v_0 = 2.5$. The image of the upper half complex plane is in green, and the image of the real line is the black curve. Notice how 1 is in the image of ζ.

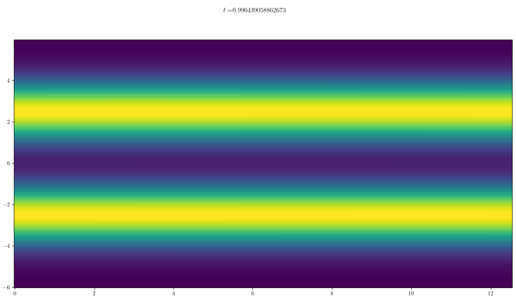

(a) Particle phase space distribution at $t = 1$

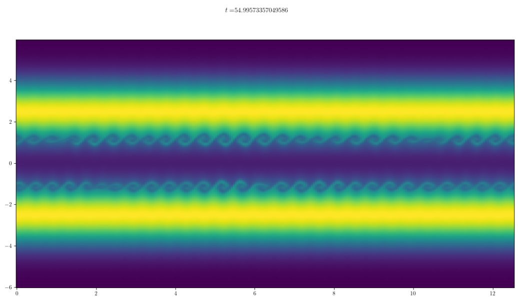

(b) Particle phase space distribution at $t = 55$

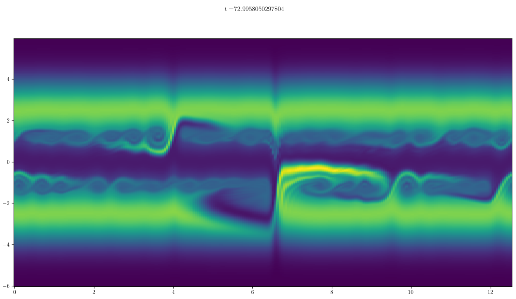

(c) Particle phase space distribution at $t = 73$

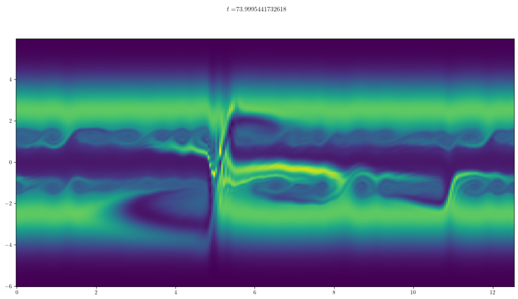

(d) Particle phase space distribution at $t = 74$

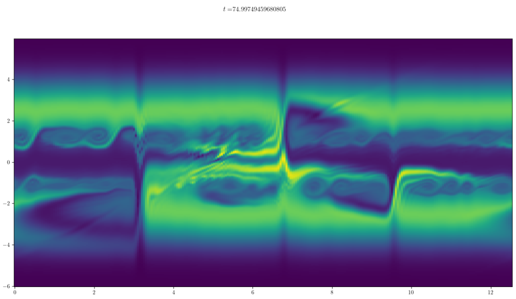

(e) Particle phase space distribution at $t = 75$

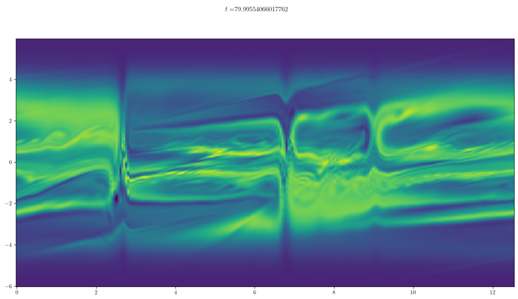

(f) Particle phase space distribution at $t = 80$

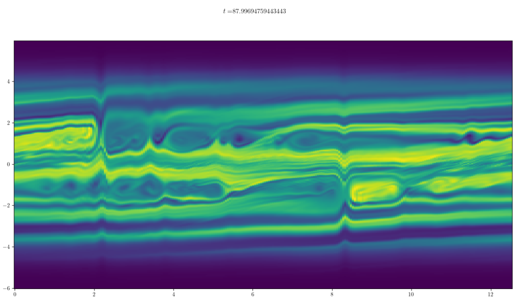

(g) Particle phase space distribution at $t = 88$

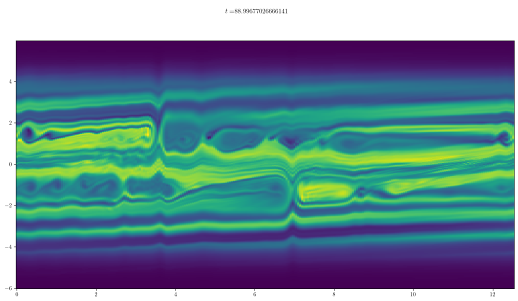

(h) Particle phase space distribution at $t = 89$

Fig. 3.9: Two stream instability

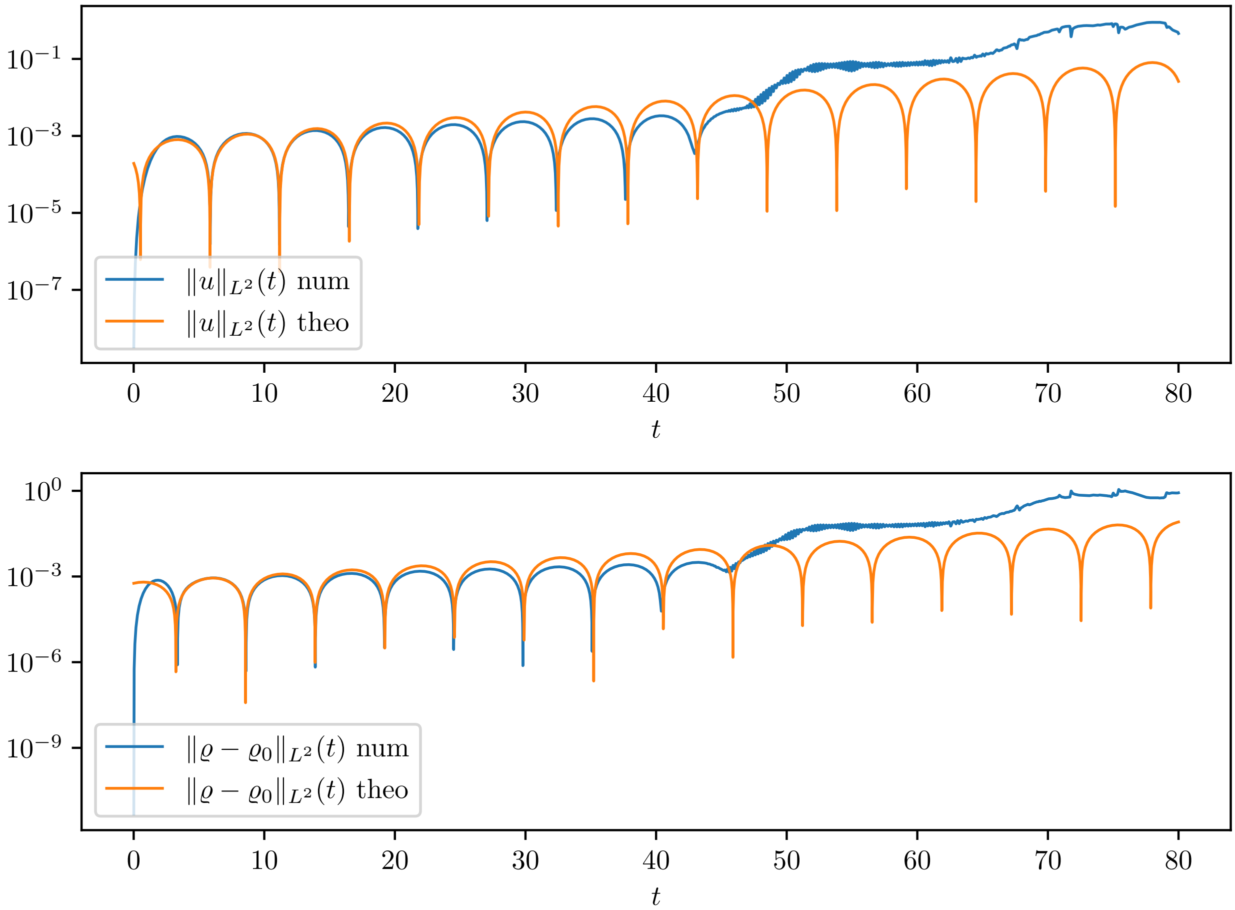

Fig. 3.10: Acoustic energy of the two stream instability

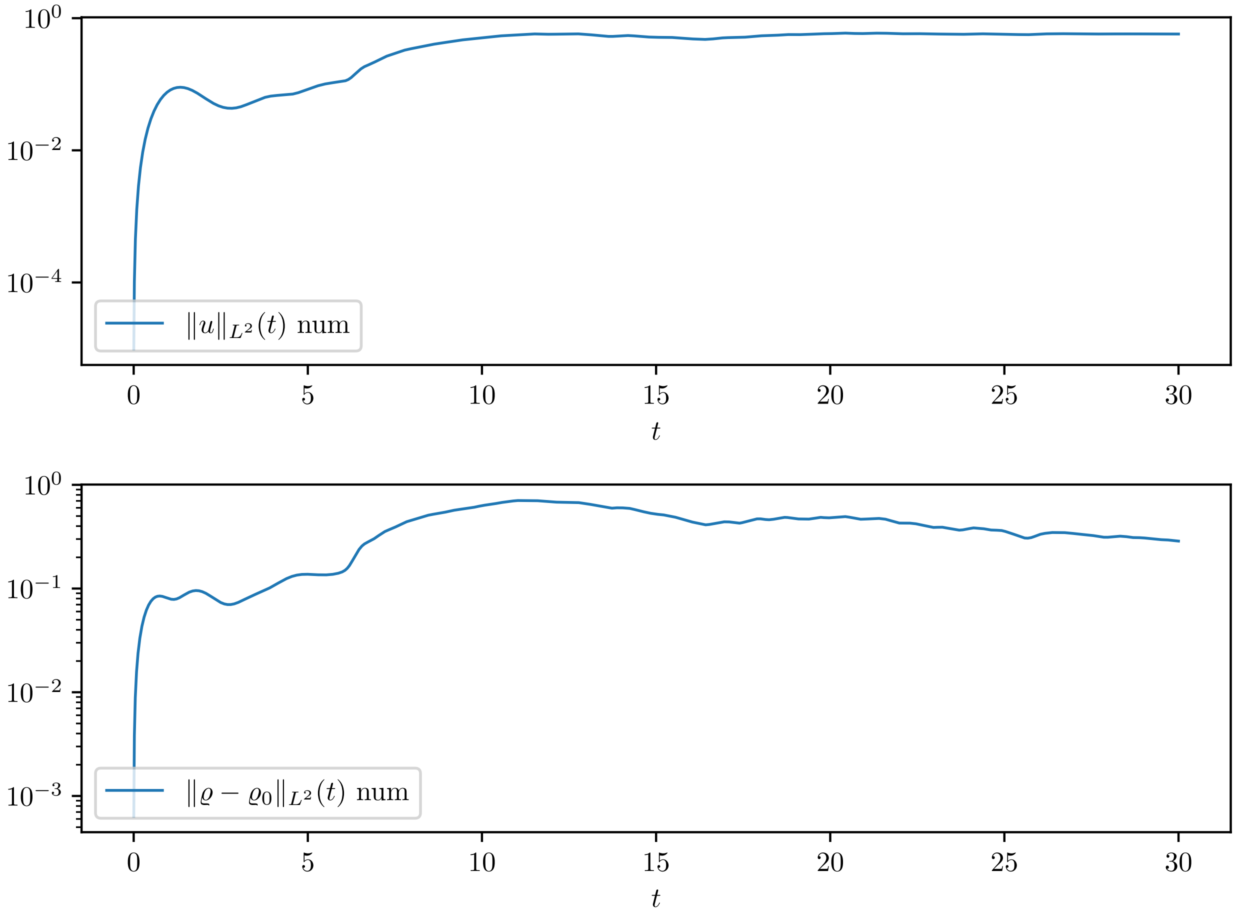

Fig. 3.11: Acoustic energy of the bump on tail instability

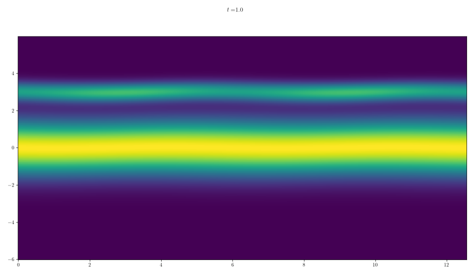

(a) Particle phase space distribution at $t = 1$

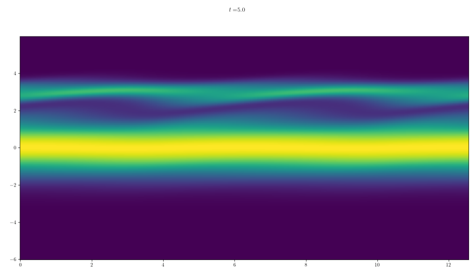

(b) Particle phase space distribution at $t = 5$

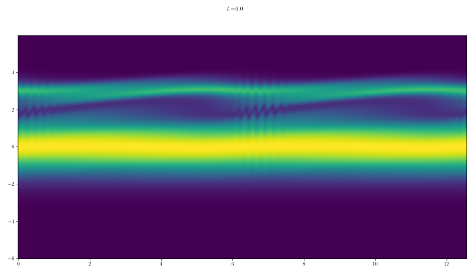

(c) Particle phase space distribution at $t = 6$

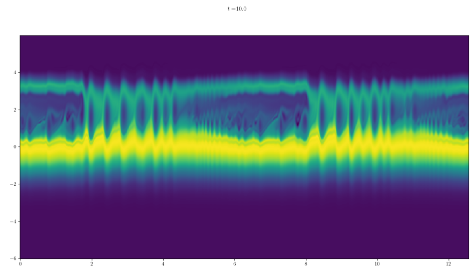

(d) Particle phase space distribution at $t = 10$

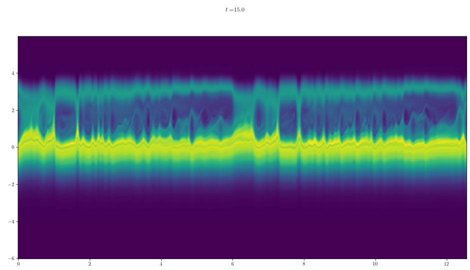

(e) Particle phase space distribution at $t = 15$

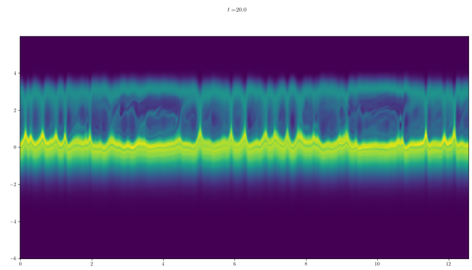

(f) Particle phase space distribution at $t = 20$

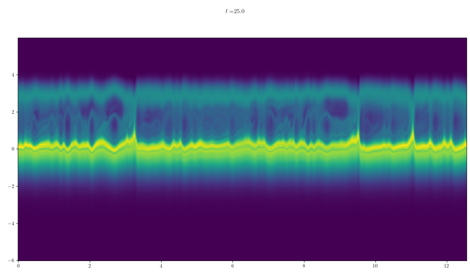

(g) Particle phase space distribution at $t = 25$

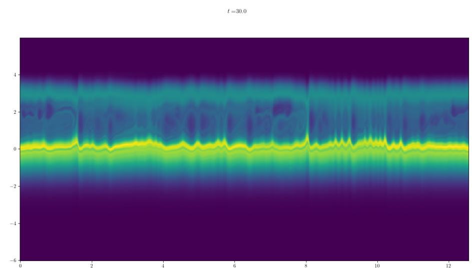

(h) Particle phase space distribution at $t = 30$

Fig. 3.12: Bump on tail instability

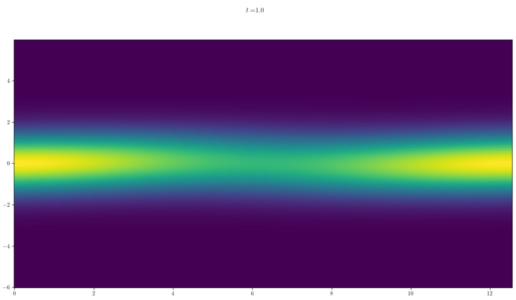

(a) Particle phase space distribution at $t = 1$

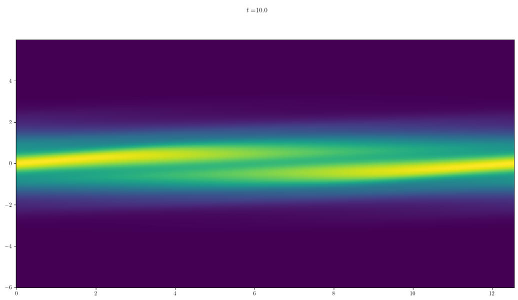

(b) Particle phase space distribution at $t = 10$

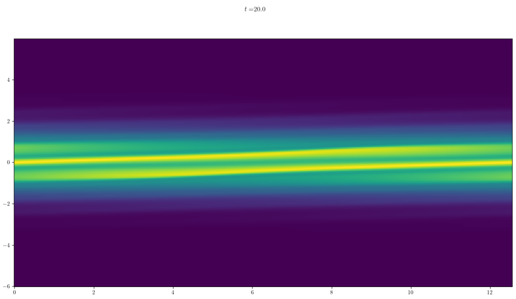

(c) Particle phase space distribution at $t = 20$

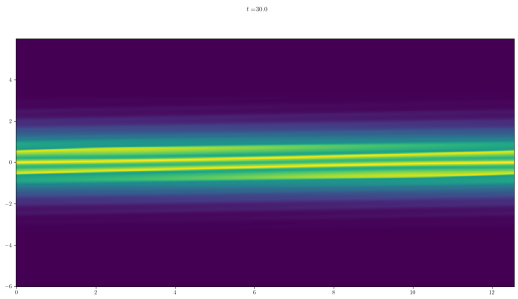

(d) Particle phase space distribution at $t = 30$

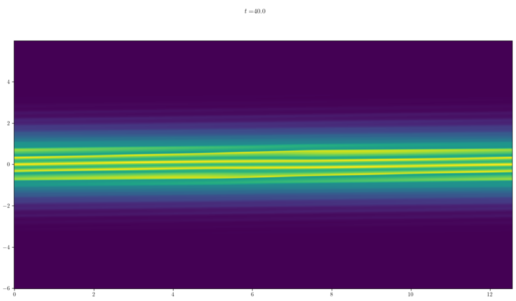

(e) Particle phase space distribution at $t = 40$

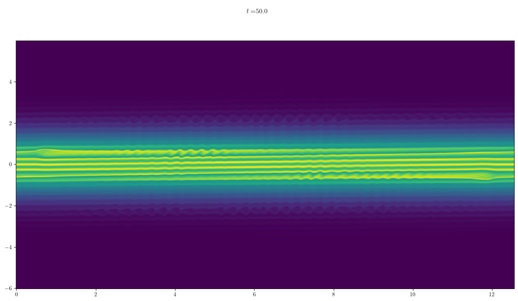

(f) Particle phase space distribution at $t = 50$

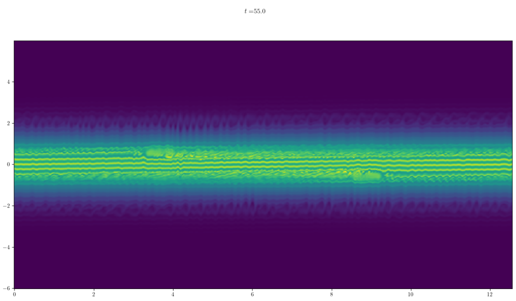

(g) Particle phase space distribution at $t = 40$

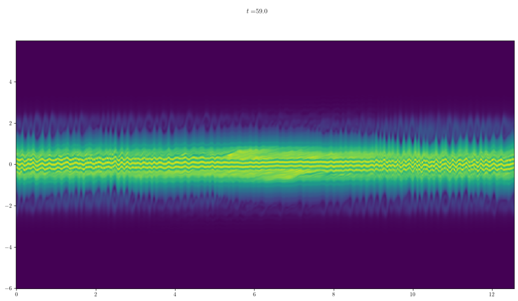

(h) Particle phase space distribution at $t = 50$

Fig. 3.13: Strong damping

Chapter 4

A coupled Finite Volume/semi-Lagrangian method for thick sprays

Summary

This chapter is dedicated to the numerical discretization of a thick spray model. We present a coupled method combining a Finite Volume scheme for the fluid phase, and a semi-Lagrangian scheme for the dispersed phase. The focus is on the discretization of the dispersed phase, for which we propose two different methods. The first one is a backward semi-Lagrangian method based on cublic B-Spline interpolation. The second one is a conservative semi-Lagrangian scheme known as Positive Flux Conservative. We also present two methods for taking into account the close-packing limit of the particles in the model.

4.1 Introduction

In this chapter, we are interested in the numerical simulation of dense suspensions of particles within a carrying fluid. The starting point of this work is the following fluid kinetic system

$$\begin{cases} \partial_t(\alpha\varrho) + \nabla_x \cdot (\alpha\varrho\boldsymbol{u}) = 0 \\ \partial_t(\alpha\varrho\boldsymbol{u}) + \nabla_x \cdot (\alpha\varrho\boldsymbol{u}\otimes\boldsymbol{u}) + \alpha\nabla_x p = D_\star \displaystyle\int_{\mathbf{R}^3} (\boldsymbol{v}-\boldsymbol{u}) f \,\mathrm{d}v \\ \partial_t f + \boldsymbol{v}\cdot\nabla_x f + \nabla_v \cdot (\boldsymbol{\Gamma} f) = 0 \\ \alpha = 1 - m_\star \displaystyle\int_{\mathbf{R}^3} f \,\mathrm{d}v \\ m_\star \boldsymbol{\Gamma} = -m_\star \nabla_x p - D_\star(\boldsymbol{v}-\boldsymbol{u}) \end{cases} \tag{4.1}$$

The first two equations are modified isentropic Euler equations, while the third equation is a Vlasov equation. The coupling between the two phases is done not only through a drag force, but also through the volume fraction of the fluid α in the fluid equations and through the presence of the pressure gradient $-\nabla_x p$ in the force field of the Vlasov equation. The system (4.1) is a prototype for describing s dense flow of particles within a carrying gas, it is sometimes refered to as a thick spray model [23, 53]. In this work, we only consider the case where $p(\varrho) = \varrho^\gamma$, where $\gamma > 1$ is the adiabatic index. It is possible to consider the full Euler system with energy transfer between the particle phase and the fluid phase [91]. For the sake of simplicity, we limit ourselves to the barotropic case.

Traditionaly, the numerical discretization of this kind of fluid-particle coupling is done with a Particle-In-Cell (PIC) method for the Vlasov equation [5, 6, 11, 49, 91]. The PIC method has the primary advantage of only discretizing the physical space x and not the velocity space v. This drastically reduces the computational cost of a direct discretization of the Vlasov equation. Indeed, the primary computational challenge comes from the fact that the distribution function f lives in an up to six-dimensional phase space. However, particle methods are known to suffer from numerical noise that decreases very slowly, as the square root of the number of particles. They are also known to be highly sensitive to sampling errors.

Recently, especially in the plasma physics community, Eulerian methods for the Vlasov equation have been developed with remarkable success [21, 35, 57–60, 88, 114]. Due to the substantial increase in computational power, 4D simulation can now be performed routinely on high performance computing (HPC) systems.

In this chapter, we present a numerical method for the discretization of thick sprays, based on semi-Lagrangian method for the Vlasov equation, and a Finite Volume method for the fluid phase [18,20]. A point of interest in this work is to take into account the *close-packing limit* in the system, characterized by a state where the particle density reaches a maximum.

4.1.1 Conservative form

If one multiplies the Vlasov equation by $m_\star \boldsymbol{v}$ and integrates with respect to $\boldsymbol{v}$, one obtains the balance law for the momentum of the particles

$$\partial_t \int_{\mathbf{R}^3} m_\star \boldsymbol{v} f \,\mathrm{d}v + \nabla_x \cdot \int_{\mathbf{R}^3} m_\star \boldsymbol{v} \otimes \boldsymbol{v} f \,\mathrm{d}v = \int_{\mathbf{R}^3} m_\star \boldsymbol{\Gamma} f \,\mathrm{d}v. \tag{4.2}$$

Adding (4.2) and the balance law of the momentum of the fluid, one obtains the equation for the total momentum of the system

$$\partial_t \left(\alpha\varrho\boldsymbol{u} + m_\star \int_{\mathbf{R}^3} \boldsymbol{v} f \,\mathrm{d}v \right) + \nabla_x \cdot \left(\alpha\varrho\boldsymbol{u} + m_\star \int_{\mathbf{R}^3} \boldsymbol{v} \otimes \boldsymbol{v} f \,\mathrm{d}v \right) + \nabla_x p = 0. \tag{4.3}$$

This equation is totally conservative, which is not the case for the fluid momentum balance law, as it contains a nonconservative product $\alpha\nabla_x p$. This term can induce additional difficulty from a numerical point of view [1,98]. For this reason, we chose to consider the system written under the form

$$\begin{cases} \partial_t(\alpha\varrho) + \nabla_x \cdot (\alpha\varrho\boldsymbol{u}) = 0, \\ \partial_t \left(\alpha\varrho\boldsymbol{u} + m_\star \int_{\mathbf{R}^3} \boldsymbol{v} f \,\mathrm{d}v\right) + \nabla_x \cdot \left(\alpha\varrho\boldsymbol{u} + m_\star \int_{\mathbf{R}^3} \boldsymbol{v}\otimes\boldsymbol{v} f \,\mathrm{d}v\right) + \nabla_x p = 0, \\ \partial_t f + \boldsymbol{v}\cdot\nabla_x f + \nabla_v \cdot (\boldsymbol{\Gamma} f) = 0. \end{cases} \tag{4.4}$$

The fluid phase is rewritten in terms of the conserved variables $n := \alpha\varrho$, $\mathbf{q} := \alpha\varrho\boldsymbol{u} + m_\star \int_{\mathbf{R}^3} \boldsymbol{v} f \,\mathrm{d}v$,

$$\begin{cases} \partial_t n + \nabla_x \cdot \left(\mathbf{q} - m_\star \int_{\mathbf{R}^3} \boldsymbol{v} f \,\mathrm{d}v\right) = 0, \\ \partial_t \mathbf{q} + \nabla_x \cdot \left(\dfrac{\left(\mathbf{q} - m_\star \int_{\mathbf{R}^3} \boldsymbol{v} f \,\mathrm{d}v\right)^{\otimes 2}}{n} + m_\star \displaystyle\int_{\mathbf{R}^3} \boldsymbol{v}\otimes\boldsymbol{v} f \,\mathrm{d}v \right) + \nabla_x p\left(\dfrac{n}{\alpha}\right) = 0. \end{cases} \tag{4.5}$$

4.1.2 Close-packing limit.

By close-packing limit, we refer to the configuration where the maximal density for the particles is reached, which typically corresponds to the case where the particles are packed on top of each other. The close-packing of particles is a part of a larger family of congestion phenomena in fluid equations. The study of such phenomena represents a prolific area of the literature, see [41,94,100,101,108] and the references therein. The system (4.1) does not take into account the modelling of close-packing limit. We would like to modify the model (4.1) so that, given a lower bound $0 \le \alpha_\star < 1$ and assuming that the initial data verifies $\alpha(t=0,\cdot) > \alpha_\star$, the solutions preserve the bound $\alpha(t,\cdot) > \alpha_\star$ for all $t > 0$. A priori, the system (4.1) does not verify this property. An interesting case is $\alpha_\star = 0$, meaning that we are interested in the positivity of the fluid volume fraction. In [27], the following result on the positivity of the volume fraction α is proved for the full Euler system.

Proposition 4.1.1 ([27]). *Assume that a solution of the system (4.1) is defined on the whole space $\mathbf{R}^3$ and is smooth on $[0,T_{\mathrm{end}})$ for some $T_{\mathrm{end}} > 0$. We assume that*

- *For all* $(\boldsymbol{x},\boldsymbol{v}) \in \mathbf{R}^3 \times \mathbf{R}^3, \quad f(0,\boldsymbol{x},\boldsymbol{v}) > 0.$
- *One has* $0 < \varrho_- = \inf_{\boldsymbol{x}\in\mathbf{R}^3} \varrho(0,\boldsymbol{x}) \leq \varrho_+ = \sup_{\boldsymbol{x}\in\mathbf{R}^3} \varrho(0,\boldsymbol{x}) < +\infty.$
- *One has* $-\infty < S_- = \inf_{\boldsymbol{x}\in\mathbf{R}^3} S(0,\boldsymbol{x}).$
- *One has* $0 < \alpha_- = \inf_{\boldsymbol{x}\in\mathbf{R}^3} \alpha(0,\boldsymbol{x}) \leq 1.$

We assume the following regularity of the velocity variables

$$\boldsymbol{u} \in W^{1,\infty}([0,T_{\text{end}}) \times \mathbf{R}^3), \quad \frac{\int_{\mathbf{R}^3} f\boldsymbol{v}\,\mathrm{d}v}{\int_{\mathbf{R}^3} f\,\mathrm{d}v} \in L^\infty([0,T_{\text{end}}) \times \mathbf{R}^3).$$

We finally assume that the pressure vanishes at infinity, that is for all $\varepsilon > 0$*, there exists* $A > 0$ *such that*

$$0 < p(t,\boldsymbol{x}) = (\gamma-1)\varrho(t,\boldsymbol{x})e(t,\boldsymbol{x}) < \varepsilon, \quad \textit{for } 0 \leq t < T_{end} \textit{ and } |\boldsymbol{x}| > A.$$

Then, there exists a constant $C > 0$ *depending on* T_{end}*,* ϱ_+*,* ϱ_-*,* α_-*,* S_-*,* A *(corresponding to* $\varepsilon = 1$*),* $\|\boldsymbol{u}\|_{W^{1,\infty}([0,T_{\text{end}})\times\mathbf{R}^3)}$ *and* $\left\|\frac{\int f\boldsymbol{v}\,\mathrm{d}v}{\int f\,\mathrm{d}v}\right\|_{L^\infty([0,T_{\text{end}})\times\mathbf{R}^3)}$ *so that the following estimate holds :*

$$0 < C \leq \alpha(t,\boldsymbol{x}) \leq 1, \quad t \in [0,T_{\text{end}}), \quad \boldsymbol{x} \in \mathbf{R}^3.$$

So for strong solutions, the positivity of the fluid volume fraction is guaranteed. However, nothing is said in the case solutions that contain discontinuities, such as shock waves, which are of paramount interest for the applications. In the remaining of this work, we assume that $\alpha_\star > 0$. In the literature, multiple ways to model the close-packing limit can be found.

For instance, a possible way [6, 20] to modify the Vlasov equation is to add a pressure term in the force field $\mathbf{\Gamma}$

$$m_\star \mathbf{\Gamma} = D_\star(\boldsymbol{u}-\boldsymbol{v}) - m_\star \nabla_x p - \frac{1}{1-\alpha}\nabla_x \pi(\alpha),$$

The function $\pi : [0,\alpha_\star) \to [0,+\infty)$ is required to satisfy $\pi(0) = 0$ and $\lim_{\alpha\to\alpha_\star} \pi(\alpha) = +\infty$. Another possibility, found for instance in [64] is to modify the free transport operator directly:

$$\partial_t f + \nabla_x \cdot (\boldsymbol{v}f - \pi(\alpha)\nabla_v f) + \nabla_v \cdot (\mathbf{\Gamma} f) = 0.$$

Our first proposition to implement close-packing effects in the model (4.4) is to modify Vlasov equation

$$\partial_t f + \nabla_x \cdot (\boldsymbol{v}f - \nabla_x \pi f) + \nabla_v \cdot (\mathbf{\Gamma} f) = 0. \tag{4.6}$$

In the literature [100], it is common to give a formula for π, which is mainly of empirical nature. A typical formula is

$$\pi(\alpha) = \varepsilon \left(\frac{\alpha_f}{\alpha_\star - \alpha_f}\right)^\beta, \quad \beta > 1.$$

The coefficient $\varepsilon > 0$ is usually taken small. Its role is to make π negligible when α_f is not very close to $\alpha_\star$. The coefficient $\beta > 1$ is given empirically. This kind of expression for π

corresponds to so-called *soft congestion models* [100]. The idea is that the singular pressure π acts as a barrier that prevents the particle volume fraction from becoming too big.

When $\varepsilon \to 0$, the singular pressure π tends to a limit pressure π_∞ such that

$$(\alpha - \alpha_\star)\pi_\infty = 0, \quad \alpha \geq \alpha_\star, \quad \pi_\infty \geq 0.$$

and the corresponding models that use this type of pressure are known as *hard congestion models* [100]. The link between the hard and soft models is interesting from a numerical point of view. The hard limit is difficult to handle because of the sharp unknown interface between the free domain (where $\pi_\infty = 0$) and the congested domain. One can instead use the soft model with small ε to approximate the hard model [41]. In this work, we only consider the case $\varepsilon > 0$. Our second proposition to take into account the close packing limit is purely of numerical nature. The idea is to introduce a correction procedure in the numerical scheme that imposes the bound $\alpha \geq \alpha_\star$. The correction procedure we propose is inspired by works done in [93, 94, 108] on the modeling of crowd motion.

To finish this section, let us write the two systems that we will study. We recall that the conserved variables are $n = \alpha\varrho$, $\mathbf{q} = \alpha\varrho\boldsymbol{u} + m_\star \int \boldsymbol{v} f \,\mathrm{d}v$. The original system without packing pressure π is

$$\begin{cases} \partial_t n + \nabla_x \cdot (\mathbf{q} - m_\star \int \boldsymbol{v} f \,\mathrm{d}v) = 0 \\ \partial_t \mathbf{q} + \nabla_x \cdot \left(\dfrac{(\mathbf{q} - m_\star \int \boldsymbol{v} f \,\mathrm{d}v)^{\otimes 2}}{n} + m_\star \int \boldsymbol{v} \otimes \boldsymbol{v} f \,\mathrm{d}v \right) + \nabla_x p \left(\dfrac{n}{\alpha}\right) = 0 \\ \partial_t f + \nabla_x \cdot (\boldsymbol{v} f) + \nabla_v \cdot (\boldsymbol{\Gamma} f) = 0 \\ \alpha = 1 - m_\star \displaystyle\int_{\mathbf{R}^3} f \,\mathrm{d}v \\ m_\star \boldsymbol{\Gamma} = -m_\star \nabla_x p - D_\star(\boldsymbol{v} - \boldsymbol{u}), \end{cases} \tag{4.7}$$

that we will refer to as the "original model". Then, the system with added packing pressure

$$\begin{cases} \partial_t n + \nabla_x \cdot (\mathbf{q} - m_\star \int \boldsymbol{v} f \,\mathrm{d}v) = 0 \\ \partial_t \mathbf{q} + \nabla_x \cdot \left(\dfrac{(\mathbf{q} - m_\star \int \boldsymbol{v} f \,\mathrm{d}v)^{\otimes 2}}{n} + m_\star \int \boldsymbol{v} \otimes \boldsymbol{v} f \,\mathrm{d}v - m_\star \partial_x \pi \int f v \,\mathrm{d}v \right) + \nabla_x p \left(\dfrac{n}{\alpha}\right) = 0 \\ \partial_t f + \nabla_x \cdot [(\boldsymbol{v} - \nabla_x \pi(\alpha)) f] + \nabla_v \cdot (\boldsymbol{\Gamma} f) = 0 \\ \alpha = 1 - m_\star \displaystyle\int_{\mathbf{R}^3} f \,\mathrm{d}v \\ m_\star \boldsymbol{\Gamma} = -m_\star \nabla_x p - D_\star(\boldsymbol{v} - \boldsymbol{u}) \\ \pi(\alpha) = \varepsilon \left(\dfrac{\alpha_f}{\alpha_\star - \alpha_f} \right)^\beta, \quad \beta > 1, \end{cases} \tag{4.8}$$

and we will refer to it as the "soft model".

4.2 Properties of the models

In this section, we recall some properties of the fluid phase and of the Vlasov equations that are useful for the numerical discretization. For the sake of simplicity, we restrict ourselves to the 1D case.

4.2.1 Fluid part

4.2.1.1 Original system.

We will consider only an isentropic gas law, where the pressure is given by

$$p(\varrho) = \varrho^\gamma = \frac{n^\gamma}{\alpha^\gamma}.$$

The fluid part of the system writes

$$\partial_t \mathbf{U} + \partial_x \mathbf{F}(\mathbf{U},f) = 0,$$

with

$$\mathbf{U} = \begin{pmatrix} n \\ q \end{pmatrix},$$

and

$$\mathbf{F}(\mathbf{U},f) = \begin{pmatrix} \alpha\varrho u \\ \alpha\varrho u^2 + p + m_\star \int_{\mathbf{R}} f v^2 \,\mathrm{d}v \end{pmatrix} = \begin{pmatrix} q - m_\star \int_{\mathbf{R}} f v \,\mathrm{d}v \\ \dfrac{(q - m_\star \int_{\mathbf{R}} f v \,\mathrm{d}v)^2}{n} + \dfrac{n^\gamma}{\alpha^\gamma} + \int_{\mathbf{R}} f v^2 \,\mathrm{d}v \end{pmatrix}.$$

The Jacobian matrix of $\mathbf{F}$ with respect to $\mathbf{U}$ is

$$\mathbf{A}(\mathbf{U},f) := \boldsymbol{\nabla}_{\mathbf{U}} \mathbf{F}(\mathbf{U},f) = \begin{pmatrix} 0 & 1 \\ \dfrac{-(q - m_\star \int_{\mathbf{R}} f v \,\mathrm{d}v)^2}{n^2} + \dfrac{\gamma n^{\gamma-1}}{\alpha^\gamma} & \dfrac{2(q - m_\star \int_{\mathbf{R}} f v \,\mathrm{d}v)}{n} \end{pmatrix}. \tag{4.9}$$

We know from Proposition 3.3.1 that the eigenvalues of the matrix $A(\mathbf{U},f)$ are

$$\lambda_\pm = u \pm \sqrt{\frac{p'(\varrho)}{\alpha}}.$$

4.2.1.2 Soft congestion system.

For the soft congested system, the total momentum equation is slightly different because of the added pressure term π.

$$\partial_t \left(\alpha\varrho u + m_\star \int_{\mathbf{R}} f v \,\mathrm{d}v \right) + \partial_x \left(\alpha\varrho u^2 + p + m_\star \int_{\mathbf{R}} v^2 f \,\mathrm{d}v - m_\star \partial_x \pi \int_{\mathbf{R}} f v \,\mathrm{d}v \right) = 0.$$

The fluid part of the system then writes

$$\partial_t \mathbf{U} + \partial_x \mathbf{F}(\mathbf{U},f) = 0,$$

with

$$\mathbf{U} = \begin{pmatrix} n \\ q \end{pmatrix} := \begin{pmatrix} \alpha\varrho \\ \alpha\varrho u + m_\star \int_{\mathbf{R}} f v \,\mathrm{d}v \end{pmatrix},$$

and

$$\mathbf{F}(\mathbf{U},f) = \begin{pmatrix} \alpha\varrho u \\ \alpha\varrho u^2 + p + m_\star \int_{\mathbf{R}} f v^2 \,\mathrm{d}v - m_\star \partial_x \pi \int f v \,\mathrm{d}v \end{pmatrix} \tag{4.10}$$

$$= \begin{pmatrix} q - m_\star \int_{\mathbf{R}} f v \,\mathrm{d}v \\ \frac{(q - m_\star \int_{\mathbf{R}} f v \,\mathrm{d}v)^2}{n} + \frac{n^\gamma}{\alpha^\gamma} + m_\star \int_{\mathbf{R}} f v^2 \,\mathrm{d}v - m_\star \partial_x \pi \int f v \,\mathrm{d}v \end{pmatrix}. \tag{4.11}$$

The jacobian of $\mathbf{F}$ with respect to $\mathbf{U}$ is the same so the eigenvalues of the system also write

$$\lambda_\pm = u \pm \sqrt{\frac{p'(\varrho)}{\alpha}}.$$

4.2.2 Particle phase

Let ϱ and u be two given smooth functions. Let us consider first the original system (4.7) in dragless case $D_\star = 0$. The Vlasov equation writes

$$\partial_t f + v \partial_x f - \partial_x p(\varrho) \partial_v f = 0. \tag{4.12}$$

The Vlasov equation admits a solution, given by the method of characteristics

$$f(t,x,v) = f_0(X(0;t,x,v), V(0;t,x,v)), \tag{4.13}$$

where the characteristics curves X and V are solutions of the following system of ODE

$$\frac{\mathrm{d}}{\mathrm{d}s} X(s;t,x,v) = V(s;t,x,v), \tag{4.14}$$

$$X(t;t,x,v) = x, \tag{4.15}$$

$$\frac{\mathrm{d}}{\mathrm{d}s} V(s;t,x,v) = -\partial_x p\left(s, X(s;t,x,v)\right), \tag{4.16}$$

$$V(t;t,x,v) = v. \tag{4.17}$$

When $D_\star > 0$ the Vlasov equation of the system (4.1) can be rewritten in the following non-conservative form

$$\partial_t f + v \partial_x f - \partial_x p(\varrho) \partial_v f + D_\star (u - v) \partial_v f = D_\star f. \tag{4.18}$$

The solution can still be computed by the method of characteristics:

$$f(t,x,v) = f_0(X(0;t,x,v), V(0;t,x,v)) e^{D_\star t}, \tag{4.19}$$

where the characteristics curves X and V are solutions of the following system of ODE

$$\frac{\mathrm{d}}{\mathrm{d}s} X(s;t,x,v) = V(s;t,x,v), \tag{4.20}$$

$$X(t;t,x,v) = x \tag{4.21}$$

$$\frac{\mathrm{d}}{\mathrm{d}s} V(s;t,x,v) = -\partial_x p\left(s, X(s;t,x,v)\right) + D_\star \left(u\left(s, X(s;t,x,v)\right) - V(s;t,x,v)\right), \tag{4.22}$$

$$V(t;t,x,v) = v. \tag{4.23}$$

Those formulae are the basic bricks of the semi-Lagrangian scheme. We deduce from the formula (4.19) the following consequences

- One has
$$\min_{x,v} f(0,x,v)e^{D_\star t} \leq f(t,x,v) \leq \max_{x,v} f(0,x,v)e^{D_\star t}.$$
This expresses the general tendency of the drag force: the velocities of the particles tend to align with the velocity of the ambient fluid u.

- When $p \neq 1$, the L^p norms of f are not conserved: $\|f(t)\|_{L^p_{x,v}} = e^{D_\star(1-1/p)t}\|f(0)\|_{L^p_{x,v}}$. This is in contrast with plasma physics models such as the Vlasov-Poisson system where all the L^p norms are conserved (in fact, for every smooth function β, the integrals of $\beta(f)$ are conserved). An interesting consequence is that the L^2 norm cannot be used to evaluate the numerical diffusion. This is due to the fact that $\mathbf{\Gamma}$ is not divergence-free in the velocity variable v. This is unusual compared to plasma physics models such as Vlasov-Poisson equations or Vlasov-Maxwell equations, see [21,50,112].

For the soft congested system (4.8), The Vlasov equation writes

$$\partial_t f + v\partial_x f - \partial_x(\partial_x \pi(\alpha) f) - \partial_x p(\varrho)\partial_v f + D_\star(u-v)\partial_v f = D_\star f. \tag{4.24}$$

The extra term introduces additionnal difficulty because the characteristic curves can no longer be computed explicitly. The characteristic curves X and V are solutions of the following system of ODE

$$\frac{\mathrm{d}}{\mathrm{d}s}X(s;t,x,v) = V(s;t,x,v) - \partial_x\pi(\alpha(s,X(s;t,x,v))), \tag{4.25}$$
$$X(t;t,x,v) = x, \tag{4.26}$$
$$\frac{\mathrm{d}}{\mathrm{d}s}V(s;t,x,v) = -\partial_x p\left(s,X(s;t,x,v)\right) + D_\star\left(u\left(s,X(s;t,x,v)\right) - V(s;t,x,v)\right), \tag{4.27}$$
$$V(t;t,x,v) = v. \tag{4.28}$$

4.3 Numerical methods

In this section, we present the numerical methods used to discretize systems (4.1) and (4.8). The main idea consists of combining a Finite Volume method for the barotropic Euler equations, for which we only consider a simple Rusanov flux [68] and a semi-Lagrangian method for the Vlasov equation. Two different semi-Lagrangian scheme are used. The first one is a semi-Lagrangian method based on cubic Spline interpolation [21] that we will refer to as the BSPL scheme. The second one is a conservative semi-Lagrangian method known as Positive Flux Conservative [60] that we will refer to as the PFC scheme.

We introduce the computational domain $[x_{\min}, x_{\max}] \times [v_{\min}, v_{\max}]$. The lenght of the space domain is denoted $L = x_{\max} - x_{\min}$. We introduce a space discretization made of N_x cells with constant step $\Delta x = \frac{L}{N_x}$. Similarly the velocity domain is discretized by N_v cells with constant step $\Delta v = \frac{v_{\max}-v_{\min}}{N_v}$. The cells are denoted $[x_{i-1/2}, x_{i+1/2}]$ and $[v_{j+1/2}, v_{j-1/2}]$ with center $x_i = \frac{1}{2}(x_{i+1/2} + x_{i-1/2})$ and $v_j = \frac{1}{2}(v_{j+1/2} + v_{j+1/2})$ respectively.

We first present the two semi-Lagrangian methods used for the Vlasov equation, then we briefly present the Finite Volume scheme used for the Euler system.

4.3.1 The Semi-Lagrangian method based on B-Spline interpolation

This method relies on the nonconservative form of the Vlasov equation (4.18) (and (4.24) for the soft congested system). Assuming that the distribution function is known at a time $t^k = k\Delta t$, the solution at time t^{k+1} is given by the formula (4.19). In this method, the distribution function is approximated at the center of the cells of the computational domain, $f^k_{i,j} = f(t^k,x_i,v_j)$. Hence, it is a pointwise discretization of the distribution function. It is updated at each time step from its value at the foot of the characteristic curve $(X(t^k;t^{k+1},x_i,v_j),V(t^k;t^{k+1},x_i,v_j))$. In general, the foot of the characteristic curve $(X(t^k;t^{k+1},x_i,v_j),V(t^k;t^{k+1},x_i,v_j))$ is not a point on the grid, so it has to be interpolated. In this work, we interpolate the foot of the characteristic using B-Spline interpolation [112]. This method is used for transport equations of the form

$$\partial_t g + A(t,y)\partial_y g = 0.$$

where $(t,y) \mapsto A(t,y)$ is a given advection field. As long as A is smooth enough, the characteristic curves

$$\frac{\mathrm{d}}{\mathrm{d}s}Y(s;t,y) = A(s,Y(s;t,y)), \quad Y(t;t,y) = y,$$

are well defined and the solution writes

$$g(t,y) = g(s,Y(s;t,y)).$$

We denote as$(y_{i+1/2})_{i\in N_y}$ a finite set of mesh points of a given computational domain $[y_{min},y_{max}]$, with constant step $\Delta y = y_{i+1/2} - y_{i-1/2}$, and y_i, the center of the cell $[y_{i-1/2},y_{i+1/2}]$. Assuming that g is known at a time $t^k = k\Delta t$, one has for $g^k(y) := g(t^k,y)$,

$$g^{k+1}(y_i) = g^k(Y(t^k;t^{k+1},y_i)).$$

Since $Y(t^k;t^{k+1},y_i)$ is not necessarily at the center of a cell, we interpolate the value $g^k(Y(t^k;t^{k+1},y_i))$ with a B-Spline. We introduce $g^k_S(y)$ the interpolation function

$$g^k_S(y) = \sum_j \sigma^k_j S^3(y - y_j),$$

with S^3 given by

$$S^3(y) = \frac{1}{6\Delta y}\begin{cases} \left(2 - \dfrac{|y|}{\Delta y}\right)^3, & \text{if } \Delta y \leq |y| \leq 2\Delta y, \\ 4 - 6\left(\dfrac{y}{\Delta y}\right)^2 + 3\left(\dfrac{|y|}{\Delta y}\right)^3, & \text{if } 0 \leq |y| \leq \Delta y, \\ 0 & \text{otherwise.} \end{cases}$$

To compute the coefficients σ^k_j, one has to construct a linear system using the constraints

$$g^k_S(y_i) = g^k(y_i).$$

We refer to [112] for details on the construction of this linear system.

This method has been developed to solve Vlasov-Poisson equations, where the advection field is divergence-free. In our case, the Vlasov equation (4.18) (and (4.24) for the soft congested system) is not divergence-free because of the friction term. To remedy this problem, we introduce an appropriate splitting between the divergence-free part (that is also splitting between the advection in x and in v) and the non divergence-free part. For the original system (4.7), it writes

$$\partial_t f + v\partial_x f = 0, \tag{4.29}$$

$$\partial_t f + \left(\frac{D_\star}{m_\star}u - \partial_x p\right)\partial_v f = 0. \tag{4.30}$$

This is solved with with the BSPL scheme. In each case the foot of the characteristic curves can be computed explicitly

$$X(t^k;t^{k+1},x_i) = x_i - \Delta t v_j,$$
$$V(t^k;t^{k+1},v_j) = v_j - \Delta t\left(\frac{D_\star}{m_\star}u_i^k - \frac{p_{i+1}^k - p_{i-1}^k}{2\Delta x}\right).$$

The non divergence-free part

$$\partial_t f - \partial_v\left(\frac{D_\star}{m_\star}vf\right) = 0$$

is solved using an implicit upwind scheme. For the soft-congested system, the splitting is done by first solving the divergence-free part (4.30) then the non divergence)-free part that writes

$$\partial_t f - \partial_x(\partial_x\pi(\alpha)f) = 0 \tag{4.31}$$

$$\partial_t f - \partial_v\left(\frac{D_\star}{m_\star}vf\right) = 0, \tag{4.32}$$

are both solved with an implicit upwind scheme.

4.3.2 A conservative semi-Lagrangian method

We present here the conservative semi-Lagrangian method used in this Chapter [18, 58, 60]. It is based on the conservative form of the Vlasov equation. For the sake of the presentation, we will explain the method for a general transport equation of the form

$$\partial_t g + \partial_y(A(t,y)g) = 0, \tag{4.33}$$

with a given advection field $(t,y) \mapsto A(t,y)$. We assume that A is smooth enough so that the characteristic curves

$$\frac{\mathrm{d}}{\mathrm{d}s}Y(s;t,y) = A(s,Y(s;t,y)), \quad Y(t;t,y) = y$$

are well defined. Then the solution of (4.33) writes

$$g(t,y) = g(s,Y(s;t,y))J(s;t,y)$$

for any t, s, y with

$$J(s;t,y) = e^{\left(\int_t^s \partial_y A(\sigma,Y(\sigma;t,y))\,\mathrm{d}\sigma\right)}.$$

Then, the solution g verifies the conservation property

$$\int_a^b g(t,y)\,\mathrm{d}y = \int_{Y(s;t,a)}^{Y(s;t,b)} g(s,y)\,\mathrm{d}y. \tag{4.34}$$

We denote as $(y_{i+1/2})_{i\in N_y}$ a finite set of mesh points of a given computational domain $[y_{\min},y_{\max}]$, with constant step $\Delta y = y_{i+1/2} - y_{i-1/2}$, and y_i, the center of the cell $[y_{i-1/2},y_{i+1/2}]$, and assuming that g is known at a time $t^k = k\Delta t$, the formula (4.34) writes

$$\int_{y_{i-1/2}}^{y_{i+1/2}} g(t^{k+1},y)\,\mathrm{d}y = \int_{Y(t^k;t^{k+1},y_{i-1/2})}^{Y(t^k;t^{k+1},y_{i+1/2})} g(t^k,y)\,\mathrm{d}y.$$

We obtain then the formulation

$$g_i^{k+1} = g_i^k - \frac{\Delta t}{\Delta y}\left(G_{i+1/2}^k - G_{i-1/2}^k\right)$$

with

$$g_i^k = \frac{1}{\Delta y}\int_{y_{i-1/2}}^{y_{i+1/2}} g(t^k,y)\,\mathrm{d}y$$

and the flux $G_{i+1/2}^k$ is

$$G_{i+1/2}^k = \frac{1}{\Delta t}\int_{Y(t^k;t^{k+1},y_{i+1/2})}^{y_{i+1/2}} g(t^k,y)\,\mathrm{d}y.$$

The idea of the PFC scheme [60] is to compute the numerical flux by introducing a primitive function $\mathcal{G}$ of g:

$$G_{i+1/2}^k = \frac{1}{\Delta t}\int_{Y(t^k;t^{k+1},y_{i+1/2})}^{y_{i+1/2}} g(t^k,y)\,\mathrm{d}y = \frac{1}{\Delta t}\left(\mathcal{G}^k(y_{i+1/2}) - \mathcal{G}^k(Y(t^k;t^{n+1},y_{i+1/2}))\right).$$

The primitive function $\mathcal{G}^k$ verifies $\mathcal{G}^k(y_{i+1/2}) - \mathcal{G}^n(y_{i-1/2}) = \Delta y g_i^n$, so that

$$\mathcal{G}^k(y_{i+1/2}) = \sum_{\mu=0}^{i} g_\mu^k.$$

Then, we need to introduce an interpolation procedure to compute $\mathcal{G}^k(Y(t^k;t^{k+1},y_{i+1/2}))$. Following [58], a third order reconstruction of the primitive function $\mathcal{G}$ leads to the following formula for the numerical flux, when A is positive

$$G_{i+1/2}^k = \frac{\alpha_i^k}{\Delta t}\left[g_i^k + \frac{L_i^+}{6}\left(1-\frac{\alpha_i^k}{\Delta y}\right)\left(2-\frac{\alpha_i^k}{\Delta y}\right)(g_{i+1}^k - g_i^k) + \frac{L_i^-}{6}\left(1-\frac{\alpha_i^k}{\Delta y}\right)\left(1+\frac{\alpha_i^k}{\Delta x}\right)(g_i^k - g_{i-1}^k)\right]$$

where L^+ and L^- are the limiters introduced by Umeda in [114]. These limiters preserve the positivity and the local extrema of the numerical solutions. The coefficient α_i is defined by

$$\alpha_i^k = y_{i+1/2} - Y(t^k;t^{k+1},y_{i+1/2}).$$

In our case, the scheme can be simplified by using a splitting procedure. For the original system (4.7), we first solve

$$\partial_t f + \partial_x(vf) = 0$$

then

$$\partial_t f + \partial_v\left((-\partial_x p(\varrho) + \frac{D_\star}{m_\star}(u-v))f\right) = 0.$$

In each case, the foot of the characteristic curves can be computed explicitly. One has

$$X(t^k;t^{k+1},x_{i+1/2}) = x_{i+1/2} - \Delta t^k v_j$$

$$V(t^k;t^{k+1},v_{j+1/2}) = v_{j+1/2}e^{\frac{D_\star}{m_\star}\Delta t^k} + u_i^k\left(1 - e^{\frac{D_\star}{m_\star}\Delta t^k}\right) - \frac{p_{i+1}^k - p_{i-1}^k}{2\Delta y}\Delta t.$$

For the soft congested system (4.8), since in this case, the charateristic curve in x can no longer be computed explicitely, we prefer to do another splitting and solve

$$\partial_t f + \partial_x(vf) = 0,$$

with the PFC scheme, then

$$\partial_t f - \partial_x(\partial_x\pi(\alpha)f) = 0,$$

with an implicit upwind scheme, then

$$\partial_t f + \partial_v\left((-\partial_x p(\varrho) + \frac{D_\star}{m_\star}(u-v))f\right) = 0,$$

with the PFC scheme.

4.3.3 Finite Volume scheme

We present here the Finite Volume scheme used in this Chapter [68]. The starting point of the method is the fluid part written in conservation form

$$\partial_t\mathbf{U} + \partial_x\mathbf{F}(\mathbf{U},f) = 0.$$

Assuming that the solution $\mathbf{U}$ is known at a time $t^k = k\Delta t$, the Finite Volume scheme write

$$\mathbf{U}_i^{k+1} = \mathbf{U}_i^k - \frac{\Delta t^k}{\Delta x}(\mathbf{F}_{i+1/2} - \mathbf{F}_{i-1/2}).$$

where

$$\mathbf{U}_i^k := \frac{1}{\Delta x}\int_{x_{i-1/2}}^{x_{i+1/2}} \mathbf{U}(t^k,x)\,\mathrm{d}x.$$

It remains to give a definition for the numerical flux $\mathbf{F}_{i+1/2}$. In this work, we restrict ourselves to a Rusanov flux:

$$\mathbf{F}_{i+1/2} = \frac{\mathbf{F}(\mathbf{U}_{i+1}^k, f_{i+1,j}^k) + \mathbf{F}(\mathbf{U}_i^k, f_{i,j}^k)}{2} - \max(\lambda_\pm(\mathbf{U}_{i+1}^k, f_{i+1,j}^k), \lambda_\pm(\mathbf{U}_i^k, f_{i,j}^k))\frac{\mathbf{U}_{i+1}^k - \mathbf{U}_i^k}{2}. \tag{4.35}$$

4.3.4 Time splitting

Here, we describe the complete algorithm and the time splitting. We first present the splitting for the BPSL scheme, then for the PFC scheme. We assume that the discrete solution $(\mathbf{U}_i^k, f_{i,j}^k)$ at a time t^k is known. To update theses quantities, we proceed as follows

B-Spline semi-Lagrangian method.

- **Transport of the particles with velocity v in the direction x.**

  We compute $f^*_{i,j}$ by solving the free transport $\partial_t f + v\partial_x f = 0$ with a BSPL scheme for a timestep $\Delta t^k/2$ with the initial condition $f^k_{i,j}$.

- **Correction of the particle distribution.**

  In this step, we take into account the close packing limit.

  – *Soft Congestion case.* We compute $f^{**}_{i,j}$ by solving the equation
  $$\partial_t f - \partial_x(\partial_x \pi_\varepsilon f) = 0$$
  with a timestep $\Delta t^k/2$ and the initial condition $f^*_{i,j}$ with an implicit upwind scheme.

  – *Original system.* We compute $f^{**}_{i,j}$ by applying the Random Repair Algorithm described in Section 4.3.4.1.

- **Transport of the divergence free part of the force field in the direction v.**

  We compute $f^{***}_{i,j}$ by solving $\partial_t f + (D_\star u - \partial_x p(\varrho))\partial_v f = 0$ with the BSPL scheme during a timestep Δt^k with initial condition $f^{**}_{i,j}$.

- **Treatment of the drift term.**

  We compute $f^{****}_{i,j}$ by solving the drift equation $\partial_t f - \partial_v(D_\star v f) = 0$ with an implicit upwind scheme.

- **Transport of the fluid.**

  We compute $\mathbf{U}^{k+1}_i$ by solving the fluid equations $\partial_t \mathbf{U} + \partial_x \mathbf{F}(\mathbf{U}, f) = 0$ with a Finite Volume scheme.
  $$\mathbf{U}^{k+1}_i = \mathbf{U}^k_i - \frac{\Delta t^k}{\Delta x}(\mathbf{F}_{i+1/2} - \mathbf{F}_{i-1/2}).$$
  The numerical flux is a Rusanov flux that depends on $\mathbf{U}^k_i$ and $f^{****}_{i,j}$:

$$\mathbf{F}_{i+1/2} = \frac{\mathbf{F}(\mathbf{U}^k_{i+1}, f^{****}_{i+1,j}) + \mathbf{F}(\mathbf{U}^k_i, f^{****}_{i,j})}{2} - \max(\lambda_\pm(\mathbf{U}^k_{i+1}, f^{****}_{i+1,j}), \lambda_\pm(\mathbf{U}^k_i, f^{****}_{i,j}))\frac{\mathbf{U}^k_{i+1} - \mathbf{U}^k_i}{2}.$$

- **Transport of the particles with velocity v the direction x.**

  Finally, we perform the last transport step of the particles. We compute $f^{*****}_{i,j}$ by solving the free transport $\partial_t f + v\partial_x f = 0$ with a BSPL scheme for a timestep $\Delta t^k/2$ with the initial condition $f^{****}_{i,j}$.

- **Correction of the particle distribution.**

  In this step, we take into account the close packing limit.

  – *Soft Congestion case.* We compute $f^{k+1}_{i,j}$ by solving the equation
  $$\partial_t f - \partial_x(\partial_x \pi_\varepsilon f) = 0$$
  with a timestep $\Delta t^k/2$ and the initial condition $f^{*****}_{i,j}$ with an implicit upwind scheme.

  – *Original system.* We compute $f^{k+1}_{i,j}$ by applying the Random Repair Algorithm described in Section 4.3.4.1.

PFC scheme.

- **Transport of the particles in the direction x.** We solve the free transport with time step $\frac{\Delta t}{2}$:
$$f^*_{i,j} = f^k_{i,j} - \frac{\Delta t}{2\Delta x}\left(F^k_{i+1/2,j} - F^k_{i-1/2,j}\right)$$
- **Correction of the particle distribution.**

  In this step, we take into account the close packing limit.
  - *Soft Congestion case.* We compute $f^{**}_{i,j}$ by solving the equation
  $$\partial_t f - \partial_x(\partial_x \pi_\varepsilon f) = 0$$
  with a timestep $\Delta t^k/2$ and the initial condition $f^*_{i,j}$ with an implicit upwind scheme.
  - *Original system.* We compute $f^{**}_{i,j}$ by applying the Random Repair Algorithm described in Section 4.3.4.1.
- **Transport of the fluid.**

  We compute $\mathbf{U}^{k+1}$ by solving the fluid equations $\partial_t \mathbf{U} + \partial_x \mathbf{F}(\mathbf{U},f) = 0$ with a Finite Volume scheme with a Rusanov flux (4.35)
$$\mathbf{U}^{k+1}_i = \mathbf{U}^k_i - \frac{\Delta t^k}{\Delta x}(\mathbf{F}_{i+1/2} - \mathbf{F}_{i-1/2})$$
  using the value $f^{**}_{i,j}$.
- **Transport in the direction v.** We update the particle distribution function in the direction v with a time step Δt
$$f^{***}_{i,j} = f^{**}_{i,j} - \frac{\Delta t^k}{\Delta v}\left(F^*_{i,j+1/2} - F^*_{i,j-1/2}\right).$$
- **Transport in the direction x** We solve the free transport with a time step $\frac{\Delta t}{2}$:
$$f^{****}_{i,j} = f^{**}_{i,j} - \frac{\Delta t^k}{2\Delta x}\left(F^{**}_{i+1/2,j} - F^{**}_{i-1/2,j}\right).$$
- **Correction of the particle distribution.**

  In this step, we take into account the close packing limit.
  - *Soft Congestion case.* We compute $f^{k+1}_{i,j}$ by solving the equation
  $$\partial_t f - \partial_x(\partial_x \pi_\varepsilon f) = 0$$
  with a timestep $\Delta t^k/2$ and the initial condition $f^{****}_{i,j}$ with an implicit upwind scheme.
  - *Original system.* We compute $f^{k+1}_{i,j}$ by applying the Random Repair Algorithm described in Section 4.3.4.1.

Remark 4.3.1 (About the timestepping). *A complete stability analysis of the proposed scheme is beyond the scope of this work. We nevertheless make some remarks about the timestepping.*

- *First, in the case of the BSPL scheme, note that the solving of the kinetic part does not impose any constraint on the time stepping. Indeed, the BSPL is free of any CFL condition because we use it for the case where the advection is constant. If the advection is not constant, we would need to impose a CFL such that characterestics curves do no cross. Furthermore, the resolution of the drift part of the drag force is done implicitly. For the PFC method, one needs to impose a CFL condition such that the characteristics do not cross each other [21, 37]. This leads to the following restriction*

$$\max_j(|v_j|)\Delta t_1^k \leq \Delta x$$

$$\Delta t_2^k \leq \frac{\Delta v}{\frac{D_\star}{m_\star}\left(\max_j(|v_j|) + \max_i\left(|u_i^k|\right)\right) + \max_i\left(|\partial_x p_i^k|\right)}$$

- *For the resolution of the fluid part, an explicit Finite Volume Scheme is used. A formal analysis of the Jacobian of the fluid part reveals that the eigenvalues write*

$$\lambda_\pm = u \pm \sqrt{\frac{p'(\varrho)}{\alpha}}.$$

For stability reasons, the timestep should verify

$$\Delta t_3^k \leq \frac{\Delta x}{\max_i(\lambda_\pm(\mathbf{U}_i^k, f_{i,j}^k))}.$$

- *In practice, we impose*

$$\Delta t_{\mathrm{BSPL}}^k = \mathrm{CFL}\,\Delta t_3^k$$

for the B-Spline semi-Lagrangian scheme, and

$$\Delta t_{\mathrm{PFC}}^k = \mathrm{CFL}\min(\Delta t_1^k, \Delta t_2^k, \Delta t_3^k)$$

for the PFC scheme. In both cases, we take CFL $= 0.5$. *With this choice of timestep, we did not observe any numerical instability for the system (4.7). For the soft congestion case, we observed instabilities in the region where α is close to $\alpha_\star$. This probably could be improved with implicit techniques for the fluid phase.*

Remark 4.3.2 (About the Finite Volume scheme.). *The weakest part of the scheme we proposed is most certainly the Finite Volume part. In this study, the main focus is on the discretization of the dispersed phase, this is why we restricted ourselves to the simplest Finite Volume scheme for the fluid phase. An improvement would be to use for instance a Lagrange + Remap scheme. See also [11, 18, 91].*

4.3.4.1 Correction procedure

The spirit of the correction procedure is to compare α_i^k with $\alpha_\star$ and check if $\alpha_i^k \geq \alpha_\star$. In this work, $\alpha_\star$ is the same in all the cells, but one could easily extend this work to a non-homogenous packing limit. Assume that $\alpha_i^k < \alpha_\star$, this means that the particle volume fraction in the cell i, $m_\star \Delta v \sum_j f_{i,j}^k$ is too big, and one has to redistribute the mass in the cells around the cell i. Taking inspiration from [94], we propose to redistribute the mass with a stochastic algorithm. Starting from the saturated cell, we initiate a random walk. When the walk encounters a cell which is not saturated, it get rids of as much mass as it can. Then the random walk continues, until the exceeding mass has been completely redistributed. The main difficulty for adapting the algorithm from [94] is that we need to modify the distribution function $f_{i,j}^k$ itself for all the velocity cells j. The algorithm reads

Random Repair algorithm. Given a discretized distribution function $f_{i,j}^k$, such that there is a cell in the space domain i such that $\alpha_i^k < \alpha_\star$:

1. We start from a cell i where $\alpha_i^k < \alpha_\star$.
2. We compute the exceeding mass Δm. Then we compute
$$f_{i,j}^{k+1} = (1 - \alpha_\star) \frac{f_{i,j}^k}{m_\star \Delta v \sum_l f_{i,l}^k}, \text{ for all } j.$$
Then $\alpha_i^{k+1} = \alpha_\star$.
3. Start a random walk (S_m), when the walk meets a cell S_m such that $\alpha_{S_m}^k > \alpha_\star$, get rid of as much mass as possible
$$f_{S_m,j}^{k+1} = f_{S_m,j}^k + \frac{\Delta m}{m_\star \Delta v \sum_l f_{i,l}^k} f_{i,j}^k, \text{ for all } j.$$

When all the exceeding mass has been distributed, the volume fraction α_i^{k+1} is admissible.

4.4 Numerical results

In this section, we present several numerical results to validate each component of our method. The first test examines linear damping [28, 62] and focuses on verifying the coupling between the volume fraction in the fluid phase and the pressure gradient in the dispersed phase. Next, we assess how the close packing limit is handled, starting with the simplest case where there is no gas. Finally, we present two tests that integrate all these aspects. We conclude with a last test in 2D-2V

4.4.1 Linear Damping in the dragless case

In this test, we consider the dragless case $D_\star = 0$. The initial data is

$$\begin{cases} \varrho(t=0,x) = \varrho_0 \\ u(t=0,x) = 0 \\ f(t=0,x,v) = \frac{1}{\sqrt{2\pi}} e^{-v^2/2} \left(1 + \varepsilon \cos(kx)\right), \end{cases}$$

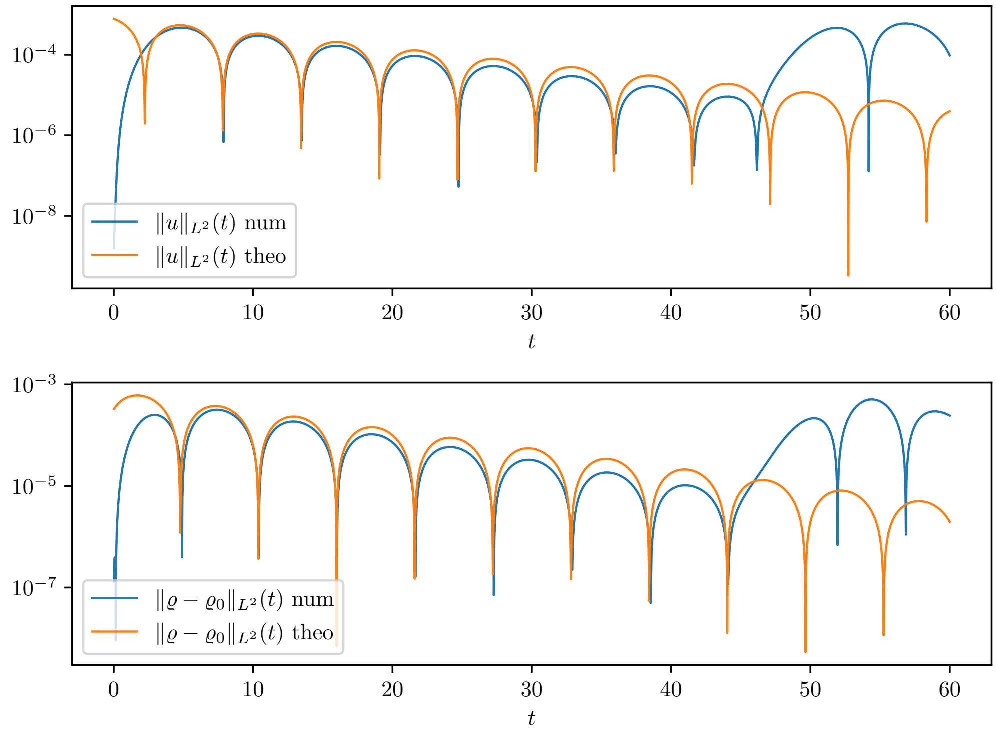

(a) The evolution of $\|\varrho - \varrho\|_{L^2}$ and $\|u\|_{L^2}$ with respect to t with the PFC scheme. Here, $N_x = 128$, $N_v = 32$. In blue the numerical result and in orange the solution predicted by the linear theory.

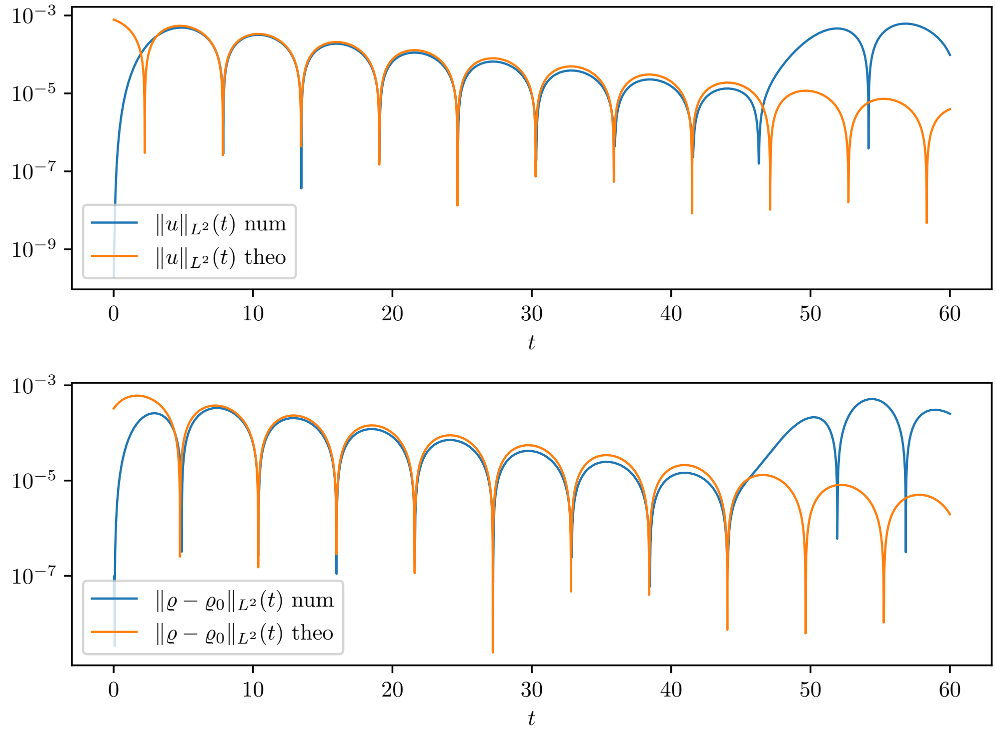

(b) The evolution of $\|\varrho - \varrho\|_{L^2}$ and $\|u\|_{L^2}$ with respect to t with the PFC scheme. Here, $N_x = 256$, $N_v = 32$. In blue the numerical result and in orange the solution predicted by the linear theory.

Fig. 4.1

where $\varepsilon = 0.001$, $k = 0.5$ and $\varrho_0 = 1$. We take $m_\star = 0.2$ and $N_v = 32$. The computational domain is $[0,4\pi]\times[-4,4]$. It has been proven in [28,62] that in this case, one expects a damping of $\|\varrho-\varrho\|_{L^2}$ and $\|u\|_{L^2}$ to 0, and, with the given initial condition, the damping is expected to be like $\cos(\Re e(\omega)t)e^{\Im m(\omega)t}$ where

$$\omega \approx 0.56 - i0.086.$$

In Figure 4.1, one can see the evolution of the L^2 norm of $\varrho-\varrho_0$ and u for the PFC scheme with $N_x = 128$ and $N_x = 256$. We observe that the decay of these quantities follows very well the linear theory developed in [28]. The observed recurrence time $T_R = 51.84$ is also well calculated as the theoretical recurrence time is $T_R = 2\pi/(k\Delta v)$. We do not present result with the BSPL scheme since this problem has been studied with this scheme in [28]. The model without packing (4.7) and the model with soft packing (4.8) give the same results since in this case, we are far from the packing limit, so we present only the results for the model without packing (4.7).

4.4.2 Pure transport of particles without coupling

In this test, we only consider the pure transport of the particles, so that the equation discretized in this subsection reads

$$\begin{cases} \partial_t f + v\partial_x f = 0, \\ f(t=0,x,v) = f_0(x,v). \end{cases}$$

We consider the initial condition

$$f_0(x,v) = \frac{1}{2\pi\sqrt{\sigma_x\sigma_v}}e^{-\frac{(v-2)^2}{2\sigma_v^2}}e^{\frac{(x-2)^2}{2\sigma_x^2}}\mathbf{1}_{v>0}(v) + \frac{1}{2\pi\sqrt{\sigma_x\sigma_v}}e^{-\frac{(v+2)^2}{2\sigma_v^2}}e^{\frac{(x-4)^2}{2\sigma_x^2}}\mathbf{1}_{v<0}(v).$$

The computational domain is $[0,6]\times[-6,6]$. The coefficients are $\sigma_x = 0.09$, $\sigma_v = 0.2$ and $m_\star = 0.2$. We take $N_x = N_v = 256$. In corresponds to the situation where there is two clouds of particles going into each other. We are interested in the behavior of the Random Repair Algorithm. The results can be found in Figure 4.2.

Initially, the two clouds are spread on opposite sides of the computational domain. As they converge at the center, particle density increases, but the Random Repair Algorithm successfully keeps it below the close-packing threshold. Eventually, some particles pass through the congested zone, and the density of the particles decreases.

4.4.3 Collision of two pack of particles

In this test, we consider the case with a gas initially at rest, with two clouds of particles going into the middle of the domain. The initial condition for the gas is

$$(\varrho_0,u_0,p_0)(x) = (1,0,1),$$

with $\gamma = 1.4$. The initial condition for the particles is

$$f_0(x,v) = \frac{1}{\sqrt{2\pi\sigma_v}}e^{-\frac{(v-6)^2}{2\sigma_v^2}}\frac{1}{\sqrt{2\pi\sigma_x}}e^{\frac{(x-2.6)^2}{2\sigma_x^2}}\mathbf{1}_{v>0}(v) + \frac{1}{\sqrt{2\pi\sigma_v}}e^{-\frac{(v+6)^2}{2\sigma_v^2}}\frac{1}{\sqrt{2\pi\sigma_x}}e^{\frac{(x-3.4)^2}{2\sigma_x^2}}\mathbf{1}_{v<0}(v).$$

with $\sigma_x = \sigma_v = 0.1$. The drag coefficient is $D_\star = 1$, and $m_\star = 0.32$, $N_x = N_v = 200$. Moreover, $\alpha_\star = 0.4$. The computational domain is $[0,6]\times[-10,10]$ with periodic boundary conditions on both dimensions, and discretization parameters $N_x = N_v = 200$.

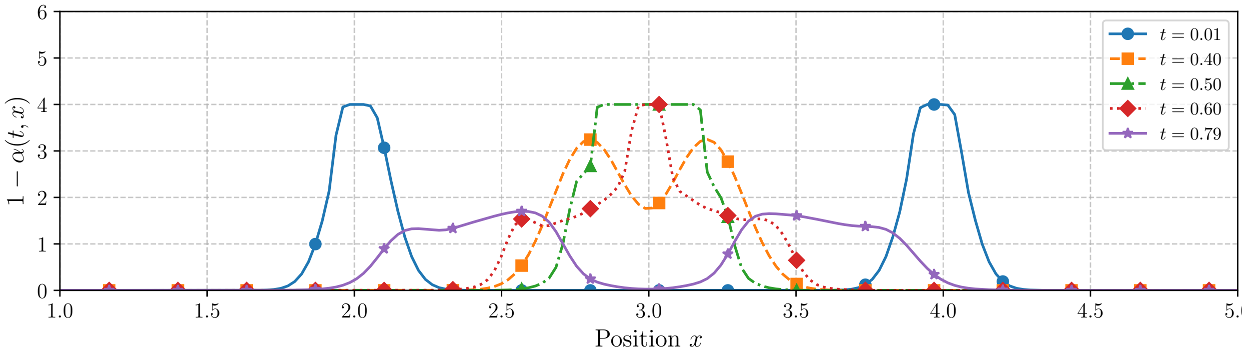

Fig. 4.2: The particle volume fraction $x \mapsto 1 - \alpha(t,x)$ with the PFC scheme for different times

The results for the PFC scheme are visible in Figure 4.3 with the system (4.7) and in Figure 4.4 with the system (4.8). The results for the BSPL scheme are visible in Figure 4.6 for the system (4.7)and in Figure 4.7 for the system (4.8).

Initially, the two particle clouds move toward each other, the particle volume fraction increases until reaching the close-packing limit, $\alpha_\star$. This collision compresses the gas, causing a sharp rise in fluid density in the congested zone. Over time, some particles begin to penetrate this dense layer, reducing both the particle concentration and gas density as the congestion dissipates.

The results from both PFC and BSPL schemes, for both systems (4.7) and (4.8), are nearly identical.

Finally, we present convergence tests using the BSPL scheme, displaying the volume fraction α at $t = 0.1$ for various mesh sizes. Figure 4.8a shows results with the original system (4.1), while Figure 4.8b uses the soft congested system (4.8). Initially, the results indicate convergence as the mesh is refined. However, with very fine meshes, we observe instabilities, suggesting potential non-convergence of the method.

4.4.4 Shock wave passing through a layer of particles

In this test, we examine the interaction between a shock wave and a stationary particle cloud. The gas is initialized with a shock front, with conditions:

$$(\varrho_0,u_0,p_0)(x) = \begin{cases} (0.54, 1.54, 1.54^\gamma) & \text{for } x < 0.2 \\ (1,0,1) & \text{for } x > 0.2. \end{cases}$$

where $\gamma = 1.4$. Immediately after the shock front, there is a cloud of particles at equilibrium, with an initial distribution function given by

$$f_0(x,v) = \frac{1}{\sqrt{2\pi\sigma_x}} e^{-\frac{(x-3)^2}{\sigma_x}} \frac{1}{\sqrt{2\pi\sigma_v}} e^{-\frac{v^2}{\sigma_v}},$$

where $\sigma_x = \sigma_v = 0.1$. The computational domain is $[0,6] \times [-10,10]$. Other parameters include a drag coefficient $D_\star = 1$, $m_\star = 0.32$, $\alpha_\star = 0.4$, and discretization parameters $N_x = N_v = 200$. The results for the PFC scheme are shown in Figures 4.9 for system (4.7) and in Figures 4.10

for system (4.8). We also display the distribution function in Figure 4.11. Similarly, results for the BSPL scheme appear in Figures 4.12 for system (4.7) and Figures 4.13 for system (4.8).

Initially, we observe that the shock wave compresses and pushes the particle cloud forward. This interaction causes a noticeable increase in the gas density on the left side of the particle cloud, as particles concentrate and reach the close-packing limit. At $t = 0.38$, the fluid volume fraction reaches the close-packing limit $\alpha_\star$, marking the peak compression phase in the congested region. Due to drag effects and the pressure of the gas, the gas shock transfers momentum to the particles, accelerating them in the shock's direction. This momentum transfer results in particle movement and spreading of the initial particle distribution as the shock front propagates. As particles disperse following the shock passage, the gas density and particle volume fraction start to decline, gradually returning to equilibrium. The density profile residual perturbations as the particles and gas adjust post-shock.

While the PFC scheme performs well with minimal oscillations, the BSPL scheme encounters difficulties in this test, showing significant spurious oscillations in the results.

4.4.5 Shock tube in 2D-2V.

In this section, we present a 2D-2V test using the BSPL scheme with linear splines. The additional dimensions are handled via directional splitting, and we use only uniform meshes. This test models a shock tube, with initial gas conditions:

$$(\varrho_0, \boldsymbol{u}_0, p_0)(x, y) = \begin{cases} (10, (0,0), 10^\gamma) & \text{for } x < 0.2, \\ (0.125, (0,0), 0.125^\gamma) & \text{for } x > 0.2, \end{cases}$$

where $\gamma = 1.4$. Immediately behind the shock front, there is a stationary particle cloud in equilibrium, with an initial distribution function:

$$f_0(x, y, v_x, v_y) = \frac{1}{\sqrt{2\pi\sigma_x}} e^{-\frac{(x-0.5)^2}{\sigma_x}} \frac{1}{\sqrt{2\pi\sigma_y}} e^{-\frac{(y-0.5)^2}{\sigma_y}} \frac{1}{\sqrt{2\pi\sigma_v}} e^{-\frac{v_x^2}{\sigma_v}} \frac{1}{\sqrt{2\pi\sigma_v}} e^{-\frac{v_y^2}{\sigma_v}},$$

where $\sigma_x = \sigma_y = \sigma_v = 0.1$. The computational domain is $[0, 1]^2 \times [-6, 6]^2$. The simulation parameters are $D_\star = 0, m_\star = 0.0375$, and discretization parameters are $N_x = N_y = N_{v_x} = N_{v_y} = 64$.

In Figure 4.14, we present a cross-section of the solution at$y = 0.5$. Figures 4.15, 4.16, and 4.17 display the complete solution across the 2D spatial domain. In Figure 4.15, the red cells indicate regions where the volume fraction reaches the close-packing limit. Due to the inherent randomness of the algorithm, we notice a loss of symmetry along the $y = 0.5$ axis. Nevertheless, the numerical behavior remains consistent with that observed in the 1D case.

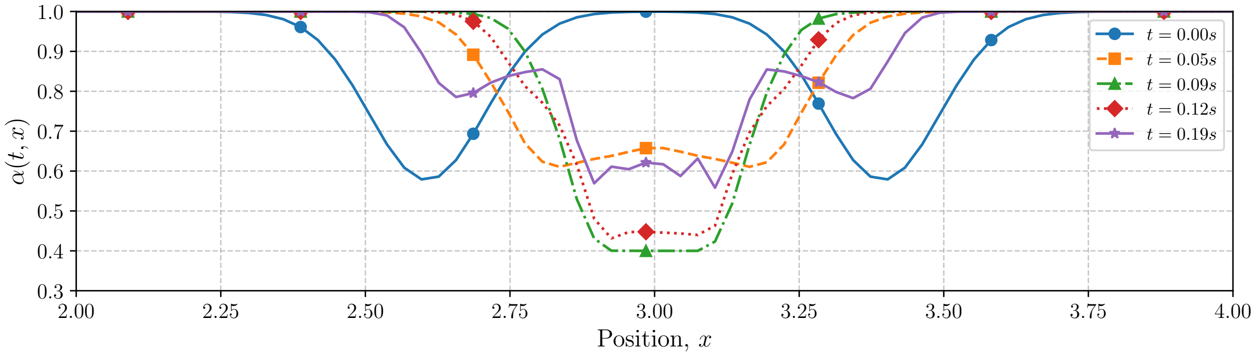

(a) The fluid volume fraction $x \mapsto \alpha(t, x)$ with the PFC scheme at different times $t = 0$, $t = 0.05$, $t = 0.09$, $t = 0.12$ and $t = 0.19$.

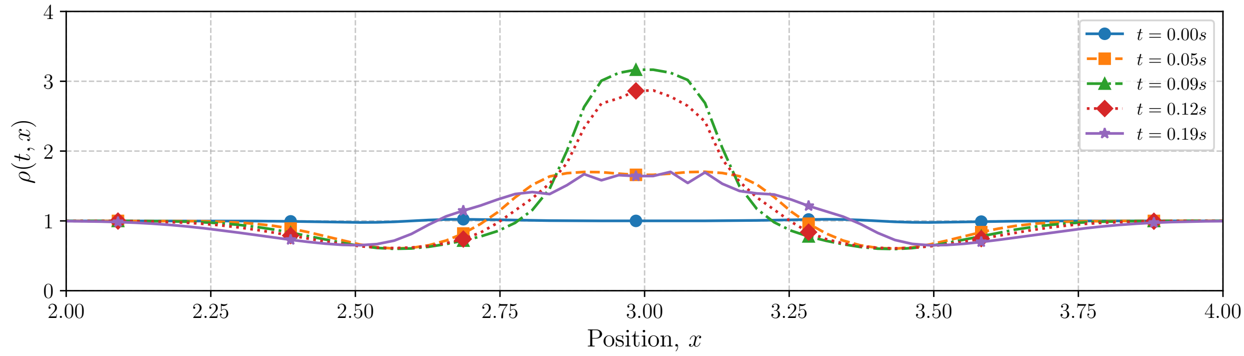

(b) The fluid density $x \mapsto \varrho(t, x)$ with the PFC scheme at different times $t = 0$, $t = 0.05$, $t = 0.09$, $t = 0.12$ and $t = 0.19$.

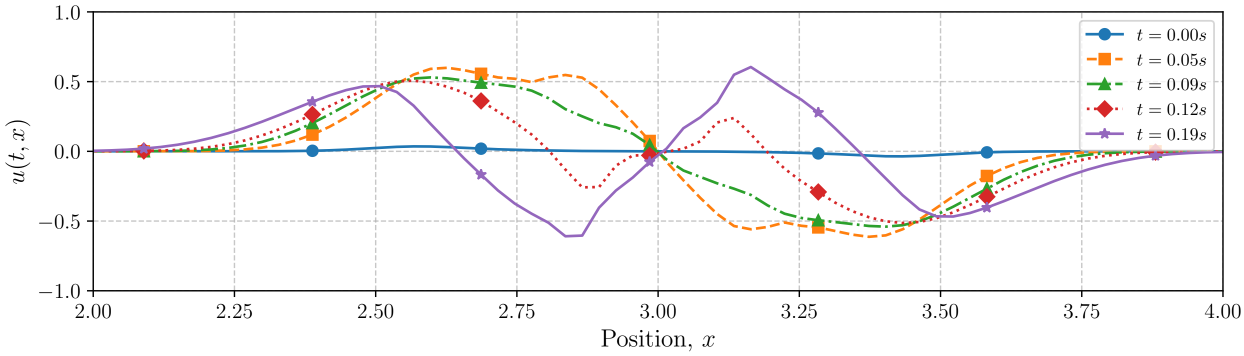

(c) The fluid velocity $x \mapsto u(t, x)$ with the PFC scheme at different times $t = 0$, $t = 0.05$, $t = 0.09$, $t = 0.12$ and $t = 0.19$.

Fig. 4.3: Collision with the original model (4.7) with the PFC scheme.

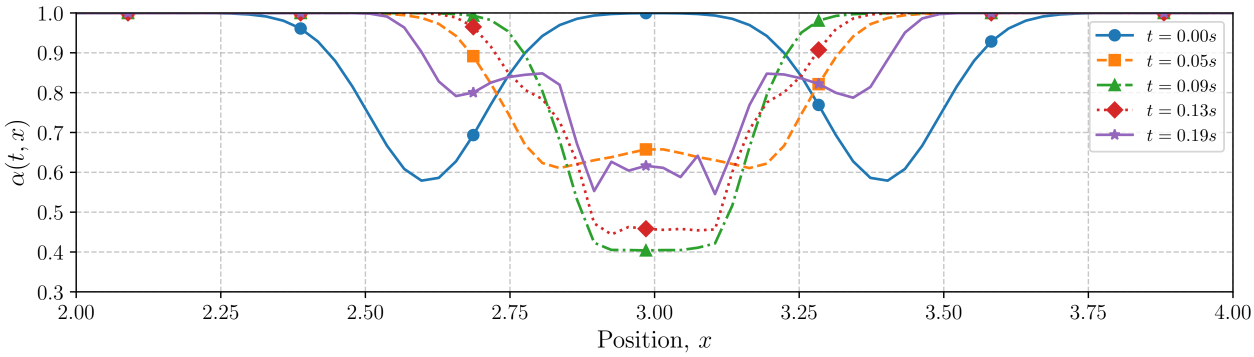

(a) The fluid volume fraction $x \mapsto \alpha(t,x)$ with the PFC scheme at different times $t = 0$, $t = 0.05$, $t = 0.09$, $t = 0.13$ and $t = 0.19$.

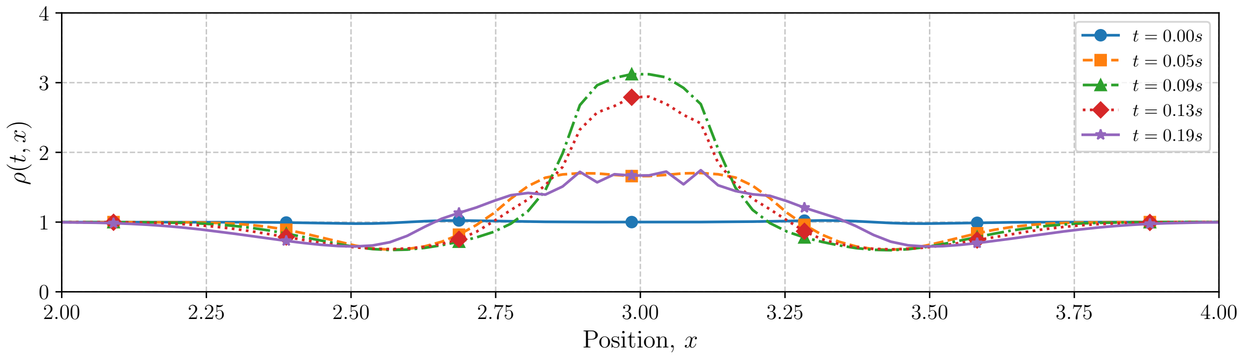

(b) The fluid density $x \mapsto \varrho(t,x)$ with the PFC scheme at different times $t = 0$, $t = 0.05$, $t = 0.09$, $t = 0.13$ and $t = 0.19$.

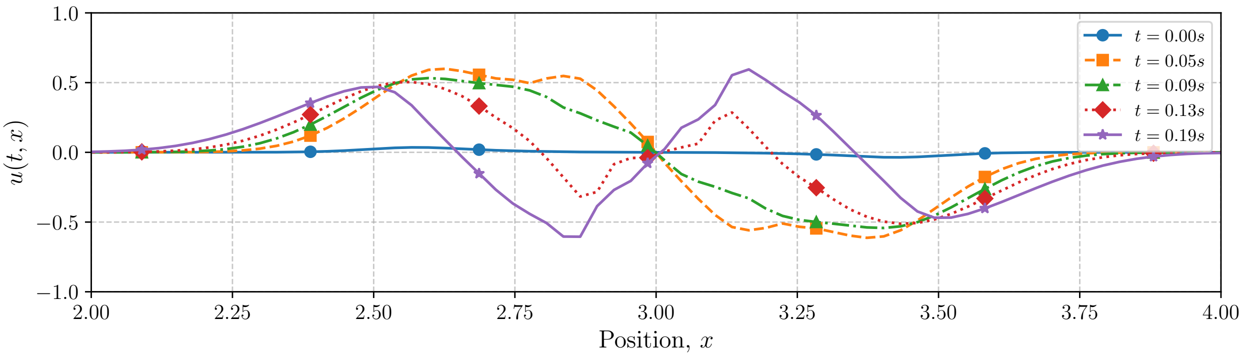

(c) The fluid velocity $x \mapsto u(t,x)$ with the PFC scheme at different times $t = 0$, $t = 0.05$, $t = 0.09$, $t = 0.13$ and $t = 0.19$.

Fig. 4.4: Collision with the soft-congested model (4.8) with $\varepsilon = 10^{-6}$ with the PFC scheme.

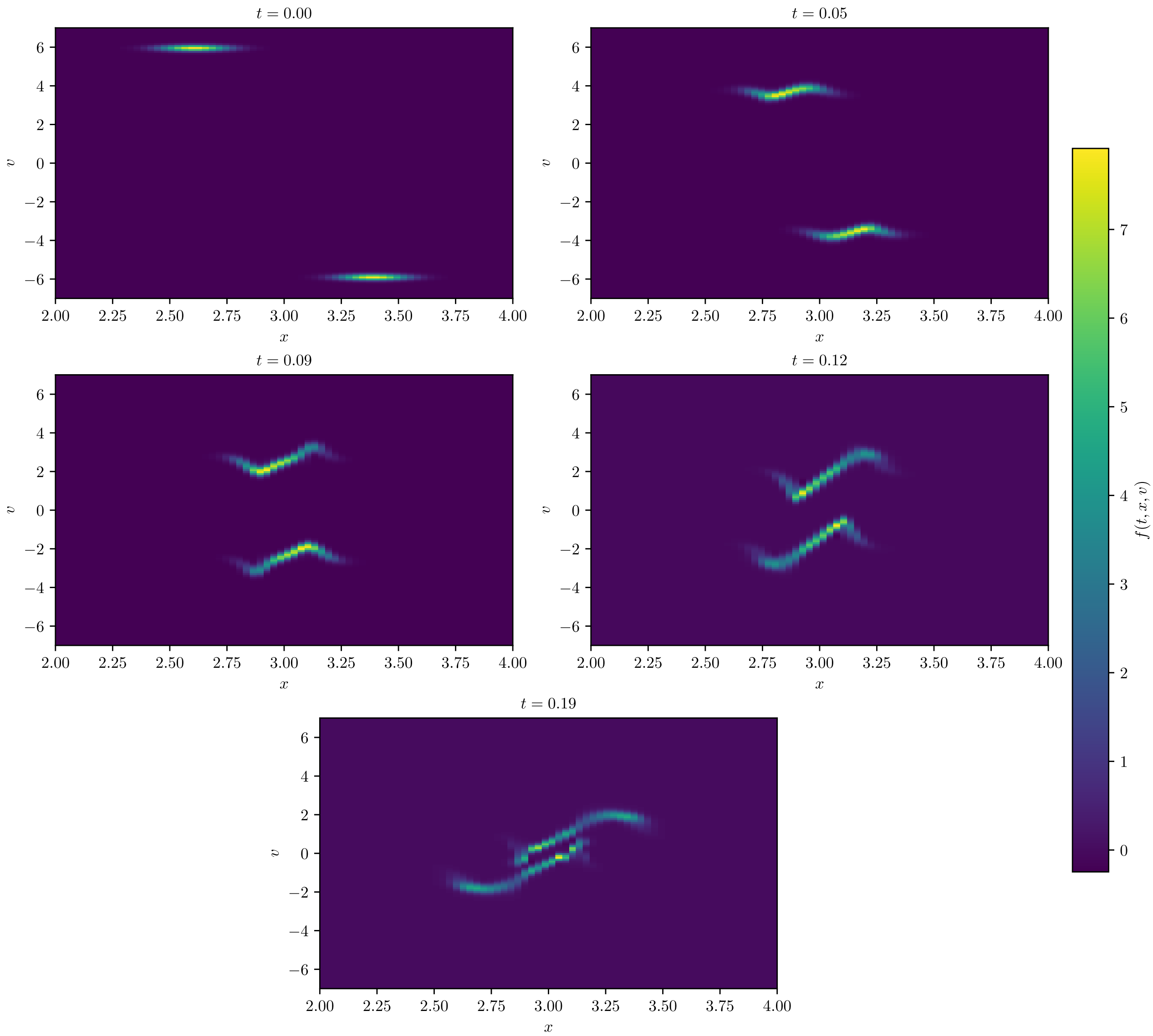

Fig. 4.5: The particle distribution function $f(t,x,v)$ for the soft-congested system (4.8) with the PFC scheme at different times.

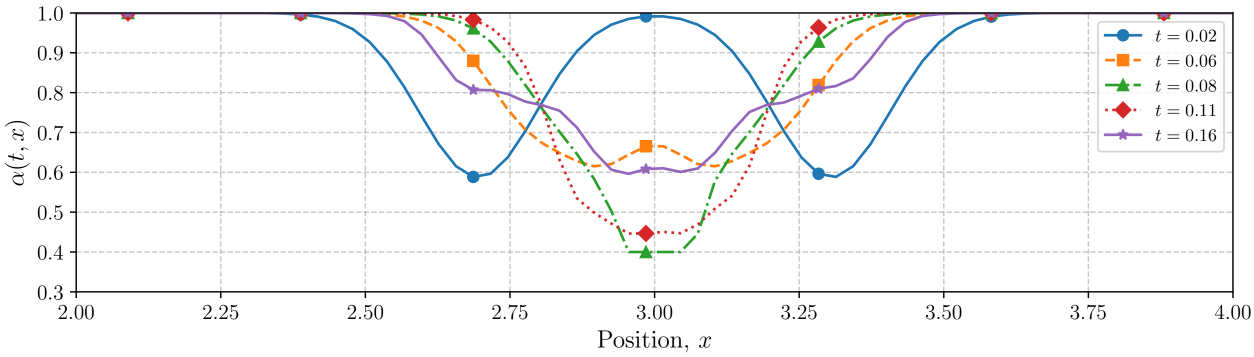

(a) The fluid volume fraction $x \mapsto \alpha(t, x)$ with the BSPL scheme at different times $t = 0$, $t = 0.06$, $t = 0.08$, $t = 0.11$ and $t = 0.16$.

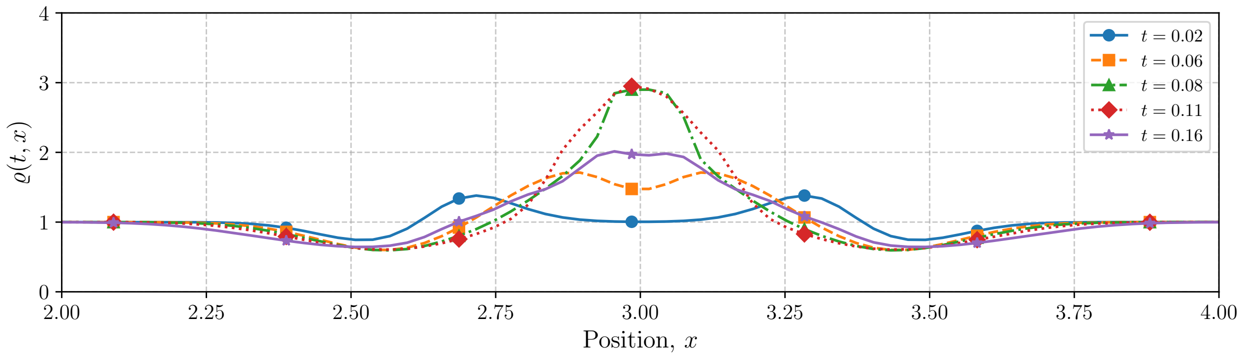

(b) The fluid density $x \mapsto \varrho(t, x)$ with the BSPL scheme at different times $t = 0$, $t = 0.06$, $t = 0.08$, $t = 0.11$ and $t = 0.16$.

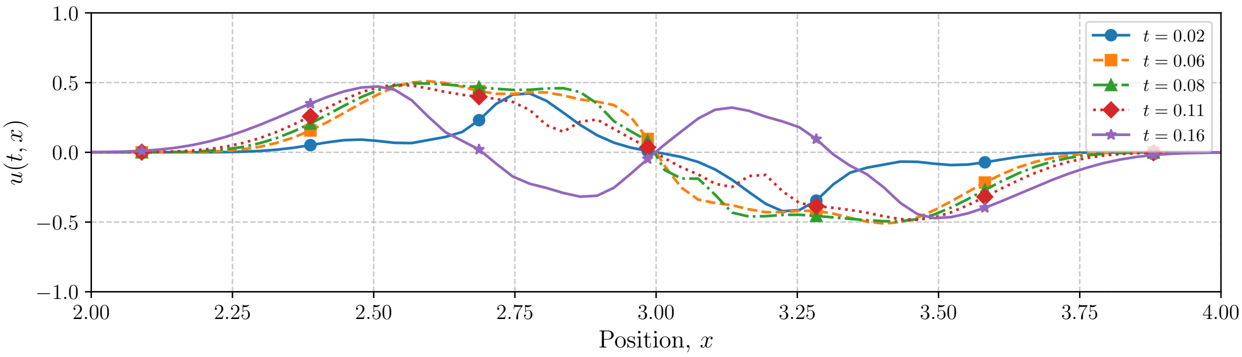

(c) The fluid velocity $x \mapsto u(t, x)$ with the BSPL scheme at different times $t = 0$, $t = 0.06$, $t = 0.08$, $t = 0.11$ and $t = 0.16$.

Fig. 4.6: Collision with the original model (4.7) with the BSPL scheme.

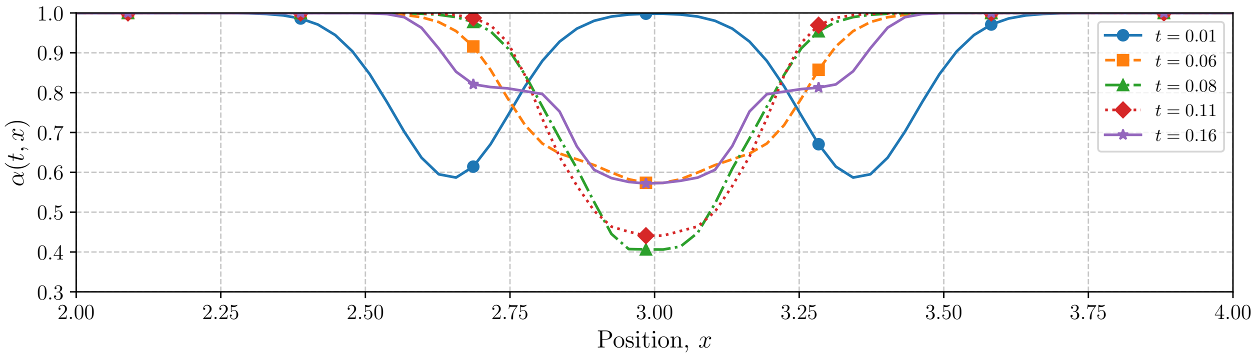

(a) The fluid volume fraction $x \mapsto \alpha(t, x)$ with the BSPL scheme at different times $t = 0$, $t = 0.06$, $t = 0.08$, $t = 0.11$ and $t = 0.16$.

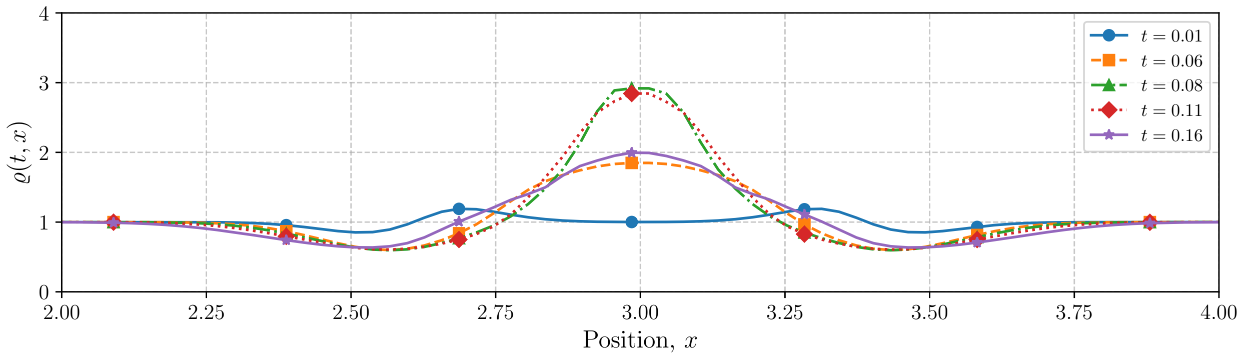

(b) The fluid density $x \mapsto \varrho(t, x)$ with the BSPL scheme at different times $t = 0$, $t = 0.06$, $t = 0.08$, $t = 0.11$ and $t = 0.16$.

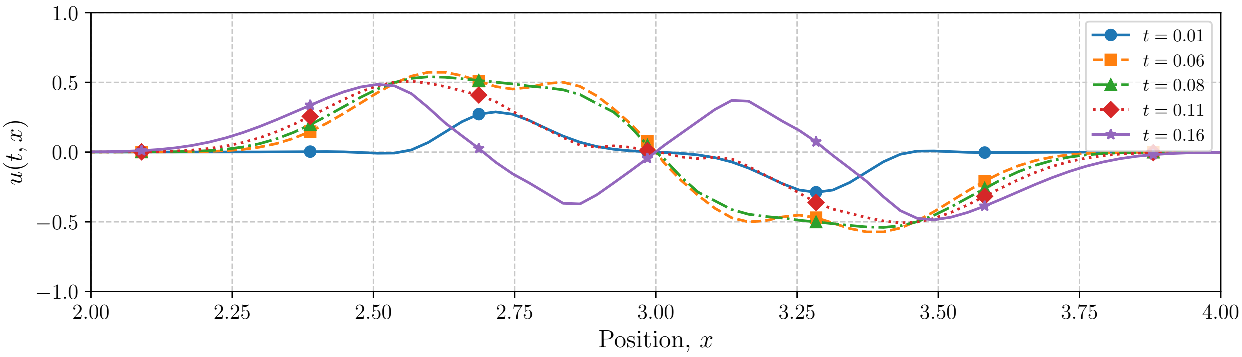

(c) The fluid velocity $x \mapsto u(t, x)$ with the BSPL scheme at different times $t = 0$, $t = 0.06$, $t = 0.08$, $t = 0.11$ and $t = 0.16$.

Fig. 4.7: Shock with the soft-congested model with $\varepsilon = 10^{-6}$ with the BSPL scheme.

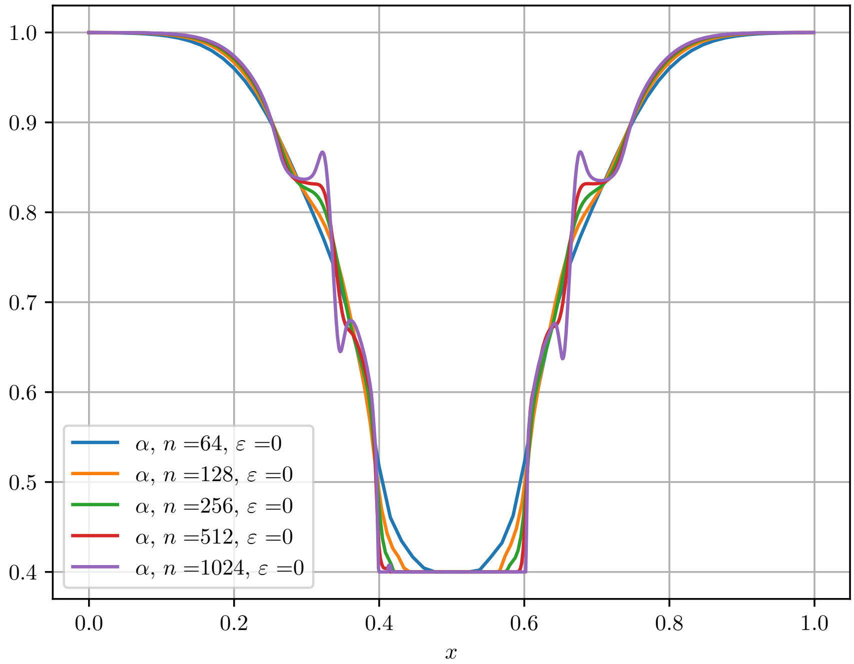

(a) The fluid volume fraction α at $T = 0.1$, with the system (4.1). The integer n denotes the number of cell in the spatial domain.

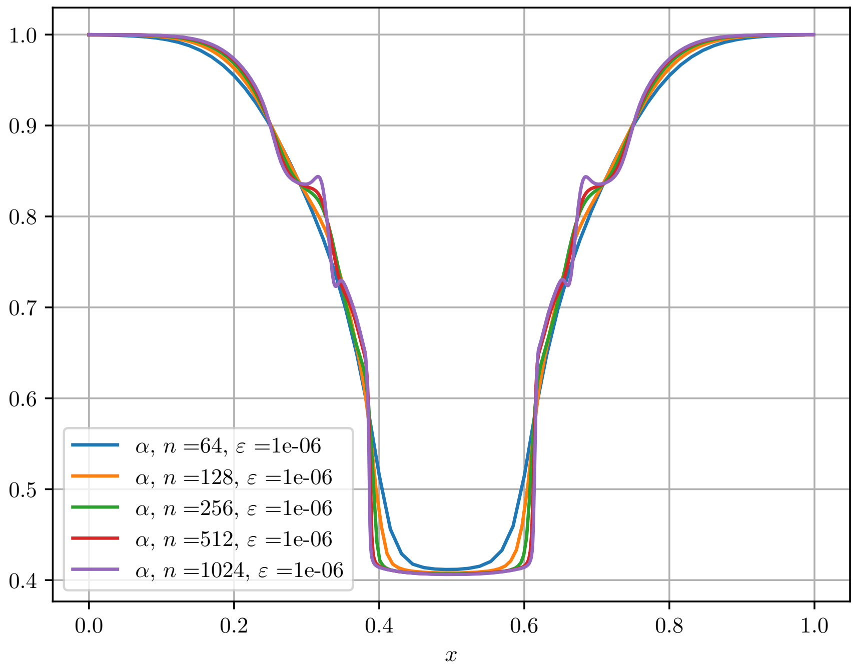

(b) The fluid volume fraction α at $T = 0.1$, with the soft congested system. $\varepsilon = 10^{-6}$. The integer n denotes the number of cell in the spatial domain.

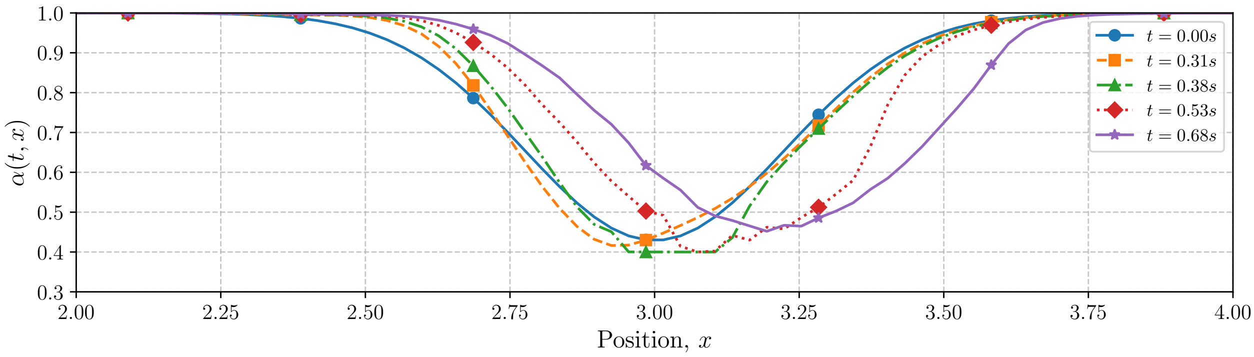

(a) The fluid volume fraction $x \mapsto \alpha(t,x)$ with the PFC scheme at different times $t = 0$, $t = 0.31$, $t = 0.38$, $t = 0.53$ and $t = 0.68$.

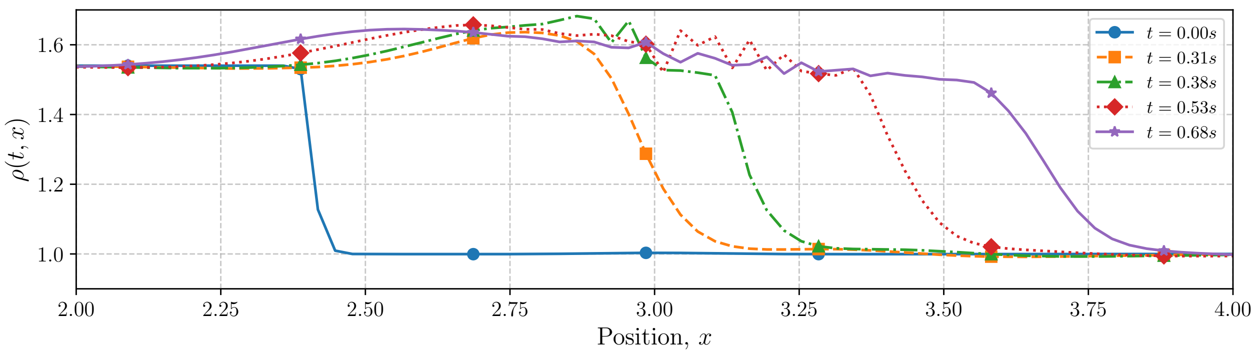

(b) The fluid density $x \mapsto \varrho(t,x)$ with the PFC scheme at different times $t = 0$, $t = 0.31$, $t = 0.38$, $t = 0.53$ and $t = 0.68$.

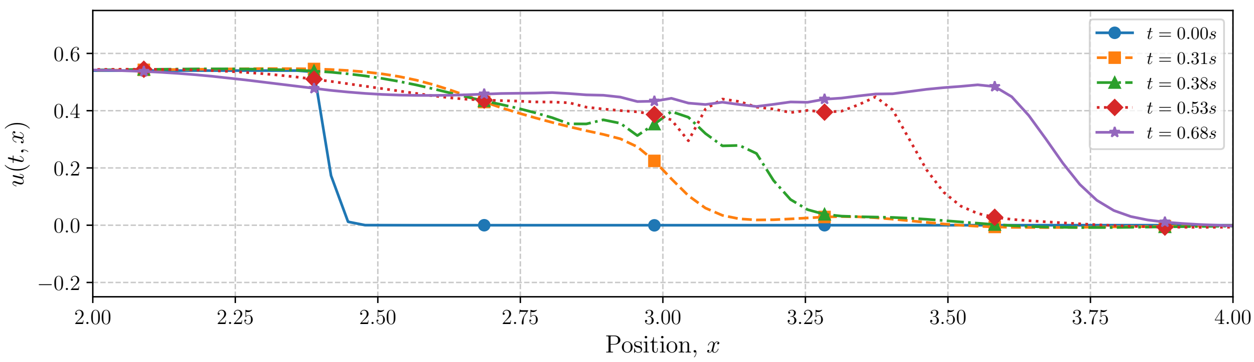

(c) The fluid velocity $x \mapsto u(t,x)$ with the PFC scheme at different times $t = 0$, $t = 0.31$, $t = 0.38$, $t = 0.53$ and $t = 0.68$.

Fig. 4.9: Shock with the original model with the PFC scheme.

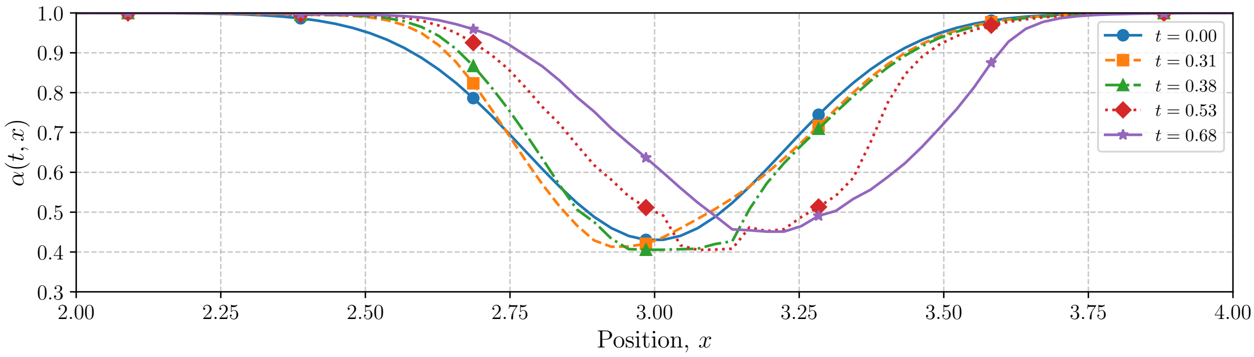

(a) The fluid volume fraction $x \mapsto \alpha(t,x)$ with the PFC scheme at different times $t = 0$, $t = 0.31$, $t = 0.38$, $t = 0.53$ and $t = 0.68$.

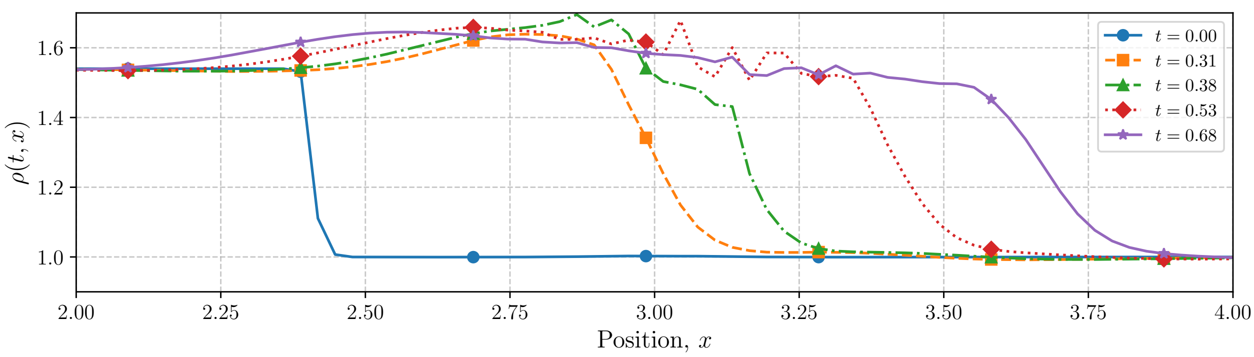

(b) The fluid density $x \mapsto \varrho(t,x)$ with the PFC scheme at different times $t = 0$, $t = 0.31$, $t = 0.38$, $t = 0.53$ and $t = 0.68$.

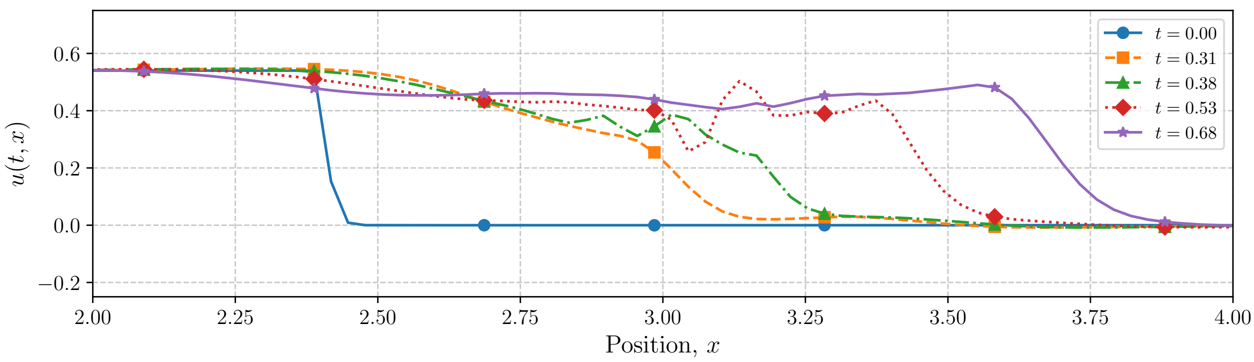

(c) The fluid velocity $x \mapsto u(t,x)$ with the PFC scheme at different times $t = 0$, $t = 0.31$, $t = 0.38$, $t = 0.53$ and $t = 0.68$.

Fig. 4.10: Shock with the soft-congested model with $\varepsilon = 10^{-6}$ with the PFC scheme.

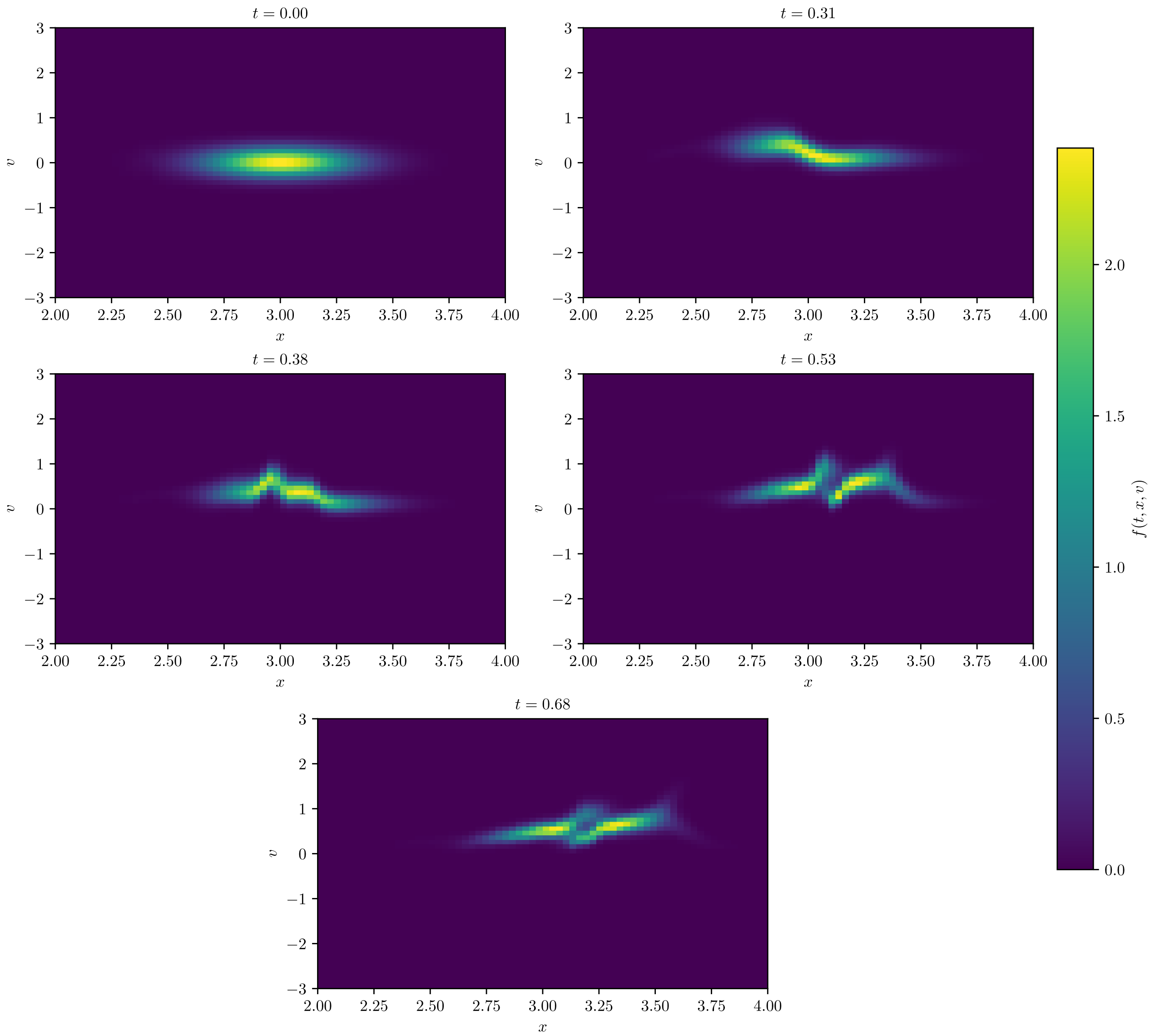

Fig. 4.11: The particle distribution function $f(t,x,v)$ for the soft-congested system (4.8) with the PFC scheme at different times.

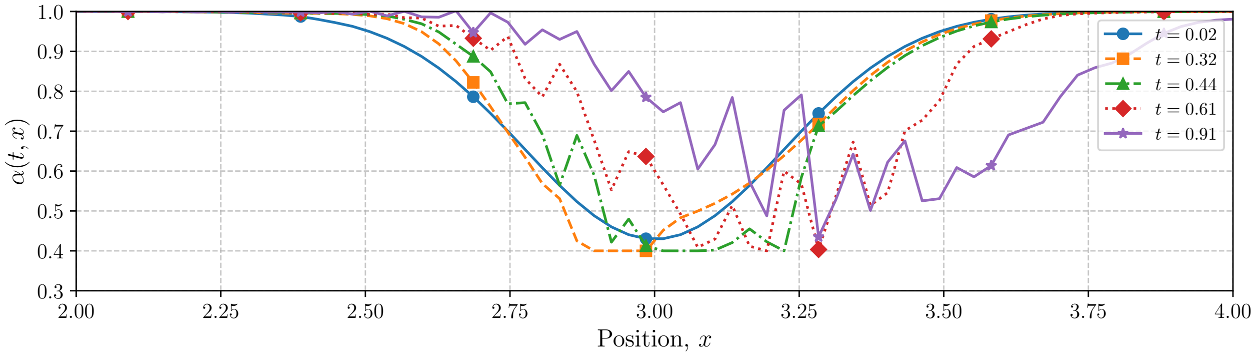

(a) The fluid volume fraction $x \mapsto \alpha(t, x)$ with the BSPL scheme at different times $t = 0.02$, $t = 0.32$, $t = 0.44$, $t = 0.61$ and $t = 0.91$.

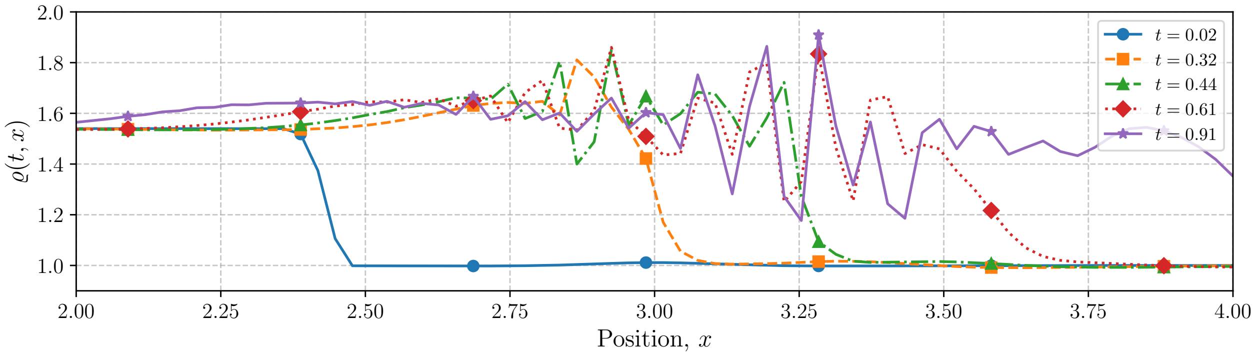

(b) The fluid density $x \mapsto \varrho(t, x)$ with the BSPL scheme at different times $t = 0.02$, $t = 0.32$, $t = 0.44$, $t = 0.61$ and $t = 0.91$.

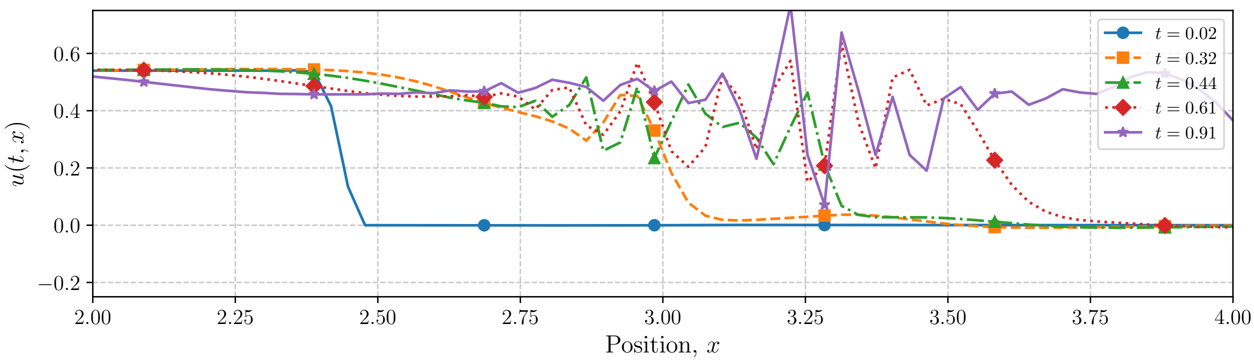

(c) The fluid velocity $x \mapsto u(t, x)$ with the BSPL scheme at different times $t = 0$, $t = 0.32$, $t = 0.44$, $t = 0.61$ and $t = 0.92$.

Fig. 4.12: Shock with the original model (4.7) with the BSPL scheme.

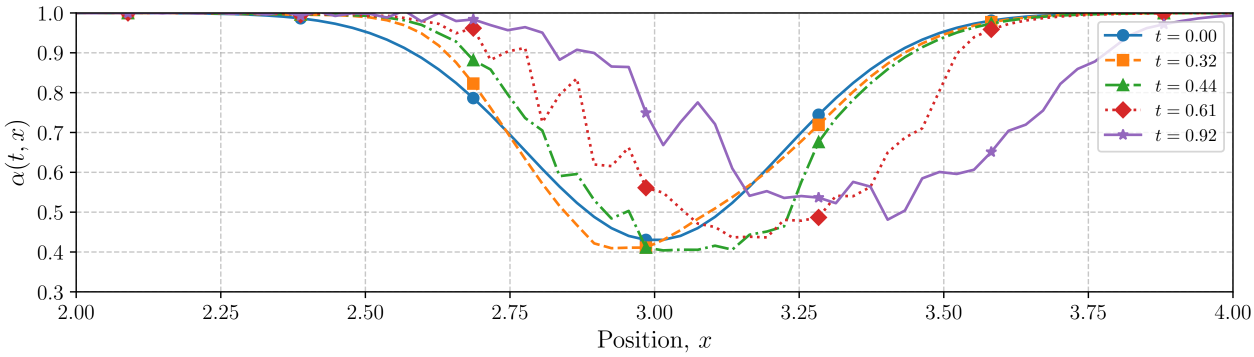

(a) The fluid volume fraction $x \mapsto \alpha(t, x)$ with the PFC scheme at different times $t = 0$, $t = 0.32$, $t = 0.44$, $t = 0.61$ and $t = 0.92$.

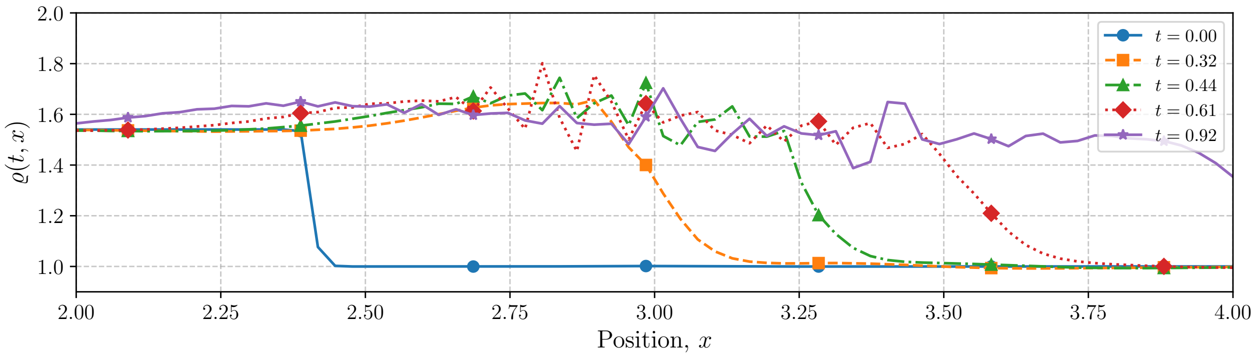

(b) The fluid density $x \mapsto \varrho(t, x)$ with the PFC scheme at different times $t = 0$, $t = 0.32$, $t = 0.44$, $t = 0.61$ and $t = 0.92$.

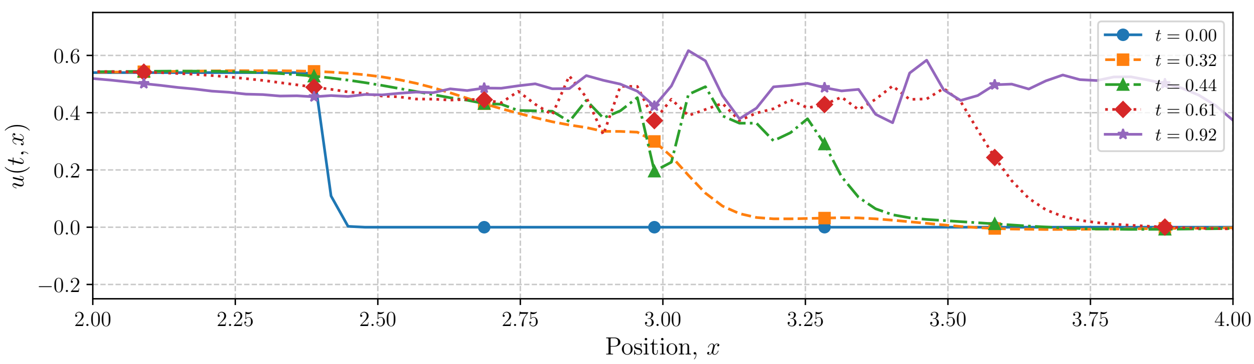

(c) The fluid velocity $x \mapsto u(t, x)$ with the PFC scheme at different times $t = 0$, $t = 0.32$, $t = 0.44$, $t = 0.61$ and $t = 0.92$.

Fig. 4.13: Shock with the soft-congested model (4.8) with $\varepsilon = 10^{-6}$ with the BSPL scheme.

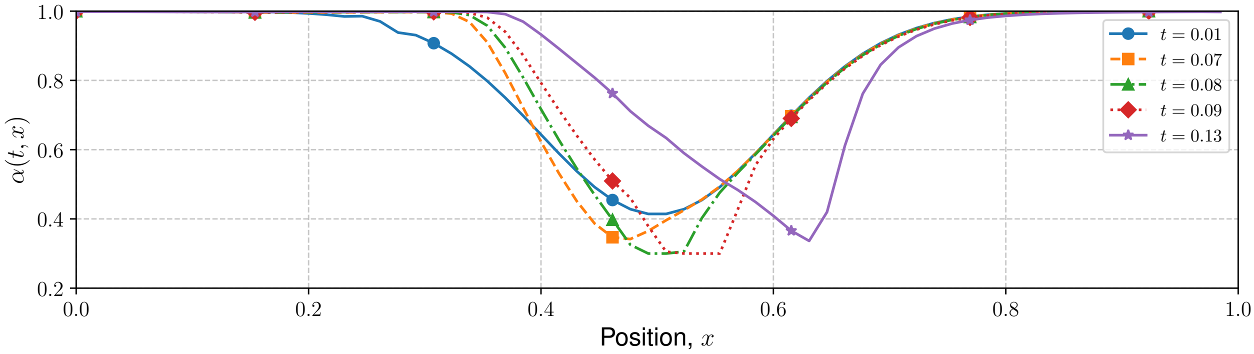

(a) Cross section of the fluid volume fraction $x \mapsto \alpha(t, x, y = 0.5)$ with the BSPL scheme at different times $t = 0$, $t = 0.32$, $t = 0.44$, $t = 0.61$ and $t = 0.92$.

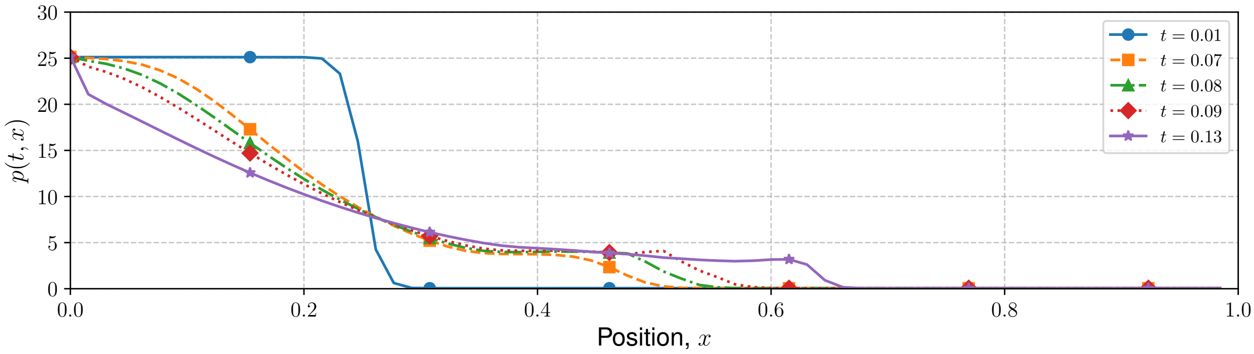

(b) Cross section of the pressure $x \mapsto p(t, x, y = 0.5)$ with the BSPL scheme at different times $t = 0$, $t = 0.32$, $t = 0.44$, $t = 0.61$ and $t = 0.92$.

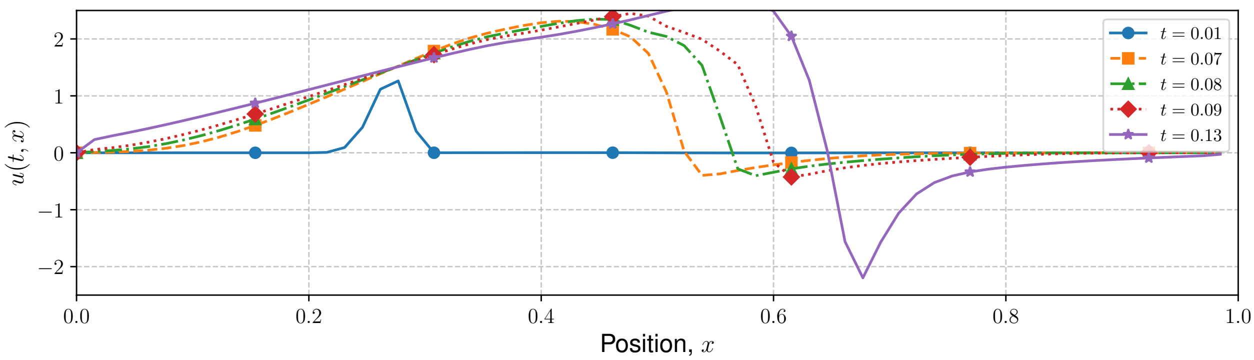

(c) Cross section of the x-component of the fluid velocity $x \mapsto u_x(t, x, = 0.5)$ with the BSPL scheme at different times $t = 0$, $t = 0.32$, $t = 0.44$, $t = 0.61$ and $t = 0.92$.

Fig. 4.14: Shock tube with the original model (4.8) in 2D-2V with the BSPL scheme.

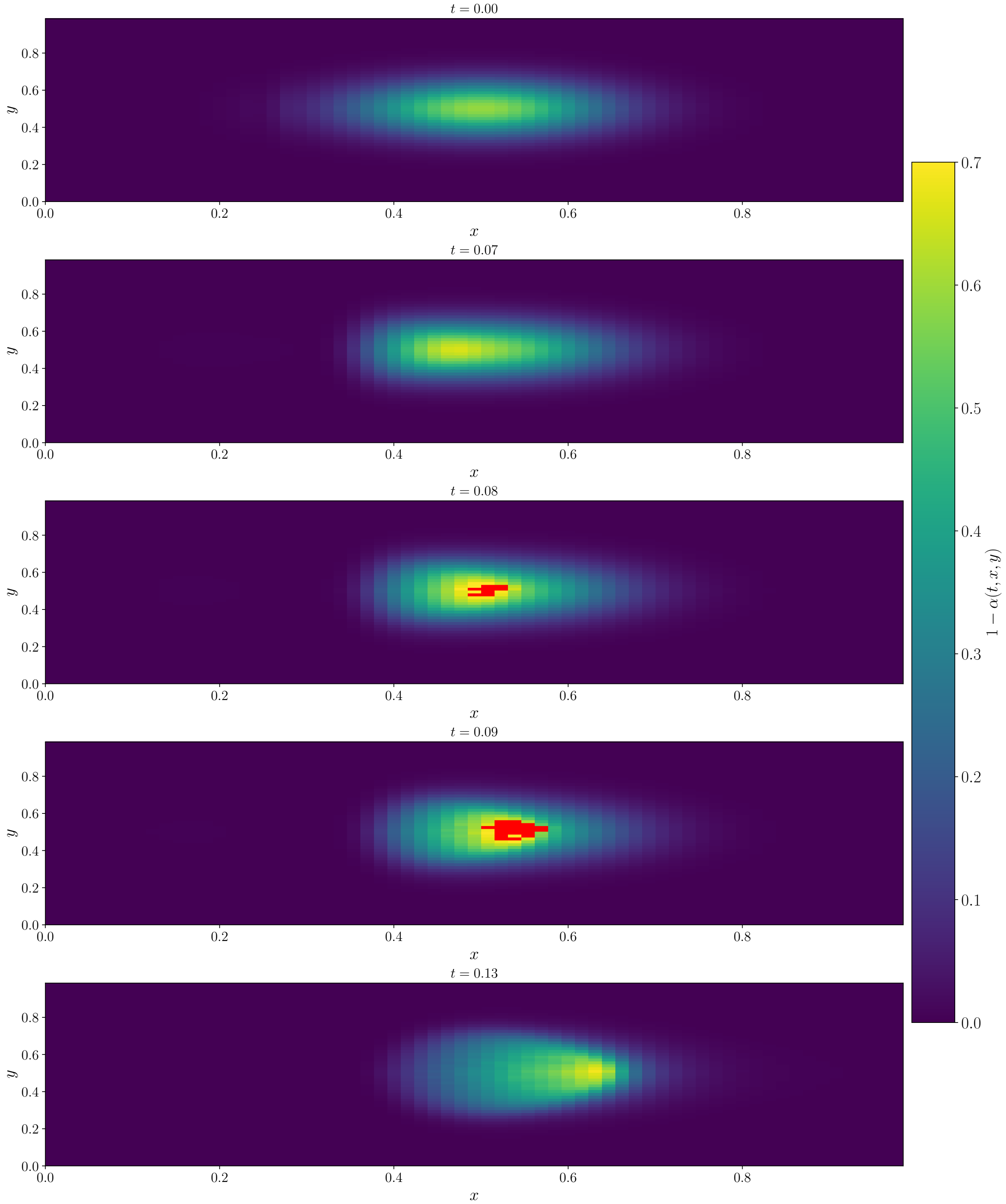

Fig. 4.15: The particle volume function $1 - \alpha(t,x,y)$ with the BSPL scheme at different times.

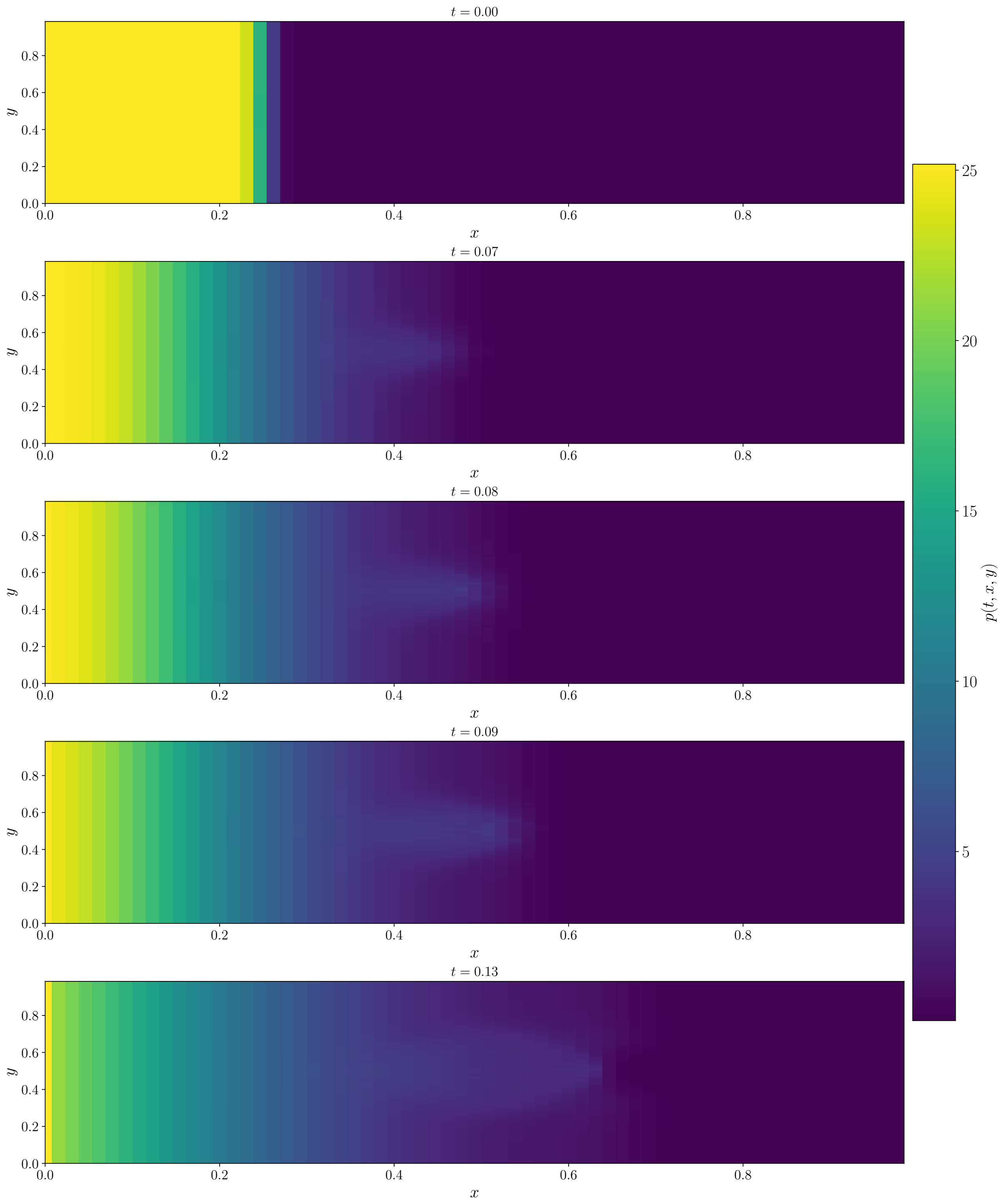

Fig. 4.16: The pressure of the fluid $p(t,x,y)$ with the BSPL scheme at different times.

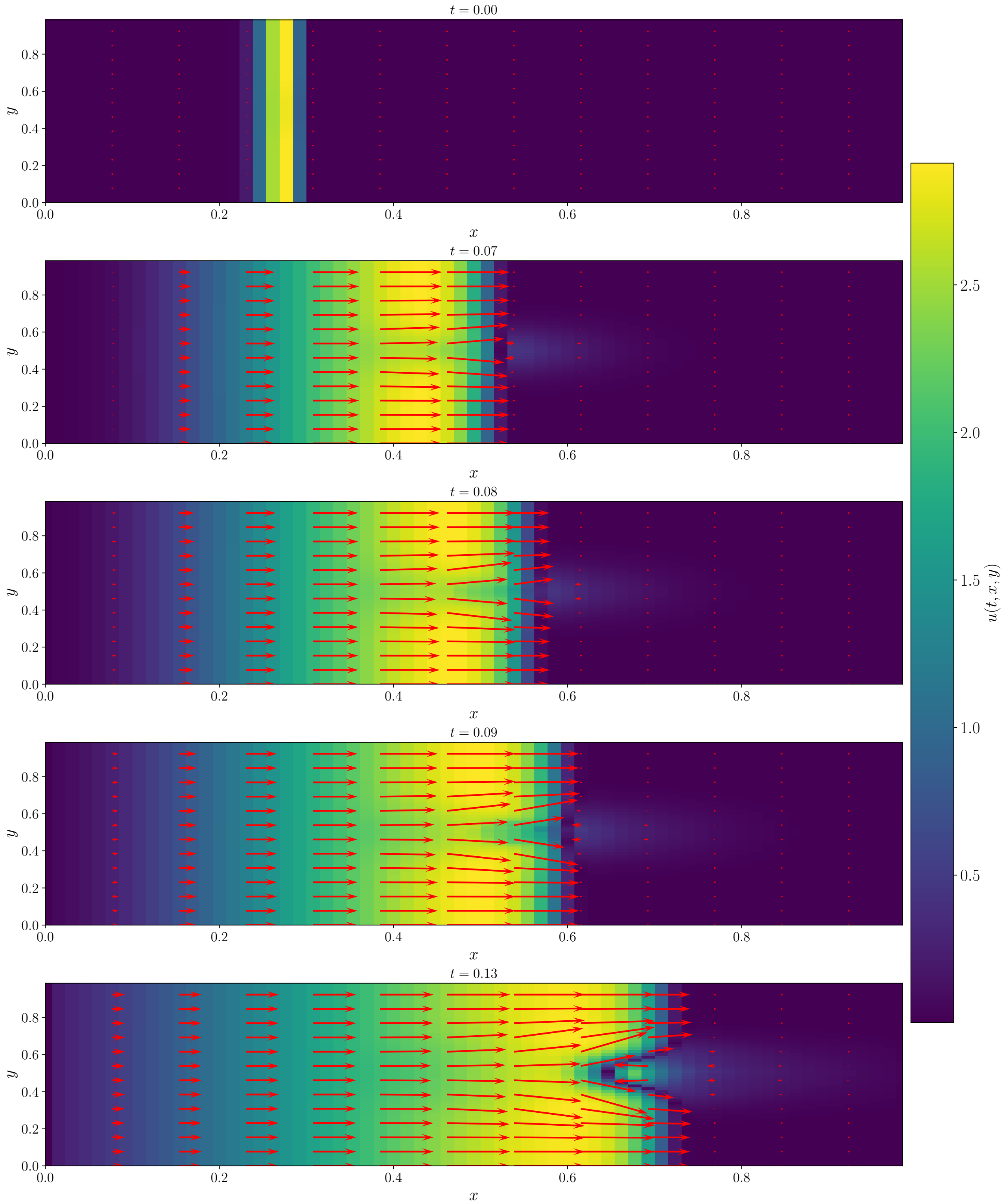

Fig. 4.17: The velocity of the fluid $\boldsymbol{u}(t,x,y)$ with the BSPL scheme at different times. The color map represents the magnitude of the velocity $|\boldsymbol{u}|$, while the arrow represents the actual velocity vector $\boldsymbol{u}$.

Conclusions and perspectives

In this thesis, we studied a fluid-kinetic coupling that describes dense suspension of particles in a carrying fluid. We proposed several contribution. The Chapter 2 is dedicated to the existence of solution for thick spray. After introducing the main difficulties to construct local-in-time strong solutions, we introduced a new averaged system for descring thick spray, by reintroducing the radius of the particles explicitely in the equations. This led to a result of local-in-time well-posedness for strong solution. The Chapter 3 study a linearized thick spray model without friction. We show that the structure of the linearized equation is reminiscient to the linearized Vlasov Poisson equations, around suitable equilibrium, and that this structure leads to a linear damping result, which present a qualitatively similar behavior to the linear Landau damping of plasma physics. We also present a numerical scheme that illustrate the damping effect. We also present some numerical result for instable equilibrium profiles, and we compare the numerical result to the correspondign test cases of plasma physics. The Chapter 4 is dedicated to the construction of a numerical scheme for thick spray models, based on a Finite Volume scheme for the fluid part, and a semi-Lagrangian scheme for the particles. We also propose methods to take into account a close packing limit of the particles in the simulations. The results show that semi-Lagrangian method can be well adapted to simulate a thick spray model, and that a close packing limit can be recovered by the proposed methodologies.

We list several natural perspectives to this work:

- It would be interesting to try to construct global weak solution in the suitable sence for the proposed averaged thick spray model. Moreover, adapting the numerical schemes proposed in Chapter 4 to the thick spray model seems to be an interesting perspective. It would be interesting to extend the local-in-time well-posedness result to an averaged system that take into account more physics: energy exchange between the particles, polydispersion, collision, fragmentation, coalescence.

- A natural question that arise in light of the linear damping result is: Can we extend this result for the full nonlinear system ? This question seems to be difficult, and the methods used for the nonlinear Landau damping [16, 96] are probably not adapted.

- The numerical methods proposed in the Chapter 4 can still be greatly improved. An immediate perspective could be to use a better numerical scheme for the gas part, for example, using a Lagrange+remap method. Moreover, the incorporation of more variable for the particles and using the full Euler system for the fluid part is important for the physical applications.

- Concerning the modification to account for the close-packing limit, it appears that this adjustment may not be ideal from a modeling perspective. Specifically, the modification is of “first order,” meaning that particles slow down as the density approaches the close-packing limit but regain their initial velocities when the density decreases. A “second-order” adjustment, where the packing pressure is included in the acceleration term of the Vlasov equation, might be more appropriate. Currently, the packing pressure is included in the transport operator, based on our conjecture—supported by numerical results—that the Random Repair algorithm approximates a hard congestion model. It would be interesting to explore methods developed for second-order hard congestion models, see the PhD thesis of Anthony Preux [103].

Bibliography

[1] R. Abgrall and S. Karni. A comment on the computation of non-conservative products. Journal of Computational Physics, 2010.

[2] K. Ait-Ameur, M. Essadki, M. Massot, and T. Pichard. Limitation strategies for high-order discontinuous Galerkin schemes applied to an Eulerian model of polydisperse sprays. preprint HAL: https://hal.science/hal-04374640/.

[3] L. Ambrosio. Transport equation and cauchy problem for BV vector fields. Inventiones mathematicae, 158:227–260, 2004.

[4] L. Ambrosio. Well posedness of ODE's and continuity equations with nonsmooth vector fields, and applications. Revista Matematica Complutense, 2017.

[5] A. A. Amsden, P. J. O'Rourke, and T. D. Butler. KIVA-II: A computer program for chemically reactive flows with sprays. Technical report, Los Alamos National Lab. (LANL), Los Alamos, NM (United States), 1989.

[6] M. Andrews and P. O'Rourke. The multiphase particle-in-cell (MP-PIC) method for dense particulate flows. International Journal of Multiphase Flow, 22(2):379–402, 1996.

[7] O. Anoshchenko and A. Boutet de Monvel-Berthier. The existence of the global generalized solution of the system of equations describing suspension motion. Mathematical Models and Methods in Applied Sciences, 1997.

[8] G. Backus. Linearized plasma oscillations in arbitrary electron velocity distributions. Journal of Mathematical Physics, 1960.

[9] R. Balescu. Statistical Mechanics of Charged Particles. Wiley-Interscience, 1963.

[10] A. Baradat. Nonlinear instability in Vlasov type equations around rough velocity profiles. Annales de l'Institut Henri Poincaré C, Analyse non linéaire, 2020.

[11] C. Baranger. Modélisation, étude mathématique et simulation des collisions dans les fluides complexes. PhD thesis, Ecole Normale supérieure - Ens Cachan, 2004.

[12] C. Baranger and L. Desvillettes. Coupling Euler and Vlasov equations in the context of sprays: The local-in-time, classical solutions. Journal of Hyperbolic Differential Equations, 03(01):1–26, 2006.

[13] C. Bardos and A. Nouri. A Vlasov equation with Dirac potential used in fusion plasmas. Journal of Mathematical Physics, 2012.

[14] H. Baumgärtel and M. Wollenberg. Mathematical Scattering Theory. Number 9 in Operator Theory: Advances and Applications. Birkhäuser, 1983.

[15] J. Bedrossian and N. Masmoudi. Inviscid damping and the asymptotic stability of planar shear flows in the 2d Euler equations. Publications mathématiques de l'IHÉS, 122, 2014.

[16] J. Bedrossian, N. Masmoudi, and C. Mouhot. Landau damping: Paraproducts and gevrey regularity. Annals of PDE, 2(4), 2016.

[17] S. Benjelloun, L. Desvillettes, J. Ghidaglia, and K. Nielsen. Modeling and simulation of thick sprays through coupling of a finite volume Euler equation solver and a particle method for a disperse phase. Note di Mathematica, 32(1), 2012.

[18] A. Bernard-Champmartin, J. Braeunig, C. Fochesato, and T. Goudon. A semi-Lagrangian approach for dilute non-collisional fluid-particle flows. Communications in Computational Physics, 19(3):801–840, 2016.

[19] F. Berthelin and D. Broizat. A model for the evolution of traffic jams in multi-lane. Kinetic and Related Models, 2012.

[20] F. Berthelin, T. Goudon, and S. Minjeaud. Multifluid flows: A kinetic approach. Journal of Scientific Computing, 66(2):792–824, 2016.

[21] N. Besse and E. Sonnendrücker. Semi-Lagrangian schemes for the Vlasov equation on an unstructured mesh of phase space. Journal of Computational Physics, 191:341–376, 2003.

[22] E. Bocchi. Floating structures in shallow water: local well-posedness in the axisymmetric case. SIAM Journal on Mathematical Analysis, 52(1), 2020.

[23] L. Boudin, L. Desvillettes, and R. Motte. A modeling of compressible droplets in a fluid. Communications if Mathematical Sciences, 1:657–669, 2003.

[24] L. Boudin, C. Grandmont, B. Grec, S. Martin, A. Mecherbet, and F. Noël. Fluid-kinetic modelling for respiratory aerosols with variable size and temperature. 67:100–119, 2020.

[25] L. Boudin, C. Grandmont, A. Lorz, and A. Moussa. Modelling and numerics for respiratory aerosols. Communications in Computational Physics, 18(3):723–756, 2018.

[26] T. J. M. Boyd and J. J. Sanderson. The Physics of Plasmas. Cambridge University Press, 2003.

[27] C. Buet, B. Després, and L. Desvillettes. Linear stability of thick sprays equations. Journal of Statistical Physics, 190(53), 01 2023.

[28] C. Buet, B. Després, and V. Fournet. Analog of linear Landau damping in a coupled Vlasov-Euler system for thick sprays. Communications in Mathematical Sciences, 2024. To appear.

[29] R. Caflisch and G. Papanicolaou. Dynamic theory of suspensions with brownian effects. SIAM J. Appl. Math, pages 885–906, 1983.

[30] M. J. Castro Diaz, A. Kurganov, and T. M. De Luna. Path-conservative central upwind schemes for nonconservative hyperbolic systems. ESAIM: Mathematical Modelling and Numerical Analysis, 2019.

[31] C. Cercignani. The Boltzmann Equation and Its Applications. Springer New York, NY, 1988.

[32] C. Cercignani and P. M. Illner, Reinhard. The Mathematical Theory of Dilute Gases. Springer-Verlag, 1994.

[33] C. Chalons and C. Frédéric. A new comment on the computation of non-conservative products using Roe-type path conservative schemes. Journal of Computational Physics, 2017.

[34] F. Charles, B. Després, A. Rege, and R. Weder. The Vlasov-Ampère system and the Bernstein-Landau paradox. Journal of Statistical Physics, 2021.

[35] C. Z. Cheng and G. Knorr. The integration of the Vlasov equation in configuration space. Journal of Computational Physics, 22(3):330–351, 1976.

[36] J. Clouet and K. Domelevo. Solution of a kinetic stochastic Equation modeling a spray in a turbulent gas flow. Mathematical Models and Methods in Applied Sciences, 07, 11 2011.

[37] N. Crouseilles, M. Mehrenberger, and E. Sonnendrücker. Conservative semi-Lagrangian schemes for the Vlasov equations. Journal of Computational Physics, 229:1927–1953, 2010.

[38] N. Crouseilles, T. Respaud, and E. Sonnendrücker. A forward semi-Lagrangian method for the numerical solution of the Vlasov equation. Computer Physics Communications, 180(10):1730–1745, 2009.

[39] G. Dal Maso, P. G. Le Floch, and F. Murat. Definition and weak stability of nonconservative products. Journal de Mathématiques Pures et Appliquées, 74(6):483–548, 1995.

[40] P. Degond. Spectral theory of the linearized Vlasov-Poisson equation. Transactions of the American Mathematical Society, 376(5), 1986.

[41] P. Degond, J. Hua, and L. Navoret. Numerical simulations of the Euler system with congestion constraint. Journal of Computational Physics, 2010.

[42] P. Degond, J. Hua, and L. Navoret. Finite volume approximations of the Euler system with variable congestion. Journal of Computational Physics, 2011.

[43] B. Després. Scattering structure and Landau damping for linearized Vlasov equations with inhomogeneous Boltzmannian states. Annales de l'Institut Henri Poincaré, 2019.

[44] B. Després. Trace class properties of the non homogeneous linear Vlasov–Poisson equation in dimension 1+1. Journal of Spectral Theory, 11(2):709–742, 2021.

[45] L. Desvillettes. Some aspects of the modelling at different scales of multiphase flows. Computer methods in applied mechanics and engineering, 2010.

[46] L. Desvillettes and J. Mathiaud. Some aspects of the asymptotics leading from gas-particles equations towards multiphase flows equations. Journal of Statistical Physics, 141, 2010.

[47] F. Doisneau, M. Arienti, and J. C. Oefelein. A semi-Lagrangian transport method for kinetic problems with application to dense-to-dilute polydisperse reacting spray flows. Journal of Computational Physics, 329:48–72, 2017.

[48] K. Domelevo and J.-M. Roquejoffre. Existence and stability of travelling wave solutions in a kinetic model of two-phase flows. Communications in Partial Differential Equations, 24(1-2):61–108, 1999.

[49] J. K. Dukowicz. A particle-fluid numerical model for liquid sprays. Journal of Computational Physics, 35(2):229–253, 1980.

[50] L. Einkemmer. A study on conserving invariants of the Vlasov equation in semi-Lagrangian computer simulations. Journal of Plasma Physics, 2017.

[51] L. Einkemmer and C. Lubich. A low-rank projector-splitting integrator for the Vlasov–Poisson equation. Computational Methods in Science and Engineering, 2018.

[52] L. Ertzbischoff. Analyse mathématique de quelques Analyse mathématique de quelques systèmes d'équations de type fluide-cinétique. PhD thesis, Ecole polytechnique, 2023.

[53] L. Ertzbischoff and D. Han-Kwan. On well-posedness for thick spray equations. Arxiv, March 2023.

[54] L. Ertzbischoff, D. Han-Kwan, and A. Moussa. Concentration versus absorption for the Vlasov-Navier-Stokes system on bounded domains. Nonlinearity, 2021.

[55] M. Essadki, S. de Chaisemartin, F. Laurent, and M. Massot. High order moment model for polydisperse evaporating sprays towards interfacial geometry description. SIAM Journal of Applied Mathematics, 2018.

[56] L. Evans and R. Gariepy. Measure Theory and Fine Properties of Functions, Revised Edition. Textbooks in Mathematics. CRC Press, 2015.

[57] F. Filbet and G. Russo. High order numerical methods for the space non-homogeneous Boltzmann equation. Journal of Computational Physics, 186:457–480, 2003.

[58] F. Filbet and E. Sonnendrücker. Comparison of Eulerian Vlasov solvers. Computer Physics Communications, 150:247–266, 2003.

[59] F. Filbet, E. Sonnendrücker, and P. Bertrand. Conservative numerical schemes for the Vlasov equation. Journal of Computational Physics, 172(1):166–187, 2001.

[60] F. Filbet, E. Sonnendrücker, and P. Bertrand. Conservative numerical schemes for the Vlasov equation. Journal of Computational Physics, 172:166–187, 2001.

[61] F. Filbet and T. Xion. Conservative discontinuous Galerkin/Hermite spectral method for the Vlasov–Poisson system. Communications on Applied Mathematics and Computation, 4:34–59, 2020.

[62] V. Fournet. Investigation on the stability in a thick spray model. ESAIM: Proceedings and Surveys, 2024. To appear.

[63] V. Fournet, C. Buet, and D. Bruno. Local-in-time existence of strong solutions to an averaged thick sprays model. Kinetic and Related Models, 17(4):606–633.

[64] R. O. Fox, J. W. Posey, R. W. Houim, and F. Laurent. A kinetic-based model for polydisperse, high-speed, fluid-particle flows. International Journal on Multiphase Flow, 171:104–698, 2024.

[65] I. Gamba, V. Panferev, and C. Villani. On the Boltzmann equation dor diffusively excited granular media. Communications in Mathematical Physics, 2004.

[66] P. Gao, H. R. Wakeford, S. E. Moran, and V. Parmentier. Aerosols in exoplanet atmospheres. Journal of Geophysical Research: Planets, 126(4), 2021.

[67] J.-M. Ghidaglia, A. Kumbaro, and G. Le Coq. On the numerical solution to two fluid models via a cell centered finite volume method. European Journal of Mechanics - B/Fluids, 20:841–867, 2001.

[68] E. Godlewki and P.-A. Raviart. Numerical Approximation of Hyperbolic Systems of Conservation Laws. Springer New York, NY, 2013.

[69] T. Goudon and L. Vivion. Numerical investigation of Landau damping in dynamical Lorentz gases. Physica D: Nonlinear Phenomena, 403:132310, 2020.

[70] T. Goudon and L. Vivion. Landau damping in dynamical Lorentz gases. Technical report, Société mathématique de France, 2021.

[71] K. Gustafson and G. Johnson. On the absolutely continuous subspace of a selt-adjoint operator. Helvetica Physica Acta, 47(2):163–166, 1976.

[72] D. Han-Kwan and M. Hauray. Stability issues in the quasineutral limit of the one-dimensional Vlasov–Poisson equation. Communications in Mathematical Physics, 2014.

[73] D. Han-Kwan, A. Moussa, and I. Moyano. Large time behavior of the Vlasov-Navier-Stokes system on the torus. Archive for Rational Mechanics and Analysis, 2020.

[74] S. Hecht and N. Vauchelet. Incompressible limit of a mechanical model for tissue growth with non-overlapping constraint. Communications if Mathematical Sciences, 2017.

[75] A. Hiltebrand, S. Mishra, and P. Carlos. Entropy-stable space-time DG schemes for non-conservative hyperbolic systems. ESAIM: Mathematical Modelling and Numerical Analysis, 2018.

[76] J. Hylkemann and P. Villedieu. A random particle method to simulate coalescence phenomena in dense liquid sprays. Sixteenth International Conference on Numerical Methods in Fluid Dynamics, 1998.

[77] J. H. Jeans. On the theory of star-streaming and the structure of the universe. Monthly Notices of the Royal Astronomical Society, 76:70–84, 1915.

[78] T. Kato. Wave operators and unitary equivalence. Pacific Journal of Mathematics, 15(1), 1965.

[79] T. Kato. Perturbation Theory for Linear Operators. Springer, 1995.

[80] N. Krall and A. Trivelpiece. Principles of plasma physics. San Francisco Press, 1986.

[81] L. Landau. On the vibration of the electronic plasma. Journal of Physics, 10(1):25–34, 1946.

[82] L. Landau and E. M. Lifshich. Fluid Mechanics. Pergamon Press, 1971.

[83] D. Lannes. On the dynamics of floating structures. Annals of PDE, 2017.

[84] P. D. Lax. Functional Analysis. Wiley, 2014.

[85] P.-L. Lions. Mathematical Topics in Fluid Mechanics, volume 2: Compressible Fluids. Oxford Lecture Series in Mathematics and Its Applications, 1998.

[86] P.-L. Lions. Mathematical Topics in Fluid Mechanics, volume 1: Incompressible Models. Oxford Lecture Series in Mathematics and Its Applications, 96.

[87] A. Majda. Compressible Fluid Flow and Systems of Conservation Laws in Several Space Variables. Springer New York, NY, 1984.

[88] A. Mangeney, F. Califano, C. Cavazzoni, and P. Travnicek. A numerical scheme for the integrations of the Vlasov-Maxwell system of equations. Journal of Computational Physics, 179:495–538, 2002.

[89] V. Maslov and M. Fedoruyk. The linear theory of Landau damping. Mathematics of the USSR-Sbornik, 1986.

[90] T. Mather, D. Pyle, and C. Oppenheimer. Tropospheric volcanic aerosol. Washington DC American Geophysical Union Geophysical Monograph Series, 139, 2003.

[91] J. Mathiaud. Etude de systèmes de type gaz-particules. PhD thesis, Ecole Normale supérieure - Ens Cachan, 2006.

[92] J. Mathiaud. Local smooth solutions of a thin spray model with collisions. Mathematical Models and Methods in Applied Sciences, (20):191–221, 2010.

[93] B. Maury, A. Roudneff-Chupin, and F. Santambrogio. A macroscopic crowd motion model of gradient flow type. Mathematical Models and Methods in Applied Sciences, 2010.

[94] B. Maury, A. Roudneff-Chupin, F. Santambrogio, and J. Venel. Handling congestion in crowd motion modeling. Networks and Heterogeneous Media, 2011.

[95] J. C. Maxwell. Illustrations of the dynamical theory of gases. The London, Edinburgh, and Dublin Philosophical Magazine and Journal of Science, 1860.

[96] C. Mouhot and C. Villani. On Landau damping. Acta Mathematica, 207(1), 2011.

[97] P. J. O'Rourke. Collective drop effects on vaporizing liquid sprays. Technical report, Los Alamos National Lab., 1981.

[98] C. Parés. Numerical methods for nonconservative hyperbolic systems: a theoretical framework. SIAM Journal on Numerical Analysis, 2006.

[99] O. Penrose. Electrostatic instabilities of a uniform non-Maxwellian plasma. Physics of Fluids, 1960.

[100] C. Perrin. An overview on congestion phenomena in fluid equations. 2018.

[101] C. Perrin and E. Zatorska. Free/congested two-phase model from weak solutions to multi-dimensional compressible Navier-Stokes equations. Communications in Partial Differential Equations, 2015.

[102] K. Pfaffelmoser. Global classical solutions of the Vlasov-Poisson system in three dimensions for general initial data. Journal of Differential Equations, 95(2):281–303, Jan. 1992.

[103] A. Preux. Transport optimal et ´equations des gaz sans pression avec contrainte de densité maximale. PhD thesis, Université Paris-Saclay, 2016.

[104] W. E. Ranz and W. R. Marshall. Evaporization from drops, part i-ii. Chemical Engineering Progress, 1952.

[105] M. Reed and B. Simon. Analysis of Operators, volume 4. Elsevier, 1978.

[106] M. Reed and B. Simon. Methods of Modern Mathematical Physics: I Functional Analysis. Academic Press, San Diego, 1980.

[107] D. D. Ruytov. Landau damping: half a century with the great discovery. Plasma Physics and Controlled Fusion, 41(3A), 1999.

[108] F. Santambrogio. Crowd motion and evolution PDEs under density constraints. ESAIM: PROCEEDINGS AND SURVEYS, 64:137–157, October 2018.

[109] R. Scardovelli and S. Zaleski. Direct numerical simulation of a free-surface and interfacial flow. Annual Review of Fluid Mechanics, 31:567–603, 1999.

[110] D. Serre. Systèmes de lois de conservation. Number vol. 1 in Fondations (Diderot). Diderot, 1996.

[111] E. Sonnendrücker. Modèles cinétiques pour la fusion. Note du cours de M2. IRMA, Université L. Pasteur, Strasbourg, France, 2008.

[112] E. Sonnendrücker, J. Roche, P. Bertand, and A. Ghizzo. The semi-Lagrangian method for the numerical resolution of the Vlasov equation. Journal of Computational Physics, 149(2):201–220, 1999.

[113] T. H. Stix. The Theory of Plasma Waves. New York et al.: McGraw-Hill Book Co., 1962.

[114] T. Umeda. A conservative and non-oscillatory scheme for Vlasov code simulations. Earth Planet SP, 60:773–779, 2008.

[115] C. Villani. A review of mathematical topics in collisional kinetic theory. Elsevier Science, 2002.

[116] A. A. Vlasov. The vibrational properties of an electron gas. Journal of Experimental and Theoretical Physics (In Russian), 1938.

[117] J. Wang. Continuum theory for dense gas-solid flow: A state-of-the-art review. Chemical Engineering Science, 2020.

[118] F. Williams. Combustion Theory, second edition. Benjamin Cummings, 1985.

[119] D. R. Yafaev. Scattering Theory: Some Old and New Problems. Springer-Verlag, 2000.

[120] X. Yang, W. Shyy, and K. Xu. Unified gas-kinetic wave-particle method for polydisperse gas-solid particle multiphase flow. Journal of Fluid Mechanics, 983:A37, 2024.

Etude Mathématique et Numérique de Modèles de Spray Épais

Résumé : Cette thèse est consacrée à la modélisation, à l'analyse mathématique et à l'analyse numérique d'un système d'équations aux dérivées partielles décrivant l'évolution d'une suspension de particules neutres dans un fluide ambiant, souvent désignée sous le nom de spray. La phase dispersée est modélisée par les équations de la théorie cinétique, tandis que la phase continue est décrite par les équations de la mécanique des fluides. Nous nous concentrons en particulier sur le cas des sprays dits épais.

Le Chapitre 2 est consacré au problème de la construction de solutions pour le système des sprays épais. Nous introduisons un nouveau système dans lequel les termes singuliers sont régularisés et nous démontrons l'existence et l'unicité de solutions avec une régularité de type Sobolev, localement en temps.

Le Chapitre 3 explore l'analogie entre le système des sprays épais et le système de Vlasov-Poisson décrivant un plasma électrostatique. Nous montrons qu'en l'absence de friction, le système des sprays épais présente une propriété d'amortissement linéaire de l'énergie acoustique, analogue à l'amortissement de Landau bien connu en physique des plasmas. Cet effet est illustré par des résultats numériques.

Le Chapitre 4 est consacré à la simulation numérique du système des sprays épais. Nous proposons une approche combinant des méthodes existantes : une méthode semi-Lagrangienne pour la phase dispersée, couplée à une méthode de type Volume Fini pour la phase continue. Nous abordons également le problème de la limite de packing et introduisons deux méthodes permettant de conserver cette limite au niveau discret. Enfin, nous présentons des résultats numériques..

Mots-clés : Equations aux dérivées partielles, théorie cinétique, mécanique des fluides, analyse.

Mathematical and Numerical Study of Thick Spray Models

Abstract: This thesis is dedicated to the modeling, mathematical analysis, and numerical analysis of a partial differential equation system describing the evolution of a suspension of neutral particles in a surrounding fluid, often referred to as a spray. The dispersed phase is modeled by the equations of kinetic theory, while the continuous phase is described by the equations of fluid mechanics. We focus particularly on the case of so-called thick sprays.

Chapter 2 is devoted to the problem of constructing solutions for the thick spray system. We introduce a new system in which singular terms are regularized, and we prove the existence and uniqueness of solutions with Sobolev regularity, locally in time.

Chapter 3 explores the analogy between the thick spray system and the Vlasov-Poisson system describing an electrostatic plasma. We demonstrate that, in the absence of friction, the thick spray system exhibits a property of linear damping of acoustic energy, analogous to Landau damping, which is well known in plasma physics. This effect is illustrated by numerical results.

Chapter 4 is dedicated to the numerical simulation of the thick spray system. We present an approach that combines existing methods: a semi-Lagrangian method for the dispersed phase, coupled with a finite volume method for the continuous phase. We also address the packing limit issue and introduce two methods to preserve this packing limit at the discrete level. Finally, we present numerical results.

Keywords: Partial differential equations, kinetic theory, fluid mechanics, analysis.

Thèse de doctorat, Victor Fournet

Établissements de recherche :
CEA/DAM/DIF
Laboratoire Jacques Louis Lions